Single-injection prime-boost vaccines based on biodegradable polymers

van der Kooij, Renée

DOI:
10.33612/diss.651650521

Publication date:
2023

Link to publication in University of Groningen/UMCG research database

Single-injection prime-boost vaccines based on biodegradable polymers

Renée S. van der Kooij

2023

Paranymphs
Hanne M. van der Kooij
Grietje H. Prins

Single-injection prime-boost vaccines based on biodegradable polymers

Layout design:	Renée van der Kooij
Cover design:	Renée van der Kooij & Maria Roosen ('Bubbles', 2004, water colour, 155 x 106 cm, collectie Amsterdam UMC)
Printing:	Ipskamp Printing (Enschede, The Netherlands)

innocore
PHARMACEUTICALS

rijksuniversiteit
groningen

Single-injection prime-boost vaccines based on biodegradable polymers

Proefschrift

ter verkrijging van de graad van doctor aan de
Rijksuniversiteit Groningen
op gezag van de
rector magnificus prof. dr. C. Wijmenga
en volgens besluit van het College voor Promoties.

De openbare verdediging zal plaatsvinden op

dinsdag 23 mei 2023 om 14.30 uur

door

Renée Suzanne van der Kooij

geboren op 16 januari 1993
te Dronten

Promotor

Prof. dr. H.W. Frijlink

Copromotor

Dr. W.L.J. Hinrichs

Beoordelingscommissie

Prof. dr. E.M.J. Verpoorte
Prof. dr. H. Almeida Santos
Prof. dr. E. Mastrobattista

Table of contents

Chapter 1

General introduction

1.1 General introduction

In December 2019, a cluster of severe cases of pneumonia was reported in Wuhan, Hubei, China [1-3], which later turned out to be the beginning of the coronavirus disease 2019 (COVID-19) pandemic [4]. This pandemic was caused by the 2019 novel coronavirus (2019-nCoV, currently designated SARS-CoV-2) [1,2,4], which was characterized by fever, dry cough, and fatigue [1], and was associated with a high mortality rate [5,6]. At this moment, more than 6 million deaths from COVID-19 have been confirmed worldwide [7], making it one of the ten deadliest pandemics in history [8]. The high infection and mortality rate of COVID-19 triggered the exceptionally rapid development of a vaccine against the disease, which on 23 August 2021 resulted in the first full regulatory approval of a COVID-19 vaccine (the Pfizer/BioNTech COVID-19 vaccine) by the US FDA [9,10]. Numerous studies have demonstrated the effectiveness of COVID-19 vaccines in protecting against infection, hospital admission, and transmission of the virus [11-14]. These studies highlight the importance of vaccination in the fight against infectious diseases. As the World Health Organization (WHO) estimated vaccination to save 3.5-5 million lives every year [15], it is considered one of the greatest medical advances of the past centuries.

Despite the great effectiveness of vaccination, coverage for many vaccines has not improved over the last decade [16]. According to the WHO, in 2021, 18.2 million infants did not receive an initial dose of the diphtheria-tetanus-pertussis (DTP) vaccine [16], which is often used as a principal indicator of full childhood vaccination coverage [17]. For the same vaccine, an additional 6.8 million infants were only partially vaccinated [16], with the majority living in low- and middle-income countries [18]. Full vaccination is important for the protection against the targeted disease and missing only the final dose of the DTP series already causes a five times greater risk of infection [19]. Numerous factors have been associated with under-vaccination, but the most frequently reported problem is limited access to vaccination services [20-22]. Also, coverage was consistently lower for multi-dose vaccines, such as the DTP3 vaccine, than for single-dose vaccines [23]. The main reason for this lower coverage is the currently applied vaccination schedules, which require multiple interactions between a health care professional and the vaccinee. These vaccination schedules, also known as a prime-boost regimen, require the administration of a first dose (primer) followed by the administration of a second and sometimes even third or fourth dose (booster) a few weeks, months, or years later (Figure 1a) [24,25]. The primer dose ensures the development of an immune response against the targeted pathogen, but the immune memory can decline over time. Therefore, a booster dose is often needed as re-exposure to the antigen in order to increase the immune response back to protective levels and ensure longer-lasting immunity [26].

Vaccination coverage could potentially be improved by developing an injectable single-administration vaccine formulation for multi-dose vaccines [25,27]. Such a single-administration vaccine formulation could provide for both the primer and the booster dose(s), thereby eliminating the need for multiple administrations, while optimally protecting the vaccinee. By incorporating the antigen into a matrix composed of a biocompatible and biodegradable polymer, controlled release of the antigen from the formulation can be obtained [25,27,28]. A well-tuned controlled release profile will,

ultimately, result in the induction of a strong and long-term immune response after only a single administration. With such a single-administration vaccine formulation, the 6.8 million infants that were only partially vaccinated with the DTP vaccine could, for instance, be prevented.
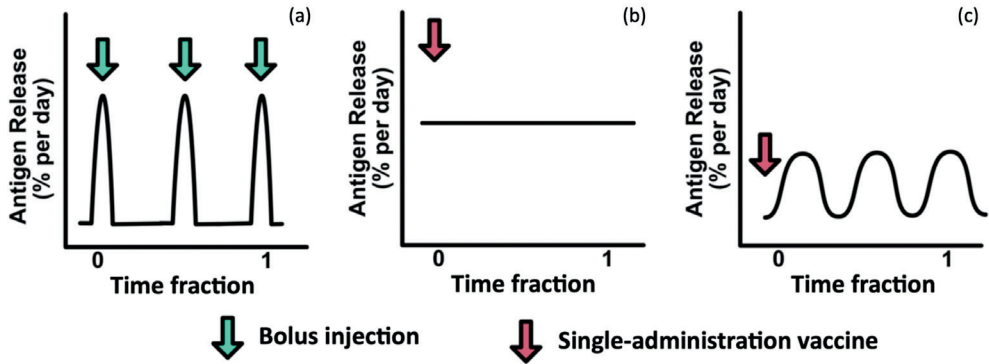
Figure 1. Comparison of the conventional prime-boost regimen and single-administration vaccine formulations and the corresponding antigen release profiles for multi-dose vaccines: (a) Conventional prime-boost regimen with multiple bolus injections at specific time points; (b) Single-administration vaccine formulation with a sustained release profile having zero-order release kinetics; (c) Single-administration vaccine formulation with a pulsatile release profile. Modified from [29] with permission from Wiley.

In the development of a single-administration vaccine formulation, the controlled-release delivery system should exhibit a sustained or pulsatile release of the antigen [25,27]. A sustained-release formulation exhibits a continuous release of the antigen over a certain period of time (Figure 1b) [29]. In this figure, a sustained release profile with zero-order release kinetics is presented, but other release kinetics such as first-order and sigmoidal release are possible as well. A pulsatile-release formulation, on the other hand, mimics the conventional prime-boost regimen with distinct pulses of antigen release, each representing a bolus dose (Figure 1c) [29]. Here, the initial release of the antigen represents the primer dose and the following pulses represent the booster doses, all released at different, predetermined time points. Both concepts are promising alternatives to the currently used multiple-injection vaccines, though they have some limitations as well. A potential issue with sustained-release formulations is the fact that they are suggested to induce tolerance toward the antigen [30-32], thereby rendering the vaccine ineffective, though previous studies have demonstrated the induction of strong immune responses as well with antibody titers similar or superior to a prime and booster injection of the antigen [33-35]. Also, sustained release might not be preferred from a regulatory point of view as it does not mimic the conventional prime-boost regimen [25]. It does, however, better resemble a natural infection than pulsatile release as the immune system is continuously exposed to a low dose of antigen over a longer period of time [36]. These low levels of antigens might also induce fewer side effects [37]. Last, a sustained-release formulation is, from a technological point of view, often easier to develop than a pulsatile-release formulation.

Many different types of formulations can be used as a single-administration

vaccine, but the most frequently investigated type of formulation is a microsphere-based technology. Microspheres are polymeric, spherical particles with a size within the micrometer range [38,39], ideally, 20 to 100 μm. A smaller particle size will cause premature uptake of the microspheres by cells engaging in phagocytosis [40], while a larger particle size disables injection through a small-gauge hypodermic needle [41]. Another type of single-administration vaccine formulation is the implant. Implants are solid polymeric drug delivery depot formulations that can be produced in various shapes and sizes, though they should still be injectable [42,43]. By varying the (internal) structure of the microspheres or implants and/or by varying the composition of the polymers they are prepared from, a pulsatile or sustained release profile can be obtained.

Most of the research performed on single-administration vaccine formulations focused on the biocompatible and biodegradable copolymer poly(DL-lactide-co-glycolide) (PLGA; Figure 2a) [25,27,28], though the homopolymer poly(DL-lactide) (PDLLA) has been used as well.
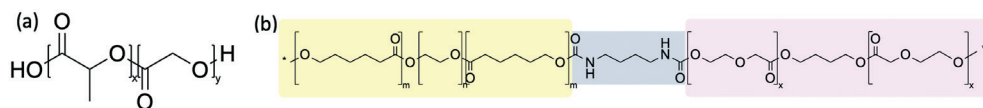
Figure 2. General chemical composition of the two main types of polymers used in this thesis: (a) Poly(DL-lactide-co-glycolide); (b) Example of a PEG-based multi-block copolymer with a hydrophilic poly(ε-caprolactone)-poly(ethylene glycol)- poly(ε-caprolactone) (PCL-PEG-PCL) block and a semi-crystalline 1,4-butanediol (BDO)-initiated poly(dioxanone) (PDO) block. In yellow shading: m: PCL, n: PEG. In blue shading: 1,4-butanediisocyanate (BDI)-based urethane linker. In purple shading: x: PDO. Reproduced from [44].

PLGA is a copolymer of both DL-lactide and glycolide monomers and is used in multiple drug delivery formulations that have been approved by the Food and Drug Administration [45]. It is the most extensively investigated polymer and its degradation rate, and thus, release kinetics, can easily be tailored by varying the DL-lactide:glycolide ratio or the molecular weight of the polymer [46]. The main disadvantage of PLGA is, however, the fact that acidic degradation products are generated upon the degradation of the polymer by hydrolysis [47]. The structural integrity of the incorporated (proteinaceous) antigen might be affected due to the formation of an acidic microclimate within the formulation [47-49]. This might also result in an incomplete release of the antigen [47,50]. Research has, therefore, focused on the development of alternative polymers that generate less or no acidic degradation products and/or exhibit a mainly diffusion-controlled release, thereby preventing a pH drop and its adverse effects on the incorporated antigen. An example is the novel poly(ether ester urethane) multi-block copolymers of which an example is shown in Figure 2b. These phase-separated multi-block copolymers consist of an amorphous, hydrophilic block and a semi-crystalline block [51,52]. These blocks are composed of variable biocompatible and biodegradable monomers, such as DL-lactide, L-lactide, ε-caprolactone and p-dioxanone. The amorphous phase also consists of poly(ethylene glycol) (PEG) blocks that swell when they come in contact with water, which can cause the incorporated antigen to be gradually released by diffusion [51-53]. The development of an acidic microclimate within the formulation is, thus,

prevented, in contrast to PLGA-based formulations. The composition and, thereby, the physicochemical properties of the multi-block copolymers can be varied to a great extent, which allows fine-tuning of the degradation and release kinetics to the specific needs of an antigen. Examples are variation of the type of monomers, the molecular weight, and the amorphous/semi-crystalline block ratio.

Overall, the development of an injectable single-administration vaccine formulation as an alternative to the currently used multiple-injection vaccines would be highly desired. By circumventing the need for booster injections while still achieving optimal protection of the vaccinee, vaccination coverage could be improved and many lives could potentially be saved.

1.2 Outline of this thesis

The overall aim of the research described in this thesis was the development of an injectable single-administration vaccine formulation that exhibits a pulsatile or sustained release profile and could, potentially, be used for the delivery of many different (types of) antigens. To achieve this, several biodegradable formulations containing a model drug or antigen were developed and evaluated, which were all based on different concepts in search of the most optimal single-administration vaccine formulation. One of these concepts was based on core-shell microspheres, so a literature overview of previously developed core-shell microsphere formulations and their characteristics (including release kinetics) is given in **chapter 2**. Also, various methods for the production of core-shell microspheres were described and evaluated in this chapter. In **chapter 3**, the core-shell concept was applied to polymeric compacts containing the small-molecule theophylline as model compound. The core of the formulations contained theophylline and the shell was composed of PDLLA. In addition, monolithic compacts were prepared from physical mixtures of a model compound (theophylline or blue dextran) and a polymer (PDLLA or PLGA) to test their suitability for the delivery of bacterial polysaccharide-based antigens. Both concepts aimed at obtaining a pulsatile release profile, though the core-shell compacts were expected to exhibit a delayed pulsatile release profile and the monolithic compacts a biphasic pulsatile release profile. Therefore, the core-shell compacts only included the booster dose, but we hypothesized that the priming dose could be included by applying an immediately dissolving coating containing the (model) antigen onto the outer surface of the compacts. Several process and formulation parameters were varied to gain insight into the release mechanisms in play. The formulations were prepared by direct compaction using a relatively large die (cylindrical core-shell compacts: ≈ 9 × 5 mm, oblong physically mixed compacts: ≈ 6 × 2 × 2 mm), and were, therefore, only intended as prototypes. Further work focused on the miniaturization of the formulations. To this end, injectable core-shell microspheres were prepared in **chapter 4** using a microfluidic setup. The cores of the microspheres contained the model antigen bovine serum albumin (BSA) and the non-porous shells were composed of PLGA. The work described in this chapter focused on obtaining a delayed pulsatile release profile that could serve as the booster dose in a single-administration vaccine formulation. We hypothesize that a solution of the antigen could be co-injected together with the microspheres, thereby serving as the primer dose. The DL-lactide:glycolide

ratio of PLGA was varied to determine its influence on the lag time. In **chapter 5**, the setup used to produce core-shell microspheres was slightly adjusted by replacing the first microfluidic chip with a flow-through ultrasonic cell in order to prevent channel blockages and improve the production rate. The relationship between the shell thickness of the microspheres and the encapsulation efficiency of BSA was assessed, and methods to reduce the shell thickness were evaluated. **Chapter 6** focused on the development of a single-administration vaccine formulation with a sustained release profile. Monolithic microspheres containing BSA were prepared using a membrane emulsification method. For this chapter, two PEG-based multi-block copolymers were tested and the weight ratio of the polymers was varied to tailor the *in vitro* release duration. Last, one of the microsphere formulations was subcutaneously administered to mice as an *in vivo* proof of concept study, after which the induced BSA-specific IgG antibody responses and the BSA plasma concentrations were measured. **Chapter 7** concludes this thesis with a general discussion of the results obtained in the previous chapters, including directions for further research.

References

[1]   C. Huang et al., "Clinical features of patients infected with 2019 novel coronavirus in Wuhan, China," Lancet, vol. 395, no. 10223, pp. 497–506, Feb. 2020.

[2]   N. Zhu et al., "A Novel Coronavirus from Patients with Pneumonia in China, 2019," N. Engl. J. Med., vol. 382, no. 8, pp. 727–733, Jan. 2020.

[3]   WHO, "COVID-19 - China," 2020. [Online]. Available: https://www.who.int/emergencies/disease-outbreak-news/item/2020-DON233. [Accessed: 14-Dec-2022].

[4]   Y.-C. Wu, C.-S. Chen, and Y.-J. Chan, "The outbreak of COVID-19: An overview," J. Chinese Med. Assoc., vol. 83, no. 3, pp. 217–220, 2020.

[5]   D. Baud, X. Qi, K. Nielsen-Saines, D. Musso, L. Pomar, and G. Favre, "Real estimates of mortality following COVID-19 infection," Lancet Infect. Dis., vol. 20, no. 7, p. 773, Jul. 2020.

[6]   E. Mathieu et al., "Mortality Risk of COVID-19," 2020. [Online]. Available: https://ourworldindata.org/mortality-risk-covid. [Accessed: 14-Dec-2022].

[7]   WHO, "Coronavirus (COVID-19) Dashboard," 2022. [Online]. Available: https://covid19.who.int/. [Accessed: 14-Dec-2022].

[8]   S. Sampath et al., "Pandemics Throughout the History," Cureus, vol. 13, no. 9, pp. e18136–e18136, Sep. 2021.

[9]   D. V Parums, "Editorial: First Full Regulatory Approval of a COVID-19 Vaccine, the BNT162b2 Pfizer-BioNTech Vaccine, and the Real-World Implications for Public Health Policy," Med. Sci. Monit., vol. 27, 2021.

[10]   FDA, "FDA News Release - FDA Approves First COVID-19 Vaccine," 2021. [Online]. Available: https://www.fda.gov/news-events/press-announcements/fda-approves-first-covid-19-vaccine. [Accessed: 14-Dec-2022].

[11]   S. P. Andeweg et al., "Protection of COVID-19 vaccination and previous infection against Omicron BA.1, BA.2 and Delta SARS-CoV-2 infections," Nat.

Commun., vol. 13, no. 1, p. 4738, 2022.

[12] B. de Gier et al., "Vaccine effectiveness against SARS-CoV-2 transmission and infections among household and other close contacts of confirmed cases, the Netherlands, February to May 2021," Eurosurveillance, vol. 26, no. 31, pp. 7–13, 2021.

[13] E. S. Rosenberg et al., "Covid-19 Vaccine Effectiveness in New York State," N. Engl. J. Med., vol. 386, no. 2, pp. 116–127, Dec. 2021.

[14] N. Andrews et al., "Covid-19 Vaccine Effectiveness against the Omicron (B.1.1.529) Variant," N. Engl. J. Med., vol. 386, no. 16, pp. 1532–1546, Mar. 2022.

[15] WHO, "Vaccines and immunization," 2022. [Online]. Available: https://www.who.int/health-topics/vaccines-and-immunization. [Accessed: 14-Dec-2022].

[16] WHO, "Immunization coverage," 2022. [Online]. Available: https://www.who.int/news-room/fact-sheets/detail/immunization-coverage. [Accessed: 14-Dec-2022].

[17] A. N. Chard, M. Gacic-Dobo, M. S. Diallo, S. V Sodha, and A. S. Wallace, "Routine Vaccination Coverage - Worldwide, 2019," MMWR. Morb. Mortal. Wkly. Rep., vol. 69, no. 45, pp. 1706–1710, Nov. 2020.

[18] H. A. Ali et al., "Vaccine equity in low and middle income countries: a systematic review and meta-analysis," Int. J. Equity Health, vol. 21, no. 1, p. 82, 2022.

[19] M. S. Rane, P. Rohani, and M. E. Halloran, "Association of Diphtheria-Tetanus–Acellular Pertussis Vaccine Timeliness and Number of Doses With Age-Specific Pertussis Risk in Infants and Young Children," JAMA Netw. Open, vol. 4, no. 8, pp. e2119118–e2119118, Aug. 2021.

[20] J. J. Rainey, M. Watkins, T. K. Ryman, P. Sandhu, A. Bo, and K. Banerjee, "Reasons related to non-vaccination and under-vaccination of children in low and middle income countries: Findings from a systematic review of the published literature, 1999–2009," Vaccine, vol. 29, no. 46, pp. 8215–8221, 2011.

[21] L. Périères, V. Séror, S. Boyer, C. Sokhna, and P. Peretti-Watel, "Reasons given for non-vaccination and under-vaccination of children and adolescents in sub-Saharan Africa: A systematic review," Hum. Vaccin. Immunother., vol. 18, no. 5, p. e2076524, Nov. 2022.

[22] M. Favin, R. Steinglass, R. Fields, K. Banerjee, and M. Sawhney, "Why children are not vaccinated: a review of the grey literature," Int. Health, vol. 4, no. 4, pp. 229–238, 2012.

[23] S. Y. Michels, "Factors Associated With Failure To Complete Multi-Dose Vaccine Series Among U.s. Children Ages 19–35 Months, National Immunization Survey-Child, 2019," Yale University, 2022.

[24] K. Kardani, A. Bolhassani, and S. Shahbazi, "Prime-boost vaccine strategy against viral infections: Mechanisms and benefits," Vaccine, vol. 34, no. 4, pp. 413–423, 2016.

[25] K. J. McHugh, R. Guarecuco, R. Langer, and A. Jaklenec, "Single-injection vaccines: Progress, challenges, and opportunities," J. Control. Release, vol. 219, pp. 596–609, 2015.

[26] J.-L. Palgen et al., "Optimize Prime/Boost Vaccine Strategies: Trained Immunity

as a New Player in the Game ," Frontiers in Immunology , vol. 12. 2021.

[27]   J. L. Cleland, "Single-administration vaccines: controlled-release technology to mimic repeated immunizations," Trends Biotechnol., vol. 17, no. 1, pp. 25–29, Jan. 1999.

[28]   C. Lemoine et al., "Technological Approaches for Improving Vaccination Compliance and Coverage," Vaccines, vol. 8, no. 2. 2020.

[29]   S. Ray, A. Puente, N. F. Steinmetz, and J. K. Pokorski, "Recent advancements in single dose slow-release devices for prophylactic vaccines," WIREs Nanomedicine and Nanobiotechnology, vol. n/a, no. n/a, p. e1832, Jul. 2022.

[30]   D. W. Dresser and G. Gowland, "Immunological Paralysis Induced in Adult Rabbits by Small Amounts of a Protein Antigen," Nature, vol. 203, no. 4946, pp. 733–736, 1964.

[31]   F. J. Dixon and P. H. Maurer, "Immunologic Unresponsiveness Induced By Protein Antigens," J. Exp. Med., vol. 101, no. 3, pp. 245–257, Mar. 1955.

[32]   N. A. Mitchison, "Induction of immunological paralysis in two zones of dosage," Proc. R. Soc. London B, vol. 161, pp. 275–292, 1964.

[33]   R. Guarecuco et al., "Immunogenicity of pulsatile-release PLGA microspheres for single-injection vaccination," Vaccine, 2017.

[34]   L. Feng et al., "Pharmaceutical and immunological evaluation of a single-dose hepatitis B vaccine using PLGA microspheres," J. Control. Release, vol. 112, no. 1, pp. 35–42, 2006.

[35]   M. Singh, A. Singh, and G. P. Talwar, "Controlled Delivery of Diphtheria Toxoid Using Biodegradable Poly(D,L-Lactide) Microcapsules," Pharm. Res., vol. 8, no. 7, pp. 958–961, 1991.

[36]   W. Li, J. Meng, X. Ma, J. Lin, and X. Lu, "Advanced materials for the delivery of vaccines for infectious diseases," Biosaf. Heal., vol. 4, no. 2, pp. 95–104, 2022.

[37]   G. Du and X. Sun, "Current Advances in Sustained Release Microneedles," Pharm. Front., vol. 2, pp. e11–e22, 2020.

[38]   K. K. Kim and D. W. Pack, "Microspheres for Drug Delivery," BioMEMS Biomed. Nanotechnology, Vol. I - Biol. Biomed. Nanotechnol., pp. 19–50, 2006.

[39]   S. P. Schwendeman, R. B. Shah, B. A. Bailey, and A. S. Schwendeman, "Injectable controlled release depots for large molecules," J. Control. Release, vol. 190, pp. 240–253, Sep. 2014.

[40]   G. Lemperle, "Biocompatibility of Injectable Microspheres," Biomed. J. Sci. & Tech. Res., vol. 2, no. 1, pp. 2296–2306, 2018.

[41]   M. Ye, S. Kim, and K. Park, "Issues in long-term protein delivery using biodegradable microparticles," J. Control. Release, vol. 146, no. 2, pp. 241–260, 2010.

[42]   S. A. Stewart, J. Domínguez-Robles, R. F. Donnelly, and E. Larrañeta, "Implantable Polymeric Drug Delivery Devices: Classification, Manufacture, Materials, and Clinical Applications," Polymers, vol. 10, no. 12. 2018.

[43]   A. Dash and G. Cudworth, "Therapeutic applications of implantable drug delivery systems," J. Pharmacol. Toxicol. Methods, vol. 40, no. 1, pp. 1–12, 1998.

[44]   R. S. van der Kooij et al., "A Single Injection with Sustained-Release Microspheres and a Prime-Boost Injection of Bovine Serum Albumin Elicit the

Same IgG Antibody Response in Mice," Pharmaceutics, vol. 15, no. 2. 2023.

[45]   K. Park et al., "Injectable, long-acting PLGA formulations: Analyzing PLGA and understanding microparticle formation," J. Control. Release, vol. 304, pp. 125–134, 2019.

[46]   H. K. Makadia and S. J. Siegel, "Poly Lactic-co-Glycolic Acid (PLGA) as Biodegradable Controlled Drug Delivery Carrier," Polymers, vol. 3, no. 3. pp. 1377–1397, 2011.

[47]   M. van de Weert, W. E. Hennink, and W. Jiskoot, "Protein Instability in Poly(Lactic-co-Glycolic Acid) Microparticles," Pharm. Res., vol. 17, no. 10, pp. 1159–1167, 2000.

[48]   T. Estey, J. Kang, S. P. Schwendeman, and J. F. Carpenter, "BSA Degradation Under Acidic Conditions: A Model For Protein Instability During Release From PLGA Delivery Systems," J. Pharm. Sci., vol. 95, no. 7, pp. 1626–1639, 2006.

[49]   K. Fu, A. M. Klibanov, and R. Langer, "Protein stability in controlled-release systems," Nat. Biotechnol., vol. 18, no. 1, pp. 24–25, 2000.

[50]   G. Zhu, S. R. Mallery, and S. P. Schwendeman, "Stabilization of proteins encapsulated in injectable poly (lactide- co-glycolide)," Nat. Biotechnol., vol. 18, no. 1, pp. 52–57, 2000.

[51]   N. Teekamp et al., "Polymeric microspheres for the sustained release of a protein-based drug carrier targeting the PDGFβ-receptor in the fibrotic kidney," Int. J. Pharm., vol. 534, no. 1, pp. 229–236, 2017.

[52]   M. Stanković et al., "Low temperature extruded implants based on novel hydrophilic multiblock copolymer for long-term protein delivery," Eur. J. Pharm. Sci., vol. 49, no. 4, pp. 578–587, 2013.

[53]   M. Stanković, J. Tomar, C. Hiemstra, R. Steendam, H. W. Frijlink, and W. L. J. Hinrichs, "Tailored protein release from biodegradable poly(ε-caprolactone-PEG)-b-poly(ε-caprolactone) multiblock-copolymer implants," Eur. J. Pharm. Biopharm., vol. 87, no. 2, pp. 329–337, 2014.

Chapter 2

An overview of the production methods for core-shell microspheres for parenteral controlled drug delivery

Renée S. van der Kooij [1]**, Rob Steendam** [2]**, Henderik W. Frijlink** [1]**, Wouter L.J. Hinrichs** [1]

[1] Department of Pharmaceutical Technology and Biopharmacy, University of Groningen, Antonius Deusinglaan 1, 9713 AV Groningen, The Netherlands
[2] InnoCore Pharmaceuticals, L.J. Zielstraweg 1, 9713 GX Groningen, The Netherlands

Abstract

Core-shell microspheres hold great promise as a drug delivery system because they offer several benefits over monolithic microspheres in terms of release kinetics, for instance a reduced initial burst release, the possibility of delayed (pulsatile) release, and the possibility of dual-drug release. Also, the encapsulation efficiency can significantly be improved. Various methods have proven to be successful in producing these core–shell microspheres, both the conventional bulk emulsion solvent evaporation method and methods in which the microspheres are produced drop by drop. The latter have become increasingly popular because they provide improved control over the particle characteristics. This review assesses various production methods for core–shell microspheres and summarizes the characteristics of formulations prepared by the different methods, with a focus on their release kinetics.

2.1 Introduction

During the last few decades, parenteral controlled release of both small-molecule drugs and biopharmaceuticals, such as peptides and proteins, has gained increasing attention. Controlled release delivery systems offer many advantages over the traditional administration of drugs because the release kinetics can be adjusted to the needs of a particular application [1,2]. The main advantage is the possibility to maintain drug levels within the therapeutic window for an extended duration which lowers the risks of side effects and systemic toxicity and allows for less frequent administrations [2]. This improves patient compliance and reduces discomfort. Furthermore, controlled release delivery systems can protect the drug in the body from most environmental influences which is especially beneficial for biopharmaceuticals that often have poor stability and a short biological half-life [1]. Therefore, the market for these drug delivery systems is growing, specifically the one for polymer-based long-acting injectables, such as microspheres [1,3]. Examples of clinically approved injectable microsphere formulations are Risperdal Consta and Vivitrol but also peptide-loaded microsphere products, such as Sandostatin LAR and Lupron Depot [4]. Most of these products consist of microspheres smaller than 200 μm [3,5,6] and can thus be administered through a rather thin, high-gauge needle of 19 to 23G [3,4]. In comparison, other controlled release delivery systems such as solid implants usually require a larger-diameter needle of e.g. 14G, which might be more painful for the patient [4]. On the other hand, the low loading capacity of specifically monolithic microspheres can sometimes be a limiting factor for their clinical application [7]. Moreover, obtaining the desired particle size, release profile, and stability of the drug remains a challenge, especially for biopharmaceuticals.

So far, most of the research has focused on traditional monolithic microspheres in which the drug is dispersed throughout the whole polymer matrix [8]. These monolithic systems have proven their suitability for sustained release drug delivery [9], but they do have some limitations with regard to the control over the release kinetics. Although methods to reduce the initial burst exist, complete elimination of burst release is often difficult or even impossible to achieve. This can be explained by the fact that drug molecules tend to preferentially accumulate at or near the surface of the microsphere, especially for water-soluble drugs [10]. Yet, for many drug products, the absence of an initial burst release is desired or even crucial as it can lead to unwanted side effects, it reduces the duration of drug release, and it compromises the efficiency of the drug delivery system [11]. Moreover, pulsatile release, zero-order release, and co-encapsulation of multiple drugs with different chemical characteristics and/or release profiles are often hard to achieve. Finally, achieving a high encapsulation efficiency (EE) can be challenging when a monolithic system is used, especially when highly water-soluble drugs with a low molecular weight are encapsulated.

Another subcategory of microspheres, the core-shell microspheres, might offer a solution for these limitations. Core-shell microspheres are compartmentalized particles consisting of a single core or multiple cores surrounded by a polymer shell [12]. Drugs can be loaded either in the inner core or in the shell layer, or in both. There are many potential advantages to the use of core-shell microspheres over monolithic microspheres but the main one is the improved control over the release kinetics of the encapsulated drugs,

as the composition and dimensions of both the core and the shell can independently be tuned. Both the initial burst release and the release duration could, respectively, be reduced and extended even further, thereby enabling sustained release over time [13-16]. This reduced initial burst release is for instance crucial for drugs with a narrow therapeutic index, such as many cytotoxic anticancer drugs [17]. Moreover, choosing the right (polymeric) excipients and fabrication process and settings also allowed for a pulsatile release profile which could be useful for the delivery of for instance vaccines [18,19]. Also, EE could significantly be improved by the addition of a shell layer and sometimes drug loading as well [14,20-23]. Therefore, core-shell microspheres offer great versatility and functionality as a controlled release drug delivery system, and have many potential pharmaceutical applications that could improve therapeutic efficiency, such as the co-delivery of two or more drugs with different functions and properties. These drugs, for instance a hydrophilic and a hydrophobic one, could be encapsulated separately in the core and shell, resulting in sequential or sometimes parallel release of the drugs [24-26]. Yet, despite these many advantages, to our best knowledge, no core-shell microsphere products have reached the market yet.

There are several methods for the production of core-shell microspheres. The choice of the method greatly influences the particle characteristics and thereby the release profile of the drug. Due to rapid advances in the field, the advantages and disadvantages of each system are not always clear. In this review, the different types of core-shell microspheres are discussed and the advantages over monolithic microspheres are assessed. Different conventional bulk emulsion methods and drop-by-drop methods for the production of core-shell microspheres are compared, and the influence of various process and formulation parameters on the particle characteristics, especially the release kinetics, is investigated.

2.2 General features and types of core-shell microspheres

In literature, the definition of what a core-shell microsphere is, varies. Both particles with a single core (mono-nuclear) and particles with multi-cores (poly-nuclear) are described as core-shell microspheres. In this review, both mono-nuclear and poly-nuclear core-shell microspheres are taken into account, as long as there is a distinct shell surrounding the core(s) and the core-shell structure is demonstrated well. Moreover, all particles with a size of approximately 1-1000 µm and a shell thickness of at least a few micrometers are considered as core-shell microspheres. As the focus of this review is on parenterally injectable controlled-release formulations, potential routes of administration are mainly the subcutaneous and the intramuscular route. However, particles with sizes of hundreds of micrometers might give injectability issues due to potential needle blockage, and they require larger needle diameters which can cause a more painful injection [3,4,27]. Core-shell microspheres smaller than 100 µm are therefore preferred as they can be administered using a 21G needle or higher [4].

Although a broad range of particles can be considered as core-shell microspheres, there are some examples in the literature where the description core-shell microsphere is unjustified. This is usually due to only partial engulfment, which means that the cores of the microspheres were not completely surrounded by a shell, or due to incomplete phase

separation. There are also some examples where it is unclear why a core-shell structure was obtained. Furthermore, the core-shell structure is often not convincingly proven. As an example, a scanning electron microscopy (SEM) photo of the cross-section of only one particle is generally inconclusive. There are several methods to confirm the existence of a core-shell structure and a combination of these methods should preferably be used. The most common method is microscopy, including light microscopy, transmission electron microscopy (TEM), and confocal laser scanning microscopy (CLSM) if the drug or another distinct component of the core or shell is fluorescent or fluorescently labeled. SEM is very informative as well but requires cross-sectional cutting of the microspheres which is often fairly difficult. In the case of core-shell microspheres with a solid core, selective dissolution of the core or shell using an organic solvent can give additional information regarding the polymeric distribution (Figure 1) [15,28,29].
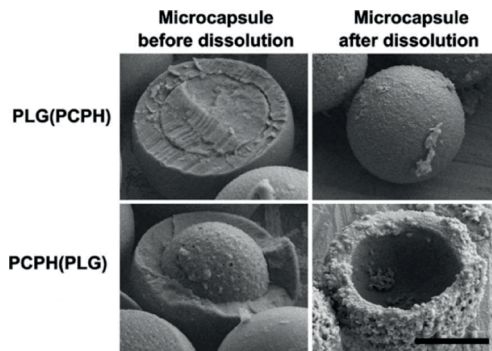
Figure 1. SEM images of PLGA/PCPH microspheres (top row) and PCPH/PLGA microspheres (bottom row). Images illustrate the effect of selectively dissolving the PLGA phase using tetrahydrofuran. Scale bar = 25 μm. Modified from [28] with permission from Elsevier.

Other less frequently used techniques to characterize the particle structure are differential scanning calorimetry (DSC) which indicates whether phase separation completely occurred, X-ray photoelectron spectroscopy (XPS) which can give information about the chemical composition of the particle surface, and attenuated total reflectance Fourier-transform infrared spectroscopy (ATR-FTIR) which can confirm the presence or absence of a certain polymer in the shell layer.

Because our definition of a core-shell microsphere is broad, there are many different types possible. First of all, a wide variety of polymers can be used for the fabrication of the shell, as long as they are biocompatible and biodegradable. In general, the same polymers are employed as for monolithic microspheres. The most frequently used polymers are poly(DL-lactide-*co*-glycolide) (PLGA), poly(DL-lactide) (PDLLA), and poly(L-lactide) (PLLA) because they have been studied extensively and have an easily adjustable degradation time. This degradation time can be adjusted by varying the lactide:glycolide monomer ratio and/or the molecular weight of the polymer [30]. Some alternatives for the shell are glucose-initiated PLGA (Glu-PLGA) [31] which is a branched polymer of PLGA chains attached to a D-glucose core, poly(ε-caprolactone) (PCL) [32,33], the polyester poly(3-hydroxybutyrate-co-3-hydroxyvalerate) (PHBV) [34],

and the polyanhydride poly[(1,6-bis-carboxyphenoxy) hexane] (PCPH) [19,28,35]. Natural polymers can also be used as shell material, for example the water-soluble sodium alginate which forms a gel after addition of calcium ions, and chitosan which is soluble at low pH but solidifies at neutral pH [23,24,36-39]. Secondly, the core contains either a gas or liquid or is composed of a polymer. Gas- or liquid-filled microspheres are also called microcapsules. In the case of liquid-filled core-shell microspheres, the core can be made of an aqueous solution or an oil. Particles with an oil-based core can have the advantage of improved solubility of hydrophobic drugs, which potentially allows an increased drug load [32]. Also, these oil-based microspheres can offer improved physical and chemical stability compared to particles with an aqueous core because many polymer degradation products are not able to reach the drug, which was for instance the case with the protein bovine serum albumin (BSA) [18]. Silicone oil was encapsulated into PLGA-based and PCL-based core-shell microspheres with injectable size, thus offering the potential for parenteral drug delivery [19,32]. Canola oil can be used as well, if needed emulsified with the aqueous drug solution into a W/O emulsion [18]. In this way, both hydrophilic and hydrophobic drugs can be encapsulated into an oily core. In the case of an aqueous core, the water can be removed by lyophilization which turns the liquid-filled microspheres into hollow (i.e. gas-filled) core-shell microspheres loaded with a drug [40]. Gas contents can also directly be encapsulated into core-shell microspheres and these gas-filled microspheres are sometimes called microbubbles, though these microbubbles are mainly used for diagnostics and imaging instead of drug delivery [41]. The last possibility for the core composition of core-shell microspheres is a biodegradable polymer. Just like the shell, PLGA, PDLLA, and PLLA are regularly used as core material but an alternative is poly(ortho ester) (POE) [42,43]. Core-shell microspheres with a solid core and a solid shell are often called double-walled microspheres, in contrast to monolithic microspheres which are sometimes called single-walled microspheres. Finally, drugs can be incorporated into the core, shell, or both, thereby enabling the production of dual-drug release products [24,25,44].

2.3 Methods for the production of core-shell microspheres

Several methods can be employed for the production of core-shell microspheres, and the type of method, as well as the process and formulation parameters, determine the formulation's physico-chemical characteristics and performance. Conventional emulsion solvent evaporation is the standard method for the bulk fabrication of microspheres and is often combined with phase separation to obtain microspheres with a core-shell structure. This method, however, involves high shear stresses and often generates particles with a broad size distribution and low EE, although modified methods have been developed that generate microspheres with improved characteristics [15,45]. Therefore, other production methods, such as microfluidics, electrospraying or coaxial electrohydrodynamic atomization (CEHDA), and precision particle fabrication (PPF) technology are becoming more widely used, because of their capability of generating highly monodisperse particles with high EEs (Table 1). These methods can make use of emulsification processes as well but in contrast to the conventional emulsion solvent evaporation method, the microspheres are produced drop by drop instead of in bulk.

Table 1. Overview of most common production methods for core-shell microspheres and the process characteristics.

Production method	Subcategories	Applied polymers	Particle size	Dispersity	EE	Advantages	Disadvantages
Conventional bulk emulsion solvent evaporation (combined with phase separation)	W/O/O/W W/O/W S/O/O/W O/O/W O/W Acetone-W/O S/Acetone-W/O	PLGA Glu-PLGA PDLLA PLLA Chitosan Alginate POE PDME PHBV	1-880 µm	Usually polydisperse (COV = 5-75%)	Variable (15-100%)	Simplicity of setup Variability of materials Broad particle size range possible	High shear stress Presence of aqueous-organic interface Difficult to scale-up Low monodispersity
Microfluidics (combined with phase separation)	W/O/W O/W/O O/W	PLGA PLLA PCL Alginate	45-350 µm	Monodisperse (COV < 10%)	Usually not measured, claimed to be high	Small volumes needed Little waste High monodispersity High EE	Low production speed Difficult to scale-up Narrow working window, low flexibility Risk of channel contamination/blockage
Electrospraying/ CEHDA	Dual-capillary Tri-capillary Coaxial Emulsion Electrodropping Electrospinning	PLGA PDLLA PLLA PCL Chitosan Alginate PCL-PPE-EA	0.2-65 µm	Variable (COV = 5-40%)	Usually high (65-100%, shell materials: 40-85%)	Simplicity of setup Single-step, continuous process Cost-effectiveness Variability of materials High EE	Limited particle size range Low throughput Stable cone-jet mode required
PPF	-	PLGA PDLLA PLLA PCPH	40-115 µm	Monodisperse (COV < 10%)	Variable (5-100%)	Continuous process High reproducibility High production speed High monodispersity	Complexity

2

This results in increased monodispersity of the particles. There are more methods that enable the production of core-shell microspheres, such as polymerization methods and self-assembly [46], but because the focus of this review is on widely used and commercially available polymers, these methods are not addressed here. The characteristics of the different methods can be found in Table 1.

2.3.1 Conventional bulk emulsion methods

Conventional bulk emulsion solvent evaporation is the most frequently used method for the production of polymeric microspheres as it is a very straightforward method, and a wide range of particle sizes can be produced from approximately 1 to 1000 μm (Table 1, Table 2). Moreover, various types of drugs can be incorporated, such as hydrophilic or hydrophobic drugs, small molecules or proteins and peptides, and a single drug or multiple drugs. This production method usually leads to the formation of monolithic microspheres but with some modifications, for instance the combination with phase separation, core-shell microspheres can be produced as well. In this process, a double emulsion (i.e. water-in-oil-in-water, W/O/W; solid-in-oil-in-water, S/O/W; oil-in-oil-in-water, O/O/W) or triple emulsion (i.e. water-in-oil-in-oil-in-water, W/O/O/W; solid-in-oil-in-oil-in-water, S/O/O/W) containing two polymers is employed. Upon solvent removal, the polymers separate into different phases to achieve the most thermodynamically stable configuration in the concentrating polymer solution(s) [47,48]. Subsequently, the combination with phase separation always leads to the formation of core-shell microspheres with a solid polymeric core. The polymers are usually dissolved in separate solutions and subsequently added together after which they phase separate. In this case, a W/O/O/W [29,31], S/O/O/W [49,50], or O/O/W [15] emulsification method is employed. Phase separation, however, can also occur when the polymers are dissolved together in one solvent, for instance with a W/O/W [42,43] or S/O/W emulsification process. This means that for double emulsions, the drug can be incorporated into an organic polymer solution as: (i) an aqueous solution (water-in-oil, W/O), (ii) a solution of the drug and another polymer in an organic solvent (oil-in-oil, O/O), or (iii) solid particles (solid-in-oil, S/O). This is the primary dispersion step. The secondary dispersion step is the emulsification of the primary dispersion, called the dispersed phase, with the external aqueous phase, called the continuous phase. After emulsification, the microspheres solidify due to the extraction of the organic solvent by the continuous phase, accompanied by solvent evaporation. In the final step, the particles are collected by centrifugation or filtration, washed, and subsequently lyophilized or bulk (vacuum) dried to remove residual solvent [51]. A schematic representation of the conventional W/O/W emulsion solvent evaporation method combined with phase separation to obtain core-shell microspheres is shown in Figure 2. For triple emulsions, an extra dispersion step is needed as a primary emulsion (for W/O/O/W) or a solid dispersion (for S/O/O/W) is generated, and subsequently emulsified with another polymer solution. A hydrophobic drug can be dissolved in one or both of the polymer phases, and then preferentially localizes within one polymer over the other, ultimately yielding an oil-in-water (O/W) or O/O/W emulsion. If the drug is hydrophilic, an aqueous solution of the drug is prepared and emulsified with either one or both polymer phases, thus yielding a W/O/W or W/O/O/W emulsion. The polymer phase that differs the least from the drug in terms of solubility parameters will contain the highest

Table 2. Representative polymeric core-shell microspheres produced via conventional bulk emulsion solvent evaporation. Presented polymer molecular weights and viscosities are the weight averaged molecular weights and the inherent viscosities, respectively, unless stated otherwise.

Ref.	Production method	Materials	Release profile	Particle size and dispersity	EE	In vivo or ex vivo data?	Comments
[31]	W/O/O/W emulsion solvent evaporation	Core: lysozyme + PLGA (50:50, intrinsic viscosity = 0.4 dL/g), shell: Glu-PLGA (50:50, M_n = 15/50 kDa)	Burst = 5-15%, slow release up to at least 70 days	2-8 μm, COV = 13-35%	71-84%	No	
[29]	W/O/O/W emulsion solvent evaporation	Core: BSA + PLGA (50:50, 0.55-0.75 dL/g), shell: PLLA (40-70 kDa)	Short solvent evaporation: 15-22% burst, a lag phase up to day 4-26, and sustained or fast release up to day 45 or almost no further release; long solvent evaporation: ≤ 15% burst, a lag phase up to day 18-30, and sustained release up to day 58	Short solvent evaporation: 33-73 μm, COV = 24-53%; long solvent evaporation: 62-80 μm, COV = 40-64%	No data	No	
[45]	W/O/O/W emulsion solvent evaporation	Core: BSA + Glu-PLGA (50:50, M_n = 15/50 kDa), shell: PLGA (50:50, intrinsic viscosity = 0.4 dL/g)	Burst = 9-16%, a lag phase up to day 8-23, and sustained release up to (at least) 90 days	4-8 μm, COV = 6-21%	95-100%	No	
[16]	W/O/O/W emulsion solvent evaporation	Core: insulin + Glu-PLGA (50:50, M_n = 15 kDa), shell: PLGA (50:50, intrinsic viscosity = 0.4 dL/g)	Burst = 13-19%, a lag phase up to day 3-14, and sustained release up to (at least) 42 days	3-9 μm, COV = 13-23%	67-78%	No	
[14]	W/O/O/W and S/O/O/W emulsion solvent evaporation	Core: meglumine antimoniate + PLGA (50:50, 48-78 kDa), shell: PLGA (75:25, 48-78 kDa)	Burst = 17-22%, sustained release up to day 30	S/O/O/W: 31 μm, COV = 42%; W/O/O/W: 52 μm, COV = 46%	S/O/O/W: 87%, W/O/O/W: 81%	No	
[13]	W/O/O/W emulsion solvent evaporation	Core: 5-FU/BSA + PLGA (50:50, 15 kDa/53:47, 137 kDa/75:25, 118 kDa), shell: PLGA (80:20, 201 kDa)/PLLA	5-FU: burst = 4-20%, a lag phase up to day 9-19, and sustained release up to 48-70 days	515 μm and 775 μm, COV = 20% and 25%	5-FU: 81-87%	No	
[110]	W/O/W and S/O/W emulsion solvent evaporation	Core: losartan potassium, shell: PLGA (75:25, 20 kDa)	Sustained release up to 18-30 days or biphasic release up to 26-30 days (i.e. slow release up to day 10-14, followed by fast release)	19-31 μm, COV = 27-52%	EE = 57-79%	Yes, in vivo pharmacodynamics study	Microspheres with a gelatine or Pluronic® F-127 core were also produced
[39]	W/O/W emulsion solvent evaporation	Core: BSA/bFGF + PLGA (75:25, 40-75 kDa), shell: CHA + glycol chitosan (28 kDa)	BSA and CHA: sustained release up to day 18, CHA faster release rate than BSA	6 μm, COV = 14-21%	BSA: 75-76%	Yes, antibacterial and cell proliferation assay	
[34]	W/O/W emulsion solvent evaporation	Core: BSA (+ HGF) + PLGA (50:50, 62 kDa), shell: PHBV (576 kDa)	BSA: burst = 18%, fast release up to day 7, hardly any release up to day 30, and fast release up to day 70	185 μm, COV = 12%	BSA: 91-92%, HGF: 89%	Yes, bioactivity assays of released proteins on cell lines and cell proliferation study with hepatocytes	Shell contained PLGA as well due to incomplete phase separation
[42]	W/O/W emulsion solvent evaporation	Core: CyA + POE (24 kDa), shell: BSA + PLGA (50:50, 43 kDa)	CyA: sustained release up to day 30 or 42, BSA: nearly complete release within 5 days	51-60 μm, COV = 24-41%	BSA: 60-61%, CyA = 79-83%	No	Shell contained POE as well due to incomplete phase separation
[43]	W/O/W emulsion solvent evaporation	Core: POE (24 kDa), shell: PLGA (50:50, 43 kDa)	No data	~100 μm	No data	No	
[49]	S/O/O/W emulsion solvent evaporation	Core: dexamethasone + PLGA (75:25), shell: PLLA	Lag phase up to day 70, sustained release up to at least 264 days	250 μm, COV = 3%	43%	Yes, histological and image analysis of adipose tissue	

Table 2. *Continued*

Ref.	Production method	Materials	Release profile	Particle size and dispersity	EE	In vivo or ex vivo data?	Comments
[103]	S/O/O/W emulsion solvent evaporation	Core: BT + PLGA (50:50, 7/13/22/24 kDa), shell: PLLA (100 kDa)	Biphasic (slow release followed by faster release) or sustained release up to (at least) 40 days	100-600 μm	No data	Yes, preparation and implantation of carrier system for microspheres and in vivo release study	
[50]	S/O/O/W emulsion solvent evaporation	Core: bupivacaine/chlorophenol red + PLGA (50:50, 7/24/33 kDa), shell: PLLA (100 kDa)	Bupivacaine: 7 kDa: fast release up to day 18; 24 kDa: fast release up to day 17, slow release up to day 33; 33 kDa: < 10% release up to day 15, fast release up to day 33	~150-200 μm	No data	Yes, implantation of microspheres into goat joint and collection of blood and synovial fluid samples + histological staining	
[54]	S/O/O/W emulsion solvent evaporation	Core: lysozyme + PLGA (50:50, 40-75 kDa), shell: PLLA (0.9-1.2 dL/g)	Small burst, slow release up to day 36, and faster release up to day 140	81 μm, COV = 42%	No data	No	
[55]	S/O/O/W emulsion solvent evaporation	Core: etanidazole + PLGA (50:50, 40-75 kDa), shell: PLLA (85-160 kDa)	Burst < 5%, a lag phase up to day 27, and linear sustained release up to day 50	422 and 432 μm, COV = 41%	55-57%	No	
[15]	O/O/W emulsion solvent evaporation	Core: aspirin + PLLA (39 kDa), shell: PLGA (50:50, 30 kDa)	Burst = 2-3%, a lag phase of 3 days, and sustained release up to day 23-31	154-179 μm, COV = 0.3-1.5%	74-81%	No	
[52]	O/O/W emulsion solvent evaporation	Core: dox + PLGA (50:50, 40-75 kDa), shell: PLLA (85-160 kDa) and the inverse	PLGA:PLLA (1:1): burst = 4%, a lag phase of 32 days, and a linear sustained release up to day 73; PLGA:PLLA (2:1 and 3:1): burst = 1 and 13%, sustained release up to day 45	167-172 μm, COV = 62-73%	60-87%	No	
[22]	O/W emulsion solvent evaporation	Core: aripiprazole, shell: PDLLA (95 kDa)	Slow release up to at least 49 days	Without homogenization: 206 μm, with homogenization: 65 μm	91-100%	Yes, in vivo release study after subcutaneous injection in rabbits	
[36]	O/W emulsion solvent evaporation	Core: paracetamol + PLGA (75:25, 10 kDa), shell: HSA + alginate	Paracetamol: lag phase up to 15 hours, near zero-order release up to 3 days, and slower near zero-order release up to at least 12 days; HSA: complete release within 3 days	9-13 μm, COV = 11-36%	HSA: 17-62%, paracetamol: 68-90%	No	
[67]	O/W emulsion solvent evaporation	Core: ABT627, shell: PLGA (50:50)	Burst = 14%, slow release up to day 13, fast release up to day 21, and slow release up to day 25	18 μm, COV ~7%	~45%	No	ABT627: hydrophobic model drug
[56]	Acetone-W/O emulsion solvent evaporation	Core: risedronate, shell: PLGA (50:50, 7-17 kDa)	Sustained release up to 6 hours	1 μm, COV = 35%	32%	No	
[57]	S/Acetone-W/O emulsion solvent evaporation	Core: theophylline, shell: PDME	Sustained or zero-order release up to (at least) 8 hours	630-878 μm	No data	No	

Abbreviations: 5-FU, 5-fluorouracil; bFGF, basic fibroblast growth factor; BT, brimonidine tartrate; CHA, chlorhexidine acetate; CyA, cyclosporin A; dox, doxorubicin; HGF, hepatocyte growth factor; HSA, human serum albumin; M_n, number averaged molecular weight
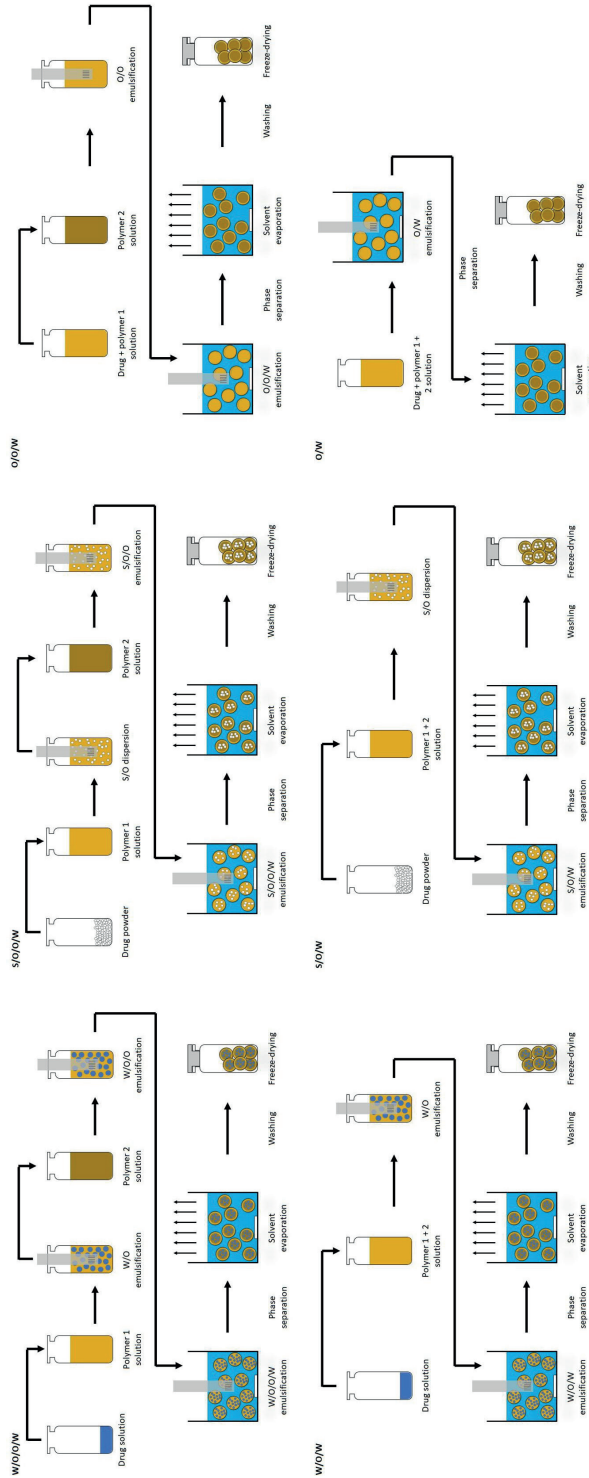
Figure 2. Schematic illustration of the conventional bulk W/O/W emulsion solvent evaporation method combined with phase separation for the production of polymeric core-shell microspheres.

drug concentration [52]. The phenomenon of phase separation can be attributed to differences in hydrophilicity and crystallinity, for instance when PLGA and PLLA are used, or incompatibility of the two polymers which is reflected in for example differences in solubility. The three possible configurations that can be obtained through phase separation are complete engulfment, partial engulfment, and no engulfment (Figure 3).
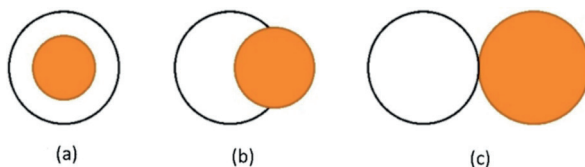

Figure 3. The three possible configurations that can be achieved through phase separation in a two-polymer system: complete engulfing (a), partial engulfing (b), and non-engulfing (c). Reproduced from [68] with permission from MDPI.

With a correct choice of the evaporation rate and the interfacial tensions between the liquid phases, complete engulfment of one polymer by the other can be achieved and thus a core-shell structure [47,53]. When the solvent evaporates too fast, complete phase separation may not occur, thereby causing only partial engulfment as shown by Zhu et al. for PLGA/PHBV composite microspheres [34]. In the case of PLGA and PLLA in equal amounts, PLGA usually forms the core and PLLA the shell [29,54,55] according to the spreading coefficient theory which is based on the surface tension of both polymer phases and the interfacial tension between the phases [47,53]. However, with increasing PLGA:PLLA mass ratio, core-shell inversion takes place as the polymer phase with the higher mass often forms the engulfing phase.

Core-shell microspheres with a non-polymeric core can be produced using conventional emulsion solvent evaporation as well, although this is less common. A few examples exist where an O/W or acetone-W/O emulsification method combined with phase separation was employed for this purpose. Production of aripiprazole-loaded core-shell microspheres with a high drug loading of up to 80% was achieved with a conventional O/W emulsion solvent evaporation method [22]. High molecular weight PDLLA and aripiprazole were dissolved in DCM, i.e. the dispersed oil phase, and the obtained solution was added drop-by-drop to an external water phase cooled to 10°C. After addition of the oil phase, the temperature of the water phase was gradually increased to 20°C, which resulted in precipitation of aripiprazole in the core and eventually evaporation of the organic solvent. This caused the polymer to slowly precipitate on the outer surface of the core resulting in microspheres with a core-shell structure. Abulateefeh and Alkilany prepared aqueous core-PLGA shell microspheres with an acetone-W/O emulsification method combined with internal phase separation [56]. An aqueous risedronate solution was added to a solution of the polymer in acetone, after which the internal acetone-water phase was emulsified with the external oil phase. Subsequently, the evaporation of acetone caused the solubility of PLGA to decrease and a part of the polymer to migrate to the surface of the droplets where it precipitated. This phase separation resulted in the formation of a poly-nuclear core-shell structure with large aqueous cores embedded in the polymeric matrix. Core-shell microspheres containing theophylline

could be produced with a similar emulsion solvent evaporation method [57]. The hydrophobic dextran derivative PDME was used as polymer. After dissolving the polymer in an acetone-water mixture, the drug was suspended in the solution and the resulting suspension was emulsified with liquid paraffin to obtain an S/acetone-W/O emulsion. At a sufficiently low acetone/water ratio, a core-shell structure was obtained as the polymer rapidly deposited on the surface of the droplets.

As already mentioned above, the conventional bulk emulsion solvent evaporation process does have some disadvantages, such as broad particle size distribution and exposure of the drug to organic solvents and high shear stresses due to high-speed homogenization. This creates hazards for the integrity of sensitive biopharmaceuticals [27,58]. Besides, the solvent evaporation rate is difficult to control, which often results in variability in particle characteristics such as size, internal structure, and EE, both within a batch and between different batches [15,59]. Another disadvantage is the difficulty of obtaining a high EE, especially with moderately or highly hydrophilic drugs with a low molecular weight [56]. There are many parameters that affect the EE, such as particle structure, stirring speed, lipophilicity of the drugs, drug loading, and polymer concentration [51,60]. In general, for all production methods that involve emulsification, the EE can be improved by decreasing the solubility of the drug in the continuous phase or by increasing the solidification rate of the microspheres but other methods are also possible [61,62]. For the conventional bulk emulsion solvent evaporation method in specific, reduction of the stirring speed during emulsification will result in lower shear forces by which a larger portion of the drug molecules will stay in the particles [63]. This might also improve the stability of drugs that are sensitive to shear stress, such as therapeutic proteins. On the other hand, a reduced stirring speed might also result in a lower solidification rate of the microspheres, and thus in a lower EE [61]. In some exceptional cases, EEs as high as 90-100% could be reached, as seen with the aripiprazole-loaded microspheres [22]. An EE of 95-100%, depending on the formulation settings, was also obtained for double-walled microspheres with a Glu-PLGA core and a PLGA shell prepared by conventional W/O/O/W emulsion solvent evaporation combined with phase separation [45]. Single-walled microspheres consisting of PLGA and Glu-PLGA were prepared as a comparison, and these particles had an EE of only 60-70%. Similar findings were obtained for PLGA-based double-walled microspheres with the hydrophilic small-molecule drug meglumine antimoniate loaded in the inner core [14]. This difference in EE between double-walled and single-walled microspheres can be attributed to the outer shell layer that acts as a barrier to the diffusion of the hydrophilic drug into the external aqueous environment during solidification of the microspheres. This also explains why core-shell microspheres generally have a higher EE than monolithic microspheres. A high EE is especially advantageous when expensive or scarcely available drugs are incorporated and a high EE can be helpful when a high drug loading is desired [22]. Higher loading may also be realized by making use of core materials that enable increased solubility of the drug. Especially for hydrophilic drugs, the target loading can significantly be increased by incorporating them into an aqueous core. When utilizing monolithic microspheres for controlled release, the maximum drug loading is usually about 30% [22]. Loadings above this value will cause the drug to also exist on the surface of the microspheres, thereby disabling slow release. Increased EE and possibly

drug loading are thus a great advantage of core-shell microspheres in comparison with monolithic microspheres. The last drawback of the conventional bulk emulsion solvent evaporation method is that industrial scale-up while preserving the particle properties is often difficult and costly. This difficulty arises from the fact that the production method involves batch operation and that it requires removal of the organic solvent, though this is a problem for all production methods that involve emulsification processes [59,64]. An organic solvent is usually needed to dissolve the polymers, but most organic solvents are toxic. Solvent removal, therefore, is a key step in the production process. The most commonly used solvent is dichloromethane as it is highly volatile and poorly soluble in water. Due to its toxicity, the residual solvent level in the final microspheres must be reduced to a minimum. Solvent removal can be promoted by stirring and using elevated temperatures for the continuous phase, though residual levels may still be present after drying [65]. Therefore, alternative solvents that are less toxic could be used, such as dimethyl carbonate [66] and ethyl acetate [15,25], though their physical properties are inferior to those of dichloromethane. For example, they are less volatile and thus harder to remove, and they are a poorer solvent for some polymers such as PLGA [65]. Mao et al. produced core-shell microspheres with an O/W emulsion solvent evaporation method using DCM, and determined the glass transition temperature of the polymer and the blank microspheres with DSC, but no significant difference was found [67]. As DCM acts as a plasticizer, this indicated that the residual solvent level was very low.

2.3.2 Drop-by-drop methods – Microfluidics

Another approach for the production of core-shell microspheres is the application of microfluidics, which offers precise control over the size of the microspheres by making use of shear forces to create new interfaces between immiscible fluids [69,70]. A schematic illustration of an example of a microfluidic device for the production of core-shell microspheres is shown in Figure 4.
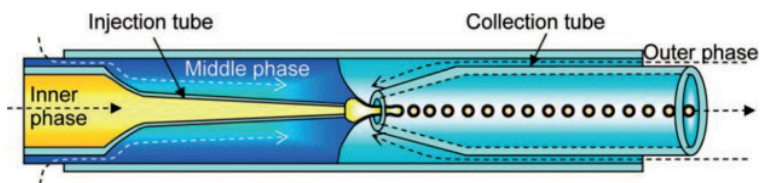
Figure 4. Schematic illustration of the generation of a double emulsion in a microfluidic device for the production of core-shell microspheres. Reprinted with permission from [83]. Copyright 2021 American Chemical Society.

Droplet microfluidics, a subcategory of microfluidics, is also an emulsification method but in contrast to the conventional bulk emulsion solvent evaporation method, the emulsion is produced drop by drop and in a continuous fashion [70]. This usually results in highly monodisperse particles with a high EE after extraction and evaporation of the organic solvent. The droplets are produced by injecting two immiscible liquid phases (an oil and a water phase) via separate inlets into the microchannels of a microfluidic device. Monodisperse W/O or O/W droplets are then generated in a highly repeatable manner at the junction where the streams meet due to the shear stresses, although these stresses

are substantially lower than with the conventional bulk emulsion solvent evaporation method. By making use of a third immiscible liquid phase that is injected via another inlet, the droplets are re-emulsified into this phase and a double emulsion is obtained [71]. W/O/W or oil-in-water-in-oil (O/W/O) double emulsions usually form the basis for the production of core-shell microspheres. In addition, microfluidics enables the formation of higher-order emulsions, such as triple (W/O/O/W, S/O/O/W) [72] or even quadruple emulsions, although extra channels are then required. The number and size of the inner droplets can be precisely controlled [70,71]. Moreover, microfluidics can be used for the incorporation of all kinds of molecules, such as hydrophilic and hydrophobic molecules, small molecules and macromolecules but the incorporation of two or more different types of drugs is also possible [73]. Hydrophilic drugs or dyes for visualization of the internal structure are often encapsulated into the core of core-shell microspheres by producing a W/O/W emulsion. When a hydrophobic drug is to be incorporated in the core, an O/W/O emulsification method is usually preferred. The hydrophobic core is then composed of polymer solution or oil and the hydrophilic shell is composed of e.g. alginate. In that particular case, an extra liquid phase consisting of calcium chloride solution is required to cross-link the alginate. In a study by Wu et al., the hydrophobic model drug rifampicin was encapsulated into PLGA-alginate core-shell microspheres in order to control its release [23]. Drug loading and EE could also be increased by applying the alginate shell around the PLGA core. Table 3 summarizes the representative core-shell microspheres that were produced using microfluidics.

Not only the conventional bulk emulsion solvent evaporation method can be combined with phase separation but the microfluidic method as well. Li et al. prepared core-shell microspheres from a single O/W emulsion using microfluidics [66]. The oil phase consisted of both PLGA and PCL in an organic solvent. By choosing the right solvent, the polymers underwent phase separation when the O/W emulsion droplets were collected in polyvinyl alcohol (PVA) solution, resulting in core-shell microspheres with a PLGA shell and a PCL core which also contained tiny PLGA beads. This was caused by an increase in polymer concentration upon extraction of the organic solvent, causing an inversion of both polymers. Acetone treatment and ATR-FTIR demonstrated the localization of PLGA and PCL in the shell and the core, respectively. Rhodamine B was added as a hydrophilic fluorescent dye that selectively distributes in the more hydrophilic PLGA which enabled the confirmation of the core-shell structure by CLSM. A similar study was carried out by Kim et al., in which the particle morphology could be controlled by varying the blend ratio of both polymers [33]. Complete phase separation could be induced by choosing the right blend ratio and by employing slow solvent evaporation. Furthermore, liquid-filled microspheres could be prepared using microfluidics combined with phase separation by adding dodecane to the organic polymer solution and subsequently generating an O/W emulsion [74]. Dodecane is a hydrophobic non-volatile non-solvent for PLLA, the polymer used in this study. PLLA precipitated at the droplet interface upon evaporation of the organic solvent, causing phase separation between the polymer and the non-solvent. Eventually, microspheres with a dodecane-filled core containing the hydrophobic dye Oil-Red-O were formed. The dodecane core could be removed by lyophilization, resulting in hollow microspheres with the dye in the core.

Table 3. Representative polymeric core-shell microspheres produced via microfluidics. Presented polymer molecular weights and viscosities are the weight averaged molecular weights and the inherent viscosities, respectively, unless stated otherwise.

Ref.	Production method	Materials	Release profile	Particle size and dispersity	EE	In vivo or ex vivo data?	Comments
[111]	Microfluidics (W/O/W)	Core: DOX-ADA + indocyanine green, shell: PLGA (50:50, 7-17 kDa)	Doxorubicin: sustained release up to 20 days	~100 μm, COV = 2%	Doxorubicin: 47%, indocyanine green: 63%	No	
[112]	Microfluidics (W/O/W)	Shell: PDLLA (89 kDa)	No data	~250 μm, monodisperse	No data	No	Microspheres with a Eudragit® S 100 core were also produced
[76]	Microfluidics (W/O/W)	Shell: PLGA (50:50, intrinsic viscosity = 0.41 dL/g / 65:35, intrinsic viscosity = 0.55-0.75 dL/g / 85:15, intrinsic viscosity = 0.66 dL/g)	No data	75-290 μm, monodisperse	No data	No	Salts (NaCl and Na_2CO_3) were added to inner water phase for osmotic annealing
[40]	Microfluidics (W/O/W)	Shell: PLGA (75:25, 66-107 kDa)	No data	Droplets: 446-921 μm, COV = 2%	No data	No	
[75]	Microfluidics (W/O/W and O/W/O)	Core: alginate, shell: PLGA (50:50, 7-17 kDa) (W/O/W) and the inverse (O/W/O)	No data	O/W/O: 69 μm, monodisperse	No data	No	
[23]	Microfluidics (O/W/O)	Core: rifampicin + PLGA (50:50, 7-17 kDa), shell: alginate	Hardly any release up to day 10, near zero-order release up to day 31	Core: 15-55 μm, whole particle: no data; COV = 8%	70%	Yes, viability studies on cell lines to confirm the biocompatibility of the microspheres	
[37]	Microfluidics (O/W/O)	Shell: alginate	No data	256 and 337 μm, COV < 2%	No data	No	
[66]	Microfluidics (O/W)	Core: PCL (130 kDa), shell: PLGA (50:50, 30 kDa)	No data	47 μm, COV = 3%	No data	No	Core contained PLGA as well due to incomplete phase separation
[33]	Microfluidics (O/W)	Core: PCL (43 kDa), shell: PLGA (65:35, 0.55-0.75 dL/g) and the inverse	No data	187-218 μm, COV = 1-4%	No data	No	
[74]	Microfluidics (O/W)	Core: Oil-Red-O, shell: PLLA (42 kDa)	Fast release up to 60 min, slow release up to 220 min	50 μm, COV = 16%	No data	No	Shell might have contained some Oil-Red-O as well

Abbreviations: DOX-ADA, doxorubicin-conjugated alginate dialdehyde

Several factors influence the size and size distribution of the inner and outer droplets, such as the geometry of the device, channel diameter, concentrations and flow rates of the different fluid phases, and ratio of the flow rates. However, when using a microfluidic junction, the geometry of the device and the channel diameter are often fixed and thus difficult to vary. Therefore, the flow rates of the different fluid phases are the most important factor in controlling the droplet characteristics but the ratio of the different flow rates influences the particle and core size as well. Ren et al. made use of this dependency to tune the dimensions of an O/W/O double emulsion. Soybean oil solution was used as the inner phase, an aqueous alginate solution as the middle phase, and another oil solution as the outer phase [37]. In the last emulsification capillary, a calcium chloride aqueous solution was injected. Due to the density difference between the O/W/O emulsion droplets and the outer oil solution, the droplets sunk to the bottom of the emulsification capillary where the aqueous alginate layer in the droplets came into contact with the calcium chloride solution, thereby allowing the alginate to gel. By increasing the ratio between the inner phase flow rate and the middle phase flow rate, the inner oil droplet size increased linearly. The outer microsphere diameter could also be varied. When the sum of the inner phase flow rate and the middle phase flow rate increased with respect to the outer phase flow rate, the outer microsphere diameter increased. Highly monodisperse particles were obtained, with coefficient of variation (COV) values of < 2% for both the core and the whole particle (Figure 5).
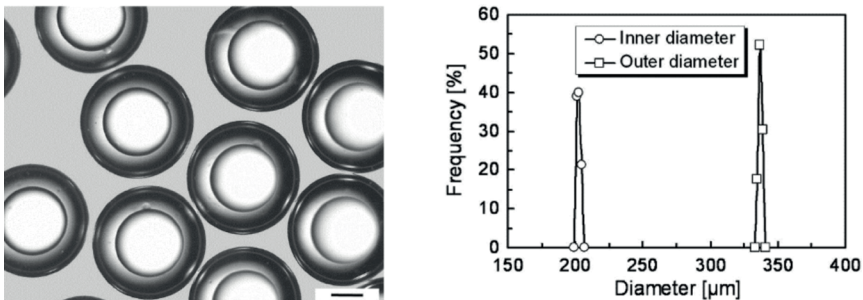
Figure 5. Optical light micrograph (left) and the size distribution (right) of highly monodisperse O/W/O core-shell microspheres with an alginate shell and soybean oil solution in the core. Scale bar = 100 μm. Modified from [37] with permission from Elsevier.

Inner and outer droplet size could also be tuned by osmotic annealing [75,76]. By varying the solute concentration ratio between the inner phase and outer phase, the inner droplet volume could be altered by more than three orders of magnitude due to the osmotic pressure difference of the inner and outer phase [76]. This osmotic annealing method circumvents the need for the fabrication of a new microfluidic device with different channel dimensions.

Microfluidic fabrication of microspheres also has some drawbacks, one of which is the need for pulseless flow and high responsiveness of the system [77]. Syringe pumps are the most frequently used devices for controlling the flow within the system, but even the most advanced pumps have some fluctuations in flow over time, which results in a broader particle size distribution. Furthermore, the pumps often have low responsiveness,

which means that it takes some time for the flow to stabilize after adjustment of the flow rate. By making use of pressure-controlled pumps, these fluctuations in flow can be minimized and response times can be decreased [78]. A second drawback is the low throughput and the difficulty of scale-up. With a single microfluidic junction, microspheres can usually be produced at a throughput of approximately 50–300 mg/h [79], depending on the viscosity of the dispersed phase and the channel diameter. Higher throughput can be achieved by increasing the polymer concentration in combination with a decreased molecular weight of the polymer or by using a larger channel diameter. However, to achieve a significant scale-up, parallelization of microfluidic devices that operate with a minimum number of pumps is needed [73,79]. Romanowsky et al. achieved a production rate of 1 kg/day of a water/octanol/water double emulsion by using a three-dimensional array of fifteen droplet-making units in parallel [80]. Additionally, large-scale production of solid lipid nanoparticles by microfluidic mixing has proven to be possible, which can for instance be used for the mRNA-based COVID-19 vaccines [81,82]. Although these vaccines do not concern core-shell particles, it does showcase the potential of microfluidics for industrial scale-up. The last shortcoming is the limited range of suitable flow rates that can be used and droplet sizes that can be generated.

2.3.3 Drop-by-drop methods – Electrospraying
Coaxial electrospraying, also called CEHDA, is a single-step continuous method for the production of core-shell microspheres. Two or three liquids are separately injected via coaxial capillaries into a nozzle or spray head, called dual-capillary and tri-capillary electrospraying, respectively. An electric field is applied to the nozzle tip and at a certain voltage, the solution interface at the tip changes shape, forming a Taylor cone jet. When the critical voltage is reached, the surface tension of the drop is overcome which causes the drop to break up into very fine highly charged droplets. These charged droplets are accelerated towards the grounded collector during which the solvent is evaporated, thereby resulting in solidified particles [84,85]. Because of this rapid drying, immiscibility of the injected solutions is not necessary for a core-shell structure. The particles are usually collected on aluminum foil but they can also be collected in ethanol, water, or another aqueous solution, although the process then demands an additional washing and/or drying step. Because a coaxial nozzle is used, the core fluid is surrounded by an annular fluid which enables the production of core-shell particles. A schematic representation of this production method is shown in Figure 6. Table 4 provides an overview of representative core-shell microspheres produced with this method.

The terms electrospraying and electrospinning are sometimes used interchangeably but in general, electrospraying refers to the production of microspheres while electrospinning refers to the production of fibers [86,87]. Both are electro-hydrodynamic techniques that use a similar setup but the methods differ in terms of applied voltage and the properties of the polymer solution, such as the molecular weight and concentration of the polymer and the solvent properties [86]. Low viscosity solutions usually cause electrospraying as stream breakup is more likely to occur, in contrast to high viscosity solutions that will rather cause electrospinning. Hiep et al. produced core-shell microspheres composed of a PLGA core and a chitosan shell with electrospinning to determine the influence of the polymer concentration and the applied voltage on the particle
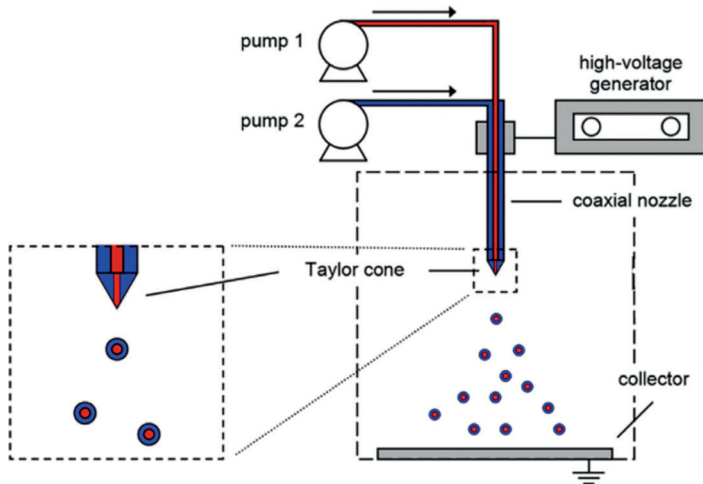
Figure 6. CEHDA setup for the production of core-shell microspheres. The inner liquid is delivered using pump 1, the outer liquid is delivered using pump 2. Modified from [85] with permission from Elsevier.

morphology [38]. Increasing the PLGA concentration from 7 to 10% w/w indeed caused the morphology of the particles to change from spheres into fibers. Furthermore, a voltage of 25 kV was required to obtain core-shell microspheres. In another study, core-shell microspheres with a PLGA (lactide:glycolide ratio 75:25) core and a PLGA (lactide:glycolide ratio 85:15) shell also showed a change in shape from microspheres to more fiber-like structures when the core polymer concentration was increased from 6 to 7.5% w/w and the shell polymer concentration from 4 to 5% w/w [86].

Some modifications have been made to the coaxial electrospraying setup, of which coaxial electro-dropping is one. Microspheres with varying sizes and a core-shell structure could be produced using this method. Similar to electrospraying, an electric field is applied to electrically charge the injected solutions but in the case of electro-dropping, the liquids are slowly pumped through coaxial needles. Core-shell microspheres of several hundred micrometers were prepared by loading a PLGA solution and an alginate solution separately in a syringe, and slowly pumping the liquids out through the inner and outer needle, respectively [24]. The two immiscible viscous liquids met at the tip of the coaxial nozzle which resulted in the formation of a droplet, and eventually in the formation of a semisolid particle upon collection in crosslinking calcium chloride solution. The collected particles were then washed and filtered. Single or multiple PLGA cores were observed in the microspheres, and the osteogenic induction factors bone morphogenetic protein 2 (BMP-2) and dexamethasone could be encapsulated separately in the core and shell, respectively, and vice versa.

Also without the coaxial setup, it is possible to obtain core-shell structured microspheres by means of electrospraying. In a study by Wu et al., core-shell microspheres were fabricated using a single-step emulsion electrospraying method with BSA encapsulated in the core and the amphiphilic biodegradable polymer poly(ε-caprolactone)-poly-amino-ethyl ethylene phosphate (PCL-PPE-EA) as shell material [88]. A W/O emulsion was prepared by adding an aqueous solution of BSA drop by drop to DCM solution

Table 4. Representative polymeric core-shell microspheres produced via electrospraying/CEHDA. Presented polymer molecular weights and viscosities are the weight averaged molecular weights and the inherent viscosities, respectively, unless stated otherwise.

Ref.	Production method	Materials	Release profile	Particle size and dispersity	EE	In vivo or ex vivo data?	Comments
[113]	CEHDA	Core: simvastatin + PLLA (85-160 kDa), shell: PDGF + alginate	Simvastatin: sustained release up to day 40; PDGF: fast release up to day 6, slow release up to day 9	~500 μm	Core materials: 73-78%, shell materials: 65%	Yes, micro-CT, histological, and immunohistochemical assessments on rats	
[114]	CEHDA	Core: BSA/PDGF/simvastatin + PDLLA (24-75 kDa), shell: BSA/simvastatin/PDGF + PLGA (50:50, 31-44 kDa)	PDGF and simvastatin: no burst, sustained release up to day 14	18-21 μm, COV = 4-10%	Core materials: 85-96%, shell materials: 54-83%	Yes, micro-CT, histological, and histomorphometric assessments on rats	
[85]	CEHDA	Core: dox + PLGA (50:50, 0.61 dL/g), shell: PDLLA (0.37 and 0.70 dL/g)	Hardly any release up to day 19, fast release up to day 43, and slower release up to day 152	28-32 μm, COV = 14-19%	71-91%	No	
[115]	CEHDA	Core: BSA/simvastatin + PDLLA (24-75 kDa), shell: BSA/PDGF + PLGA (31-44 kDa)	Sustained release up to day 14	14-17 μm, COV = 22-29%	Core materials: 81-90%, shell materials: 65-73%	Yes, placement of microspheres in rats, micro-CT assessments and histological examination	
[106]	CEHDA	Core: simvastatin/BSA/PDGF + PDLLA (24-75 kDa), shell: BSA/simvastatin/PDGF + PLGA (50:50, 31-44 kDa)	Sustained release up to (at least) 14 days	15-22 μm, COV = 13-21%	Core materials: 83-92%, shell materials: 51-71%	Yes, in vivo biocompatibility assay	
[109]	CEHDA	Core: BSA/simvastatin/PDGF + PDLLA, shell: BSA/PDGF/simvastatin + PLGA	Sustained release up to (at least) 14 days	15-20 μm	Core materials: 65-92%, shell materials: 41-71%	Yes, micro-CT, histological, inflammation, cell viability, and bone resorption studies	
[25]	CEHDA	Core: paclitaxel/suramin + PLLA (85-160 kDa), shell: suramin/paclitaxel + PLGA (50:50, 40-75 kDa)	Sustained release up to day 30; resp. sequential and parallel release of both drugs	~20 μm	Core materials: 81-91%, shell materials: 39-59%	Yes, cytotoxicity assay and cellular apoptosis study	
[44]	CEHDA	Core: paclitaxel/suramin + PLLA (85-160 kDa), shell: suramin/paclitaxel + PLGA (50:50, 40-75 kDa)	Sustained release up to 30 days; resp. sequential and parallel release of both drugs	~10-20 μm	No data	Yes, cytotoxicity and cellular apoptosis assays; tumor inhibition and imaging study, histological and immunohistochemical analysis	
[104]	Coaxial electrospraying	Core: VEGF, shell: PLGA (50:50, 120 kDa)	Burst = 20-35%, fast release up to day 6	6 μm, COV = 28-29%	65-70%	Yes, cell culture and staining	
[116]	Coaxial electrospraying	Core: reGFP, shell: PLGA (50:50)	No data	2-6 μm, COV = 13-26%	No data	No	
[117]	Dual-capillary electrospraying	Core and shell: budesonide/theophylline + PLGA (50:50, 7-17 kDa/50:50, 24-38 kDa/85:15, 50-75 kDa)	Both drugs: sustained release up to at least 50 hours	0.4 and 1.1 μm, geometric standard deviation = 1.4	Both drugs: 88-97%	No	

Table 4. *Continued*

Ref.	Production method	Materials	Release profile	Particle size and dispersity	EE	In vivo or ex vivo data?	Comments
[32]	Coaxial electrospraying	Core: Sudan Red G, shell: PCL (45 kDa)	Fast release up to day 1, slow release up to day 5	30-62 µm, monodisperse	No data	Yes, biological evaluation/*in vitro* cell studies: cytotoxicity and cell growth behavior	
[26]	Coaxial electrospraying	Core: BMP-2 + PLGA (75:25, 10 kDa), shell: VEGF + PDLLA (10 kDa)	Sustained release up to day 28; VEGF faster release than BMP-2	0.7 µm, COV = 37-40%	BMP-2: 80-85%, VEGF: 73-80%	Yes, cell tests and implantation of microspheres into rat calvarium	
[86]	Coaxial electrospraying	Core: lacosamide + PLGA (72:25, 60 kDa), shell: PLGA (85:15, 60 kDa)	Sustained release up to day 18, ~50% release within the 1st day	4 µm, COV = 24%	94%	No	
[20]	Coaxial electrospraying	Core: BSA, shell: PLGA (50:50, 31-58 kDa and 58-92 kDa)	PLGA 58-92 kDa: fast release up to day 3, a lag phase up to at least 43 days; PLGA 31-58 kDa: fast release up to day 3, a lag phase up to day 29, and near zero-order release up to at least 43 days	3-6 µm, COV = 17-38%	48-75%	No	
[107]	Dual-capillary electrospraying	Core: budesonide/EGCG, shell: PLGA (50:50, 5-15 kDa)	Budesonide: burst = 5-60%, two-stage release up to 25-225 hours	0.2-1.2 µm, COV = 3-11%	Budesonide: 90-95%, EGCG: 88-92%	No	
[90]	Coaxial tri-capillary electrospraying	Core: EGCG (+ PLGA), middle phase: budesonide (+ PLGA), shell: PLGA (50:50, 40-75 kDa)	EGCG: biphasic release (slow release followed by faster release) up to 18-24 days, budesonide: sustained release up to 18-24 days	3 µm, COV = 7-18%	EGCG: 90-93%, budesonide: 87-92%	No	
[88]	Emulsion electrospraying	Core: BSA, shell: PCL-PPE-EA	Sustained release up to day 20	3 µm	90%	No	
[24]	Coaxial electro-dropping	Core: BMP-2 + BSA + PLGA (50:50, 40 kDa), shell: dexamethasone + alginate	Sustained release up to day 30; faster release of shell drug than of core drug	200-1000 µm	No data	No	BSA added as stabilizer. Position of BMP-2 and dexamethasone could be switched
[38]	Electrospinning	Core: PLGA (85:15), shell: chitosan	No data	0.2-20 µm	No data	Yes, cytotoxicity and cell proliferation test on cells	

Abbreviations: EGCG, epigallocatechin gallate; PDGF, platelet-derived growth factor; reGFP, recombinant enhanced green fluorescent protein; VEGF, vascular endothelial growth factor

containing the polymer, after which this emulsion was electrosprayed. Due to the amphiphilic properties of the polymer, core-shell structured particles instead of monolithic particles were formed, as agglomeration of the small water droplets in the W/O emulsion resulted in a monolithic protein core. This core-shell structure was verified by both TEM and CLSM photos and by an SEM photo of a freeze-fractured particle.

A great advantage of electrospraying is the variety in the combination of polymers and drugs that can be used, even materials that are sensitive to high shear stresses and elevated temperatures, such as proteins [87,89]. The ability to operate at ambient temperature and pressure makes it a very versatile and convenient production method. For the shell, PLGAs of different monomer ratios are the most commonly used polymers, but also PDLLA, PLLA, PCL, chitosan, and alginate have been used. Gao et al. produced monodisperse core-shell microspheres with a PCL shell and a silicon oil core containing the hydrophobic model drug Sudan Red G [32]. Oil-based cores have gained increased attention as problems related to drug solubility can be reduced and the chemical or physical stability of moisture-sensitive drugs can be improved in comparison with aqueous cores. This shows the potential of coaxial electrospraying for hydrophobic drug encapsulation without the need for a polymeric core. Furthermore, particle size and shell thickness can easily be controlled by varying the polymer concentration, inner and outer flow rate, applied voltage, and collection distance [32]. Another advantage of CEHDA over the conventional bulk emulsion solvent evaporation method is the fact that there is no need for stirring to create emulsions so high shear rates are circumvented. Also, the formulation does not require contact with an outer aqueous environment, which enhances the ability to load hydrophilic drugs in the core. This makes CEHDA very suitable for producing core-shell microspheres with hydrophilic drugs loaded in the core and hydrophobic drugs loaded in the shell but also vice versa in a single step. In a study by Nie et al., core-shell microspheres were fabricated as a multi-drug release system of which the core consisted of PLLA and the shell of PLGA [25]. The hydrophobic small molecule paclitaxel was incorporated into the shell whereas the hydrophilic small molecule suramin was incorporated into the core but the reverse was also constructed for comparison. Although the EE of the core material was high, i.e. 81-91%, the EE of the shell material was compromised. Paclitaxel was encapsulated in the shell at an EE of 54-59% but a significantly lower EE of 39-46% was obtained for suramin in the shell. The low EE of suramin in the shell was ascribed to its hydrophilicity and to jet instability caused by the mixture of ethyl acetate (EtAc), ethanol, and water which was used as solvent for the drug. Also, the microspheres were collected in anhydrous ethanol instead of on aluminum foil so the drug on the surface might have washed off. The EE of the core materials for CEHDA in general is relatively high (approximately 65-100%), although this is also dependent on the formulation parameters, such as polymer concentration and drug loading. The reason for these high EE values is that the core materials are loaded through the inner needle which reduces the chance of diffusion of the core drugs into the outer phase. This in turn reduces the possibility that the materials get wasted in the atomization process. This is a great advantage in comparison with some of the other production methods. The EE, for instance, significantly improved when BSA-loaded microspheres were produced with coaxial electrospraying instead of emulsion electrospraying. The core-shell microspheres prepared with coaxial electrospraying had an EE of 69-72%, in contrast to the

monolithic microspheres prepared with emulsion electrospraying that had an EE of only 47-54% while using the same theoretical BSA loading and polymer concentration [20]. This again shows the benefit of a core-shell structure.

Coaxial electrospraying also allows for the production of small particles in the nanometer to micrometer range but the production of particles larger than 100 μm does not seem to be possible (Table 1, Table 4). Moreover, precise control over size and shape, i.e. microspheres or fibers, of the product is complicated. COV values of < 10% could be achieved, especially when operated in cone-jet mode but the formation of a stable cone-jet is much more difficult with dual-capillary electrospraying than with single-capillary electrospraying. This is caused by the differences in the electrical properties of both phases [20]. Lee et al., however, did succeed in producing monodisperse tri-layered microspheres with COV values of 7-18% by using acetonitrile as the solvent for both the inner, middle, and outer phase. The miscibility of the three liquids resulted in a stable cone-jet and, thus, a narrow particle size distribution [90].

2.3.4 Drop-by-drop methods – PPF

A less common method for the fabrication of core-shell microspheres is PPF, which uses multiple concentric nozzles to coaxially spray a jet that is composed of the core and annular shell material. The jet is acoustically excited via an ultrasonic transducer and subsequently broken up into uniform core-shell droplets by piezoelectric vibration. The frequency of the vibrations and the concentrations and flow rates of the solutions control the droplet size. An additional coaxial nozzle generates a co-flowing non-solvent carrier stream that surrounds the polymer jet. This carrier stream can reduce the jet diameter and thus allows for the production of droplets smaller than the nozzle diameter [28,91]. The reported diameter of the obtained microspheres is 40-115 μm and thus within a size range that is suitable for parenteral administration. After collecting the droplets in PVA solution, the organic solvent is extracted and evaporated, the particles are washed, and eventually freeze-dried. Table 5 gives an overview of representative core-shell microspheres produced with PPF. Because this technique offers great control over the particle size and shell thickness due to both the carrier stream and the use of acoustic excitation, a narrow size distribution is often achieved (Table 5). Also, microspheres can be produced with a high production speed and reproducibility and in a continuous fashion which makes it a very profitable method, and there is no need for high-speed homogenization. Figure 7 provides a schematic representation of the production method.

In most of the studies, a PLGA or a P(D)LLA solution was used for the core jet so that core-shell microspheres with a solid core were produced. For the shell phase, the same polymers were primarily employed. The PPF method is not confined to the use of immiscible polymers or polymers solutions. In some studies, however, the use of miscible polymers, for instance PLGA and PCPH, resulted in the presence of some domains of the core polymer in the shell layer [19,35]. Furthermore, both a hydrophobic and a hydrophilic model small-molecule drug, i.e. piroxicam [92,93] and doxorubicin [94-96], respectively, could be loaded in the core phase in order to control their release rate. In the case of doxorubicin, the drug was first dissolved in water and subsequently emulsified with the polymeric core phase. Chi-p53 (gene delivery vectors comprising chitosan and a plasmid DNA encoding p53) nanoparticles were added to the shell phase to obtain a

Table 5. Representative polymeric core-shell microspheres produced via PPF. Presented polymer molecular weights and viscosities are the weight averaged molecular weights and the inherent viscosities, respectively, unless stated otherwise.

| Ref.	Production method	Materials	Release profile	Particle size and dispersity	EE	In vivo or ex vivo data?	Comments
[18]	PPF	Core: BSA, shell: PLGA (50:50, 15/38/88 kDa)	15 kDa: fast release up to day 5; 38 kDa: sustained release up to day 40; 88 kDa: slow release (up to 10-30%) followed by a pulse over ~7 days from day 22, 32, or 35	73-85 μm, monodisperse	15 kDa: 5-10%, 38 kDa: 15-30%, 88 kDa: 55-65%	No	
[21]	PPF	Core: BSA + PLGA (50:50, 4 kDa), shell: PLLA (43/106/192 kDa)	Fast release up to day 10, sustained release up to 70 days	55 μm, COV = 3-5%	Only DCM: 20-35%, EtAc + DCM: 40-55%	No	
[96]	PPF	Core: dox + PLGA (50:50, 0.61 dL/g), shell: Chi-p53 nanoparticles + PLLA (1.05 dL/g)	Chi-p53: burst = 15%, near zero-order release up to at least 125 days; dox: burst = 10-30%, lag phase up to day 20, sustained release up to at least 125 days	50-75 μm	No data	Yes, cytotoxicity and cellular expression study, and immuno-fluorescence staining	
[95]	PPF	Core: dox + PLGA (50:50, 0.61 dL/g), shell: PDLLA (0.37 and 0.70 dL/g)/PLLA (1.05 dL/g)	Burst = 2-10%, lag phase up to day 26, sustained release up to at least 125 days	50-75 μm	79-80%	No	
[97]	PPF	Core: BSA + PLGA (50:50, 4 kDa), shell: PDLLA (43 kDa)	EtAc + DCM: fast release of 35% up to day 10, sustained or near zero-order release up to day 140	60-77 μm, COV = 2-4%	Only DCM: 25-30%, EtAc + DCM: 45-50%	No	
[94]	PPF	Core: dox + PLGA (50:50, 0.61 dL/g), shell: Chi-p53 nanoparticles + PDLLA (0.37 and 0.70 dL/g)/PLLA (1.05 dL/g)	Dox: burst = 2-30%, lag phase up to day 26, sustained release up to at least 125 days; chi-p53: burst = 2-15%, slow release up to at least 125 days	63-75 μm, COV = 4-7%	Dox: 79-83%, Chi-p53: 25-37%, Dox+Chi-p53: 32-47% and 27-37%, resp.	No	
[19]	PPF	Core: dextran/BSA, silicone/canola oil, and PLGA; shell: resp. PLGA, PLGA, and PCPH (n.b. PLGA 50:50, 10-65 kDa)	BSA and dextran: burst < 5%, lag phase up to day 20, pulse over ~5 days from day 30, slow release up to day 60	Aqueous core: 115 μm, oil core: 110 μm, solid core: 60 μm; monodisperse	No data	No	
[93]	PPF	Core: piroxicam + PLGA (50:50, 0.39 dL/g), shell: PDLLA (0.24 dL/g)	Burst = 4-12%, biphasic release (slow release followed by faster release) up to 40-50 days	47-86 μm, COV = 5-16%	74-97%	No	
[35]	PPF	Core: PCPH, shell: PLGA (50:50, 0.82 dL/g) and the inverse	No data	44 μm, COV = 4-6%	No data	No	
[92]	PPF	Core: piroxicam + PLGA (50:50, 35 kDa), shell: PLLA (100 kDa)	Burst ~10%, sustained release up to day 90	40-60 μm, monodisperse	3-8%	No	
[28]	PPF	Core: PLGA (50:50, 85/130 kDa), shell: PCPH and the inverse	No data	58 μm, monodisperse	No data	No	
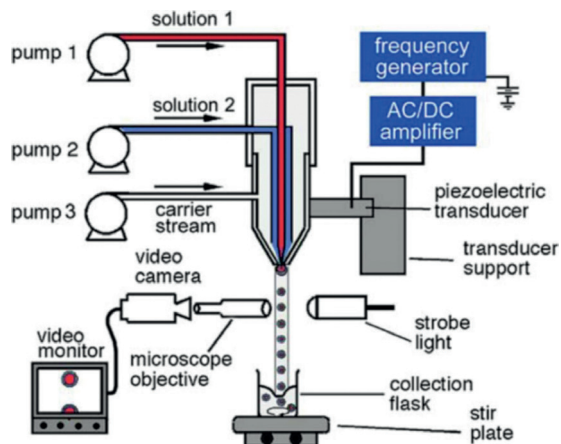
Figure 7. Schematic PPF setup for the production of uniform core-shell microspheres. The inner liquid is delivered using pump 1, the outer liquid is delivered using pump 2, and the carrier stream is delivered using pump 3. Modified from [28] with permission from Elsevier.

dual-drug delivery system for anticancer therapy by combining both chemotherapy and gene therapy [94,96]. Proteins can be also be incorporated into microspheres using PPF. BSA was successfully encapsulated in a PLGA core surrounded by a PLLA or PDLLA shell [21,97]. An exception to the use of PLGA, PDLLA, and PLLA is the surface-eroding polyanhydride polymer PCPH. Berkland et al. prepared double-walled microspheres with a PCPH core and a PLGA shell [28]. However, reversing the arrangement of the two polymers while keeping all other production conditions unchanged, resulted in incomplete encapsulation of the PLGA core by PCPH. By adjusting the polymer concentrations and flow rates, full engulfment could eventually be achieved. This shows that there are no standard settings for microsphere production with PPF, and that the production conditions have to be optimized when a different polymer is used or a different arrangement is desired.

A great advantage of PPF is the possibility of easily achieving a non-solid core that only contains the drug. For example, Berkland et al. demonstrated that liquid-filled core-shell microspheres with either an oil or aqueous core could be produced using PPF technology [19]. Three different core types were tested: a solid PLGA core with a PCPH shell, a silicone or canola oil core with a PLGA shell, and an aqueous dextran or BSA core with a PLGA shell. For all arrangements, a distinct core-shell structure was visible and a narrow size distribution was obtained. However, for the solid and oil core formulations, some mixing of phases did take place at the interface of the materials as portrayed by SEM photos of cross-sectioned particles. Microspheres with a canola oil core displayed small unconnected pores at the particle surface, indicating the breaching of canola oil into the PLGA shell. Aqueous core microspheres did not display this minimal intrusion of the core phase into the shell phase as these phases are less miscible.

A drawback of this production method is the fact that the obtained EE is variable from as low as 3% to up to 97%, though the low EE values are often the consequence of the chosen production settings instead of being inherent to the production method.

Xia et al. prepared both BSA-loaded single-walled and double-walled microspheres, from PLGA and PLGA/PLLA [21] or PLGA/PDLLA [97], respectively. Double-walled microspheres had an EE of only 20-35% when dichloromethane (DCM) was used as the solvent. However, the EE increased to 40-55% when both DCM and EtAc were used for the core and the shell phase, respectively, which was ascribed to differences in the particle hardening time. The EE also appeared to increase with increasing molecular weight of PLLA, i.e. the shell polymer, due to an increase in the solution viscosity which prevented the protein from diffusing out of the core [21]. These EE values are relatively low in comparison with microfluidics and CEHDA. The single-walled microspheres had an EE of only 20% or 30%, depending on the production settings. The improved EE values for the double-walled microspheres can again be attributed to the presence of a drug-free shell layer. However, the opposite was observed in a study by Berkland et al. [92], where the EE drastically decreased from 49% (PLGA microspheres) or 85% (PLLA microspheres) to only 3-8% (PLGA/PLLA core-shell microspheres). It is said that the large volume of solvent in the shell phase of each droplet is a driving force for the diffusion of the drug towards the droplet surface. When doxorubicin was incorporated into the core of the previously described PLGA/PLLA double-walled microspheres, the EE increased from 61% for single-walled PLGA-based microspheres to 79-83% [94]. Yet, when chi-p53 nanoparticles were added to the shell, the EE of doxorubicin decreased from 79-83% to 32-47% as the nanoparticle dispersion was emulsified with the shell phase, thereby facilitating the diffusion of doxorubicin out of the particles during microsphere solidification. The EE of the nanoparticles was only 25-37%. It has to be noted that the EE of drugs in the shell phase is generally 40-80% and thus much lower than the EE of drugs in the core, which can be explained by the shorter diffusion distance from the shell. Another disadvantage of PPF is the complexity of the production method and so far, only a few studies have used the technique for the production of core-shell microspheres for pharmaceutical use. Therefore, the information on the possible applications and the optimal production conditions is limited, and further research is required.

2.4 Drug release profiles from core-shell microspheres

One of the major advantages of core-shell microspheres over monolithic microspheres is the increased control over the release kinetics of the encapsulated drugs because the properties of the shell, such as shell material and shell thickness, can be tailored. Examples of improved release kinetics are a reduced initial burst release [14,31,45], a prolonged total release [14,21,23,92,97], and a delayed (pulsatile) release [18,19,29,50,55,85] as the shell layer presents a diffusion barrier to the drugs in the core. A prolonged release is especially advantageous for drugs that frequently have to be administered via parenteral injection which is very uncomfortable and unpractical for the patient. Another example of improved release kinetics is the dual-drug release of, for example, a hydrophobic and a hydrophilic drug with different release patterns [24,26]. Dual-drug release is especially beneficial in the therapy for tissue regeneration and cancer, as these are multistage processes that can be influenced by several growth factors or inhibition factors and other proteins and drugs that can regulate the tissue or tumor growth [44,98]. These therapies often require sequential or parallel delivery of the different drugs, which can be achieved

by loading these drugs separately in the core and shell. In order to mimic the natural bone healing process, Wang et al. produced PLGA/PDLLA core–shell microspheres using coaxial electrospraying, with vascular endothelial growth factor (VEGF) incorporated in the shell layer and BMP-2 in the core (Figure 8) [26].
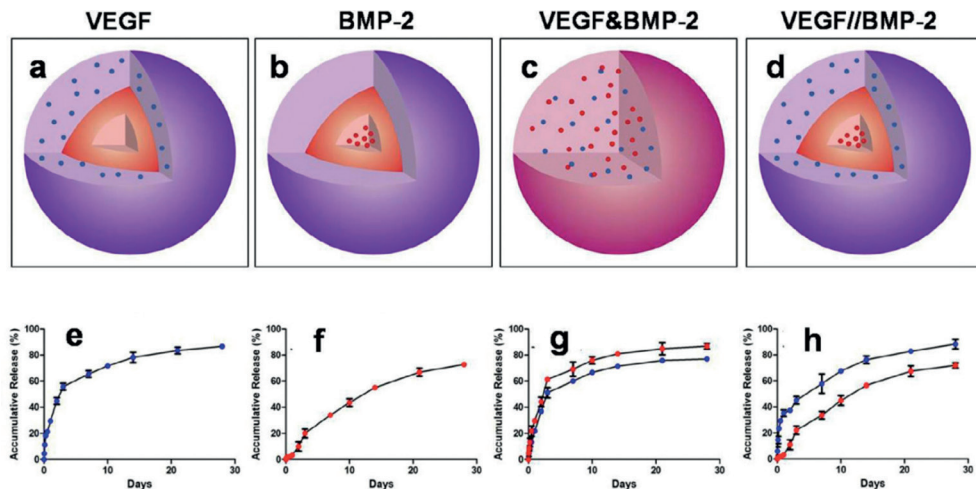

Figure 8. Schematic illustration of VEGF (●) and BMP-2 (●) releasing monolithic and core-shell microspheres (a-d): core-shell microsphere with only VEGF in the shell (a), core-shell microsphere with only BMP-2 in the core (b), monolithic microsphere with both VEGF and BMP-2 (c), core-shell microsphere with both VEGF and BMP-2 in the shell and core, respectively. *In vitro* release profiles of VEGF and BMP-2 from microspheres a-d (e-h). Modified from [26] with permission from Elsevier.

Both drugs exhibited a sustained release profile up to 28 days, although they were delivered at different release rates and thus in a sequential manner. As VEGF was loaded in the shell, this growth factor exhibited an initial burst release of nearly 40% and a total release of approximately 70% within the first ten days, while only 3% of BMP-2 was released from the core within the first 24 hours. The released VEGF can promote angiogenesis, followed by the release of BMP-2 inducing osteoblast differentiation. Choi et al. prepared core-shell microspheres with two osteogenic induction factors, BMP-2 and dexamethasone, loaded separately in the core and shell, thereby establishing a dual-drug delivery system [24]. In this way, both drugs could be released simultaneously at different release rates, which means that stem cell differentiation could be regulated in a coordinated fashion. Additionally, the respective drugs could be switched from core to shell position and vice versa, while maintaining the physical separation. The drugs displayed a sustained release profile for at least thirty days, with the drug incorporated in the shell displaying a higher burst release and a faster overall release than the drug incorporated in the core. Although the incorporation of two drugs into a single microsphere has some advantages, such as the need for only one production line, it is also possible to incorporate two drugs into two different batches of microspheres. By adding these batches together into one syringe, a dual-drug release formulation can be obtained.

The desired release profile depends on the intended application of the drug(s)

in the microspheres. A pulsatile release profile, such as a delayed pulsatile release (i.e. a pulse after a certain lag time) or a triphasic release profile, is often aimed for when core-shell microspheres are employed. There are various indications for which continuous drug delivery is not optimal and where a pulsatile release profile might be preferred [99]. Examples are drugs with a high first-pass effect or with specific chronopharmacological demands, for example hormones. Hormones regulate many internal functions in the body, often following the circadian rhythm, which means that pulsatile release is required to mimic certain endogenous patterns and thus improve therapeutic efficiency. Moreover, a triphasic-release formulation might be beneficial for the delivery of vaccines that generally demand a second and sometimes third booster dose to confer protective immunity against the targeted pathogen [100]. A single injection of a vaccine delivery system with such a triphasic release covers both the primer and the booster dose, and thus circumvents the need for multiple injections [65]. This improves vaccinee's convenience and compliance and reduces the costs. A sustained-release formulation can also be applied for vaccine delivery but a pulsatile release profile gives a better imitation of the current multiple injection regimen used for conventional vaccines, and a sustained release profile might induce immune tolerance [65,101]. Sanchez et al. developed a single-shot tetanus vaccine formulation using PLGA-based microspheres with an oily core containing the model antigen tetanus toxoid surrounded by a vaccine-free polymer shell [102]. Two formulations with different grades of PLGA were tested and both exhibited a delayed pulsatile release of tetanus toxoid as seen in Figure 9.
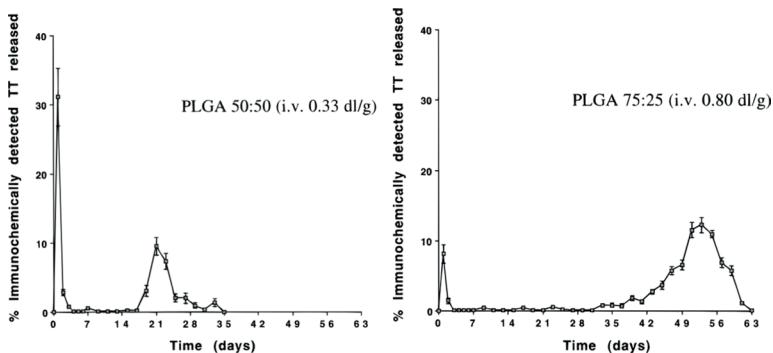
Figure 9. *In vitro* release profiles of immunochemically detected TT from oil-based core-shell microspheres with a PLGA shell. PLGA with a lactide:glycolide ratio of 75:25 and an inherent viscosity (i.v.) of 0.33 dL/g (left) and PLGA with a lactide:glycolide ratio of 75:25 and an i.v. of 0.80 dL/g (right) were compared. Modified from [102] with permission from Elsevier.

Delayed release of the highly water-soluble radiosensitizer etanidazole was achieved by incorporating the drug as solid crystals into core-shell microspheres with a PLLA shell and a PLGA core, although the lag phase was not followed by a pulsatile release but by a sustained release (Figure 10) [55]. A low initial burst of less than 5% was observed, followed by a lag phase of four weeks and a nearly linear release for two weeks. Such a release profile might greatly improve the treatment of tumors. The initial release was diffusion controlled while the subsequent release was controlled by the degradation of

Figure 10. *In vitro* release profiles of etanidazole from PLGA-PLLA core-shell microspheres with different polymer mass ratios (w/w) of PLLA to PLGA (2:1 (▲) and 1:1 (♦)). Reproduced from [55] with permission from Elsevier.

the polymeric shell layer as the formation of pores and channels, caused by the presence of PLGA domains in the shell, predominated. Similar microspheres were prepared with a conventional W/O/O/W emulsion solvent evapora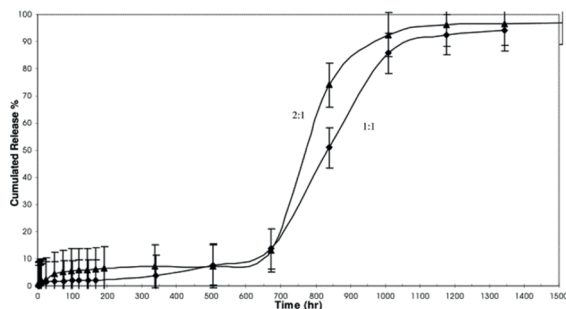tion method combined with phase separation with BSA as model protein [29]. The release profile could be altered by saturating the aqueous continuous phase with DCM, thereby changing the solvent evaporation kinetics, and by adding ethanol to the PLLA solution, i.e. the shell phase. The first reduced the solvent efflux from the dispersed oil phase into the aqueous continuous phase and the last caused an increased solubility of DCM in the aqueous continuous phase. Both methods ultimately influenced the protein distribution within the microspheres. For all formulations, an initial burst release of less than 20% was obtained that was followed by a lag time in which hardly any protein was released. The lag time duration could be varied from 4 to 30 days and the total release period from 30 to at least 58 days by altering the solvent evaporation kinetics and/or the ethanol content. For PLGA-based core-shell microspheres with an oily core, a delayed pulsatile release of BSA was obtained as well when the molecular weight of the polymer was high enough, i.e. 88 kDa [18]. For lower molecular weight PLGA, i.e. 15 and 38 kDa, fast or sustained release was obtained without a lag phase as the liquid-core engulfment efficiencies were significantly lower for these formulations, which indicates that a high percentage of the microspheres did actually not have a core-shell structure. Pek et al. also demonstrated this dependency of the *in vitro* release profile on the molecular weight of the polymer for PLGA/PLLA core-shell microspheres loaded with bupivacaine powder in the inner core [50]. In a study by Berkland et al., PLGA-based core-shell microspheres with an aqueous core containing BSA and dextran were produced [19]. Both compounds generated a pulsatile release after a lag time of approximately twenty days with minimal initial burst release. In this case, however, a low molecular weight of PLGA (15 kDa) was enough to obtain a high core engulfment efficiency, and thus, such a pulsatile release profile. In summary, polymeric core-shell microspheres can provide a delayed pulsatile release profile as long as they meet certain structural criteria. The core should be completely surrounded by a drug-free shell layer with minimal porosity, and distinct phase separation of the core and shell phase is essential, with the drug being spatially localized in the core.

One of the aims that is often pursued with delayed (pulsatile) release core-shell

microspheres, is the ability to modulate the lag time by tuning the properties of the core and/or shell. In this way, the microspheres are suitable for numerous applications. The lag time could be modulated by adding ethanol to the polymer solution which altered the protein distribution and the microsphere structure but many more mechanisms are possible [29]. PLGA/PLLA core-shell microspheres that were γ-irradiated with a sterilization dosage of 25 kGy displayed a decrease in lag time of two weeks compared to the nonirradiated microspheres [55]. This was explained by a reduction in molecular weight of the shell polymers as a result of irradiation, which caused a decrease in degradation time. The duration of the lag time was, on the other hand, independent of the polymer mass ratio of PLLA and PLGA, and thus independent of the shell thickness of the microspheres as shown in Figure 10. This might be explained by the fact that PLLA and PLGA are bulk-degrading polymers and not surface-eroding which means that the lag time is only determined by the polymer characteristics. The influence of the polymer molecular weight on the release characteristics has been demonstrated multiple times [18,20,50], although the polymer composition and primarily the monomer ratio in the case of PLGA, have a greater influence, mainly on the onset of the pulse. An increase in lactide content results in a more hydrophobic and thus a slower degrading polymer which eventually could lead to a longer lag time. In the case of the single-shot tetanus vaccine formulation, PLGAs with two different monomer ratios and molecular weights were used to vary the lag time [102]. For both formulations, the antigen was released in a pulsatile manner after a certain lag time. The lag time was three weeks for PLGA with a lactide:glycolide ratio of 50:50 and a relatively low molecular weight, and seven weeks for PLGA with a lactide:glycolide ratio of 75:25 and a relatively high molecular weight. Both the monomer ratio and the molecular weight might have caused the difference in lag time. An initial burst release of 30 and 10%, respectively, was observed which is presumably due to the migration of some of the antigen-loaded droplets towards the particle surface. However, no other studies could be found in which the influence of the lactide:glycolide ratio of the polymer used as shell material on the lag time of core-shell microspheres was investigated. Zheng determined the influence of the polymer composition of the core material on the release profile [13]. Core-shell microspheres with 5-fluorouracil loaded in a PLGA core surrounded by a PLLA shell were produced and the monomer ratio and molecular weight of PLGA in the core were varied. The lag phase was the shortest for microspheres made from PLGA with a relatively low lactide content and molecular weight and the longest for microspheres made from PLGA with a relatively high lactide content and molecular weight, although the differences were marginal. The *in vitro* release rate after the lag phase decreased as well with increasing lactide content and molecular weight. Both observations could be explained by the occurrence of autocatalytic degradation of the shell polymer. PLGA with the lowest lactide content and molecular weight will degrade the fastest once water has reached the core and thus generate more carboxylic acids that cause faster autocatalytic degradation of the shell. The lag time also increased with increasing shell thickness, which relationship was also shown in some other studies [18,93]. On the other hand, BSA release studies of different core-shell microsphere formulations with a shell made from PLGA with a lactide:glycolide ratio of 50:50 all demonstrated similar lag times of approximately three to four weeks [18-20]. These results indicate that the lag time is indeed solely dependent

on the polymer composition and not on the particle size and/or shell thickness which was also demonstrated by Xu et al. [85]. It is unclear why different results were obtained. More research should be conducted on the dependence of the lag time on various particle characteristics such as size and hydrophilicity of the drug, polymer composition, polymer and drug localization, and shell thickness.

Another interesting finding is the fact that core-shell microspheres often do not exhibit a delayed (pulsatile) release profile. In the majority of the studies, a sustained release profile was obtained, whether or not preceded by an initial burst release. In some cases, (near) zero-order [24,103] or even immediate [104] release was obtained. Drug release from polymeric core-shell microspheres is influenced by a combination of water penetration, drug diffusion, and polymer degradation [105]. There are several causes for a high initial burst release and/or the absence of a lag phase, one of which is incomplete phase separation. This can occur during the solvent evaporation and microsphere hardening process, for instance when the solvent evaporation is too fast [16]. As a result, two discontinuous layers of polymer are formed with tiny beads of the core polymer embedded in the shell layer, which causes some of the drug molecules to be present in the shell layer as well. These drug molecules in the vicinity of the surface can cause an initial burst release or release during the lag phase [29,52,54,56]. Moreover, a completely non-porous shell is necessary to prevent any drug from being released during the lag phase and to prevent an initial burst release. Many examples can be found of core-shell microspheres with small or large pores in the shell through which the drug can diffuse out [14,21,42,44,88,94,106]. Furthermore, drug diffusion can sometimes occur through the polymer matrix. This is mainly the case for small hydrophobic drugs [32,92,107] but whether the shell layer can act as a diffusive barrier depends on both the properties of the shell material and the properties of the drug. Large hydrophilic proteins, for example, can sometimes diffuse through the polymer shell as well if this shell is made of for example glycol chitosan [39]. In some cases, however, core-shell microspheres with a non-porous, non-permeable shell are formed in which the drug molecules are solely encapsulated in the core but still no delayed pulsatile release is obtained [97]. This shows that release mechanisms are often still unclear and that research into the release mechanisms of especially core-shell microspheres is desired.

Lastly, *in vitro* release data are often lacking, especially for microfluidically produced core-shell microspheres (Table 3). These studies often focus on the technical part of the production process and on the influence of the production settings on the particle characteristics. Incorporation of a drug and measurement of the *in vitro* release of this drug, however, would definitely be of added value. *In vivo* data are even more scarce and because for many drugs, the release is difficult to measure *in vivo*, the therapeutic effect of the administered drug is often measured instead, for instance tumor weight and volume [108] or bone resorption [109]. Because *in vitro* release data are often not an accurate predictor of the *in vivo* performance, the acquisition of *in vivo* data should be prioritized in the future. Additionally, *in vitro* release studies are often terminated after a few weeks, even when drug release still seems to continue. In order to get a complete picture of the release profile and to determine the underlying release mechanisms, continuation of the release studies over a longer period is warranted.

2.5 Conclusion

Core-shell microspheres seem to have multiple advantages over monolithic microspheres, and the addition of a shell might offer improved functionality and versatility for parenteral drug delivery. In the first place, core-shell microspheres can provide increased control over the release kinetics of the incorporated drugs. Examples are reduction of the initial burst, increased circulation time of the drug in the body, and the ability to obtain a pulsatile or dual-drug release. Secondly, core-shell microspheres generally have a higher EE than monolithic microspheres. Many different types of core-shell microspheres are possible, both with a solid polymeric, gas-filled, or liquid-filled core, and various polymers can be employed although PLGA, PDLLA, and PLLA are used in the majority of the studies. Unfortunately, data that prove the existence of a core-shell structure are frequently lacking, and a combination of confirmation methods is desired. Various methods can be applied for the production of core-shell microspheres but drop-by-drop methods, such as microfluidics, CEHDA, and PPF are the most attractive because they allow for better control over the particle structure and size and because there is no high-speed homogenization involved. PPF is a very promising method but rather complex and CEHDA is only feasible for the production of small particles. Therefore, microfluidics is the preferred method although large-scale production is still a challenge. Yet, conventional bulk emulsion solvent evaporation (combined with phase separation) is still the most common production method but the obtained particles usually have a broad size distribution and it makes use of harsh production conditions. Various release profiles can be obtained with core-shell microspheres but the release mechanisms are often unclear and many studies lack *in vivo* or even *in vitro* release data. Hence, future research should focus on elucidating the mechanism behind the different release profiles and release profiles should be determined more often, especially *in vivo* and for a longer period of time. Overall, core-shell microspheres have many potential implications on clinical practice, for instance the incorporation of drugs with a narrow therapeutic index that, therefore, require complete absence of burst release. Another example is the use of core-shell microspheres with a pulsatile release profile as a single-injection vaccine formulation.

References

[1] K. K. Kim and D. W. Pack, "Microspheres for Drug Delivery," BioMEMS Biomed. Nanotechnology, Vol. I - Biol. Biomed. Nanotechnol., pp. 19–50, 2006.

[2] Y. Zhang, H. F. Chan, and K. W. Leong, "Advanced Materials and Processing for Drug Delivery: The Past and the Future," Adv. Drug Deliv. Rev., vol. 65, no. 1, pp. 104–120, Jan. 2013.

[3] S. P. Schwendeman, R. B. Shah, B. A. Bailey, and A. S. Schwendeman, "Injectable controlled release depots for large molecules," J. Control. Release, vol. 190, pp. 240–253, Sep. 2014.

[4] K. Park et al., "Injectable, long-acting PLGA formulations: Analyzing PLGA and understanding microparticle formation," J. Control. Release, vol. 304, pp. 125–134, 2019.

[5]   A. Jain, K. R. Kunduru, A. Basu, B. Mizrahi, A. J. Domb, and W. Khan, "Injectable formulations of poly(lactic acid) and its copolymers in clinical use," Adv. Drug Deliv. Rev., vol. 107, pp. 213–227, 2016.

[6]   Y. Hua et al., "Key Factor Study for Generic Long-Acting PLGA Microspheres Based on a Reverse Engineering of Vivitrol®," Molecules, vol. 26, no. 5. 2021.

[7]   T. R. S. Kumar and K. S. and S. K. Nachaegari, "Novel Delivery Technologies for Protein and Peptide Therapeutics," Current Pharmaceutical Biotechnology, vol. 7, no. 4. pp. 261–276, 2006.

[8]   M. N. Singh, K. S. Y. Hemant, M. Ram, and H. G. Shivakumar, "Microencapsulation: A promising technique for controlled drug delivery," Res. Pharm. Sci., vol. 5, no. 2, pp. 65–77, Jul. 2010.

[9]   Y. Ogawa, H. Okada, Y. Yamamoto, and T. Shimamoto, "In Vivo Release Profiles of Leuprolide Acetate from Microcapsules Prepared with Polylactic Acids or Copoly(Lactic/Glycolic) Acids and in Vivo Degradation of These Polymers," Chem. Pharm. Bull., vol. 36, no. 7, pp. 2576–2581, 1988.

[10]   J. Wang, B. M. Wang, and S. P. Schwendeman, "Characterization of the initial burst release of a model peptide from poly(d,l-lactide-co-glycolide) microspheres," J. Control. Release, vol. 82, no. 2, pp. 289–307, 2002.

[11]   X. Huang and C. S. Brazel, "On the importance and mechanisms of burst release in matrix-controlled drug delivery systems," J. Control. Release, vol. 73, no. 2, pp. 121–136, 2001.

[12]   F. M. Galogahi, Y. Zhu, H. An, and N.-T. Nguyen, "Core-shell microparticles: Generation approaches and applications," J. Sci. Adv. Mater. Devices, vol. 5, no. 4, pp. 417–435, 2020.

[13]   W. Zheng, "A water-in-oil-in-oil-in-water (W/O/O/W) method for producing drug-releasing, double-walled microspheres," Int. J. Pharm., vol. 374, no. 1, pp. 90–95, 2009.

[14]   A. Navaei, M. Rasoolian, A. Momeni, S. Emami, and M. Rafienia, "Double-walled microspheres loaded with meglumine antimoniate: preparation, characterization and in vitro release study.," Drug Dev. Ind. Pharm., vol. 40, no. 6, pp. 701–710, Jun. 2014.

[15]   C.-D. Xiao, X.-C. Shen, and L. Tao, "Modified emulsion solvent evaporation method for fabricating core–shell microspheres," Int. J. Pharm., vol. 452, no. 1–2, pp. 227–232, Aug. 2013.

[16]   R. H. Ansary, M. M. Rahman, M. B. Awang, H. Katas, H. Hadi, and A. A. Doolaanea, "Preparation, characterization, and in vitro release studies of insulin-loaded double-walled poly(lactide-co-glycolide) microspheres," Drug Deliv. Transl. Res., vol. 6, no. 3, pp. 308–318, Jun. 2016.

[17]   A. Paci et al., "Review of therapeutic drug monitoring of anticancer drugs part 1 - Cytotoxics," Eur. J. Cancer, vol. 50, no. 12, pp. 2010–2019, Aug. 2014.

[18]   Y. Xia and D. W. Pack, "Pulsatile Protein Release from Monodisperse Liquid-Core Microcapsules of Controllable Shell Thickness," Pharm. Res., vol. 31, no. 11, pp. 3201–3210, 2014.

[19]   C. Berkland, E. Pollauf, N. Varde, D. W. Pack, and K. (Kevin) Kim, "Monodisperse Liquid-filled Biodegradable Microcapsules," Pharm. Res., vol.

24, no. 5, pp. 1007–1013, 2007.

[20] M. Zamani, M. P. Prabhakaran, E. S. Thian, and S. Ramakrishna, "Protein encapsulated core–shell structured particles prepared by coaxial electrospraying: Investigation on material and processing variables," Int. J. Pharm., vol. 473, no. 1–2, pp. 134–143, Oct. 2014.

[21] Y. Xia, Q. Xu, C. Wang, and D. W. Pack, "Protein Encapsulation in and Release from Monodisperse Double-Wall Polymer Microspheres," J. Pharm. Sci., vol. 102, no. 5, pp. 1601–1609, May 2013.

[22] S. Hiraoka, S. Uchida, and N. Namiki, "Preparation and Characterization of High-Content Aripiprazole-Loaded Core–Shell Structure Microsphere for Long-Release Injectable Formulation," Chem. Pharm. Bull., vol. 62, no. 7, pp. 654–660, 2014.

[23] J. Wu et al., "Fabrication and characterization of monodisperse PLGA–alginate core–shell microspheres with monodisperse size and homogeneous shells for controlled drug release," Acta Biomater., vol. 9, no. 7, pp. 7410–7419, Jul. 2013.

[24] D. H. Choi, C. H. Park, I. H. Kim, H. J. Chun, K. Park, and D. K. Han, "Fabrication of core–shell microcapsules using PLGA and alginate for dual growth factor delivery system," J. Control. Release, vol. 147, no. 2, pp. 193–201, 2010.

[25] H. Nie, Z. Dong, D. Y. Arifin, Y. Hu, and C.-H. Wang, "Core/shell microspheres via coaxial electrohydrodynamic atomization for sequential and parallel release of drugs," J. Biomed. Mater. Res. Part A, vol. 95A, no. 3, pp. 709–716, Dec. 2010.

[26] Y. Wang et al., "PLGA/PDLLA core–shell submicron spheres sequential release system: Preparation, characterization and promotion of bone regeneration in vitro and in vivo," Chem. Eng. J., vol. 273, no. Supplement C, pp. 490–501, 2015.

[27] M. Ye, S. Kim, and K. Park, "Issues in long-term protein delivery using biodegradable microparticles," J. Control. Release, vol. 146, no. 2, pp. 241–260, 2010.

[28] C. Berkland, E. Pollauf, D. W. Pack, and K. (Kevin) Kim, "Uniform double-walled polymer microspheres of controllable shell thickness," J. Control. Release, vol. 96, no. 1, pp. 101–111, 2004.

[29] D. Dutta, C. Fauer, K. Hickey, M. Salifu, and S. E. Stabenfeldt, "Tunable delayed controlled release profile from layered polymeric microparticles," J. Mater. Chem. B, vol. 5, no. 23, pp. 4487–4498, 2017.

[30] H. K. Makadia and S. J. Siegel, "Poly Lactic-co-Glycolic Acid (PLGA) as Biodegradable Controlled Drug Delivery Carrier," Polymers (Basel)., vol. 3, no. 3, pp. 1377–1397, Sep. 2011.

[31] H. R. Ansary et al., "Controlled Release of Lysozyme from Double-Walled Poly(Lactide-Co-Glycolide) (PLGA) Microspheres," Polymers, vol. 9, no. 10. 2017.

[32] Y. Gao, D. Zhao, M.-W. Chang, Z. Ahmad, and J.-S. Li, "Optimising the shell thickness-to-radius ratio for the fabrication of oil-encapsulated polymeric microspheres," Chem. Eng. J., vol. 284, no. Supplement C, pp. 963–971, 2016.

[33] S. W. Kim, K.-H. Hwangbo, J. H. Lee, and K. Y. Cho, "Microfluidic fabrication of microparticles with multiple structures from a biodegradable polymer blend,"

RSC Adv., vol. 4, no. 87, pp. 46536–46540, 2014.

[34] X. H. Zhu, C.-H. Wang, and Y. W. Tong, "In vitro characterization of hepatocyte growth factor release from PHBV/PLGA microsphere scaffold," J. Biomed. Mater. Res. Part A, vol. 89A, no. 2, pp. 411–423, May 2009.

[35] E. J. Pollauf, C. Berkland, K. (Kevin) Kim, and D. W. Pack, "In vitro degradation of polyanhydride/polyester core-shell double-wall microspheres," Int. J. Pharm., vol. 301, no. 1, pp. 294–303, 2005.

[36] W. Wang, S. Zhou, L. Sun, and C. Huang, "Controlled delivery of paracetamol and protein at different stages from core–shell biodegradable microspheres," Carbohydr. Polym., vol. 79, no. 2, pp. 437–444, 2010.

[37] P.-W. Ren, X.-J. Ju, R. Xie, and L.-Y. Chu, "Monodisperse alginate microcapsules with oil core generated from a microfluidic device," J. Colloid Interface Sci., vol. 343, no. 1, pp. 392–395, Mar. 2010.

[38] N. T. Hiep, N. D. Hai, and V. Van Toi, "Fabrication of Core-Shell PLGA-Chitosan Microparticles Using Electrospinning: Effects of Polymer Concentration," Int. J. Polym. Sci., 2017.

[39] M.-M. Chen et al., "Sequential delivery of chlorhexidine acetate and bFGF from PLGA-glycol chitosan core-shell microspheres," Colloids Surfaces B Biointerfaces, vol. 151, pp. 189–195, Mar. 2017.

[40] S.-W. Choi, Y. Zhang, and Y. Xia, "Fabrication of Microbeads with a Controllable Hollow Interior and Porous Wall Using a Capillary Fluidic Device," Adv. Funct. Mater., vol. 19, no. 18, pp. 2943–2949, Sep. 2009.

[41] S. Tinkov, R. Bekeredjian, G. Winter, and C. Coester, "Microbubbles as ultrasound triggered drug carriers," J. Pharm. Sci., vol. 98, no. 6, pp. 1935–1961, Jun. 2009.

[42] M. Shi et al., "Double walled POE/PLGA microspheres: encapsulation of water-soluble and water-insoluble proteins and their release properties," J. Control. Release, vol. 89, no. 2, pp. 167–177, 2003.

[43] Y.-Y. Yang, M. Shi, S.-H. Goh, S. M. Moochhala, S. Ng, and J. Heller, "POE/PLGA composite microspheres: formation and in vitro behavior of double walled microspheres," J. Control. Release, vol. 88, no. 2, pp. 201–213, 2003.

[44] H. Nie, Y. Fu, and C.-H. Wang, "Paclitaxel and suramin-loaded core/shell microspheres in the treatment of brain tumors," Biomaterials, vol. 31, no. 33, pp. 8732–8740, 2010.

[45] R. H. Ansary et al., "Preparation, characterization and in vitro release study of BSA-loaded double-walled glucose-poly(lactide-co-glycolide) microspheres," Arch. Pharm. Res., vol. 39, no. 9, pp. 1242–1256, Sep. 2016.

[46] D. He et al., "Core-shell particles for controllable release of drug," Chem. Eng. Sci., vol. 125, pp. 108–120, 2015.

[47] K. J. Pekarek, J. S. Jacob, and E. Mathiowitz, "Double-walled polymer microspheres for controlled drug release," Nature, vol. 367, no. 6460, pp. 258–260, 1994.

[48] N. A. Rahman and E. Mathiowitz, "Localization of bovine serum albumin in double-walled microspheres," J. Control. Release, vol. 94, no. 1, pp. 163–175, 2004.

2

[49]   A. Kelmendi-Doko, J. P. Rubin, K. Klett, C. Mahoney, S. Wang, and K. G. Marra, "Controlled dexamethasone delivery via double-walled microspheres to enhance long-term adipose tissue retention," J. Tissue Eng., vol. 8, p. 2041731417735402, Jan. 2017.

[50]   Y. S. Pek, P. Pitukmanorom, and J. Y. Ying, "Sustained release of bupivacaine for post-surgical pain relief using core-shell microspheres," J. Mater. Chem. B, vol. 2, no. 46, pp. 8194–8200, 2014.

[51]   S. Freitas, H. P. Merkle, and B. Gander, "Microencapsulation by solvent extraction/evaporation: reviewing the state of the art of microsphere preparation process technology," J. Control. Release, vol. 102, no. 2, pp. 313–332, 2005.

[52]   E. C. Tan, R. Lin, and C.-H. Wang, "Fabrication of double-walled microspheres for the sustained release of doxorubicin," J. Colloid Interface Sci., vol. 291, no. 1, pp. 135–143, 2005.

[53]   K. J. Pekarek, J. S. Jacob, and E. Mathiowitz, "One-step preparation of double-walled microspheres," Adv. Mater., vol. 6, no. 9, pp. 684–687, Sep. 1994.

[54]   L. E. Kokai, H. Tan, S. Jhunjhunwala, S. R. Little, J. W. Frank, and K. G. Marra, "Protein bioactivity and polymer orientation is affected by stabilizer incorporation for double-walled microspheres," J. Control. Release, vol. 141, no. 2, pp. 168–176, 2010.

[55]   T. H. Lee, J. Wang, and C.-H. Wang, "Double-walled microspheres for the sustained release of a highly water soluble drug: characterization and irradiation studies," J. Control. Release, vol. 83, no. 3, pp. 437–452, 2002.

[56]   S. R. Abulateefeh and A. M. Alkilany, "Synthesis and Characterization of PLGA Shell Microcapsules Containing Aqueous Cores Prepared by Internal Phase Separation," AAPS PharmSciTech, vol. 17, no. 4, pp. 891–897, 2016.

[57]   Y. Miyazaki, S. Yakou, and K. Takayama, "Effect of Amount of Water in Dispersed Phase on Drug Release Characteristics of Dextran Microspheres Prepared by Emulsion-Solvent Evaporation Process," Biol. Pharm. Bull., vol. 30, no. 3, pp. 543–546, 2007.

[58]   Y. Yeo, N. Baek, and K. Park, "Microencapsulation methods for delivery of protein drugs," Biotechnol. Bioprocess Eng., vol. 6, no. 4, pp. 213–230, 2001.

[59]   N. Teekamp, L. F. Duque, H. W. Frijlink, W. L. Hinrichs, and P. Olinga, "Production methods and stabilization strategies for polymer-based nanoparticles and microparticles for parenteral delivery of peptides and proteins," Expert Opin. Drug Deliv., vol. 12, no. April 2017, pp. 1–21, 2015.

[60]   K. Park et al., "Formulation composition, manufacturing process, and characterization of poly(lactide-co-glycolide) microparticles," J. Control. Release, vol. 329, pp. 1150–1161, 2021.

[61]   Y. Yeo and K. Park, "Control of encapsulation efficiency and initial burst in polymeric microparticle systems," Arch. Pharm. Res., vol. 27, no. 1, p. 1, 2004.

[62]   M. Ali, X. F. Walboomers, J. A. Jansen, and F. Yang, "Influence of formulation parameters on encapsulation of doxycycline in PLGA microspheres prepared by double emulsion technique for the treatment of periodontitis," J. Drug Deliv. Sci. Technol., vol. 52, pp. 263–271, 2019.

[63]   V. Jakub, M. Kejdušová, K. Dvořáč, and D. Vetchý, "Influence of formulation and process parameters on the characteristics of PLGA-based microparticles with controlled drug release," Ces. a Slov. Farm., vol. 62, no. 3, pp. 120–126, 2013.

[64]   N. K. Varde and D. W. Pack, "Microspheres for controlled release drug delivery," Expert Opin. Biol. Ther., vol. 4, no. 1, pp. 35–51, Jan. 2004.

[65]   J. L. Cleland, "Single-administration vaccines: controlled-release technology to mimic repeated immunizations," Trends Biotechnol., vol. 17, no. 1, pp. 25–29, Jan. 1999.

[66]   W. Li, H. Dong, G. Tang, T. Ma, and X. Cao, "Controllable microfluidic fabrication of Janus and microcapsule particles for drug delivery applications," RSC Adv., vol. 5, no. 30, pp. 23181–23188, 2015.

[67]   S. Mao, Y. Shi, L. Li, J. Xu, A. Schaper, and T. Kissel, "Effects of process and formulation parameters on characteristics and internal morphology of poly(d,l-lactide-co-glycolide) microspheres formed by the solvent evaporation method," Eur. J. Pharm. Biopharm., vol. 68, no. 2, pp. 214–223, 2008.

[68]   Z. Kang, P. Zhu, T. Kong, and L. Wang, "A Dewetting Model for Double-Emulsion Droplets," Micromachines, vol. 7, no. 11, p. 196, Nov. 2016.

[69]   S.-Y. Teh, R. Lin, L.-H. Hung, and A. P. Lee, "Droplet microfluidics," Lab Chip, vol. 8, no. 2, pp. 198–220, 2008.

[70]   R. K. Shah et al., "Designer emulsions using microfluidics," Mater. Today, vol. 11, no. 4, pp. 18–27, Apr. 2008.

[71]   W. Wang, M.-J. Zhang, and L.-Y. Chu, "Microfluidic approach for encapsulation via double emulsions," Curr. Opin. Pharmacol., vol. 18, pp. 35–41, Oct. 2014.

[72]   L.-Y. Chu, A. S. Utada, R. K. Shah, J.-W. Kim, and D. A. Weitz, "Controllable Monodisperse Multiple Emulsions," Angew. Chemie Int. Ed., vol. 46, no. 47, pp. 8970–8974, Dec. 2007.

[73]   W. J. Duncanson, T. Lin, A. R. Abate, S. Seiffert, R. K. Shah, and D. A. Weitz, "Microfluidic synthesis of advanced microparticles for encapsulation and controlled release," Lab Chip, vol. 12, no. 12, pp. 2135–2145, 2012.

[74]   D. Lensen, K. van Breukelen, D. M. Vriezema, and J. C. M. van Hest, "Preparation of Biodegradable Liquid Core PLLA Microcapsules and Hollow PLLA Microcapsules Using Microfluidics," Macromol. Biosci., vol. 10, no. 5, pp. 475–480, May 2010.

[75]   T. Kong et al., "Microfluidic fabrication of polymeric core-shell microspheres for controlled release applications," Biomicrofluidics, vol. 7, no. 4, p. 44128, Jul. 2013.

[76]   F. Tu and D. Lee, "Controlling the Stability and Size of Double-Emulsion-Templated Poly(lactic-co-glycolic) Acid Microcapsules," Langmuir, vol. 28, no. 26, pp. 9944–9952, Jul. 2012.

[77]   N. Mavrogiannis, M. Ibo, X. Fu, F. Crivellari, and Z. Gagnon, "Microfluidics made easy: A robust low-cost constant pressure flow controller for engineers and cell biologists," Biomicrofluidics, vol. 10, no. 3, p. 34107, May 2016.

[78]   J. R. Lake, K. C. Heyde, and W. C. Ruder, "Low-cost feedback-controlled syringe pressure pumps for microfluidics applications," PLoS One, vol. 12, no.

4, pp. e0175089–e0175089, Apr. 2017.

[79]	F. Ramazani et al., "Strategies for encapsulation of small hydrophilic and amphiphilic drugs in PLGA microspheres: State-of-the-art and challenges," Int. J. Pharm., vol. 499, no. 1–2, pp. 358–367, 2016.

[80]	M. B. Romanowsky, A. R. Abate, A. Rotem, C. Holtze, and D. A. Weitz, "High throughput production of single core double emulsions in a parallelized microfluidic device," Lab Chip, vol. 12, no. 4, pp. 802–807, 2012.

[81]	C. B. Roces et al., "Manufacturing Considerations for the Development of Lipid Nanoparticles Using Microfluidics," Pharmaceutics, vol. 12, no. 11. 2020.

[82]	Y.-S. Lin, C.-M. Cheng, and C.-F. Chien, "How Smart Manufacturing Can Help Combat the COVID-19 Pandemic," Diagnostics, vol. 11, no. 5. 2021.

[83]	H. C. Shum, J.-W. Kim, and D. A. Weitz, "Microfluidic Fabrication of Monodisperse Biocompatible and Biodegradable Polymersomes with Controlled Permeability," J. Am. Chem. Soc., vol. 130, no. 29, pp. 9543–9549, Jul. 2008.

[84]	P. Davoodi et al., "Coaxial electrohydrodynamic atomization: Microparticles for drug delivery applications," J. Control. Release, vol. 205, no. Supplement C, pp. 70–82, 2015.

[85]	Q. Xu, H. Qin, Z. Yin, J. Hua, D. W. Pack, and C.-H. Wang, "Coaxial electrohydrodynamic atomization process for production of polymeric composite microspheres," Chem. Eng. Sci., vol. 104, no. Supplement C, pp. 330–346, 2013.

[86]	Y. Chen, Z. Yue, S. E. Moulton, P. Hayes, M. J. Cook, and G. G. Wallace, "A simple and versatile method for microencapsulation of anti-epileptic drugs for focal therapy of epilepsy," J. Mater. Chem. B, vol. 3, no. 36, pp. 7255–7261, 2015.

[87]	D. N. Nguyen, C. Clasen, and G. Van den Mooter, "Pharmaceutical Applications of Electrospraying," J. Pharm. Sci., vol. 105, no. 9, pp. 2601–2620, 2016.

[88]	Y. Wu et al., "Electrosprayed core-shell microspheres for protein delivery," Chem. Commun., vol. 46, no. 26, pp. 4743–4745, 2010.

[89]	A. Abeyewickreme, A. Kwok, J. R. McEwan, and S. N. Jayasinghe, "Bio-electrospraying embryonic stem cells: interrogating cellular viability and pluripotency," Integr. Biol., vol. 1, no. 3, pp. 260–266, Mar. 2009.

[90]	Y.-H. Lee, M.-Y. Bai, and D.-R. Chen, "Multidrug encapsulation by coaxial tri-capillary electrospray," Colloids Surfaces B Biointerfaces, vol. 82, no. 1, pp. 104–110, 2011.

[91]	C. Berkland, K. (Kevin) Kim, and D. W. Pack, "Fabrication of PLG microspheres with precisely controlled and monodisperse size distributions," J. Control. Release, vol. 73, no. 1, pp. 59–74, 2001.

[92]	C. Berkland, A. Cox, K. (Kevin) Kim, and D. W. Pack, "Three-month, zero-order piroxicam release from monodispersed double-walled microspheres of controlled shell thickness," J. Biomed. Mater. Res. Part A, vol. 70A, no. 4, pp. 576–584, Sep. 2004.

[93]	E. J. Pollauf, K. K. Kim, and D. W. Pack, "Small-Molecule Release from poly(D,L-Lactide)/Poly(D,L-Lactide-co-Glycolide) Composite Microparticles," J. Pharm. Sci., vol. 94, no. 9, pp. 2013–2022, 2005.

[94]   Q. Xu, Y. Xia, C.-H. Wang, and D. W. Pack, "Monodisperse double-walled microspheres loaded with chitosan-p53 nanoparticles and doxorubicin for combined gene therapy and chemotherapy," J. Control. Release, vol. 163, no. 2, pp. 130–135, 2012.

[95]   Q. Xu, S. E. Chin, C.-H. Wang, and D. W. Pack, "Mechanism of drug release from double-walled PDLLA(PLGA) microspheres," Biomaterials, vol. 34, no. 15, pp. 3902–3911, 2013.

[96]   Q. Xu et al., "Combined modality doxorubicin-based chemotherapy and chitosan-mediated p53 gene therapy using double-walled microspheres for treatment of human hepatocellular carcinoma," Biomaterials, vol. 34, no. 21, pp. 5149–5162, 2013.

[97]   Y. Xia, P. F. Ribeiro, and D. W. Pack, "Controlled protein release from monodisperse biodegradable double-wall microspheres of controllable shell thickness," J. Control. Release, vol. 172, no. 3, pp. 707–714, 2013.

[98]   R. A. Perez and H.-W. Kim, "Core–shell designed scaffolds for drug delivery and tissue engineering," Acta Biomater., vol. 21, pp. 2–19, Jul. 2015.

[99]   D. Jain, R. Raturi, V. Jain, P. Bansal, and R. Singh, "Recent technologies in pulsatile drug delivery systems," Biomatter, vol. 1, no. 1, pp. 57–65, 2011.

[100]   K. Kardani, A. Bolhassani, and S. Shahbazi, "Prime-boost vaccine strategy against viral infections: Mechanisms and benefits," Vaccine, vol. 34, no. 4, pp. 413–423, 2016.

[101]   S. Lofthouse, "Immunological aspects of controlled antigen delivery," Adv. Drug Deliv. Rev., vol. 54, no. 6, pp. 863–870, 2002.

[102]   A. Sanchez, R. K. Gupta, M. J. Alonso, G. R. Siber, and R. Langer, "Pulsed controlled-release system for potential use in vaccine delivery," J. Pharm. Sci., vol. 85, no. 6, pp. 547–552, Jun. 1996.

[103]   Y. S. Pek, H. Wu, S. T. Mohamed, and J. Y. Ying, "Long-Term Subconjunctival Delivery of Brimonidine Tartrate for Glaucoma Treatment Using a Microspheres/Carrier System," Adv. Healthc. Mater., vol. 5, no. 21, pp. 2823–2831, 2016.

[104]   Q. Zhao and M. Wang, "Manipulating the release of growth factors from biodegradable microspheres for potentially different therapeutic effects by using two different electrospray techniques for microsphere fabrication," Polym. Degrad. Stab., vol. 162, pp. 169–179, 2019.

[105]   S. Fredenberg, M. Wahlgren, M. Reslow, and A. Axelsson, "The mechanisms of drug release in poly(lactic-co-glycolic acid)-based drug delivery systems--a review.," Int. J. Pharm., vol. 415, no. 1–2, pp. 34–52, 2011.

[106]   P.-C. Chang, M.-C. Chung, C. Lei, L. Y. Chong, and C.-H. Wang, "Biocompatibility of PDGF-simvastatin double-walled PLGA (PDLLA) microspheres for dentoalveolar regeneration: A preliminary study," J. Biomed. Mater. Res. Part A, vol. 100A, no. 11, pp. 2970–2978, Nov. 2012.

[107]   Y.-H. Lee, F. Mei, M.-Y. Bai, S. Zhao, and D.-R. Chen, "Release profile characteristics of biodegradable-polymer-coated drug particles fabricated by dual-capillary electrospray," J. Control. Release, vol. 145, no. 1, pp. 58–65, 2010.

[108]   H. Zhao et al., "Local antitumor effects of intratumoral delivery of rlL-2 loaded

sustained-release dextran/PLGA–PLA core/shell microspheres," Int. J. Pharm., vol. 450, no. 1, pp. 235–240, 2013.

[109] P.-C. Chang et al., "PDGF-Simvastatin Delivery Stimulates Osteogenesis in Heat-induced Osteonecrosis," J. Dent. Res., vol. 91, no. 6, pp. 618–624, Apr. 2012.

[110] M. Yu et al., "Core/shell PLGA microspheres with controllable in vivo release profile via rational core phase design," Artif. Cells, Nanomedicine, Biotechnol., vol. 46, no. sup1, pp. 1070–1079, Oct. 2018.

[111] L. Huang, J. Zhou, Y. Chen, W. Li, X. Han, and L. Wang, "Engineering Microcapsules for Simultaneous Delivery of Combinational Therapeutics," Adv. Mater. Technol., vol. 5, no. 11, p. 2000623, Nov. 2020.

[112] E. E. Ekanem, Z. Zhang, and G. T. Vladisavljević, "Facile microfluidic production of composite polymer core-shell microcapsules and crescent-shaped microparticles," J. Colloid Interface Sci., vol. 498, pp. 387–394, 2017.

[113] M. Yan, J. Ni, H. Shen, D. Song, M. Ding, and J. Huang, "Local controlled release of simvastatin and PDGF from core/shell microspheres promotes bone regeneration in vivo," RSC Adv., vol. 7, no. 32, pp. 19621–19629, 2017.

[114] P.-C. Chang et al., "Sequential Platelet-Derived Growth Factor–Simvastatin Release Promotes Dentoalveolar Regeneration," Tissue Eng. Part A, vol. 20, no. 1–2, pp. 356–364, Jan. 2014.

[115] P.-C. Chang, A. S. Dovban, L. P. Lim, L. Y. Chong, M. Y. Kuo, and C.-H. Wang, "Dual delivery of PDGF and simvastatin to accelerate periodontal regeneration in vivo," Biomaterials, vol. 34, no. 38, pp. 9990–9997, 2013.

[116] D. Lee et al., "Factors affecting the co-axial electrospraying of core–shell-structured poly(d,l-lactide-co-glycolide) microparticles," Jpn. J. Appl. Phys., vol. 57, no. 11, p. 116702, 2018.

[117] H.-W. Yeh and D.-R. Chen, "In vitro release profiles of PLGA core-shell composite particles loaded with theophylline and budesonide," Int. J. Pharm., vol. 528, no. 1, pp. 637–645, 2017.

2

Chapter 3

The mechanism behind the biphasic pulsatile drug release from physically mixed poly(DL-lactic(-co-glycolic) acid)-based compacts

Max Beugeling [1,*], Niels Grasmeijer [1,*], Philip A. Born [1], Merel van der Meulen [1], Renée S. van der Kooij [1], Kevin Schwengle [1], Lieven Baert [2], Katie Amssoms [3], Henderik W. Frijlink [1], and Wouter L.J. Hinrichs [1]

[1] Department of Pharmaceutical Technology and Biopharmacy, University of Groningen, Antonius Deusinglaan 1, 9713 AV, Groningen, the Netherlands
[2] Jalima Pharma bvba, Jozef Van Walleghemstraat 11, 8200 Brugge, Belgium
[3] Infectious Diseases & Vaccines Therapeutic Area, Janssen Research & Development, A Division of Janssen Pharmaceutica NV, Turnhoutseweg 30, 2340 Beerse, Belgium
* Authors contributed equally

Abstract

Successful immunization often requires a primer, and after a certain lag time, a booster administration of the antigen. To improve the vaccinees' comfort and compliance, a single-injection vaccine formulation with a biphasic pulsatile release would be preferable. Previous work has shown that such a release profile can be obtained with compacts prepared from physical mixtures of various poly(dl-lactic(-*co*-glycolic) acid) types [1]. However, the mechanism behind this release profile is not fully understood. In the present study, the mechanism that leads to this biphasic pulsatile release was investigated by studying the effect of the glass transition temperature (T_g) of the polymer, the temperature of compaction, the compression force, the temperature of the release medium, and the molecular weight of the incorporated drug on the release behavior. Compaction resulted in a porous compact. Once immersed into release medium with a temperature above the T_g of the polymer, the drug was released by diffusion through the pores. Simultaneously, the polymer underwent a transition from the glassy state into the rubbery state. The pores were gradually closed by viscous flow of the polymer and further release was inhibited. After a certain period of time, the polymer matrix ruptured, possibly due to a build-up in osmotic pressure, resulting in a pulsatile release of the remaining amount of drug. The compression force and the molecular weight of the incorporated drug did not influence the release profile. Understanding this mechanism could contribute to further develop single-injection vaccines.

3.1 Introduction

Annually, vaccination prevents approximately 2–3 million deaths caused by more than thirty different infectious diseases [2,3]. Successful vaccination, i.e. providing protection by creating pools of long-term memory B- and T-cells, often requires a primary (primer) and after a certain lag time, a secondary (booster) administration of the vaccine [4,5]. Hence, most traditional vaccines are administered using a multi-injection regime [6]. This multi-injection regime is discomforting for the vaccinee and might compromise compliance [6,7]. Improved vaccinees' comfort and compliance would be achieved with an injectable device with a biphasic pulsatile release profile. Such an implant releases one part of the antigenic substance instantly (primer), while the remainder is released after a certain lag time (booster) [6,7]. Ideally, this lag time can be tailored to the requirements of the specific antigen that is used.

Previous work on the development of such a single-injection vaccine has shown the use of various polymers [7]. Of these polymers, poly(dl-lactic(-*co*-glycolic) acid) (PL(G)A) is most widely investigated. PL(G)A is a biodegradable and biocompatible copolymer that has been used in many drug products approved by the Food and Drug Administration [8,9]. The copolymer consists of lactic and glycolic acid monomers. By changing the lactic:glycolic acid ratio of the copolymer, physicochemical characteristics (e.g. glass transition temperature (T_g) and degradation rate) of the polymer can be tailored [8-10]. Other ways to tailor the physicochemical characteristics of the polymer are using different molecular weights of the polymer and changing the end group of the polymer [8-10].

A common method to achieve a biphasic pulsatile release profile is to develop a core-shell device. In such a device, a water-soluble core containing the active component is encapsulated in a water-insoluble biodegradable polymer shell to enable a delayed pulsatile release. This device can be combined with an additional water-soluble outer layer containing the active component, or can simply be co-injected with a solution containing the active component to obtain the desired biphasic pulsatile release profile. A great disadvantage of core-shell devices is that they require complicated production methods, amongst which emulsification, coating, multiple-compaction processes, and more recently, a microfabrication production method named StampEd Assembly of polymer Layers [7,11-15].

However, in 2000, Murakami et al. [1] reported a device consisting of a physical mixture of theophylline as a model drug and several types of PL(G)A, simply prepared by a single compaction procedure. This device exhibited the desired biphasic pulsatile release profile. The mechanism behind the biphasic pulsatile drug release from these PL(G)A-based compacts, however, is not fully understood. Furthermore, although the single compaction step seems a simple process, the authors used a complicated emulsion technique to prepare polymeric nanoparticles for compaction and it is unclear whether similar results can be obtained if larger polymer particles are used.

Based on literature, monolithic PL(G)A-based systems, such as the physically mixed compacts described by Murakami et al. [1] seem less suitable for protein-based vaccines. An incomplete release of native protein from monolithic devices due to protein instability is often observed [16-18]. Major reasons for protein instability within these

devices are the formation of an acidic microclimate within the matrix and incompatibility of the polymer degradation products and proteins, leading to aggregation and inactivation of the protein [19-22]. To overcome these issues, several excipients (e.g. magnesium hydroxide and shellac) could potentially be incorporated to stabilize proteins within monolithic PL(G)A-based devices [23,24]. However, polysaccharides, used as antigens in bacterial vaccines (e.g. pneumococcal polysaccharide vaccine) [25] are more stable and compatible with polymer degradation products. Therefore, a device based on a physical mixture might be more interesting for the biphasic delivery of a polysaccharide-based vaccine.

We hypothesize that compaction at a temperature below the T_g of the polymer results in a porous compact, as the polymer is in the glassy state. Once immersed into release medium with a temperature above the T_g of the polymer, the drug can diffuse through the pores of the compact, leading to a pulsatile burst release. However, at the same time, the polymer undergoes a transition from the glassy state into the rubbery state. Therefore, the pores of the compact are gradually closed by viscous flow of the polymer and further release is inhibited. After a certain period of time, the polymer matrix ruptures, resulting in a pulsatile boost release. To investigate this hypothesis, physically mixed compacts based on theophylline as a model drug and various types of PL(G)A were produced. The influence of the T_g of the polymer, the temperature of compaction, the compression force, and the temperature of the release medium on the release of theophylline from physically mixed PL(G)A-based compacts were investigated. To investigate the influence of the molecular weight of the incorporated drug on the release, blue dextran (BD) with a molecular weight of either 70 kDa or 2000 kDa was incorporated in the physically mixed compact. As bacterial vaccines are often polysaccharide-based, BD was also used to mimic bacterial vaccines. Furthermore, core-shell compacts consisting of a theophylline containing core tablet and a nonporous and a porous shell composed of PLA with a high T_g were used as a control. Understanding the mechanism behind the biphasic pulsatile release could contribute to the further development of an effective single-injection vaccine.

3.2 Materials and methods

3.2.1 Materials
Poly(dl-lactic-*co*-glycolic acid) with a lactic:glycolic acid ratio of 50:50 and an intrinsic viscosity of 0.2 dL/g (PLGA5002), poly(dl-lactic acid) with an intrinsic viscosity of 0.2 dL/g (PLA02), and 0.5 dL/g (PLA05) were purchased from Corbion Purac Biomaterials (Gorinchem, The Netherlands). Theophylline anhydrous was obtained from Boehringer Ingelheim (Ingelheim am Rhein, Germany). BD with molecular weights of 70 kDa and 2000 kDa were purchased from TdB Consultancy (Uppsala, Sweden). Sodium dihydrogen phosphate and disodium hydrogen phosphate were purchased from Merck (Darmstadt, Germany). Sodium azide was obtained from Acros Organics (Geel, Belgium). Inulin (4 kDa) with a degree of polymerization of 23 was a generous gift from Sensus (Roosendaal, The Netherlands). Sodium chloride was purchased from Fluka Chemie GmbH (Buchs, Switzerland). Mannitol was purchased from Roquette (Nord-Pas-de-Calais, France). All experiments were performed with Millipore, type 1 water.

3.2.2 Powder formulations for physically mixed compacts

For theophylline containing compacts, an aqueous solution containing 5 mg/ml theophylline and 50 mg/ml inulin was prepared. Of this solution, amounts of 2 ml were transferred to 20 ml vials. The solutions were freeze-dried using a Christ Epsilon 2-4 LSC freeze-dryer (Salm & Kipp, Breukelen, The Netherlands) at 0.220 mBar and a shelf temperature of −35 °C for 24 h, after which the pressure was reduced to 0.050 mBar while the shelf temperature was increased to 25 °C over a period of 24 h. The obtained freeze-dried powder was then ground and mixed with mannitol in a smooth agate mortar. This powder mixture was then physically mixed with PLGA5002 or PLA02 in a smooth agate mortar. Prior to mixing, PLGA5002 and PLA02 were ground with an AR100 mill (Moulinex, Écully, France) and subsequently sieved with a 150 μm sieve. The resulting powder blends were used for the production of the physically mixed PL(G)A-based compacts. The final powder formulation consisted of 4 wt-% freeze-dried theophylline and inulin (in a 1:10 w/w ratio), 5.1 wt-% mannitol, and 90.9 wt-% polymer.

For BD containing compacts, an aqueous solution containing 5 mg/ml BD with either a molecular weight of 70 kDa or 2000 kDa and 6.4 mg/ml mannitol was prepared. Solutions were freeze-dried as described above. The obtained freeze-dried powder was then physically mixed with PLGA5002 with a particle size of ≤150 μm in a smooth agate mortar. The final powder formulation consisted of 4 wt-% BD (with a molecular weight of either 70 kDa or 2000 kDa), 5.1 wt-% mannitol, and 90.9 wt-% polymer.

3.2.3 Production of physically mixed PL(G)A-based compacts

The powder blends containing theophylline were compacted using a hydraulic press (Hydro Mooi, Appingedam, The Netherlands) and an oblong tablet die (6 × 2 mm). Approximately 26 mg of the powder formulation described above was compressed at room temperature (RT) with a compaction load of 7 kN and a compaction rate of 0.7 kN/s, or a compaction load of 2.8 kN and a compaction rate of 0.28 kN/s. In both cases the hold time was 10 s. To investigate the influence of temperature, the compact containing tablet die compressed at a compaction load of 2.8 kN was stored in an oven for 1 h at 48 °C to allow viscous flow of the polymer. After removal from the oven, the compact was immediately re-compressed using the same settings as described above. For BD containing compacts, approximately 27.5 mg of the powder formulation was compressed at RT with a compaction load of either 3 kN and a compaction rate of 0.3 kN/s, or a compaction load of 9 kN and a compaction rate of 0.9 kN/s. In both cases the hold time was 10 s. These compaction loads were chosen to further investigate the influence of compression force on the release profile. Note that with the specific oblong tablet die, three tablets were simultaneously prepared, resulting in a compaction force per tablet that was three times lower than the total compaction force.

3.2.4 Production of PLA core-shell compacts

First, PLA05 pellets were milled with a Pulverisette 14 (Fritsch GmbH, Idar-Oberstein, Germany) at 6000–10,000 rpm and sieved with a 200 μm sieve. To produce the core tablet, approximately 25 mg of a physical mixture consisting of 44 wt-% freeze-dried theophylline and inulin (in a 1:10 w/w ratio) and 56 wt-% mannitol was compressed in a 7 mm diameter tablet die at a compaction load of 5 kN, a compaction rate of 0.5 kN/s,

and a hold time of 10 s. Subsequently, the core was inserted into a 9 mm diameter tablet die, in which ground PLA02 or PLA05 was added as top layer (23.5 mg) and as bottom layer (93 mg). The PLA02 or PLA05 shell was then compressed at a compaction load of 12.5 kN, a compaction rate of 1.25 kN/s, and a hold time of 10 s. To investigate the effect of heating on the release characteristics of PLA05 core-shell compacts, the same procedure was used except that compression was at a compaction load of 5 kN, a compaction rate of 0.5 kN/s, and a hold time of 10 s. Thereafter, the core-shell compact containing tablet die was stored in an oven for 1 h at 80 °C to allow for sufficient viscous flow of the polymer. After removal from the oven, the core-shell compact was immediately re-compressed using the same settings as described above. The resulting core-shell compact had a shell thickness of approximately 300 μm on top and 1000 μm at the bottom and the sides.

3.2.5 Differential scanning calorimetry (DSC)

DSC measurements of PLGA5002, PLA02, and PLA05 were done with a Q2000 differential scanning calorimeter (TA Instruments, New Castle, DE, United States). Dry samples were weighed in open Tzero pans at ambient conditions. The samples were preheated to a temperature of 120 °C prior to scanning at a rate of 20 °C/min and a temperature range of −20 °C to 90 °C. The same samples were used to determine the T_g when moisturized. To achieve this, 40 μL of water was added to the sample and the sample was moisturized over a period of 30 min. The excess of water was subsequently removed. Finally, the pan was hermetically sealed, after which the sample was cooled to -50 °C and then heated at a rate of 20 °C/min to a temperature of 90 °C. Each sample was measured directly and 2, 5, and 7.5 h after moisturizing. To gain insight in the degradation process of PL(G)A, DSC measurements were conducted on physically mixed theophylline containing PLGA5002 compacts after different exposure times to the release medium. At predetermined time points, compacts exposed to the release medium at 37 °C were removed from the release medium and cut to pieces using a scalpel. The samples were weighed in open T_{zero} pans at ambient conditions and were first preheated for 10 min at a temperature of 120 °C. After this preheating step, the samples were cooled to −20 °C and then heated with a rate of 20 °C/min to 90 °C. The T_g was defined as the onset of the transition.

3.2.6 In vitro *release of theophylline and blue dextran from physically mixed PL(G)A-based compacts and PLA core-shell compacts*

The *in vitro* release tests were performed in 20 ml (for physically mixed theophylline containing compacts) or 50 ml (for core-shell compacts) 100 mM phosphate buffered saline (PBS) (pH 7.4) supplemented with 0.02% (w/v) sodium azide. The temperature of the release medium in the standard procedure was 37 °C. However, to investigate the influence of release medium temperature, physically mixed compacts were immersed into release medium of either 4 °C, RT, or 37 °C. The release medium was first preheated or precooled to the temperature at which the release was studied. The release studies were performed in a shaking water bath (80 rpm) to allow refreshment of the release medium at the surface of the compacts. Theophylline release was measured with a UV–visible spectrophotometer (Thermo Spectronic Unicam UV-540, Waltham, MA, United States) at $\lambda = 272$ nm and at $\lambda = 325$ nm (reference wavelength). Sampling was performed by taking 2.5–3 ml of the release medium through a flow-through cuvette (L = 10 mm)

and returning the sample back to the release medium. The in vitro release tests with BD containing compacts were performed in 1 ml release medium at a temperature of 37 °C. At predetermined time points, samples of 0.9 ml were taken and 0.9 ml of fresh preheated (37 °C) release medium was added to the vial to keep the volume constant. The samples were centrifuged for 15 min at 14,800 rpm and the supernatant was used to measure BD release at $\lambda = 616$ nm using a flow-through cuvette (L = 50 mm).

3.2.7 Scanning electron microscopy (SEM)

SEM images of physically mixed compacts were taken with a JEOL 6460 microscope (JEOL, Tokyo, Japan). To investigate the influence of the compression force on surface porosity, SEM images of PLA02 compacts compressed at 2.8 kN and 7 kN were taken prior to release. Theophylline containing PLA02 compacts were imaged after 3 days of release at 4 °C, RT, or 37 °C. In addition, physically mixed PLA02 compacts were imaged after 4, 8, and 72 h of release at 37 °C. To gain insight in the boost release, theophylline containing PLGA5002 compacts were imaged after 18 days of exposure to the release medium. Prior to imaging, incubated compacts were freeze-dried using the same program as described above. The dry compacts were stuck on top of double-sided adhesive carbon tape on aluminum disks and coated with a 17 nm layer of gold in a JFC-1300 sputtering device fitted with an MTM-20 thickness controller system (JEOL, Tokyo, Japan). An acceleration voltage of 10 kV, a spot size of 25, and a Z-distance of 15 mm was used for all recordings.

3.2.8 Comparison of the release profiles

The release profiles were compared by using the similarity factor (f_2), which is calculated using the following equation [26,27]:

$$f_2 = 50 * \log\{[1 + 1/n \sum n_{t=1}(R_t - T_t)^2]^{-0.5} * 100\}$$

where n is the number of release sampling times, and R_t and T_t are the average percentage drug released at each time point from the reference formulation and the test formulation, respectively. The time point t = 0 was excluded and only one point after more than 85% drug release was included, as recommended by Shah et al. [27]. If the $f_2 > 50$, the release profiles can be considered similar.

3.3. Results

3.3.1 Glass transition temperatures of the polymers

The T_g's of PLGA5002, PLA02, and PLA05 were measured with DSC. The average onset of the transition of two measurements were 31.6 °C, 33.5 °C, and 44.3 °C, respectively. Furthermore, moisturizing the polymers with water reduced the T_g to 19.1 °C, 24.3 °C, and 37.1 °C, respectively. The latter values were measured 5 h after moisturizing, this was when the T_g reached a plateau value.

3.3.2 In vitro *release of theophylline from physically mixed PLGA5002- and PLA02-based compacts*

Figure 1 shows the release at 37 °C of theophylline from compacts with either a PLGA5002 or a PLA02 polymer matrix prepared at a compaction load of 7 kN and RT.
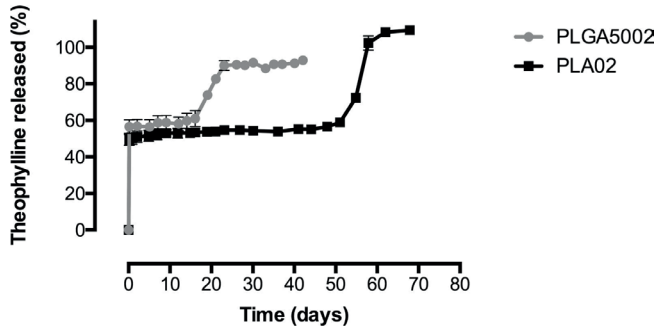

Figure 1. Release of theophylline from physically mixed compacts with either a PLGA5002 (grey) or a PLA02 (black) polymer matrix at 37 °C, prepared at a compaction load of 7 kN and RT. Standard deviation is indicated (n = 3).

The physically mixed compacts released 56.6 ± 3.7% and 49.3 ± 2.9% of the total theophylline content during the initial burst release, respectively. The remaining content was released as a pulse after a lag phase. The lag phase was substantially shorter for PLGA5002-based compacts (approximately 18 days) than for PLA02-based compacts (approximately 50 days).

3.3.3 Effect of compression force and heating on theophylline release from PLA02-based compacts

Physically mixed compacts with PLA02 were compressed at 2.8 kN, instead of 7 kN to study the effect of a possibly more porous compact on the burst release. Furthermore, compacts compressed at 2.8 kN were heated in an oven set at 48 °C for 1 h in between two compaction procedures to study the effect of heating. A lower compression force resulted in a visibly more porous surface of the compact (Figure 2-8, Figure 9A and B), but only in a minor increase in burst release (Figure 2-8, Figure 9C). The burst release was 55.8 ± 0.9% and 49.3 ± 2.9% for compacts compressed at 2.8 kN and 7 kN, respectively. However, based on the f_2, which was 63.3, the two release profiles were found to be similar. Heating of the compact resulted in a reduction of the burst release of theophylline from 55.8 ± 0.9% to 22.6 ± 5.8% (Figure 3). The lag phase duration was unaffected, and although a small fraction appeared to release during the lag phase, most of the remaining theophylline was released as a pulse after the lag phase. Based on the f_2, which was 27.4, the two release profiles were not similar.

Figure 2. (A–C) SEM images (top view) of a physically mixed PLA02 compact prepared at RT and a compaction load of 2.8 kN (A) and 7 kN (B) at a magnification of 30× and the release of theophylline at 37 °C from these compacts (2.8 kN (grey) and 7 kN (black)) (C). Standard deviation is indicated (n = 3).
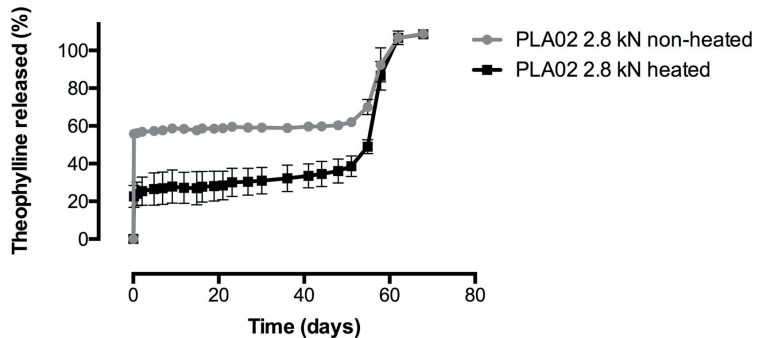
Figure 3. Release of theophylline at 37 °C from physically mixed PLA02 compacts compressed at 2.8 kN that are either heated for 1 h at 48 °C (black) or not heated (grey) during compaction. Standard deviation is indicated (n = 3).

3.3.4 Effect of release medium temperature on theophylline release from PLA02-based compacts
Physically mixed PLA02-based compacts compressed at a compaction load of 7 kN and RT were set to release at 4 °C, RT, and 37 °C (Figure 4). At RT and below, all theophylline was released during the burst in the first 3 days, whereas at 37 °C, $51.1 \pm 3.1\%$ of theophylline was released. In addition, based on the f_2, which was 26.9, the release profiles at 4 °C and RT were different. SEM images from physically mixed PLA02-based

compacts containing theophylline directly after compaction (Figure 2-8, Figure 9B) and after 3 days of release at 4 °C, RT, and 37 °C showed a noticeable difference in the surface structure of the compacts (Figure 5A–C). Directly after compaction, a rough, porous structure was observed. After 3 days of release at 4 °C and RT, the compacts still showed a rough, porous structure. However, after 3 days of release at 37 °C, the surface appeared to be completely smooth and nonporous. Figure 6A–C shows SEM images of PLA02 compacts after 4, 8, and 72 h of release at 37 °C. After 4 and 8 h of release at 37 °C, a few pores can still be seen on the surface of the compact. However, after 72 h, the compact showed a smooth, nonporous surface.
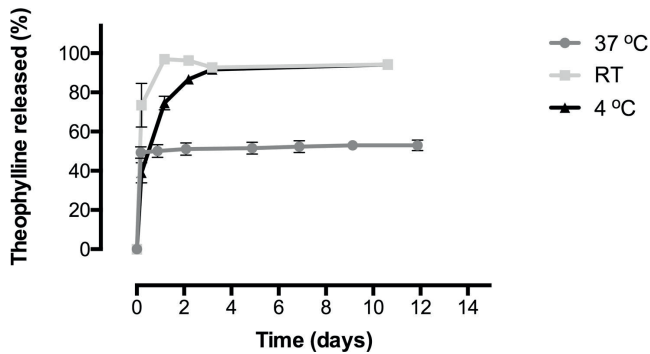
Figure 4. Release of theophylline from physically mixed PLA02 compacts prepared at a compaction load of 7 kN and RT, at 4 °C (black), RT (light grey), and 37 °C (dark grey). Standard deviation is indicated (n = 3).
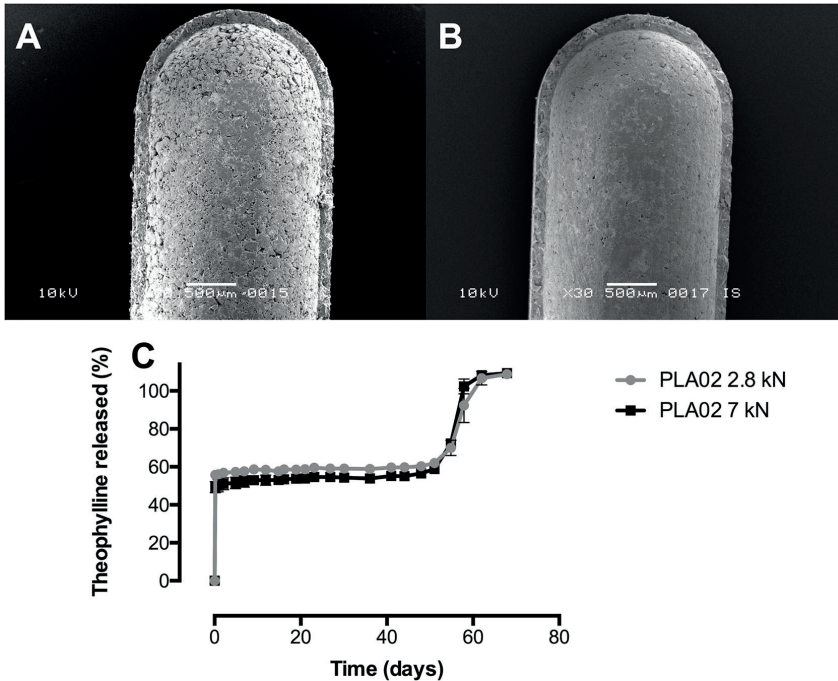

Figure 5. (A–C) SEM images (top view) of a physically mixed PLA02 compact prepared at a compaction load of 7 kN and RT after 3 days of release at 4 °C (A), RT (B), and 37 °C (C) at a magnification of 30×.

Figure 6. (A–C) SEM images (top view) of a physically mixed PLA02 compact prepared at a compaction load of 7 kN and RT after 4 h (A), 8 h (B), and 72 h (C) of release at 37 °C at a magnification of 30×.

3.3.5 Degradation of PLGA: DSC measurements after different exposure times to the release medium and boost release

Figure 7A shows thermograms of theophylline containing PLGA5002-based compacts compressed at 7 kN and RT after different exposure times to the release medium at 37 °C.

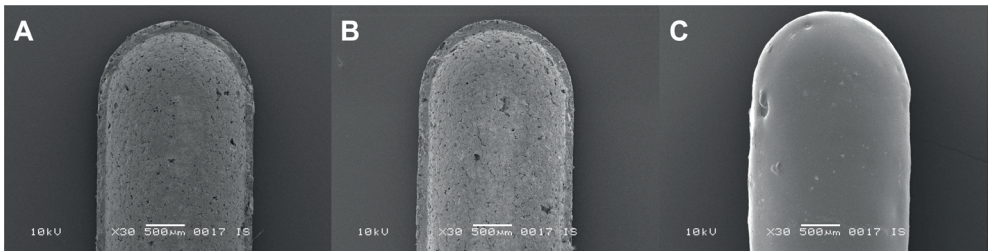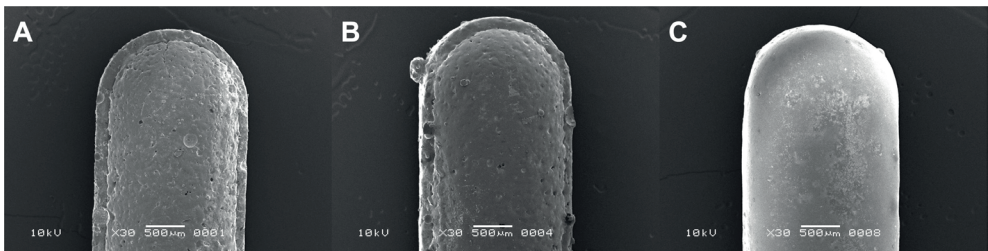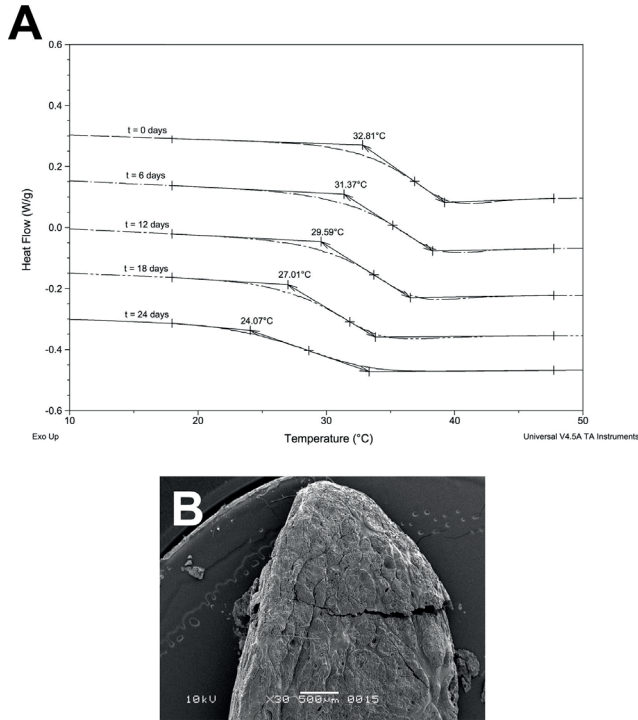**Figure 7.** A and B DSC thermograms of a physically mixed PLGA5002 compact prepared at a compaction load of 7 kN and RT after different times of exposure to the release medium at 37 °C (A) and SEM image (top view) of a physically mixed PLGA5002 compact after 18 days of exposure to the release medium at 37 °C at a magnification of 30× (B).

The results clearly show that the T_g of the polymer decreased over time. Prior to exposure to the release medium, the T_g was 32.8 °C. After 18 days of release, when the pulse was observed for theophylline containing PLGA5002-based compacts (Figure 1), the T_g was found to be 27.0 °C. After 24 days of release at 37 °C, the T_g further decreased to 24.1 °C. Figure 7B shows a SEM image of a PLGA5002-based compact after 18 days of release at 37 °C. The image clearly shows a ruptured compact.

3.3.6 In vitro *release of BD from physically mixed PLGA5002-based compacts*

Figure 8A and B shows the release at 37 °C of BD with a molecular weight of 70 kDa (Figure 8A) and 2000 kDa (Figure 8B) from compacts with a PLGA5002 polymer matrix prepared at RT and a compression force of 3 kN or 9 kN. A larger difference between the two compression forces than previously (2.8 kN and 7 kN) was chosen to further investigate the influence of compression force on the release profile. Physically mixed

Figure 8. A and B Release of BD with a molecular weight of 70 kDa (A) or 2000 kDa (B) at 37 °C from physically mixed PLGA5002 compacts prepared at RT with a compaction load of 3 kN (grey) or 9 kN (black). Standard deviation is indicated (n = 3).

compacts compressed at 3 kN and 9 kN containing BD with a molecular weight of 70 kDa released 58.4 ± 9.8% and 54.3 ± 6.1% of the total BD content during the initial pulsatile burst release, respectively. Based on the f_2, which was 69.9, the two release profiles were similar. Physically mixed compacts compressed at 3 kN and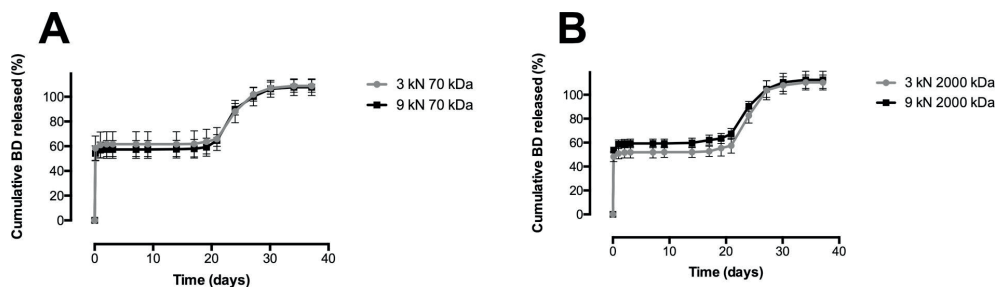 9 kN containing BD with a molecular weight of 2000 kDa released 48.3 ± 4.1% and 53.8 ± 1.8% of the total BD content during the initial pulsatile burst release, respectively. Based on the f_2, which was 55.0, the release profiles were similar. The release profiles of the different BD molecular weights (70 kDa and 2000 kDa) compressed at either 3 kN or 9 kN were also similar, with f_2 values of 51.7 and 78.8, respectively. The remaining content was released as a pulse after a lag phase. The lag phase was approximately 21 days for both molecular weights of BD.

3.3.7 Effect of a nonporous shell on the burst release
Three different core-shell compacts were prepared by either omitting the heating step with PLA02 or PLA05 as shell material and compressing with a compaction load of 12.5 kN, or by heating at 80 °C for 1 h during compaction and compressing at a compaction load of 5 kN with PLA05 as shell material. The non-heated PLA02 core-shell compact exhibited a delayed release profile without any initial burst release. The lag time was approximately 40 days. All the theophylline was released within 2 days from the non-heated PLA05 core-shell compact, however, if the PLA05 core-shell compact was heated at 80 °C for 1 h, a delayed release without any initial burst release was exhibited. The lag time was approximately 100 days (Figure 9).

3.4 Discussion

The compacts prepared at RT from a physical mixture of PLGA5002 or PLA02 and theophylline exhibited a biphasic pulsatile release profile at 37 °C, similar to the previous findings [1] (Figure 1). Furthermore, the lag time could be adjusted by changing the polymer composition, which is also in line with the previous study [1]. These results imply that the release mechanism may be independent of the polymer particle size, as in the study of Murakami et al. [1] nanoparticles were used, while in the present study more coarse particles were used. However, head-to-head experiments should be performed to
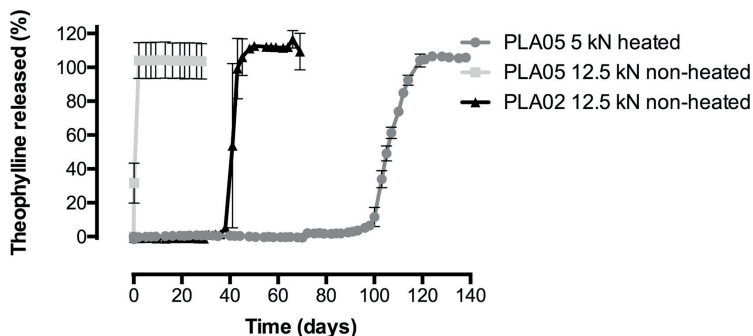
Figure 9. Release of theophylline at 37 °C from core-shell compacts with a PLA02 shell that was non-heated and compressed at 12.5 kN (black), a PLA05 shell that was non-heated and compressed at 12.5 kN (light grey), and a core-shell compact with a PLA05 shell that was heated at 80 °C for 1 h and compressed at 5 kN (grey). Standard deviation is indicated (n = 3).

confirm this. Not all compacts exhibited a biphasic pulsatile release profile. It was found that the release profile was greatly dependent on the T_g of the polymer, the temperature during compaction, and the temperature of the release medium. If the temperature during compaction was below and the temperature during release was above the T_g of the polymer, a biphasic pulsatile release profile was obtained with a 50–60% burst release and a 40–50% boost release. According to the results shown in this study, this biphasic pulsatile release profile can be attributed to the transition from the glassy state into the rubbery state of the polymer, as will be made clear in the following discussion.

As described by Fredenberg et al. [8], four release mechanism should be considered when investigating drug release from a PL(G)A-based device, namely: diffusion through water-filled pores, diffusion through the polymer, osmotic pumping, and polymer erosion. During compaction at RT, a porous matrix was formed, as confirmed by SEM for PLA02-based compacts (Figure 2-8, Figure 9A and B). This porous structure is typical for a glassy polymer and is caused by the relatively high T_g of dry PLGA5002 and PLA02 of 31.6 °C and 33.5 °C, respectively. When the compact is set to release at 37 °C, the polymer will heat up and absorb water. As the T_g of the moisturized polymer is below environmental temperatures, i.e. 19.1 °C for PLGA5002 and 24.3 °C for PLA02, a transition from the glassy state into the rubbery state will occur. This causes the polymer chains to become mobile and viscous flow will close the pores that were originally present after compaction (Figure 5C). The phenomenon of pore closure has been described in several other studies [28-31]. However, different PL(G)A-based devices were studied and therefore the mechanisms of pore closure may be different. Because pore closure of the physically mixed compacts was not instantly (Figure 6A–C), part of the drug could diffuse through the pores of the compact before the pores were sealed, resulting in a pulsatile burst release. The diffusion through pores has also been described as a possible drug release mechanism from various other types of PL(G)A-based devices in literature [8,32-34]. This release mechanism is further supported by the fact that the burst release was reduced from $55.8 \pm 0.9\%$ to $22.6 \pm 5.8\%$ when the PLA02-based compacts were heated for 1 h at 48 °C (a temperature above the T_g of dry PLA02) prior to starting the release experiment (Figure 3). A small amount of burst release can be

expected, as some of the dispersed drug will be at or near the surface of the compact. The burst release was followed by a lag phase, since the hydrophilic drug molecules were not able to diffuse through the nonporous polymer matrix of the physically mixed compacts.

To further support our hypothesis, a release experiment was performed in which the release temperature was lowered to refrigerated conditions (4 °C) or RT (Figure 4). At these temperatures, the T_g of PLA02 is above the environmental temperature during release, and the polymer does not transition into the mobile rubbery state. Consequently, no pore closure occurred, as confirmed by SEM (Figure 5A and B). Therefore, all the theophylline was released during the burst. At RT, the burst release was faster than at refrigerated conditions, this is due to a higher diffusion rate of theophylline through the porous compact to the release medium at higher temperatures. These results show that the temperature of the release medium affects pore closure.

Although decreasing the compression force from 7 kN to 2.8 kN resulted in a visibly more porous surface of the compact (Figure 2-8, Figure 9A and B), the release profiles from both compacts were similar (Figure 2-8, Figure 9C). Apparently, the initial porosity of the surface of the compact did not influence the burst release. This may be explained by the fact that the water-soluble mannitol in the formulation acts as a pore former, creating a more porous compact when immersed into the release medium. As pore closure was not instantly (Figure 6A–C), this led to a rapid initial burst release, which was independent of the initial porosity of the compact. It is known from literature that additives may act as pore formers and affect the structure of various PL(G)A-based devices [8].

The T_g of PLGA-based compacts clearly decreased over time (Figure 7A). According to the Fox-Flory equation, the T_g decreases with a decrease in molecular weight of the polymer [35,36]. Therefore, these results indicate that the molecular weight of the polymer decreases over time due to degradation. After 18 days of release at 37 °C, the compact showed a ruptured surface (Figure 7B), which might be ascribed by the following mechanism. The dissolved acidic byproducts of the degrading polymer are trapped in the polymer matrix and accumulate over time. This accumulation possibly led to an increase of the osmotic pressure within the compact, which has recently been described by Mylonaki et al. [37] for PLGA-based microparticles. Eventually, the osmotic pressure within the compact may build up to such an extent that it ruptured the compact, leading to the pulsatile boost release. Such osmotic pressure induced rupturing of polymeric matrices has been described in literature [8,29,36].

Incorporation of BD with a molecular weight of 70 kDa or 2000 kDa into the physically mixed compacts showed similar results as the theophylline containing compacts (Figure 8A and B). As with the theophylline containing compacts, the compression force did not influence the release profile. However, the lag phase for BD containing physically mixed compacts was approximately 3 days longer than with theophylline containing compacts. This difference in lag time might be explained by the difference in sampling procedure. These results indicate that molecular weight does not influence the release. The independence of molecular weight supports the fact that the compact ruptures, possibly due to a build-up in osmotic pressure.

Finally, using PLA05, a polymer with a higher T_g (onset at 37.1 °C when moisturized), resulted in all of the theophylline being released during the initial burst

(Figure 9). This even occurred despite the fact that a core-shell configuration was used, resulting in a thicker polymer layer for the theophylline to diffuse through. This is due to the fact that the T_g of moisturized PLA05 is slightly above the environmental temperature during release. However, heating the PLA05 core-shell compact for 1 h at 80 °C (a temperature far above the T_g) prior to release reduced the initial burst release to zero. This is because there was no theophylline at or near the surface and the shell surrounding the core becomes nonporous upon the heating step. Non-heated PLA02 core-shell compacts exhibited a delayed release without any initial burst release. This can be explained by the fact that the T_g of moisturized PLA02 (24.3 °C) is below the environmental temperature during release.

Understanding the mechanism behind the biphasic pulsatile release from physically mixed compacts could contribute to further develop single-injection vaccines. The release profile can be tailored to specific therapies, opening up new ways to optimize the protection against various pathogens. Specifically, a device based on a physical mixture might be interesting for the development of a single-injection polysaccharide-based vaccine, as it is possible to successfully incorporate polysaccharides into the compact. Because the release profile is not influenced by the molecular weight of the incorporated drug, multiple antigens with different molecular weights can be incorporated into the same device.

3.5 Conclusion

As described by Murakami et al. [1], a biphasic pulsatile release could be obtained from a physically mixed PL(G)A-based compact. However, the mechanism behind this biphasic pulsatile release profile was previously not fully understood. We found that the pulsatile release was greatly influenced by the T_g of the polymer. After compaction, a porous compact was formed from which one part of the active component released instantly by diffusion through the pores of the compact. However, if a polymer with a T_g below the environmental temperature was used, the pores closed due to viscous flow of the polymer and release of the active component was inhibited, since the hydrophilic drug is not able to diffuse through the nonporous polymer matrix. Instead, the burst release was followed by a lag time and a second pulsatile release (booster) was obtained. This pulsatile boost release was not influenced by the molecular weight of the incorporated drug, as it was caused by rupturing of the compact, possibly due to a build-up of osmotic pressure. Furthermore, the initial porosity of the compact did not influence the release profile. The physically mixed compact prototype might be interesting for the development of a single-injection polysaccharide-based vaccine, as BD could successfully be incorporated into the compact.

Acknowledgements

References

[1] H. Murakami, M. Kobayashi, H. Takeuchi, and Y. Kawashima, "Utilization of poly(dl-lactide-co-glycolide) nanoparticles for preparation of mini-depot tablets by direct compression," J. Control. Release, vol. 67, pp. 29–36, 2000.

[2] K. Kardani, A. Bolhassani, and S. Shahbazi, "Prime-boost vaccine strategy against viral infections: Mechanisms and benefits," Vaccine, vol. 34, pp. 413–423, 2016.

[3] World Health Organization, "Immunization," 2018. [Online]. Available: http://www.who.int/topics/immunization/en/. [Accessed: 7-Mar-2018].

[4] L. J. McHeyzer-Williams and M. G. McHeyzer-Williams, "Antigen-specific memory B cell development," Annu. Rev. Immunol., vol. 23, pp. 487–513, 2005.

[5] C.-A. Siegrist, "Vaccine immunology," in Vaccines, 6th ed., S. Plotkin and P. Offit, Eds. London: Saunders, 2013, pp. 14–32.

[6] K. J. McHugh, R. Guarecuco, R. Langer, and A. Jaklenec, "Single-injection vaccines: Progress, challenges, and opportunities," J. Control. Release, vol. 219, pp. 596–609, 2015.

[7] J. L. Cleland, "Single-administration vaccines: controlled-release technology to mimic repeated immunizations," Trends Biotechnol., vol. 17, pp. 25–29, 1999.

[8] S. Fredenberg, M. Wahlgren, M. Reslow, and A. Axelsson, "The mechanisms of drug release in poly(lactic-co-glycolic acid)-based drug delivery systems—A review," Int. J. Pharm., vol. 415, pp. 34–52, 2011.

[9] H. K. Makadia and S. J. Siegel, "Poly Lactic-co-Glycolic Acid (PLGA) as Biodegradable Controlled Drug Delivery Carrier," Polymers (Basel), vol. 3, pp. 1377–1397, 2011.

[10] Y. Xu, C.-S. Kim, D. M. Saylor, and D. Koo, "Polymer degradation and drug delivery in PLGA-based drug-polymer applications: A review of experiments and theories," J. Biomed. Mater. Res. Part B Appl. Biomater., vol. 105, pp. 1692–1716, 2017.

[11] B. G. De Geest, S. De Koker, J. Demeester, S. C. De Smedt, and W. E. Hennink, "Pulsed in vitro release and in vivo behavior of exploding microcapsules," J. Control. Release, vol. 135, pp. 268–273, 2009.

[12] S.Y. Tzeng, K.J. McHugh, A.M. Behrens, S. Rose, J.L. Sugarman, S. Ferber, R. Langer, A. Jaklenec, "Stabilized single-injection inactivated polio vaccine elicits a strong neutralizing immune response," Proc. Natl. Acad. Sci., vol. 115, no. 24, pp. E5269-E5278, Jun. 2018.

[13] S. Sungthongjeen, S. Puttipipatkhachorn, O. Paeratakul, A. Dashevsky, R. Bodmeier, "Development of pulsatile release tablets with swelling and rupturable layers," J. Control. Release, vol. 95, no. 1, pp. 147-159, Jan. 2004.

[14] C. Guse, S. Koennings, T. Blunk, J. Siepmann, A. Goepferich, "Programmable implants—From pulsatile to controlled release," Int. J. Pharm., vol. 314, no. 2, pp. 161-169, Dec. 2006.

[15] K.J. McHugh, T.D. Nguyen, A.R. Linehan, D. Yang, A.M. Behrens, S. Rose, Z.L. Tochka, S.Y. Tzeng, J.J. Norman, A.C. Anselmo, X. Xu, S. Tomasic, M.A. Taylor, J. Lu, R. Guarecuco, R. Langer, A. Jaklenec, "Fabrication of fillable

microparticles and other complex 3D microstructures," Science, vol. 357, no. 6356, pp. 1138-1142, Sep. 2017.

[16]   Z. Ghalanbor, M. Körber, R. Bodmeier, "Protein release from poly(lactide-co-glycolide) implants prepared by hot-melt extrusion: Thioester formation as a reason for incomplete release," Int. J. Pharm., vol. 438, no. 1-2, pp. 302-306, Dec. 2012.

[17]   D.J. Hines, D.L. Kaplan, "Poly(lactic-co-glycolic acid) controlled release systems: experimental and modeling Insights," Crit. Rev. Ther. Drug Carrier Syst., vol. 30, no. 4, pp. 257-276, 2013.

[18]   M. van de Weert, W.E. Hennink, W. Jiskoot, "Protein instability in poly(lactic-co-glycolic acid) microparticles," Pharm. Res., vol. 17, no. 10, pp. 1159-1167, Oct. 2000.

[19]   T. Estey, J. Kang, S.P. Schwendeman, J.F. Carpenter, "BSA Degradation Under Acidic Conditions: A Model For Protein Instability During Release From PLGA Delivery Systems," J. Pharm. Sci., vol. 95, no. 7, pp. 1626-1639, Jul. 2006.

[20]   J. Kang and S. P. Schwendeman, "Comparison of the effects of Mg(OH)2 and sucrose on the stability of bovine serum albumin encapsulated in injectable poly(d,l-lactide-co-glycolide) implants," Biomaterials, vol. 23, pp. 239-245, 2002.

[21]   Y. Liu and S. P. Schwendeman, "Mapping Microclimate pH Distribution inside Protein-Encapsulated PLGA Microspheres Using Confocal Laser Scanning Microscopy," Mol. Pharm., vol. 9, pp. 1342-1350, 2012.

[22]   M. Stanković et al., "Protein release from water-swellable poly(d,l-lactide-PEG)-b-poly(ε-caprolactone) implants," Int. J. Pharm., vol. 480, pp. 73-83, 2015.

[23]   G. Zhu and S. P. Schwendeman, "Stabilization of proteins encapsulated in cylindrical poly(lactide-co-glycolide) implants: mechanism of stabilization by basic additives," Pharm. Res., vol. 17, pp. 351-357, 2000.

[24]   L. Duque, M. Körber, and R. Bodmeier, "Improving release completeness from PLGA-based implants for the acid-labile model protein ovalbumin," Int. J. Pharm., vol. 538, pp. 139-146, 2018.

[25]   A. Weintraub, "Immunology of bacterial polysaccharide antigens," Carbohydr. Res., vol. 338, pp. 2539-2547, 2003.

[26]   V. P. Shah et al., "In vitro dissolution profile comparison--statistics and analysis of the similarity factor, f2.," Pharm. Res., vol. 15, pp. 889-896, 1998.

[27]   P. Srinarong et al., "Strongly enhanced dissolution rate of fenofibrate solid dispersion tablets by incorporation of superdisintegrants," Eur. J. Pharm. Biopharm., vol. 73, pp. 154-161, 2009.

[28]   S. Fredenberg et al., "Pore formation and pore closure in poly(D,L-lactide-co-glycolide) films," J. Control. Release, vol. 150, pp. 142-149, 2011.

[29]   J. Kang and S. P. Schwendeman, "Pore Closing and Opening in Biodegradable Polymers and Their Effect on the Controlled Release of Proteins," Mol. Pharm., vol. 4, pp. 104-118, 2007.

[30]   J. Wang, B. M. Wang, and S. P. Schwendeman, "Characterization of the initial burst release of a model peptide from poly(d,l-lactide-co-glycolide) microspheres," J. Control. Release, vol. 82, pp. 289-307, 2002.

[31]   Y. Yamaguchi et al., "Insulin-loaded biodegradable PLGA microcapsules: initial

3

burst release controlled by hydrophilic additives," J. Control. Release, vol. 81, pp. 235-249, 2002.

[32] H. Gao, Y. Gu, and Q. Ping, "The implantable 5-fluorouracil-loaded poly(l-lactic acid) fibers prepared by wet-spinning from suspension," Journal of Controlled Release, vol. 118, pp. 325-332, 2007.

[33] H. Yushu and S. Venkatraman, "The effect of process variables on the morphology and release characteristics of protein-loaded PLGA particles," Journal of Applied Polymer Science, vol. 101, pp. 3053-3061, 2006.

[34] A. S. Zidan, O. A. Sammour, M. A. Hammad, N. A. Megrab, M. D. Hussain, M. A. Khan, and M. J. Habib, "Formulation of anastrozole microparticles as biodegradable anticancer drug carriers," AAPS PharmSciTech, vol. 7, pp. E38-E46, 2006.

[35] T. G. Fox and P. J. Flory, "Second-Order Transition Temperatures and Related Properties of Polystyrene. I. Influence of Molecular Weight," Journal of Applied Physics, vol. 21, pp. 581-591, 1950.

[36] T. G. Park, "Degradation of poly(lactic-co-glycolic acid) microspheres: effect of copolymer composition," Biomaterials, vol. 16, pp. 1123-1130, 1995.

[37] I. Mylonaki, E. Allémann, F. Delie, and O. Jordan, "Imaging the porous structure in the core of degrading PLGA microparticles: The effect of molecular weight," Journal of Controlled Release, vol. 286, pp. 231-239, 2018.

3

Chapter 4

Microfluidic production of polymeric core-shell microspheres for the delayed pulsatile release of bovine serum albumin as a model antigen

Renée S. van der Kooij [1], Rob Steendam [2], Johan Zuidema [2], Henderik W. Frijlink [1], and Wouter L. J. Hinrichs [1]

[1] Department of Pharmaceutical Technology and Biopharmacy, University of Groningen, Antonius Deusinglaan 1, 9713 AV Groningen, The Netherlands
[2] InnoCore Pharmaceuticals, L.J. Zielstraweg 1, 9713 GX Groningen, The Netherlands

Abstract

For many vaccines, multiple injections are required to confer protective immunity against targeted pathogens. These injections often consist of a primer administration followed by a booster administration of the vaccine a few weeks or months later. A single-injection vaccine formulation that provides for both administrations could greatly improve the convenience and vaccinee's compliance. In this study, we developed parenterally injectable core–shell microspheres with a delayed pulsatile release profile that could serve as the booster in such a vaccine formulation. These microspheres contained bovine serum albumin (BSA) as the model antigen and poly(DL-lactide-*co*-glycolide) (PLGA) with various DL-lactide:glycolide monomer ratios as the shell material. Highly monodisperse particles with different particle characteristics were obtained using a microfluidic setup. All formulations exhibited a pulsatile *in vitro* release of BSA after an adjustable lag time. This lag time increased with the increasing lactide content of the polymer and ranged from 3 to 7 weeks. Shell thickness and bovine serum albumin loading had no effect on the release behavior, which could be ascribed to the degradation mechanism of the polymer, with bulk degradation being the main pathway. Co-injection of the core–shell microspheres together with a solution of the antigen that serves as the primer would allow for the desired biphasic release profile. Altogether, these findings show that injectable core–shell microspheres combined with a primer are a promising alternative for the current multiple-injection vaccines.

4.1 Introduction

Immunization is widely recognized as one of the greatest and most successful medical advances of the past centuries, saving two to three million lives every year by preventing or even eliminating infectious diseases [1]. However, the global coverage for many vaccines is still too low, especially in low-income countries [2–4]. One of the reasons for this low coverage is the limited access to routine immunization services, which is mainly a problem when multiple injections are required to obtain protective immunity against the targeted pathogens [3,4]. A multiple-injection schedule generally consists of a first immunization (primer) followed by a second or even third immunization (booster) after a certain period of time [5]. Such a prime-boost schedule does not only cause logistical problems and high costs, it is also very uncomfortable and thus jeopardizes the compliance of the vaccinee [5,6]. An example of a prime-boost vaccine is the diphtheria-tetanus-pertussis (DTP) vaccine of which, in 2020, 17.1 million infants did not receive a primer dose, and an additional 5.6 million were only partially vaccinated [2]. The latter could be prevented by developing a single-injection vaccine formulation that exhibits a pulsatile release profile and thus includes both the primer and the booster doses [5–8]. Such a pulsatile release formulation could provide for a prolonged immunological response, hence circumventing the need for multiple injections. The administration of the primer dose can easily be achieved by co-injection of a solution of the antigen or by the addition of a separate immediate-release formulation of the antigen. However, the development of the booster part of such a formulation, characterized by a pulsatile release after a predefined lag time, is challenging. Therefore, the development of a formulation providing a delayed pulsatile release is the focus of this study.

In a previous proof of concept study, the feasibility of a single-injection vaccine using a polymeric core–shell implant (oblong: ≈9 × 5 × 5 mm) was investigated [8]. This implant contained ovalbumin as a model antigen in a core that was surrounded by a non-porous shell of the biocompatible and biodegradable polymer poly(DL-lactide-*co*-glycolide) (PLGA). Initially, the polymeric shell formed an impermeable barrier to the *in vitro* release of the antigen, thereby resulting in a lag phase during which no antigen was released. Once the shell had sufficiently degraded, it lost its barrier function, which caused the antigen to diffuse out of the implant [9]. This ultimately resulted in a delayed pulsatile release profile [8]. The implant was also subcutaneously inserted in mice, and after a specified lag time, an ovalbumin-specific IgG1 antibody response was induced as expected. Moreover, it was shown that the lag time of the formulation could be tailored from 3 to 6 weeks by simply adjusting the DL-lactide:glycolide ratio of PLGA, as the monomer ratio directly influenced the degradation rate of the polymer [10–12]. However, such an implant has to be surgically inserted, which is obviously not ideal and therefore cannot be developed into a commercially viable vaccine product [8]. Thus, a formulation that is suitable for subcutaneous or intramuscular injection would be an interesting alternative.

To this end, we incorporated a model antigen into PLGA-based core–shell microspheres. Core–shell microspheres are vesicular particles consisting of a single core containing the therapeutic agent, which is surrounded by a polymer shell [13]. In order to prevent premature uptake by immune cells or other cells, the core–shell microspheres

should be larger than approximately 20 μm but smaller than approximately 100 μm to enable parenteral administration [14,15]. Furthermore, we hypothesize that the shell thickness of the microspheres does not influence the *in vitro* release profile as the degradation of PLGA occurs mainly through bulk erosion [11,16]. This means that the release profile is only dependent on the polymer composition. However, there is controversy over the influence of the shell thickness, as some studies did demonstrate an increase in lag time with an increasing shell thickness [17–19]. In that case, a narrow particle size distribution and uniform shell thickness are necessary for obtaining a pulsatile release instead of a sustained release after the lag time. To test both hypotheses, monodisperse core–shell microspheres with shells of uniform thickness are desired. For this reason, we used droplet microfluidics as a production method, as it enables the generation of highly monodisperse particles in the micrometer range by providing great control over the size of the droplets [20,21]. In addition, the emulsion that ultimately forms the microspheres is produced drop by drop, which is in contrast to the conventional emulsion solvent evaporation method where the microspheres are produced in bulk [21]. By placing two microfluidic chips in series, a water-in-oil-in-water (W/O/W) emulsion could be produced. In the first microfluidic chip, a primary water-in-oil (W/O) emulsion of aqueous droplets containing a model antigen in an organic polymer phase was formed. In the second microfluidic chip, the W/O emulsion was encapsulated into another aqueous phase, which enabled the generation of a W/O/W double emulsion that formed the basis for the core–shell microspheres. Hence, the aim of this study was to develop core–shell microspheres containing bovine serum albumin (BSA) as a model antigen using a microfluidic setup. In previous studies, PLGA-based core–shell microspheres were produced using microfluidics but, in all cases, no therapeutic agent was incorporated [22–26]. To the best of our knowledge, this is the first time that microfluidics was used to produce core–shell microspheres with a PLGA shell and a core containing a (model) antigen. To assess the potential of these microspheres for application as the booster part of a single-injection vaccine formulation, *in vitro* release studies were conducted, and the influence of the polymer composition on the lag time was investigated by using PLGA copolymers with various monomer ratios. In a study by Sanchez et al., this relationship was already investigated using tetanus toxoid-containing core–shell microspheres, but here, both the PLGA monomer ratio and the molecular weight were varied at the same time [27]. Therefore, in this study, solely the monomer ratio was varied to determine the influence on the lag time.

4.2 Materials and methods

4.2.1 Materials

PLGA with an inherent viscosity of 0.2 dL/g and DL-lactide:glycolide molar ratios of 50:50 (PDLG5002) and 72:25 (PDLG7502) were obtained from Corbion Purac Biomaterials (Gorinchem, The Netherlands). Polyglycerol polyricinoleate (PGPR) was a generous gift from TER Ingredients GmbH & CO. KG (Hamburg, Germany). Polyvinyl alcohol (PVA, M_w 9-10 kDa, 80% hydrolyzed), BSA, and fluorescein isothiocyanate (FITC) were purchased from Sigma-Aldrich Co. (St. Louis, MO, USA). Dichloromethane (DCM) and phosphate-buffered saline (PBS; 155 mM NaCl, 1.06 mM KH_2PO_4, 2.97 mM Na_2H-

$PO_4 \cdot 7H_2O$, pH 7.4) were obtained from Fisher Scientific (Leicestershire, UK). For the *in vitro* release medium, potassium dihydrogen phosphate, disodium hydrogen phosphate, and sodium azide were purchased from Fisher Scientific (Leicestershire, UK) and Tween 80 from Merck (Darmstadt, Germany). Trifluoroacetic acid (TFA) was obtained from VWR International Ltd. (Amsterdam, The Netherlands) and acetonitrile from Actu-All Chemicals B.V. (Oss, The Netherlands). Ultrapure water with a resistivity of 18.2 MΩ was obtained using a Millipore Milli-Q Integral 3 (A10) purification system and used for all experiments.

4.2.2 FITC-BSA synthesis and analysis

For the synthesis of FITC-labeled BSA (FITC–BSA), 3.2 mL of 1 mg/mL FITC in absolute ethanol was added to 20 mL of BSA solution (10 mg/mL in PBS adjusted to pH 9.4 with 1 M NaOH), after which the reaction mixture was kept under magnetic stirring for 45 min at room temperature. This resulted in a fluorophore-to-protein molar ratio of approximately 3:1. Subsequently, the mixture was dialyzed (Slide-A-Lyzer™ Dialysis Cassettes (Extra Strength), 10K MWCO, 12–30 mL Capacity, Thermo Scientific, Waltham, MA, USA) against ultrapure water for 3 days at 8 °C to remove any uncoupled FITC. The final product was obtained by freeze drying of the resulting solution.

The labeling of BSA with FITC was assessed by thin-layer chromatography (TLC). In short, 10 μL aliquots of 1 mg/mL FITC, 10 mg/mL FITC–BSA, and 10 mg/mL BSA were applied on a TLC Silica gel 60 F_{254} plate (Merck, Darmstadt, Germany). The plate was run with a mixture of acetonitrile, DCM, and glacial acetic acid (volumetric ratio 90:10:1) as eluent and subsequently air-dried. The spots on the plate were detected at two different wavelengths (254 nm for BSA and 366 nm for FITC) with a UV lamp (Universal, CAMAG, Muttenz, Switzerland).

4.2.3 Production of core-shell microspheres

Monodisperse core–shell microspheres with different particle characteristics were produced by a W/O/W double emulsion solvent evaporation method using a capillary microfluidic setup (Dolomite Ltd., Royston, UK), as shown in Figure 1.
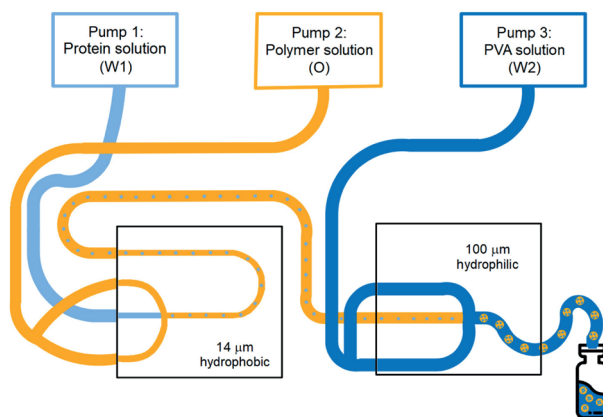

Figure 1. Schematic representation of the microfluidic setup used for the production of core–shell microspheres.

For the primary water-in-oil emulsion, a microfluidic glass chip with a flow-focusing geometry, a channel diameter of 14 μm at the junction, and a hydrophobic coating was used. This coating enabled the formation of water droplets containing the model antigen dispersed in an organic polymer phase. For the secondary W/O/W emulsion, a similar glass chip was used with a channel diameter of 100 μm. This chip did not have a coating, thereby rendering the channel surface naturally hydrophilic. This hydrophilic surface enabled the formation of W/O emulsion droplets in an outer water phase, resulting in such a W/O/W double emulsion. The inner water phase (W_1) was an aqueous 200 mg/mL BSA or 40 mg/mL FITC–BSA solution. A solution of PLGA (7.5 wt-% or 10 wt-%) and PGPR (0.75 wt-% or 1 wt-%, respectively) in DCM was used as oil phase (O). To investigate the effect of the PLGA monomer ratio on the release characteristics of the microspheres, PDLG5002, PDLG7502, and a blend of PDLG5002 and PDLG7502 (mass ratio 1:1) were evaluated. A 2 wt-% aqueous solution of PVA served as the outer water phase (W_2). All liquids were injected at independently adjustable flow rates using pressure pumps (Mitos P-Pump, Dolomite Ltd., Royston, UK). Flow and pressure were monitored using flow rate sensors (Mitos Flow Rate Sensor, Dolomite Ltd., Royston, UK). Various flow rates were used for the injection of the different phases (Table 1) in order to adjust the droplet size and thus the particle dimensions.

Table 1. Experimental parameters and settings of different bovine serum albumin (BSA)-loaded microsphere formulations.

Formulation	Model Compound	Polymer	Polymer Concentration (wt-%)	Flow Rates (W_1–O–W_2, μL/min)	Theoretical Loading (wt-%)
A	BSA	PDLG5002	10	0.58–7.8–50	9.3
B	BSA	PDLG5002	10	0.47–7.8–50	7.7
C	BSA	PDLG5002	10	0.40–7.8–50	6.7
D	BSA	PDLG5002	10	0.35–7.8–50	5.9
E	BSA	PDLG5002 + PDLG7502 (1:1)	7.5	0.28–7.8–30	6.4
F	BSA	PDLG7502	7.5	0.28–7.8–30	6.4
G	FITC-BSA	PDLG5002	10	0.20–5.4–40	1.0

In the first chip, the inner water phase was hydrodynamically focused by the oil phase, resulting in the continuous production of W/O emulsion droplets at the junction of the microchannels. In the second chip, the oil phase containing the inner water droplets was hydrodynamically flow focused by the outer water phase, thereby generating a W/O/W double emulsion. In both emulsification steps, the controlled break-up of the dispersed phase jet immediately at the junction of the chip ensured the formation of highly monodisperse single- and double-emulsion droplets. The obtained double-emulsion droplets were collected in an excess of PVA solution at room temperature to extract and evaporate the DCM overnight by magnetic stirring. As a result, solid microspheres were obtained that were washed three times with 0.05 wt-% Tween 80 solution and three times with ultrapure water. Then, the washed microspheres were freeze-dried using a Christ Alpha 2–4 LSC plus freeze-dryer (Martin Christ Gefriertrocknungsanlagen GmbH, Osterode am Harz, Germany) of which the shelf was pre-cooled to a temperature of −45 °C. Sub-

sequently, the pressure was gradually reduced to 2 mBar, after which the particles were dried for 3 h at a shelf temperature of −10 °C and then for 8 h at 20 °C. During this primary drying phase, ice is removed by sublimation. Eventually, the pressure was further reduced to 1 mBar during 2 h, which was followed by a final drying step of 2 h at approximately 0.05 mBar and 20 °C. During this secondary drying phase, unfrozen water molecules are removed by desorption. The settings of several process and formulation parameters were altered to obtain core–shell microspheres with varying dimensions and BSA loading. The experimental parameters and settings are summarized in Table 1. The theoretical BSA loading was calculated using Equation (1).

$$\text{Theoretical loading} = \frac{W_1 \text{ flow rate} \times W_1 \text{ conc.}}{W_1 \text{ flow rate} \times W_1 \text{ conc.} + O \text{ flow rate} \times O \text{ conc.}} \times 100\% \tag{1}$$

where the W_1 flow rate is the flow rate of the inner water phase; W_1 conc. is the mass concentration of the inner water phase; the O flow rate is the flow rate of the oil phase; and O conc. is the mass concentration of the oil phase.

4.2.4 Characterization of particle size and morphology

All microsphere batches were examined before washing and freeze drying with an ME.2665 Euromex optical microscope (Arnhem, The Netherlands), and images were taken at 100×, 200×, and 400× magnification. Images of the dried microspheres were acquired with a NeoScope JCM-5000 scanning electron microscope (SEM; JEOL Ltd., Tokyo, Japan) under high vacuum at an acceleration voltage of 10 kV. For all recordings, the probe current was set to standard, and the filament setting was set to long life. The particles were mounted onto metal stubs using double-sided adhesive carbon tape and sputter-coated with gold prior to examination. The surface morphology of the microspheres was investigated at different magnifications ranging from 50× to 1500×. For each batch, ImageJ software (National Institutes of Health, Bethesda, MD, USA) was used to measure the diameter (d_y) of the whole particle and the core of fifty randomly selected particles from several representative optical microscopy images. The volume median diameter (d50, Equation (2)) ± the standard deviation (SD, Equation (3)) and the coefficient of variation (CV, Equation (4)) of the whole microspheres and the cores were calculated to determine the particle size and particle size distribution of the different microsphere batches.

$$d50 = \sum V\%_y \times d_y \tag{2}$$

where $V\%_y = \frac{V_y}{V_{total}}$; $V_y = \frac{4}{3} \times \pi \times (\frac{d_y}{2})^3$ and $V_{total} = \sum V_y$

where V_y is the volume of the measured particle; V_{total} is the total volume of the measured particles; and $V\%_y$ is the percentage V_y of V_{total}.

$$SD = \sqrt{\frac{\sum 100 \times V\%_y \times (d_y - d50)^2}{V\%_{total}}} \tag{3}$$

where $V\%_{total}$ is the total volume percentage of the measured particles; $V\%_{total} = 100\%$.

$$CV = \frac{SD}{d50} \times 100\% \qquad (4)$$

Average shell thickness was also calculated using Equation (5).

$$Shell\ thickness\ = \frac{\sum \frac{d_{y,particle} - d_{y,core}}{2}}{N} \qquad (5)$$

where $N = 50$.

The $d50 \pm SD$ and CV of the dried microspheres were determined as well, but as the differences from the wet microspheres were minimal, these values were not listed. The internal morphology was examined by first embedding the freeze-dried particles in an organic solvent-free adhesive (UHU® Twist & Glue Renature, Bühl, Germany). Then, the samples were air-dried for 2 days, subsequently cooled for 30 min at −70 °C, and cut into five equal pieces using a razor blade. Finally, the cross-sectioned microspheres were examined with SEM.

4.2.5 FITC-BSA localization analysis

FITC–BSA was incorporated into the microspheres at a theoretical loading of 1 wt-%, as described in Section 2.3, to determine the localization of the protein in the microspheres. To this end, FITC–BSA was dissolved in ultrapure water at a concentration of 40 mg/mL, and the obtained solution was used as the inner water phase. The obtained microspheres were examined after freeze drying on a glass slide using a Leica TCS SP8 confocal laser scanning microscope (CLSM, Leica Microsystems GmbH, Wetzlar, Germany). Both fluorescence and transmitted light images were obtained using a plan-apochromat CS2 63x oil-immersion objective with 1.4 numerical aperture. FITC was excited with a 488 nm argon laser, and green fluorescence emission was collected with a 489–549 nm band-pass filter. The pinhole diameter was set at 0.7 AU (67.3 μm). To determine the protein distribution at the center of the microspheres, multiple optical cross-sections were collected at different points along the z-axis.

4.2.6 BSA loading assay

The actual BSA loading of the microspheres was determined by measuring the total nitrogen content of the microspheres using a Vario MICRO Cube elemental analyzer (Elementar, Ronkonkoma, NY, USA) in CHNS mode. The analysis was carried out at a combustion temperature of 1150 °C. The actual BSA loading was used to calculate the encapsulation efficiency (EE) according to Equation (6).

$$EE = \frac{Actual\ loading}{Theoretical\ loading} \times 100\% \qquad (6)$$

4.2.7 BSA in vitro *release assay*

All BSA-loaded core–shell microsphere batches were analyzed for their *in vitro* release profiles by suspending 20 mg particles in 2 mL vials containing 1 mL of 100 mM phosphate buffer (pH 7.4) supplemented with 0.05 *v/v*% Tween 80 and 0.02 wt-% sodium azide. The vials were placed on a roller mixer (40 rpm) in an oven to maintain the release medium at 37 °C. At predetermined time points, the vials were centrifuged for 5 min at 1500 rpm, and 0.5 mL of the supernatant was taken and replaced with 0.5 mL of fresh release medium to keep the volume constant. The concentration of BSA in the release samples was determined by reverse phase ultra-performance liquid chromatography (RP-UPLC) with an ACQUITY UPLC Protein BEH C4 column (300 Å, 2.1 × 50 mm, 1.7 μm particle size, Waters, Milford, MA, USA) and fluorescence detection at λ_{ex} = 276 nm and λ_{em} = 345 nm. The mobile phase was a mixture of ultrapure water with 0.1 *v/v*% TFA and acetonitrile with 0.1 *v/v*% TFA in the volumetric ratio of 75:25 from t = 0 – 1 min and t = 1.1 – 2 min, and 50:50 from t = 1 – 1.1 min. The liquid flow rate of this mobile phase was 0.8 mL/min. The peak areas were integrated at a retention time of 1.1 min for the quantification of BSA. BSA concentrations were calculated using an 8-point calibration curve. Of some microsphere formulations, optical microscopy and SEM images were taken (see Section 2.4) both before and after 2 h, 14 days, and 25 days of *in vitro* release. For SEM examination of the microspheres during *in vitro* release, the particles were first washed and freeze-dried as described in Section 2.3. For the optical microscopy image at t = 0 days, washed and freeze-dried microspheres were suspended in *in vitro* release medium, after which they were immediately examined under the microscope.

4.2.8 Statistics

All core–shell microsphere formulations (A to G, Table 1) were produced once (*n* = 1). All measurements were performed in triplicate (*n* = 3), and data were expressed as mean ± SD, unless otherwise stated.

4.3 Results and discussion

4.3.1 Production and characterization of monodisperse BSA-loaded core-shell microspheres

Several BSA-loaded core–shell microsphere batches with a PLGA shell and varying particle characteristics, such as particle dimensions, BSA loading, and PLGA monomer ratio, were produced using microfluidics. This allowed for the generation of particles in a highly controlled manner as the emulsion was produced drop by drop instead of in bulk. As a result, all formulations had a very narrow particle size distribution with CV values of < 10% (Table 2). The variation in core diameter was somewhat larger, although the CV values were generally still less than 10%. The average particle size of the different formulations ranged from 37.1 ± 2.8 to 48.2 ± 1.8 μm, which makes the microspheres ideal for parenteral administration through a small-gauge hypodermic needle and prevents premature endocytosis by immune cells and other cells [14,15].

Table 2. Characteristics of BSA-loaded core-shell microspheres of different grades of poly(DL-lactide-*co*-glycolide) (PLGA) and theoretical loading.

Formulation	Actual Loading (wt-%)	EE (%)	$d50_{particle}$ (µm)	$CV_{particle}$ (%)	$d50_{core}$ (µm)	CV_{core} (%)	Shell Thickness (µm)
A	8.46 [1]	90.56 [1]	48.2 ± 1.8	3.8	41.3 ± 1.7	4.2	3.5 ± 0.6
B	6.91 ± 0.01	89.87 ± 0.17	43.4 ± 0.8	1.8	33.0 ± 1.2	3.6	5.2 ± 0.5
C	6.60 ± 0.06	98.48 ± 0.94	40.8 ± 1.2	2.9	29.5 ± 1.5	5.0	5.7 ± 0.6
D	1.37 ± 0.02	23.01 ± 0.41	38.1 ± 0.7	1.7	23.1 ± 0.6	2.6	7.4 ± 0.2
E	4.95 ± 0.43	77.74 ± 6.68	37.1 ± 2.8	7.6	28.5 ± 2.8	9.9	4.6 ± 1.2
F	5.73 ± 0.07	90.07 ± 1.03	46.0 ± 1.9	4.2	34.9 ± 3.9	11.2	6.3 ± 1.5
G	0.87 ± 0.04	86.72 ± 3.95	46.1 ± 2.8	6.1	35.0 ± 4.5	12.7	5.8 ± 0.9

[1] For the determination of the actual loading, only one sample was analyzed so no standard deviation is given.

Furthermore, all microspheres were highly spherical, had a smooth and non-porous surface, and presented a distinct core–shell structure. Representative optical microscopy and SEM images of BSA-loaded core–shell microspheres composed of PDLG7502 are depicted in Figure 2.

(**a**)　　　　　　　　　　　　　　　　(**b**)
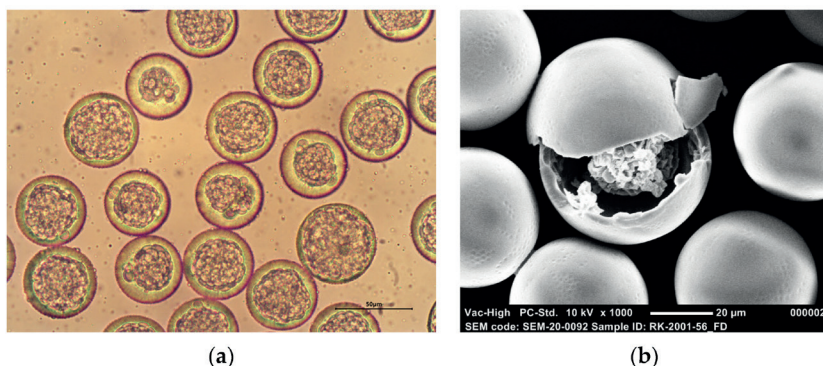
Figure 2. Representative images of BSA-loaded core–shell microspheres: (**a**) Optical microscopy image at 400× magnification; (**b**) Scanning electron microscopy (SEM) image at 1000× magnification. The shell of the microspheres was composed of PDLG7502, and the actual BSA loading was 5.7 wt-% (Formulation F).

Before freeze drying, the cores of the particles are composed of multiple small inner water droplets (Figure 2a), as the encapsulation of one large inner water droplet posed a problem. Small fluctuations in flow are inevitable, which makes it difficult to encapsulate exactly one inner water droplet in an outer droplet. The impact of these fluctuations on the internal morphology of the microspheres will be smaller for particles with multiple inner water droplets, as these fluctuations will only alter the core diameter slightly. The inner water droplets became close-packed upon collection in PVA solution, thereby forming a distinct core, although this core still consisted of multiple separate droplets. Water was removed from the cores by freeze drying, yielding hollow single-core particles containing BSA, as shown in Figure 2b, which presumably shows the presence of BSA inside the core of a fractured particle. This indicates that the inner water droplets coalesced upon freeze drying.

The EE of the model antigen was consistently high with typical values of 80–

100%, except for one formulation that had a significantly lower EE of only 23.01% (Table 2). These microspheres had slightly thicker shells than the other formulations due to the lower inner phase flow rate that was used. These thicker shells probably caused the particles to solidify slower, giving BSA the possibility to diffuse out of the cores. However, the EE seemed to be unaffected by the polymer composition, polymer concentration, BSA loading, and particle size.

Moreover, formulation G, which contained FITC–BSA, was produced to further elucidate the spatial distribution of BSA within the core–shell microspheres. The FITC–BSA loading was only 0.9 wt-%, as the concentration and flow rate of the inner water phase were lower than for the other formulations. However, the EE was as high as 87.0%, and both the particles and the cores showed high monodispersity, which indicates that the coupling of FITC to the model antigen did not have any impact on the particle characteristics. The internal structure of the microspheres containing FITC–BSA is demonstrated in Figure 3a, and the surface morphology is demonstrated in Figure 3b.
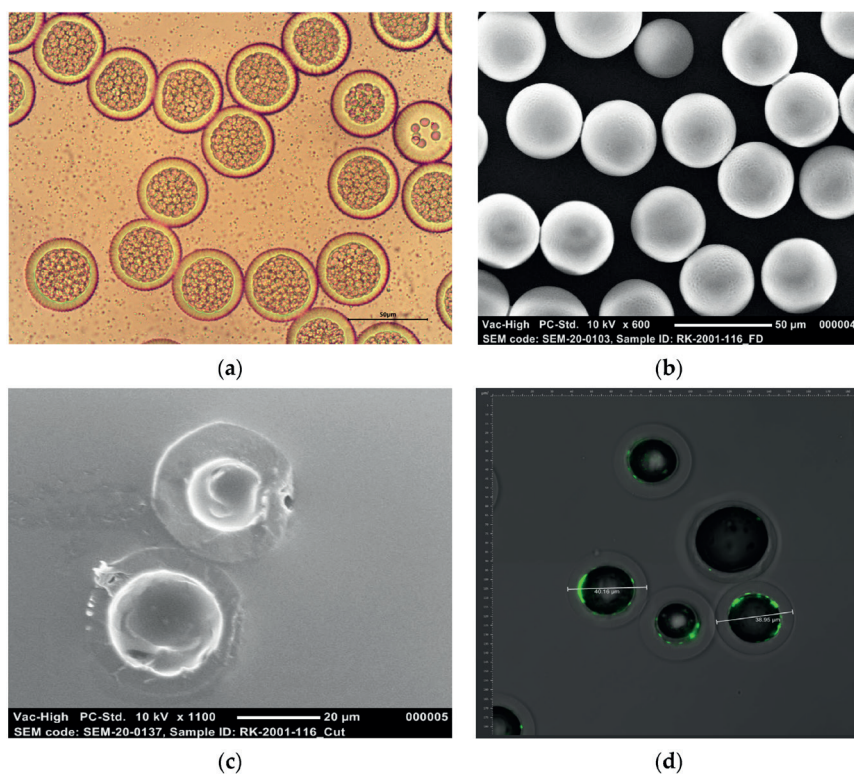
(a)

(b)

(c)

(d)

Figure 3. Representative microscopy images of PDLG5002-based core–shell microspheres loaded with 0.9 wt-% fluorescein isothiocyanate (FITC) labeled–BSA (Formulation G): (**a**) Optical microscopy image at 400× magnification; (**b**) SEM image at 600× magnification; (**c**) SEM image of cross-sectioned microspheres at 1100× magnification; (**d**) overlay of an optical microscopy image and a confocal laser scanning microscopy (CLSM) image showing the distribution of the green fluorescent FITC–BSA.

A core–shell structure is clearly visible, although before freeze drying, the separate inner

water droplets are still to be seen as well (Figure 3a). A SEM image of cross-sectioned microspheres (Figure 3c) shows that the particles had obtained a single-core structure after freeze drying. The cores are virtually hollow, but some FITC–BSA seems to be present on the inner surface of the microsphere shells. This assumption is confirmed by a CLSM image (Figure 3d) that shows that the green fluorescent FITC–BSA tended to be concentrated near the inner surface of the shells and that the inner part of the cores is completely protein-free. This could be attributed to the hydrophobicity of FITC, which caused the labeled model antigen to migrate toward the polymer layer. Due to the relatively low FITC–BSA loading (0.9 wt-%), only the periphery of the core was filled with the labeled model antigen. However, its fluorescence was clearly confined to the core area, and the shells of the microspheres appear to be completely free of the labeled model antigen. This indicates no or only limited diffusion of FITC–BSA into the polymer phase during microsphere formation and, thus, a clear distinction between the polymer phase and the protein phase. In turn, this might enable a delayed pulsatile release profile. A movie that visualizes the 3D structure of FITC–BSA fluorescence in core–shell microspheres can be found in the Supplementary Information (Movie S1).

4.3.2 *Effect of production process and formulation parameters on particle characteristics*
Different inner phase flow rates were used for the production of BSA-loaded core–shell microspheres to obtain microsphere formulations with varying shell thicknesses and BSA loadings. As expected, an increased inner phase flow rate generally resulted in an increased BSA loading and a decreased shell thickness (Table 1, Table 2). In addition, the particle size somewhat increased upon increasing the inner phase flow rate. The PLGA monomer ratio was varied as well to determine its influence on the *in vitro* release profile. In the case of PDLG7502, the polymer concentration was reduced to 7.5 wt-% to enable the production of core–shell microspheres as with 10 wt-%, no primary emulsion droplets could be formed in the first chip. Therefore, the inner and outer phase flow rate were reduced as well to obtain microspheres with a similar BSA loading and shell thickness as the PDLG5002-based microspheres. Changing the polymer composition did not seem to affect the particle characteristics, as the EE was still sufficiently high, and the d50 of the particles was within the desired size range.

4.3.3 *Effect of BSA loading and shell thickness on the* in vitro *release of BSA from PDLG5002-based core–shell microspheres*
To determine whether the shell thickness is a key determinant of the lag time, PDLG5002-based core–shell microspheres with a narrow particle size distribution but different shell thicknesses were produced (Table 2). The shell thickness was tuned from 3.5 to 7.5 μm by varying the inner phase flow rate. Figure 4 shows the influence of the shell thickness on the BSA *in vitro* release profiles for these formulations. All formulations exhibited a delayed release profile with a lag phase of 3 weeks followed by a clear increase in BSA release over 1 to 2 weeks. A limited initial burst release was found for formulation A, but for all formulations, no additional BSA release was observed during the lag phase. The observed lag time is in line with previous studies where drug was released from core–shell microspheres [28,29] and implants [8,30] with a PDLG5002 shell after a lag time of 3 to 4 weeks. Thus, it can be concluded that the lag time does not depend on the shell
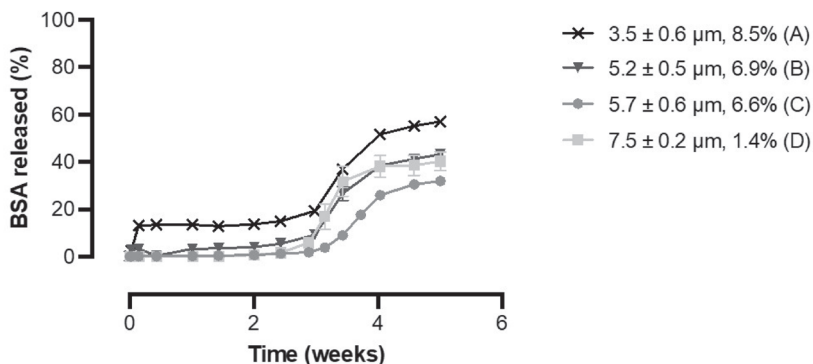
Figure 4. Cumulative *in vitro* release of BSA from PDLG5002-based core–shell microspheres with different shell thicknesses and BSA loadings ($n = 3$).

thickness, at least for core–shell microspheres within the investigated size range and perhaps even for formulations with a much thicker shell, such as the abovementioned core–shell implants [8,30]. These implants had a shell thickness of approximately 1.5 mm, which is 200 to 450 times the shell thickness of the core–shell microspheres developed in this study. A possible explanation for this finding is that PLGA is a bulk-degrading polymer and not surface eroding [11,16]. Consequently, water is able to permeate through the PLGA shell, resulting in swelling and eventually bulk degradation [31–33]. Initially, the non-porous shell serves as a barrier to drug release, thereby causing a lag phase during which no BSA is released. However, water penetration can directly occur throughout the whole polymer layer, but this uptake of water does not lead to such swelling that BSA directly diffuses out of the microspheres [32,33]. Upon water penetration, bulk degradation of the polymer starts, and when the degradation of the shell reaches a critical level, it can no longer serve as a barrier. This causes BSA to diffuse out of the microspheres. Consequently, the lag time solely depends on the polymer characteristics and not on the thickness of the shell, which is in accordance with our hypothesis. However, other studies have demonstrated a clear relationship between the shell thickness and the onset of the pulse [17–19]. In those studies, the lag time ranged from 3 to even 5 weeks. The pulse occurred at the time that the shell of the microspheres ruptured, which was also shown by SEM [17]. It is unclear why different results were obtained.

BSA loading also seemed to have no effect on the *in vitro* release profile (Figure 4). The non-porous shell entirely prevented the release of BSA during the lag phase, and once the shell had sufficiently degraded, a large part of the encapsulated BSA was released at once, independent of the BSA loading. The formulation with the highest BSA loading did show a minimal burst release of $14.0 \pm 1.6\%$, but this could rather be attributed to BSA release from some fractured particles with thin shells that were visible on SEM images (data not shown) than to the BSA loading.

However, for all formulations, the percentage of the total BSA content that was released during the pulse was only 30 to 50%. Incomplete release of proteins is a common problem for PLGA-based drug delivery formulations, even for relatively stable model antigens such as BSA, and it is often ascribed to protein instability within the formula-

tion [8,34,35]. Possible explanations for protein instability are the polymer degradation products that are formed upon hydrolysis of the polymer, which can both create an acidic microclimate within the formulation and can cause protein aggregation due to the incompatibility of the protein with the polymer degradation products [36–38]. In addition, adsorption of the protein to the hydrophobic polymer surface can cause part of the protein to remain entrapped [36–38]. Therefore, further research into alternative polymers that generate less or no acidic degradation products while maintaining a delayed pulsatile release profile is desired. However, the BSA release does seem to continue after the pulse, although at a lower rate. This is caused by ongoing hydrolysis of the polymer, leading to a second phase of release in which BSA slowly diffuses out [11]. Nonetheless, it is not expected that this phase will ultimately lead to complete release of the encapsulated protein.

4.3.4 Particle morphology of PDLG5002-based core-shell microspheres during BSA in vitro release

To further clarify the BSA *in vitro* release mechanism, PDLG5002-based core–shell microspheres containing BSA (Formulation C) were imaged by optical microscopy and SEM at different time points during the *in vitro* release study (Figure 5). Before incubation in *in vitro* release medium, highly monodisperse core–shell microspheres with thin shells and a single core are visible (Figure 5a, Figure 5b). The cores seem free of water due to the freeze drying, but the imprint of the inner water droplets can still be seen in the shells, and in some microspheres, an accumulation of BSA is visible in the cores. Upon incubation in *in vitro* release medium at 37 °C, the microspheres retained a smooth surface for at least 14 days, although the sphericity of the particles reduced (Figure 5e, Figure 5f). In addition, after 2 h, some agglomeration had already occurred (Figure 5c, Figure 5d). Moreover, water seems to have penetrated into the cores, as BSA is not visible anymore, and the imprint of the small inner water droplets has disappeared. This can be attributed to the glass transition temperature of the polymer, which was 31.6 °C as dry product and 19.1 °C after adding a small volume of water to the sample and allowing it to moisturize for 30 min [7]. Subsequently, the excess of water was removed, and the sample was measured with differential scanning calorimetry 5 h later. The measured glass transition temperature is below environmental temperature when set at 37 °C, which causes the polymer to change from the glassy state into the rubbery state [7]. This increases the mobility of the polymer chains, thereby enabling water influx into the cores [39,40]. Additionally, the polymer heats up and absorbs water, which is reflected in the swollen shells [11]. This transition into the rubbery state might also have caused the agglomeration of some of the microspheres. After 25 days, the microspheres had collapsed and presented a raisin-like structure (Figure 5g, Figure 5h). These results are in accordance with the *in vitro* release profile (Figure 4) that demonstrated a clear increase in BSA release from week 3 to 5. At this point, polymer degradation has reached a critical level, which caused BSA to diffuse out of the microspheres.
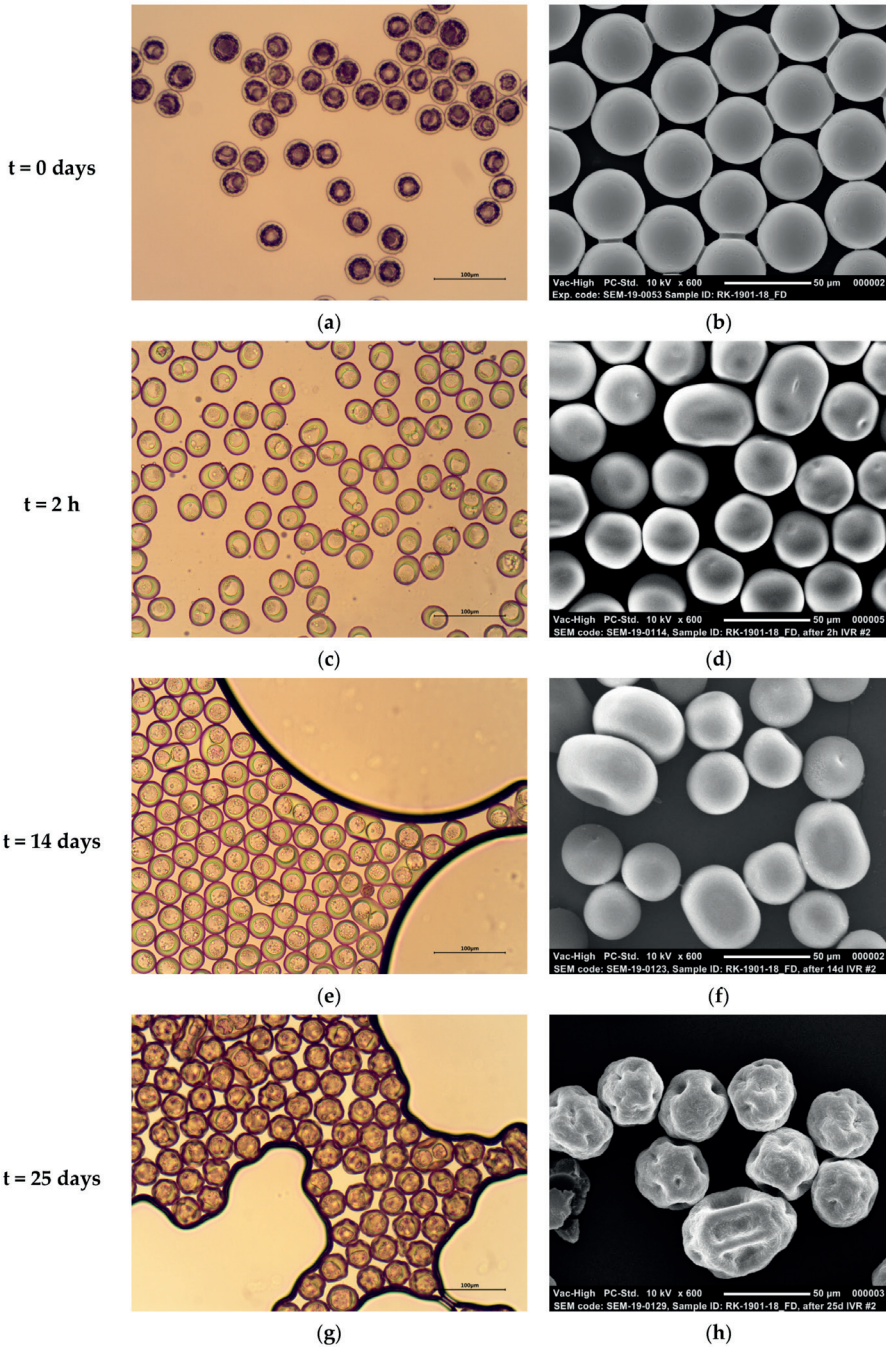
Figure 5. Representative microscopy images depicting the morphology of PDLG5002-based core–shell microspheres (formulation C) at different stages before and during the *in vitro* release of BSA. (**a**) and (**b**) Images of the initial microspheres after washing and freeze drying and before release; (**c**) and (**d**) 2 h after release; (**e**) and (**f**) 14 days after release; (**g**) and (**h**) 25 days after release. Left panel: optical microscopy images, right panel: SEM images.

BSA-containing core–shell microspheres with different shell compositions were produced to determine the influence of the PLGA monomer ratio on the *in vitro* release profile, as this monomer ratio greatly influences the degradation rate of PLGA. Figure 6 shows that all three formulations exhibited a delayed release profile without any BSA release during the lag phase.
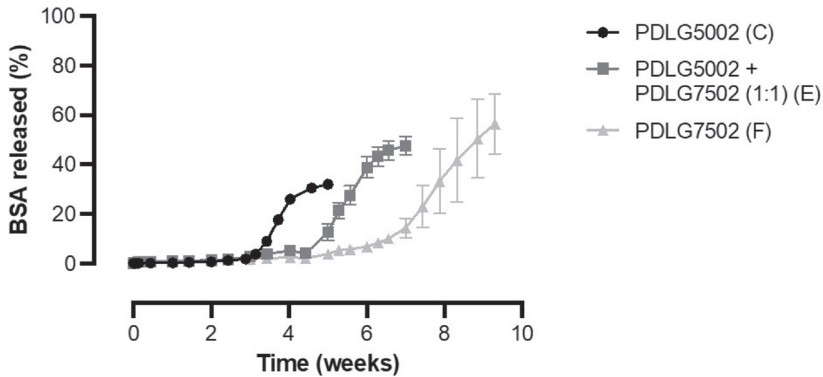
Figure 6. Cumulative *in vitro* release of BSA from core–shell microspheres composed of PLGA of different monomer ratios (*n* = 3).

For formulation E, the release of BSA out of the microspheres indeed continued after the pulse, albeit at a decreased rate (data not shown). Moreover, there was a clear relationship between the monomer ratio of PLGA and the lag time, as the lag phase substantially increased with the increasing lactide content of the polymer. The lag time was approximately 3, 4.5, and 7 weeks for a PDLG5002, PDLG5002 + PDLG7502 (mass ratio 1:1), and PDLG7502 shell, respectively. A higher lactide content causes the hydrophilicity and thus the degradation rate to decrease [10–12]. In comparison, the lag time of the previously studied core–shell implants with a PDLG7502 shell was only 4.5 weeks [8]. A possible reason for this difference in lag time is that autocatalytic degradation starts after a few weeks of release. This autocatalytic degradation might play a bigger role in the large implants than in the thin-shelled microspheres [10,41]. A potential application of the produced core–shell microspheres is the current vaccine against SARS-CoV-2: for instance, the Pfizer-BioNTech vaccine that requires two doses given 3 weeks apart [42]. So far, only PDLG5002, PDLG7502, and a blend of both polymers were tested, but alternative monomer ratios could be used to tailor the *in vitro* release profile to the specific needs of different vaccines. Moreover, other studies with core–shell microspheres and implants have demonstrated that the lag time could be varied by altering the molecular weight of the polymer [29,43]. This opens many possibilities for the use of core–shell microspheres as single-injection vaccines.

4.4 Conclusion

This research demonstrates that monodisperse PLGA-based core–shell microspheres containing BSA can be produced using a microfluidic setup. *In vitro* release studies showed that after an adjustable lag time of 3 to 7 weeks, BSA released from the microspheres in a pulsatile manner, although the release was incomplete. This lag time was dependent on the monomer ratio of PLGA, with a higher lactide content causing a longer lag time. However, neither the shell thickness nor BSA loading had an influence on the release profile. These parenterally injectable delayed pulsatile release microspheres are a promising candidate for single-injection vaccine formulations when combined with a primer, as the lag time could be altered by varying the composition of the polymer shell. The primer dose could be included by injecting the core–shell microspheres together with an immediate-release formulation or a solution of the antigen. Moreover, even a second booster dose could be included by simply co-injecting core–shell microspheres with a different lag time. In this way, the release profiles can be tailored to the particular needs of a vaccine, which enables the use of core–shell microspheres for a wide variety of vaccines. Future research should focus on using alternative polymers that do not generate acidic degradation products to avoid incomplete protein release, and incorporating a therapeutically relevant vaccine.

Acknowledgments

References

[1]   WHO, "Vaccines and Immunization," 2021. [Online]. Available: https://www.who.int/health-topics/vaccines-and-immunization. [Accessed: Sep. 29, 2021].

[2]   WHO, "Immunization Coverage," 2021. [Online]. Available: https://www.who.int/news-room/fact-sheets/detail/immunization-coverage. [Accessed: Sep. 29, 2021].

[3]   N.C. Galles et al., "Measuring routine childhood vaccination coverage in 204 countries and territories, 1980–2019: A systematic analysis for the global burden of disease study 2020, release 1," The Lancet, vol. 398, pp. 503–521, 2021.

[4]   WHO and UNICEF, "Progress and Challenges with Achieving Universal Immunization Coverage," 2019. [Online]. Available: https://www.who.int/immunization/monitoring_surveillance/who-immuniz.pdf?ua=1. [Accessed: Sep. 29, 2021].

[5]   K.J. McHugh, R. Guarecuco, R. Langer, and A. Jaklenec, "Single-injection vaccines: Progress, challenges, and opportunities," Journal of Controlled Release, vol. 219, pp. 596–609, 2015.

4

[6]   J.L. Cleland, "Single-administration vaccines: Controlled-release technology to mimic repeated immunizations," Trends in Biotechnology, vol. 17, pp. 25–29, 1999.

[7]   M. Beugeling et al., "The mechanism behind the biphasic pulsatile drug release from physically mixed poly(DL-lactic(-co-glycolic) acid)-based compacts," International Journal of Pharmaceutics, vol. 551, pp. 195–202, 2018.

[8]   K. Amssoms et al., "Ovalbumin-containing core-shell implants suitable to obtain a delayed IgG1 antibody response in support of a biphasic pulsatile release profile in mice," PLoS ONE, vol. 13, p. e0202961, 2018.

[9]   J.M. Anderson and M.S. Shive, "Biodegradation and biocompatibility of PLA and PLGA microspheres," Advanced Drug Delivery Reviews, vol. 28, pp. 5–24, 1997.

[10]   L. Lu, C.A. Garcia, and A.G. Mikos, "In vitro degradation of thin poly(DL-lactic-co-glycolic acid) films," Journal of Biomedical Materials Research, vol. 46, pp. 236–244, 1999.

[11]   S. Fredenberg, M. Wahlgren, M. Reslow, and A. Axelsson, "The mechanisms of drug release in poly(lactic-co-glycolic acid)-based drug delivery systems—A review," International Journal of Pharmaceutics, vol. 415, pp. 34–52, 2011.

[12]   H.K. Makadia and S.J. Siegel, "Poly Lactic-co-Glycolic Acid (PLGA) as biodegradable controlled drug delivery carrier," Polymers, vol. 3, pp. 1377–1397, 2011.

[13]   F. M. Galogahi, Y. Zhu, H. An, and N.-T. Nguyen, "Core-shell microparticles: Generation approaches and applications," J. Sci. Adv. Mater. Devices, vol. 5, pp. 417-435, 2020.

[14]   G. Lemperle, "Biocompatibility of injectable microspheres," Biomed. J. Sci. Tech. Res., vol. 2, pp. 2296-2306, 2018.

[15]   M. Ye, S. Kim, and K. Park, "Issues in long-term protein delivery using biodegradable microparticles," J. Control. Release, vol. 146, pp. 241-260, 2010.

[16]   X. Chen, C. P. Ooi, and T. H. Lim, "Effect of ganciclovir on the hydrolytic degradation of poly(lactide-co-glycolide) microspheres," J. Biomater. Appl., vol. 20, pp. 287-302, 2006.

[17]   Y. Xia and D. W. Pack, "Pulsatile protein release from monodisperse liquid-core microcapsules of controllable shell thickness," Pharm. Res., vol. 31, pp. 3201-3210, 2014.

[18]   E. J. Pollauf, K. K. Kim, and D. W. Pack, "Small-molecule release from poly(D,L-Lactide)/Poly(D,L-lactide-co-glycolide) composite microparticles," J. Pharm. Sci., vol. 94, pp. 2013-2022, 2005.

[19]   W. Zheng, "A water-in-oil-in-oil-in-water (W/O/O/W) method for producing drug-releasing, double-walled microspheres," Int. J. Pharm., vol. 374, pp. 90-95, 2009.

[20]   S.-Y. The, R. Lin, L.-H. Hung, and A. P. Lee, "Droplet microfluidics," Lab Chip, vol. 8, pp. 198-220, 2008.

[21]   R. K. Shah, H. C. Shum, A. C. Rowat, D. Lee, J. J. Agresti, A. S. Utada, L.-Y. Chu, J.-W. Kim, A. Fernandez-Nieves, C. Martinez et al., "Designer emulsions using microfluidics," Mater. Today, vol. 11, pp. 18-27, 2008.

[22]   S. W. Kim, K.-H. Hwangbo, J. H. Lee, and K. Y. Cho, "Microfluidic fabrication of microparticles with multiple structures from a biodegradable polymer blend," RSC Adv., vol. 4, pp. 46536-46540, 2014.

[23]   S.-W. Choi, Y. S. Zhang, and Y. Xia, "Fabrication of microbeads with a controllable hollow interior and porous wall using a capillary fluidic device," Adv. Funct. Mater., vol. 19, pp. 2943-2949, 2009.

[24]   W. Li, H. Dong, G. Tang, T. Ma, and X. Cao, "Controllable microfluidic fabrication of Janus and microcapsule particles for drug delivery applications," RSC Adv., vol. 5, pp. 23181-23188, 2015.

[25]   T. Kong, J. Wu, K. Yeung, M.K.T. To, and L. Wang, "Microfluidic fabrication of polymeric core-shell microspheres for controlled release applications," Biomicrofluidics, vol. 7, p. 044128, 2013.

[26]   F. Tu and D. Lee, "Controlling the stability and size of double-emulsion-templated poly(lactic-co-glycolic) acid microcapsules," Langmuir, vol. 28, pp. 9944-9952, 2012.

[27]   A. Sanchez, R.K. Gupta, M.J. Alonso, G.R. Siber, and R. Langer, "Pulsed controlled-release system for potential use in vaccine delivery," J. Pharm. Sci., vol. 85, pp. 547-552, 1996.

[28]   C. Berkland, E. Pollauf, N. Varde, D.W. Pack, and K. Kim, "Monodisperse liquid-filled biodegradable microcapsules," Pharm. Res., vol. 24, pp. 1007-1013, 2007.

[29]   M. Zamani, M.P. Prabhakaran, E.S. Thian, and S. Ramakrishna, "Protein encapsulated core–shell structured particles prepared by coaxial electrospraying: Investigation on material and processing variables," Int. J. Pharm., vol. 473, pp. 134-143, 2014.

[30]   M. Beugeling, K. Amssoms, F. Cox, B. De Clerck, E. Van Gulck, J.A. Verwoerd, G. Kraus, D. Roymans, L. Baert, H.W. Frijlink, et al., "Development of a stable respiratory syncytial virus pre-fusion protein powder suitable for a core-shell implant with a delayed release in mice: A proof of concept study," Pharmaceutics, vol. 11, p. 510, 2019.

[31]   C. Berkland, E. Pollauf, D.W. Pack, and K. Kim, "Uniform double-walled polymer microspheres of controllable shell thickness," J. Control. Release, vol. 96, pp. 101-111, 2004.

[32]   F.Y. Han, K.J. Thurecht, A.K. Whittaker, and M.T. Smith, "Bioerodable PLGA-based microparticles for producing sustained-release drug formulations and strategies for improving drug loading," Front. Pharmacol., vol. 7, p. 185, 2016.

[33]   N.K. Varde and D.W. Pack, "Microspheres for controlled release drug delivery," Expert Opin. Biol. Ther., vol. 4, pp. 35-51, 2004.

[34]   Z. Ghalanbor, M. Koerber, and R. Bodmeier, "Interdependency of protein-release completeness and polymer degradation in PLGA-based implants," Eur. J. Pharm. Biopharm., vol. 85, pp. 624–630, 2013.

[35]   L. Duque, M. Koerber, and R. Bodmeier, "Improving release completeness from PLGA-based implants for the acid-labile model protein ovalbumin," Int. J. Pharm., vol. 538, pp. 139–146, 2018.

[36]   G. Zhu, S. R. Mallery, and S. P. Schwendeman, "Stabilization of proteins

encapsulated in injectable poly (lactide-co-glycolide)," Nat. Biotechnol., vol. 18, pp. 52–57, 2000.

[37]   M. van de Weert, W. E. Hennink, and W. Jiskoot, "Protein instability in poly(lactic-co-glycolic acid) microparticles," Pharm. Res., vol. 17, pp. 1159–1167, 2000.

[38]   K. Fu, A.M. Klibanov and R. Langer, "Protein stability in controlled-release systems," Nat. Biotechnol., vol. 18, pp. 24-25, 2000.

[39]   K. K. L. Phua, E. R. H. Roberts, and K. W. Leong, "Degradable polymers," in Comprehensive Biomaterials, P. Ducheyne, K. E. Healy, D. W. Hutmacher, D. W. Grainger, and C. J. Kirkpatrick, Eds. Elsevier Ltd., 2011, vol. 1, pp. 381–415.

[40]   N. Kamaly, B. Yameen, J. Wu, and O. C. Farokhzad, "Degradable controlled-release polymers and polymeric nanoparticles: Mechanisms of controlling drug release," Chem. Rev., vol. 116, pp. 2602–2663, 2016.

[41]   Y. Xia and D. W. Pack, "Uniform biodegradable microparticle systems for controlled release," Chem. Eng. Sci., vol. 125, pp. 129–143, 2015.

[42]   Centers for Disease Control and Prevention (CDC), "Different COVID-19 Vaccines," 2021. [Online]. Available: https://www.cdc.gov/coronavirus/2019-ncov/vaccines/different-vaccines.html. [Accessed: 15-Oct-2021].

[43]   C. Guse, S. Koennings, T. Blunk, J. Siepmann, and A. Goepferich, "Programmable implants—From pulsatile to controlled release," Int. J. Pharm., vol. 314, pp. 161–169, 2006.

Supplementary materials

Video S1. Video obtained with CLSM that visualizes the 3D structure of FITC–BSA fluorescence in PDLG5002-based core-shell microspheres (available online at https://www.mdpi.com/article/10.3390/pharmaceutics13111854/s1).

4

Chapter 5

The use of inline ultrasonic and microfluidic emulsification for the production of poly(DL-lactide-*co*-glycolide)-based core-shell microspheres

Renée S. van der Kooij [1], Rob Steendam [2], Johan Zuidema [2], Henderik W. Frijlink [1], and Wouter L. J. Hinrichs [1]

[1] Department of Pharmaceutical Technology and Biopharmacy, University of Groningen, Antonius Deusinglaan 1, 9713 AV Groningen, The Netherlands
[2] InnoCore Pharmaceuticals, L.J. Zielstraweg 1, 9713 GX Groningen, The Netherlands

Abstract

In order to reduce under-vaccination, the development of a single-administration vaccine formulation for vaccines that require a multiple-dose schedule would be highly desired. An example of such a formulation is injectable core-shell microspheres with a biphasic release profile of the antigen, which means that the initial release of the antigen is followed by the pulsatile release of the remaining antigen a few weeks or months later. In this study, core-shell microspheres were prepared from a water-in-oil-in-water double emulsion, where the primary emulsion was generated in a flow-through ultrasonic cell and the double emulsion was generated in a microfluidic chip. Monodisperse particles with a poly(DL-lactide-*co*-glycolide) (PLGA) shell, having different particle dimensions, were obtained with this setup. Various attempts to incorporate the model antigen bovine serum albumin (BSA) into the microspheres, however, failed. This was probably due to the relatively thick shells of the microspheres, which caused slow solidification and diffusion of BSA out of the cores. We hypothesize that the shell thickness could be reduced by decreasing the flow rate ratio of the shell/core phase (< 12) in combination with a low polymer concentration (< 7.5 wt-%). Successful incorporation of BSA into these microspheres would enable the development of a delayed pulsatile release formulation. Such delayed pulsatile release microspheres could be co-injected together with a solution of the antigen, thereby enabling the desired biphasic release profile and ultimately a single-administration vaccine formulation.

5.1 Introduction

Over the past decades, a lot of research has been focused on the development of single-administration vaccine formulations. Such a formulation could provide complete protection against the targeted pathogen after only a single administration, thereby offering the potential of improving the vaccination coverage [1,2]. One example of a single-administration vaccine formulation is an injectable biphasic release formulation in which the initial release of the antigen (i.e. the primer dose) is followed by the pulsatile release of the remaining antigen (i.e. the booster dose) after a certain lag time [1-3]. In a previous study, a delayed pulsatile release of the model antigen bovine serum albumin (BSA) was achieved by developing core-shell microspheres with a shell composed of the biocompatible and biodegradable polymer poly(DL-lactide-co-glycolide) (PLGA) [4]. Initially, the non-porous polymer shell acted as a barrier to antigen release, thereby causing a lag phase in which no antigen was released. After a few weeks, the polymer shell had sufficiently degraded which caused the antigen to be released in a pulsatile manner. These core-shell microspheres only served as the booster dose, but we hypothesized that the primer dose can easily be administered by co-injecting a solution of the antigen or by adding a separate immediate-release formulation of the antigen.

The core-shell microspheres developed in the abovementioned study were produced using droplet microfluidics to generate a water-in-oil-in-water (W/O/W) emulsion that formed the basis for the microspheres. The W/O/W double emulsion was generated by placing two microfluidic chips in series. The first chip featured channels with a diameter of 14 μm, in which an aqueous solution of BSA was dispersed into a solution of PLGA in dichloromethane (DCM), thereby forming a primary water-in-oil (W/O) emulsion. The second chip featured channels with a diameter of 100 μm. In this chip, the primary emulsion was encapsulated into an aqueous polyvinyl alcohol (PVA) solution, thereby forming a W/O/W double emulsion. After extraction and evaporation of DCM, core-shell microspheres were obtained. This setup allowed the development of highly monodisperse core-shell microspheres, but it also had some disadvantages. First of all, the first chip was very prone to clogging due to the narrow diameter of its microchannels, which often caused failure of the microsphere production. Second, with the typical flow rate of the polymer solution in the first chip being 7.8 μL/min, the yield was usually only 100 mg/h or less. Last, as the microspheres will be administered via the parenteral route, product sterility is required, which can only be achieved by aseptic manufacturing as has been previously explained by Freitas et al. [5]. Steam sterilization is the preferred method due to its safety, low costs, short cycle time, and ease of use [6,7], but steam sterilizing the first chip is not possible as it contains a hydrophobic coating that is damaged by this method [8].

Here, we present an alternative setup for the production of core-shell microspheres that could overcome the limitations of the first microfluidic chip by replacing it with a flow-through ultrasonic cell. With this setup, PLGA-based core-shell microspheres were developed by means of a W/O/W double emulsion solvent evaporation method. The primary W/O emulsion was generated in the flow-through ultrasonic cell, while the W/O/W double emulsion was generated in the 100 μm microfluidic chip. The produced microspheres were characterized in terms of particle size, morphology, and BSA loading,

and the influence of the flow rates and polymer concentration on the shell thickness was evaluated.

5.2 Materials and methods

5.2.1 Materials
PLGA with an inherent viscosity of 0.2 dL/g and a DL-lactide:glycolide molar ratio of 50:50 (PDLG5002) was purchased from Corbion Purac Biomaterials (Gorinchem, The Netherlands). Polyglycerol polyricinoleate (PGPR) was a generous gift from TER Ingredients GmbH& CO. KG (Hamburg, Germany). DCM was purchased from Fisher Scientific (Leicestershire, UK). BSA and PVA (M_w 9–10 kDa, 80% hydrolyzed) were obtained from Sigma-Aldrich Co. (St. Louis, MO, USA). For all experiments, ultrapure water was used with a resistivity of 18.2 MΩ obtained from a Millipore Milli-Q Integral 3 (A10) purification system.

5.2.2 Fabrication of core-shell microspheres
Monodisperse core-shell microspheres with a PDLG5002-based shell were prepared with a W/O/W double emulsion solvent evaporation method using an inline ultrasonic and microfluidic setup (Figure 1).
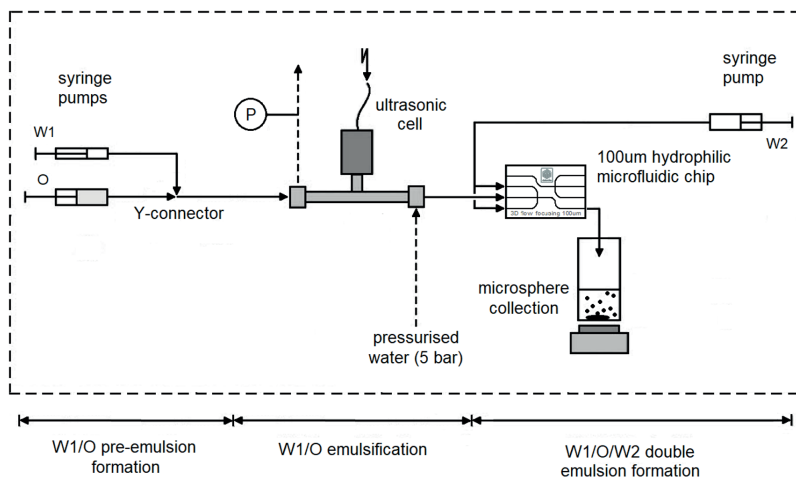
Figure 1. Schematic representation of the ultrasonic and microfluidic emulsification setup used for the production of core-shell microspheres. Modified from [5] with permission from Elsevier.

First, a coarse primary W/O emulsion was produced by injecting an inner water phase (W1) and an oil phase (O, i.e. the organic polymer phase) through separate capillaries that were connected at the ends with a Y-connector assembly. For these capillaries, fluorinated ethylene propylene (FEP) tubing with an OD of 1.59 mm and an ID of 0.25 mm was used. The hydrophobic nature of FEP and the use of a sufficiently high flow rate ratio of shell to core phase allowed for the formation of an emulsion of inner water phase droplets in the organic polymer phase. Subsequently, this coarse W/O emulsion

was transported into the flow-through ultrasonic cell (Hielscher Ultrasonics, Teltow, Germany; Figure 2) for further homogenization.
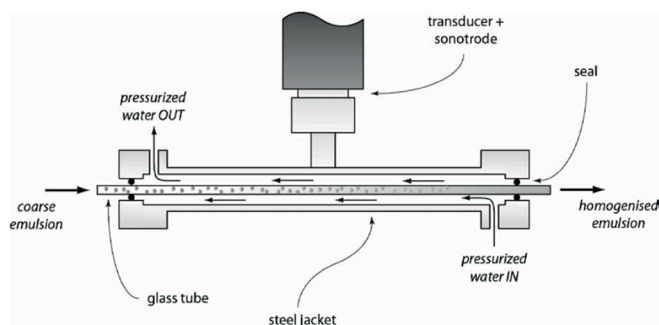
Figure 2. Design of the ultrasonic flow-through cell for the production of the primary water-in-oil (W/O) emulsion. Reproduced from [5] with permission from Elsevier.

The working principle of this ultrasonic cell has been extensively described previously [9]. In short, the setup consists of a 24.5 cm long glass tube with a 1.2 mm inner diameter that is inserted into a steel jacket. The obtained emulsion is pumped through this glass tube where further droplet break-up occurs through ultrasonic cavitation. The ultrasound waves causing this cavitation are introduced by a 20 kHz sonotrode that is attached to the steel jacket. Pressurized water (5 bar) is pumped through the open space between the steel jacket and the glass tube for conduction of the ultrasound waves and for cooling of the emulsion in the glass tube. The total power applied by the ultrasonic unit could be controlled by the amplitude of the transducer's oscillation which was varied between 50 and 90% of the maximum amplitude. Previously, the power intake at the maximum amplitude was quantified to be 32 W for a similar setup employing the flow-through ultrasonic cell [9]. The fine W/O emulsion formed in the ultrasonic flow-through cell was transported into a glass flow-focusing microfluidic chip with a channel diameter of 100 μm at the junction (Dolomite Ltd., Royston, UK). In contrast to the abovementioned 14 μm chip, the microchannel surface of this chip did not have a hydrophobic coating and was, therefore, naturally hydrophilic. This hydrophilic surface enabled the formation of a W/O/W double emulsion by pumping an outer water phase (W2) into the microfluidic chip together with the W/O emulsion. The primary W/O emulsion was hydrodynamically flow focused by the outer water phase, which resulted in the continuous production of monodisperse W/O/W emulsion droplets at the junction of the microchannels. An excess of PVA solution at room temperature was used to collect the produced double-emulsion droplets. Extraction and evaporation of DCM took place overnight at room temperature by gentle stirring of the dispersion, after which solid microspheres remained. The obtained microspheres were washed three times with an aqueous 0.05 wt-% Tween 80 solution and three times with water, and eventually freeze-dried using a Christ Alpha 2–4 LSC plus freeze-dryer (Martin Christ Gefriertrocknungsanlagen GmbH, Osterode am Harz, Germany) according to a program previously described [4].

Water or an aqueous 200 mg/mL BSA solution were used as the inner water phase. For the oil phase, a solution of PDLG5002 (5, 7.5, 10, or 15 wt-%) and PGPR

(0.5, 0.75, 0.1, or 1.5 wt-%, respectively) in DCM was prepared. A 2 wt-% aqueous PVA solution served as the outer water phase. All liquids were injected into the setup using Nexus 3000 syringe pumps (Chemyx Inc., Stafford, TX, USA) and the flow rates could be adjusted independently. Various flow rates and flow rate ratios were tested (Table 1) to determine their influence on the particle size, shell thickness, and BSA loading. The theoretical BSA loading was calculated according to Equation (1).

$$\text{Theoretical loading} = \frac{W_1 \text{ flow rate} \times W_1 \text{ conc.}}{W_1 \text{ flow rate} \times W_1 \text{ conc.} + O \text{ flow rate} \times O \text{ conc.}} \times 100\% \qquad (1)$$

All core-shell microsphere formulations were prepared at least once (n = 1), but for some formulations, 2, 3, or 7 batches were prepared (Table 1). This was done to evaluate the reproducibility of the production method and enable a linear regression analysis on the shell thickness data in relation to the polymer concentration and flow rate ratio shell/core phase. Also, for some batches, the microsphere collection conditions were varied (Table 1) to determine the influence on the BSA loading. An overview of all formulations can be found in Table 1.

Table 1. Experimental parameters and settings of different PDLG5002-based core-shell microsphere formulations.

Formulation	Number of Batches	Model Compound	Polymer Concentration (wt-%)	Flow Rate Ratio Shell/Core Phase	Flow Rates (W₁–O–W₂, µL/min)	Theoretical Loading (wt-%)	Amplitude (%)
1	1	-	10	19.5	0.8–15.6–20	-	80
2	1	-	10	19.5	0.8–15.6–50	-	50
3	1	-	10	19.5	0.8–15.6–50	-	60
4	2	-	10	19.5	0.8–15.6–50	-	70
5	1	-	10	19.5	0.8–15.6–50	-	80
6	1	-	10	19.5	0.8–15.6–50	-	90
7	1	BSA	5	19.5	0.8–15.6–60	12.5	70
8	2	BSA	7.5	19.5	0.8–15.6–60	8.7	70
9	1	BSA	10	13	0.8–10.4–60	9.6	70
10	2	BSA	10	13	1.2–15.6–60	9.6	70
11	1	BSA	10	13	1.6–20.8–120	9.6	70
12	1	BSA	10	13	2.4–31.2–120	9.6	70
13	2	BSA	10	15	0.8–12.0–60	8.4	70
14	1	BSA	10	15	0.8–12.0–100	8.4	70
15	7 [1]	BSA	10	19.5	0.8–15.6–60	6.6	70
16	1	BSA	10	19.5	0.8–15.6–100	6.6	70
17	3 [2]	BSA	10	19.5	1.6–31.2–120	6.6	70
18	1	BSA	15	19.5	0.4–7.8–30	4.5	70
19	2 [3]	BSA	15	19.5	1.6–31.2–120	4.5	70

[1] Batch 4: microsphere collection in 2 wt-% PVA solution at 30°C, followed by extraction at room temperature. Batch 5: microsphere collection in 2 wt-% PVA + 5 wt-% sodium chloride solution.
[2] Batch 3: microsphere collection in 2 wt-% PVA solution cooled on ice. Extraction and evaporation of DCM overnight at room temperature, followed by one hour at 25°C and one hour at 30°C.
[3] Batch 2: microsphere collection in 2 wt-% PVA solution cooled on ice. Extraction and evaporation of DCM overnight at room temperature, followed by one hour at 25°C and one hour at 30°C.

5.2.3 Characterization of microsphere size and morphology

All microsphere batches were characterized before washing and freeze-drying in terms of size and morphology. Light microscopy images were taken at 100×, 200×, and 400× magnification with an ME.2665 Euromex optical microscope (Arnhem, The Netherlands), after which they were analyzed using ImageJ software (National Institutes of Health, Bethesda, MD, USA). For twenty randomly selected particles, the diameter (d_y) of the whole particle and the core was measured from several representative images. The volume median diameter (d50, Equation (2)) ± the standard deviation (SD, Equation (3)) and the coefficient of variation (CV, Equation (4)) of the whole microspheres and the cores were calculated to determine the particle size and particle size distribution of the different microsphere batches.

$$d50 = \sum V\%_y \times d_y \tag{2}$$

where $V\%_y = \dfrac{V_y}{V_{total}}$; $V_y = \dfrac{4}{3} \times \pi \times (\dfrac{d_y}{2})^3$ and $V_{total} = \sum V_y$

where V_y is the volume of the measured particle; V_{total} is the total volume of the measured particles; and $V\%_y$ is the percentage V_y of V_{total}.

$$SD = \sqrt{\frac{\sum 100 \times V\%_y \times (d_y - d50)^2}{V\%_{total}}} \tag{3}$$

where $V\%_{total}$ is the total volume percentage of the measured particles; $V\%_{total} = 100\%$.

$$CV = \frac{SD}{d50} \times 100\% \tag{4}$$

Average shell thickness was calculated as well (Equation (5)).

$$Shell\ thickness = \frac{\sum \frac{d_{y,particle} - d_{y,core}}{2}}{N} \tag{5}$$

where N = 20.

For the dried microspheres, scanning electron microscopy (SEM) images were acquired with a NeoScope JCM-5000 (JEOL Ltd., Tokyo, Japan). The acceleration voltage was set at 10 kV, the probe current to standard, and the filament setting to long life. Prior to examination, the microspheres were mounted onto metal stubs using double-sided adhesive carbon tape and sputter-coated with gold. Images were taken at different magnifications ranging from 50× to 1500×. The d50 ± SD and CV of the dried microspheres are not listed, as the differences from the wet microspheres were only minimal.

For some microsphere batches, the internal morphology was examined as well by taking SEM images of the cross-sectioned particles. To this end, the dried microspheres were embedded in an organic solvent-free adhesive (UHU® Twist & Glue Renature, Bühl, Germany). The prepared samples were air-dried for 2 days, after which they were cooled for 30 min at −70 °C and cut into five equal pieces using a razor blade.

5.2.4 BSA loading of microspheres

For the determination of the actual BSA loading of the core-shell microspheres, the total nitrogen content was measured using a Vario MICRO Cube elemental analyzer (Elementar, Ronkonkoma, NY, USA) in CHNS mode. The samples were combusted at a temperature of 1150 °C. The encapsulation efficiency (EE) was calculated from both the theoretical and the actual BSA loading according to Equation (6).

$$EE = \frac{\text{Actual loading}}{\text{Theoretical loading}} \times 100\% \tag{6}$$

5.2.5 Statistics and data analysis

All measurements were performed in triplicate (n = 3), unless otherwise stated, and data were expressed as mean ± SD. The graphs and linear regression analyses were performed using GraphPad Prism version 9.1.2 (La Jolla, CA, USA).

5.3. Results and discussion

5.3.1 Preparation of monodisperse PDLG5002-based core-shell microspheres with the flow-through ultrasonic cell

Monodisperse core-shell microspheres with a PDLG5002 shell were prepared with the inline ultrasonic and microfluidic emulsification setup as depicted in Figure 1. The characteristics of these batches, such as BSA loading and particle dimensions, are listed in Table 2. All batches showed a clear distinction between the core and shell domain, with representative optical microscopy and SEM images of one of these batches as an example shown in Figure 3. This demonstrates that the replacement of the 14 μm microfluidic chip by the flow-through ultrasonic cell did not affect the ability to produce microspheres with a core-shell structure. Similar to the core-shell microspheres produced with the 14 μm microfluidic chip (Figure 4), the cores of the wet particles consisted of many small inner water droplets before freeze-drying (Figure 3a). Yet, after freeze-drying, hollow single-core particles were obtained (Figure 3c) due to coalescence of the inner water droplets [4].
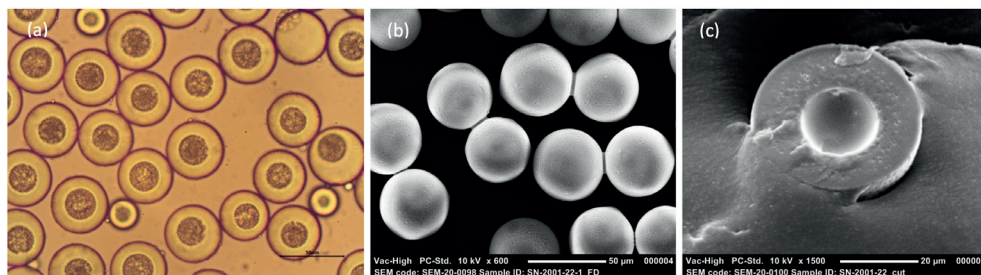

Figure 3. Representative microscopy images of PDLG5002-based core-shell microspheres loaded with 0.27 wt-% BSA (Formulation 15, Batch 1): (a) Optical microscopy image at 400× magnification; (b) Scanning electron microscopy (SEM) image at 600× magnification; (c) SEM image of cross-sectioned microsphere at 1500× magnification.
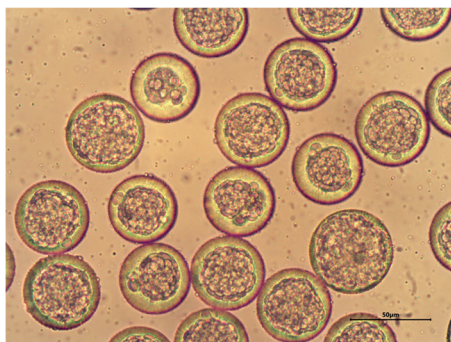
Figure 4. Representative optical microscopy image at 400× magnification of core-shell microspheres produced with a 14 μm microfluidic chip for the primary emulsification step. The microspheres contained 5.7 wt-% BSA and the shells were composed of PLGA with an inherent viscosity of 0.2 dL/g and a DL-lactide:glycolide molar ratio of 75:25. Reproduced from [4].

Though the microspheres in Figure 4 are composed of PLGA with a different DL-lactide:glycolide molar ratio than the microspheres is Figure 3, it is not expected that this difference has affected the particle dimensions and EE, as this was also not observed in the study with the 14 μm microfluidic chip [4].

The change in preparation method of the primary W/O emulsion did, however, alter the particle dimensions. First of all, the average droplet size of the inner water droplets considerably decreased. Though for both preparation methods, the droplet size of the primary W/O emulsion has not been measured, optical microscopy images clearly demonstrate that a much finer primary emulsion is obtained when prepared with the flow-through ultrasonic cell (Figure 3a) than when prepared with the 14 μm microfluidic chip (Figure 4). This indicates that sonication could reduce the emulsion droplet size more effectively than microfluidization, as the latter is limited by the microchannel diameter of the chip which is suitable for generating droplets between 5 and 12 μm [10]. In contrast, mean droplet sizes of < 700 nm were obtained for a primary emulsion of BSA in PLGA solution produced with the flow-through ultrasonic cell [5]. Second, a broader particle size distribution was obtained for both the whole particle and the core diameter, which is reflected in the relatively higher CV values (Table 2). This could be attributed to the fact that the primary emulsion is no longer produced drop by drop, which resulted in reduced control over the droplet generation and, therefore, a broader droplet and particle size distribution. Moreover, in this study, syringe pumps instead of pressure-driven pumps were used for the injection of the liquids into the system, though it is possible to exchange the syringe pumps for pressure-driven pumps in this setup. Syringe pumps introduce higher levels of pulsation into the flow due to the stepper motor inside the pump [11-13]. Nevertheless, nearly all batches still had CV values of < 15% for the whole particle diameter and < 20% for the core diameter (Table 2). In comparison, for the microspheres produced with the 14 μm chip, all CVparticle values were < 10% and all CVcore values were < 15% [4]. Finally, the shell thickness was generally higher with values of 7.5 to 16.7 μm (Table 2) compared to 4.2 to 10.0 μm for the microspheres produced with the 14 μm chip [4]. Previous studies, however, have shown that the

Table 2. Characteristics of core-shell microsphere batches with different bovine serum albumin (BSA) loading and particle dimensions.

Formulation	Batch no.	Actual Loading (wt-%)	EE (%)	$d50_{particle}$ (µm)	$CV_{particle}$ (%)	$d50_{core}$ (µm)	CV_{core} (%)	Shell Thickness (µm)
1	1	-	-	62.1 ± 5.7	9.1	28.8 ± 3.7	12.8	16.7 ± 1.6
2	1	-	-	41.3 ± 5.3	12.3	17.7 ± 3.3	18.5	11.6 ± 1.0
3	1	-	-	38.2 ± 2.3	6.1	16.8 ± 1.5	9.0	10.8 ± 0.9
4	1	-	-	38.9 ± 0.6	1.5	18.8 ± 1.1	6.1	10.2 ± 0.5
4	2	-	-	46.2 ± 4.8	10.4	22.0 ± 2.6	12.0	11.6 ± 1.6
5	1	-	-	43.5 ± 1.7	4.0	18.0 ± 1.5	8.4	12.7 ± 1.1
6	1	-	-	46.5 ± 2.1	4.4	18.9 ± 1.0	5.5	13.5 ± 0.9
7	1	n.d. [1]	n.d.	32.3 ± 0.8	2.4	14.3 ± 0.8	5.6	9.0 ± 0.6
8	1	0.14 [2]	1.58 [2]	38.7 ± 5.0	12.9	18.4 ± 3.0	16.3	9.8 ± 1.5
8	2	n.d.	n.d.	39.1 ± 2.1	5.5	21.5 ± 1.5	6.8	8.8 ± 1.2
9	1	n.d.	n.d.	33.5 ± 2.8	8.3	15.4 ± 1.1	7.1	8.8 ± 1.0
10	1	n.d.	n.d.	36.8 ± 5.3	14.3	19.1 ± 4.1	21.6	8.7 ± 1.6
10	2	n.d.	n.d.	46.0 ± 10.5	22.9	37.8 ± 13.3	35.2	10.0 ± 2.1
11	1	n.d.	n.d.	33.7 ± 4.7	14.0	17.8 ± 3.0	16.7	7.5 ± 1.7
12	1	0.00 ± 0.00	0.00 ± 0.00	33.0 ± 3.0	9.0	14.6 ± 1.3	9.0	9.0 ± 1.0
13	1	0.00 ± 0.00	0.00 ± 0.00	40.0 ± 6.4	16.0	19.0 ± 3.0	15.7	9.7 ± 1.9
13	2	n.d.	n.d.	29.5 ± 1.1	3.8	12.6 ± 1.0	8.2	8.6 ± 0.6
14	1	n.d.	n.d.	38.5 ± 4.4	11.1	18.8 ± 2.6	13.7	10.1 ± 1.5
15	1	0.27 [2]	4.23 [2]	41.8 ± 3.4	8.1	21.2 ± 2.1	9.7	10.2 ± 1.2
15	2	0.01 ± 0.01	0.10 ± 0.17	46.5 ± 1.7	3.6	25.8 ± 1.2	4.7	10.3 ± 1.0
15	3	0.00 [2]	0.05 [2]	41.6 ± 2.6	6.4	20.4 ± 2.6	12.6	10.7 ± 1.6
15	4	0.00 ± 0.00	0.00 ± 0.00	41.3 ± 2.0	4.7	18.8 ± 1.0	5.5	11.2 ± 0.6
15	5	0.00 ± 0.00	0.00 ± 0.00	41.4 ± 2.7	6.6	15.6 ± 1.3	8.3	12.8 ± 0.7
15	6	n.d.	n.d.	41.6 ± 0.9	2.1	18.5 ± 0.5	2.6	11.5 ± 0.4
15	7	n.d.	n.d.	42.2 ± 3.6	8.5	19.3 ± 1.9	9.8	11.3 ± 1.0
16	1	0.09 [2]	1.38 [2]	38.4 ± 6.2	16.2	18.5 ± 3.6	19.6	9.4 ± 1.2
17	1	0.00 ± 0.00	0.00 ± 0.00	37.1 ± 0.8	2.2	17.0 ± 0.5	3.2	10.0 ± 0.3
17	2	0.00 ± 0.00	0.00 ± 0.00	37.2 ± 3.3	8.8	17.4 ± 1.6	9.2	9.7 ± 0.8
17	3	0.00 ± 0.00	0.00 ± 0.00	39.6 ± 5.2	13.1	18.2 ± 2.7	14.6	10.0 ± 1.8
18	1	0.00 ± 0.00	0.00 ± 0.00	48.5 ± 4.0	8.3	20.6 ± 1.7	8.3	13.5 ± 1.5
19	1	0.00 ± 0.00	0.00 ± 0.00	42.1 ± 4.7	11.1	19.5 ± 2.2	11.3	10.7 ± 1.8
19	2	0.00 ± 0.00	0.00 ± 0.00	46.2 ± 1.3	2.9	20.8 ± 0.7	3.5	12.7 ± 0.6

[1] n.d. = not determined

[2] For the determination of the BSA actual loading, measurements were performed in duplicate (n = 2) so no standard deviation is given.

in vitro release profiles from core-shell microspheres only depend on the polymer characteristics, which means that the differences in particle size distribution and shell thickness should neither affect the lag time nor the total release duration [4,14,15]. Moreover, the average particle size of most batches was still in the range of 30 to 50 µm, which is small enough for parenteral administration through a small-gauge hypodermic needle, and large enough to avoid undesired uptake by immune cells and other cells [16,17]. As expected, the yield of the production method was higher than with the 14

μm chip, with theoretical production rates of up to 425 mg/h and actual yields of up to 310 mg/h. In comparison, the maximally achieved yield with the 14 μm chip was 110 mg/h (unpublished data). We hypothesize that the production rates could increase even further by increasing the flow rates of all fluid phases.

5.3.2 *Effect of amplitude of the ultrasound on the primary W/O emulsion*

Unloaded core-shell microspheres were prepared at varying amplitudes ranging from 50 to 90% of the maximum amplitude to determine the influence on the primary W/O emulsion. Other parameters, such as polymer concentration and flow rates, were kept constant. For all amplitudes, microspheres with a clear core-shell structure were obtained (Figure 5), though the inner water droplet density in the core varied as visualized by optical microscopy images.
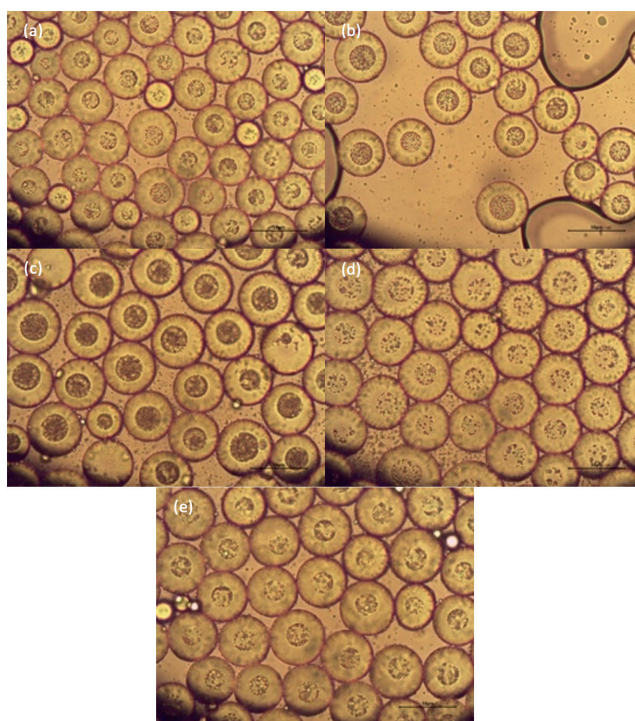
Figure 5. Representative optical microscopy images of unloaded PDLG5002-based core-shell microspheres prepared at different amplitudes. (a) Image of core-shell microspheres prepared at 50% (Formulation 2), (b) 60% (Formulation 3), (c) 70% (Formulation 4, Batch 2), (d) 80% (Formulation 5), (e) 90% (Formulation 6) of the maximum amplitude.

The average droplet size of the primary W/O emulsion has not been determined, as Freitas et al. had found that the droplet size was hardly influenced by the sonication power and time [5]. In contrast, other studies have described the existence of an optimal sonication power for the highest process efficiency [9,18]. If the sonication power is too low, the number and intensity of the cavitation events is not high enough to achieve

an effective droplet size reduction, but if the sonication power is too high, coalescence becomes predominant which may re-increase the average droplet size. Based on visual examination of the optical microscopy images (Figure 5), inner water droplet size cannot really be determined, though the differences seem small. For future research, droplet size analysis would thus be recommended. It is, however, evident that the highest inner water droplet density and the clearest distinction between the core and shell was obtained at 70% of the maximum amplitude. For the other percentages, some polymer seemed to be present between the inner water droplets in the core. For this reason, an amplitude of 70% was used for all further experiments.

5.3.3 Assessment of the reproducibility of the production process

Multiple batches of the same formulation were prepared to evaluate the reproducibility of the production method (Table 1). The particle characteristics of these batches were compared in terms of particle size (distribution) and shell thickness. For Formulation 15, seven batches were prepared and compared as shown in Table 3.

Table 3. Characteristics of microspheres prepared with 200 mg/mL BSA solution, 10 wt-% polymer solution and W_1–O–W_2 flow rates of 0.8–15.6–60 µL/min (Formulation 15), produced to assess the reproducibility of the production process.

Batch no.	d50$_{particle}$ (µm)	CV$_{particle}$ (%)	d50$_{core}$ (µm)	CV$_{core}$ (%)	Shell Thickness (µm)
1	41.8	8.1	21.2	9.7	10.2
2	46.5	3.6	25.8	4.7	10.3
3	41.6	6.4	20.4	12.6	10.7
4	41.3	4.7	18.8	5.5	11.2
5	41.4	6.6	15.6	8.3	12.8
6	41.6	2.1	18.5	2.6	11.5
7	42.2	8.5	19.3	9.8	11.3
Average ± SD	42.3 ± 1.9	n.a. [1]	19.9 ± 3.1	n.a.	11.1 ± 0.9

[1] n.a. = not applicable

Slightly different collection conditions were used for batch 4 and 5, but this seemed to have a negligible effect on the particle characteristics. The average median diameter of the seven batches was 42.3 ± 1.9 µm (CV = 4.5%), the average median diameter of the core was 19.9 ± 3.1 µm (CV = 15.6%), and the average shell thickness was 11.1 ± 0.9 µm (CV = 8.1%). The low CV values demonstrate that the setup enables a highly reproducible preparation of core-shell microspheres. Besides, all seven batches consisted of uniformly sized particles with all CV$_{particle}$ and most CV$_{core}$ values below 10%. For some formulations that were prepared in duplicate, the differences in particle dimensions were somewhat bigger, but this was probably due to higher CV values of one of the batches (e.g. Formulation 13).

5.3.4 Incorporation of BSA into core-shell microspheres and the influence of shell thickness

In order to test the suitability of the described setup for the preparation of single-administration vaccine formulations, PDLG5002-based core-shell microspheres were prepared using an aqueous BSA solution as the inner water phase. Multiple microsphere

batches were prepared with varying flow rates (W1 = 0.4–2.4 µL/min, O = 7.8–31.2 µL/min, W2 = 30–120 µL/min) and polymer concentrations (5–15 wt-%) to tune the BSA loading. The theoretical BSA loading ranged from 4.5 to 12.5 wt-%. Unfortunately, we did not succeed in incorporating the model antigen into the core-shell microspheres, while the microsphere surface seemed completely non-porous (Figure 3b). The highest actual BSA loading achieved was as low as 0.27 wt-% and the EE ranged from 0 to only 4.23% (Table 2). Various attempts to increase the EE, for instance by increasing the temperature of the collection medium to 30°C (Formulation 15, batch 4) or by adding 5 wt-% sodium chloride to the PVA solution (Formulation 15, batch 5), were unsuccessful (Table 2). The temperature of the collection medium was increased to increase the DCM removal rate, that is, the DCM diffusion and evaporation rate, and thus the solidification rate of the microspheres [19]. Salt was added to the collection medium to reduce the solubility, and thus the diffusion rate, of BSA in the collection medium [20]. The EE also did not seem to improve upon increasing the polymer concentration (Formulation 18 and 19), which normally causes a reduced drug diffusion rate due to a faster polymer precipitation and an increased viscosity of the polymer solution [21,22]. Moreover, the EE seemed to be independent of the BSA loading and particle size. The striking difference in EE in comparison with the core-shell microspheres produced with the 14 µm chip can most likely be ascribed to the differences in shell thickness [4]. In Figure 6, the EE of the PLGA-based microsphere batches prepared with both production setups is plotted as a function of the shell thickness.
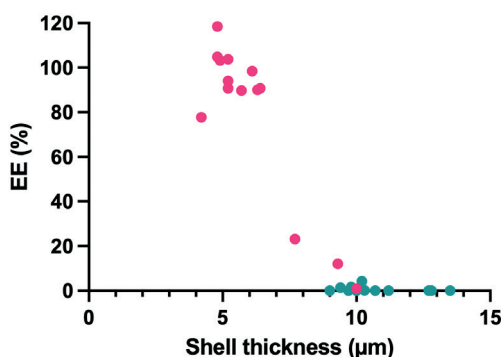
Figure 6. Effect of the shell thickness on the encapsulation efficiency (EE) of PLGA-based core-shell microspheres. (●) Core-shell microspheres produced with a 14 µm microfluidic chip for the primary emulsification step [4], and (●) core-shell microspheres produced with the flow-through ultrasonic cell for the primary emulsification step.

There seems to be a clear cut-off value for the shell thickness between 7 and 8 µm above which the EE drastically decreases, independent of the production method used. As previously described, a higher shell thickness is probably related to a lower solidification rate, thereby increasing the risk of BSA diffusing out of the cores [4]. The low EE values are also reflected in the SEM images of cross-sectioned microspheres, for instance the microsphere in Figure 3c (Formulation 15) that has a virtually hollow core. As expected, the actual BSA loading of this batch was only 0.27 wt-% and the EE was 4.23%.

5.3.5 Effect of polymer concentration and flow rates on the shell thickness

The obtained results indicate that reduction of the shell thickness is required to improve the EE. The shell thickness is influenced by both the polymer concentration and the flow rates of the inner water and oil phase. Therefore, the shell thickness was plotted as a function of the polymer concentration and the flow rate ratio of the shell/core phase (Figure 7).

Figure 7. Effects of the polymer concentration and the flow rate ratio shell/core phase on the shell thickness of PDLG5002-based core-shell microspheres produced with the flow-through ultrasonic cell for the primary emulsification step and a 200 mg/mL BSA solution as the inner water phase. Solid line is the line of regression, dashed lines indicate the 95% confiden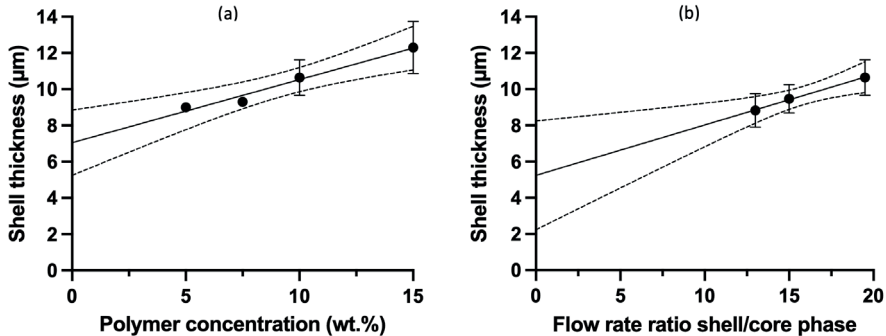ce interval limits of the best-fitting linear regression line. (a) Shell thickness as a function of polymer concentration for microspheres prepared with a flow rate ratio shell/core phase of 19.5. The best-fitting linear regression line was expressed by the formula: Shell thickness = 0.3480 x Polymer concentration + 7.050 (R^2 = 0.9723). As for 5 and 7.5 wt-% polymer concentration only one (n = 1) and two (n = 2) batches were prepared, respectively, no standard deviation is given for these datapoints. (b) Shell thickness as a function of the flow rate ratio shell/core phase for microspheres prepared with a 10 wt-% polymer concentration. The best-fitting linear regression line was expressed by the formula: Shell thickness = 0.2783 x Flow rate ratio shell/core phase + 5.241 (R^2 = 0.9972). The variation ranges for the flow rates of the core phase (W_I phase flow rate) and shell phase (O phase flow rate) were W_I = 0.4–2.4 µL/min and O = 7.8–31.2 µL/min, respectively.

Linear fitting of shell thickness vs. polymer concentration and flow rate ratio shell/core phase was performed using simple linear regression analysis, and a relative regression equation was generated. The shell thickness was found to be directly proportional to both parameters as expected, with an increase in polymer concentration or flow rate ratio causing an increase in the shell thickness [23-25]. Both relationships can simply be ascribed to the presence of more polymer, while remaining the quantity of the core unchanged. Figure 7a, however, shows that a shell thickness of < 7 µm can probably not be achieved by a further reduction of the polymer concentration to < 5 wt-% when a flow rate ratio shell/core phase of 19.5 is used. According to the linear regression plot, a negative value for the polymer concentration is required to obtain a shell thickness of 7 µm, and at a polymer concentration of ≥ 4 wt-%, a shell thickness of < 7 µm even lies outside the 95% confidence interval. Moreover, a well-controlled, uniform droplet formation with low CV values is promoted by relatively similar viscosities of the polymer and PVA solution [26]. This means that a certain polymer concentration is minimally required to improve the viscosity match since DCM is less viscous than 2 wt-% PVA solution. The linear regression plot in Figure 7b indicates that the flow rate ratio of the shell/core phase

should be reduced to at least < 7 to obtain a shell thickness of < 7 μm when a polymer concentration of 10 wt-% is used. The upper bound of the 95% confidence interval, however, is > 7 μm for all flow rate ratios, which means that a sufficient decrease in shell thickness is still not guaranteed. In order to reduce the flow rate ratio, a decrease of the oil phase flow rate relative to the inner water phase flow rate or an increase of the inner water phase flow rate relative to the oil phase flow rate are both a promising option. No formulations, however, have been prepared with both a low polymer concentration (i.e. < 7.5 wt-%) and a low flow rate ratio of the shell/core phase (i.e. < 12), while this appears to be the only option for obtaining core-shell microspheres with thin shells. In a study by Freitas et al., BSA-loaded microspheres were prepared with a similar setup, though the W/O/W double emulsion was generated with a static micromixer [5]. For the inner water phase, a 5 wt-% solution of BSA in PBS was used, for the oil phase a 6 wt-% solution of PLGA (M_w 24–38 kDa, DL-lactide:glycolide molar ratio 50:50) in DCM, and for the outer water phase a 0.5 wt-% PVA solution. The flow rates were set at 67 μL/min for the inner water phase (i.e. the core phase), 750 μL/min for the oil phase (i.e. the shell phase), and 6000 μL/min for the outer water phase, which means that the flow rate ratio of the shell/core phase was 11.3. With these settings, microspheres with a BSA loading of 3.8 to 4.1 wt-% and an EE of 67.1 to 73.0% could be prepared. Although the production method was slightly different and the internal morphology of the microspheres is unknown, it does show that a combination of a relatively low polymer concentration and flow rate ratio shell/core phase might solve the issue of low EE. A lower polymer concentration, however, also results in a slower solidification of the microspheres and, hence, might counteract the improvement of the EE. To compensate for this effect, PLGA with a higher molecular weight could be used to increase the solidification rate, as polymers with a higher molecular weight (and thus glass transition temperature [27]) are less soluble in the organic solvent [28-30]. In this study, a low-molecular weight PLGA with an inherent viscosity of 0.2 dL/g was used, but similar grades with inherent viscosities up to 1.0 dL/g could be tested as well.

Another possibility to reduce the shell thickness is to prepare core-shell microspheres with a smaller diameter. Decreasing the particle diameter while keeping all the other settings, such as flow rate ratio shell/core phase and polymer concentration, constant, might result in a lower absolute shell thickness. The average diameter of the microspheres can be reduced by tuning the ratio of the outer water phase flow rate to the inner water plus oil phase flow rate [23]. An increase in this ratio will generally result in a decreased microsphere diameter, provided that the particles do not become smaller than 20 μm to prevent their uptake by immune cells and other cells [16].

5.4 Conclusion

In this study, monodisperse PLGA-based core-shell microspheres were produced using ultrasonic and microfluidic emulsification. The prepared microspheres were highly spherical, had a non-porous surface and exhibited a distinct core-shell structure. Overall, the flow-through ultrasonic cell seems to be a promising alternative for the 14 μm microfluidic chip, with the possibility of higher production rates, absence of channel blockages, and fairly good reproducibility. Additionally, aseptic microsphere

preparation using steam sterilization is enabled with this setup. Incorporation of the model antigen BSA, however, has not been achieved, as the maximum EE value obtained was only 4.23%. These low EE values could be attributed to the relatively thick shells of the microspheres, which facilitated the diffusion of BSA out of the cores during production. Attempts to reduce the shell thickness failed, but a combination of a relatively low polymer concentration (< 7.5 wt-%) and a reduced flow rate ratio of the shell/core phase (< 12) might be the answer to this problem. Once BSA has been incorporated into the core-shell microspheres, *in vitro* release studies should be executed to confirm that a delayed pulsatile release can be obtained. This would enable the formulation being used as a single-administration vaccine formulation when combined with a primer.

Acknowledgements

References

[1]   J. L. Cleland, "Single-administration vaccines: controlled-release technology to mimic repeated immunizations," Trends Biotechnol., vol. 17, no. 1, pp. 25–29, Jan. 1999.

[2]   K. J. McHugh, R. Guarecuco, R. Langer, and A. Jaklenec, "Single-injection vaccines: Progress, challenges, and opportunities," J. Control. Release, vol. 219, pp. 596–609, 2015.

[3]   M. Beugeling et al., "The mechanism behind the biphasic pulsatile drug release from physically mixed poly(DL-lactic(-co-glycolic) acid)-based compacts," Int. J. Pharm., vol. 551, no. 1–2, 2018.

[4]   R. S. van der Kooij, R. Steendam, J. Zuidema, H. W. Frijlink, and W. L. J. Hinrichs, "Microfluidic Production of Polymeric Core-Shell Microspheres for the Delayed Pulsatile Release of Bovine Serum Albumin as a Model Antigen," Pharmaceutics, vol. 13, no. 11. 2021.

[5]   S. Freitas, B. Rudolf, H. P. Merkle, and B. Gander, "Flow-through ultrasonic emulsification combined with static micromixing for aseptic production of microspheres by solvent extraction," Eur. J. Pharm. Biopharm., vol. 61, no. 3, pp. 181–187, 2005.

[6]   S. Adler, M. Scherrer, and F. D. Daschner, "Costs of low-temperature plasma sterilization compared with other sterilization methods," J. Hosp. Infect., vol. 40, no. 2, pp. 125–134, Oct. 1998.

[7]   L. Joslyn, "Sterilization by heat," in Block SS, ed. Disinfection, sterilization, and preservation., Philadelphia: Lippincott Williams & Wilkins, 2001, pp. 695–728.

[8]   Dolomite Microfluidics, "FAQ." [Online]. Available: https://www.dolomite-microfluidics.com/support/faq/. [Accessed: 09-Sep-2022].

[9]   S. Freitas, G. Hielscher, H. P. Merkle, and B. Gander, "Continuous contact- and contamination-free ultrasonic emulsification—a useful tool for pharmaceutical

development and production," Ultrason. Sonochem., vol. 13, no. 1, pp. 76–85, 2006.

[10]   Dolomite Microfluidics, "3D Flow Focusing Chips - Product Datasheet." [Online]. Available: https://go.blacktrace.com/l/659183/2020-03-16/ x3lvp/659183/63428/Product_Datasheet___3d_Flow_Focusing_Chips_v.3.0.pdf. [Accessed: 09-Sep-2022].

[11]   J. R. Lake, K. C. Heyde, and W. C. Ruder, "Low-cost feedback-controlled syringe pressure pumps for microfluidics applications," PLoS One, vol. 12, no. 4, pp. e0175089–e0175089, Apr. 2017.

[12]   Z. Li, S. Y. Mak, A. Sauret, and H. C. Shum, "Syringe-pump-induced fluctuation in all-aqueous microfluidic system implications for flow rate accuracy," Lab Chip, vol. 14, no. 4, pp. 744–749, 2014.

[13]   Dolomite Microfluidics, "Mitos P-Pump Droplet Monodispersity - Application Note." [Online]. Available: https://go.blacktrace. com/l/659183/2019-01-08/l6g/659183/3389/Dolomite___MitosP_ PumpDropletMonodispersityApplicationNote___pdf.pdf. [Accessed: 09-Sep-2022].

[14]   T. H. Lee, J. Wang, and C.-H. Wang, "Double-walled microspheres for the sustained release of a highly water soluble drug: characterization and irradiation studies," J. Control. Release, vol. 83, no. 3, pp. 437–452, 2002.

[15]   Q. Xu, H. Qin, Z. Yin, J. Hua, D. W. Pack, and C.-H. Wang, "Coaxial electrohydrodynamic atomization process for production of polymeric composite microspheres," Chem. Eng. Sci., vol. 104, no. Supplement C, pp. 330–346, 2013.

[16]   G. Lemperle, "Biocompatibility of Injectable Microspheres," Biomed. J. Sci. & Tech. Res., vol. 2, no. 1, pp. 2296–2306, 2018.

[17]   M. Ye, S. Kim, and K. Park, "Issues in long-term protein delivery using biodegradable microparticles," J. Control. Release, vol. 146, no. 2, pp. 241–260, 2010.

[18]   J. P. Canselier, H. Delmas, A. M. Wilhelm, and B. Abismaïl, "Ultrasound Emulsification—An Overview," J. Dispers. Sci. Technol., vol. 23, no. 1–3, pp. 333–349, Jan. 2002.

[19]   Y.-Y. Yang, H.-H. Chia, and T.-S. Chung, "Effect of preparation temperature on the characteristics and release profiles of PLGA microspheres containing protein fabricated by double-emulsion solvent extraction/evaporation method," J. Control. Release, vol. 69, no. 1, pp. 81–96, 2000.

[20]   T. Arakawa and S. N. Timasheff, "Preferential interactions of proteins with salts in concentrated solutions," Biochemistry, vol. 21, no. 25, pp. 6545–6552, Dec. 1982.

[21]   R. Bodmeier and J. W. McGinity, "Solvent selection in the preparation of poly(dl-lactide) microspheres prepared by the solvent evaporation method," Int. J. Pharm., vol. 43, no. 1, pp. 179–186, 1988.

[22]   H. Rafati, A. G. A. Coombes, J. Adler, J. Holland, and S. S. Davis, "Protein-loaded poly(dl-lactide-co-glycolide) microparticles for oral administration: formulation, structural and release characteristics," J. Control. Release, vol. 43,

5

no. 1, pp. 89–102, 1997.

[23]   P.-W. Ren, X.-J. Ju, R. Xie, and L.-Y. Chu, "Monodisperse alginate microcapsules with oil core generated from a microfluidic device," J. Colloid Interface Sci., vol. 343, no. 1, pp. 392–395, Mar. 2010.

[24]   S.-W. Choi, Y. Zhang, and Y. Xia, "Fabrication of Microbeads with a Controllable Hollow Interior and Porous Wall Using a Capillary Fluidic Device," Adv. Funct. Mater., vol. 19, no. 18, pp. 2943–2949, Sep. 2009.

[25]   T. Kong et al., "Microfluidic fabrication of polymeric core-shell microspheres for controlled release applications," Biomicrofluidics, vol. 7, no. 4, p. 44128, Jul. 2013.

[26]   Dolomite Microfluidics, "Microfluidic Production of 20 to 50 μm Core-Shell PLGA Beads - Application Note," 2019. [Online]. Available: https://go.blacktrace.com/l/659183/2019-09-30/3x3hq/659183/44855/Dolomite___MicrofluidicProductionOf20to50__mCore_ShellPLGABeads_v.1.0AppNote_.pdf. [Accessed: 09-Sep-2022].

[27]   H. K. Makadia and S. J. Siegel, "Poly Lactic-co-Glycolic Acid (PLGA) as Biodegradable Controlled Drug Delivery Carrier," Polymers, vol. 3, no. 3. pp. 1377–1397, 2011.

[28]   F. Ramazani et al., "Strategies for encapsulation of small hydrophilic and amphiphilic drugs in PLGA microspheres: State-of-the-art and challenges," Int. J. Pharm., vol. 499, no. 1–2, pp. 358–367, 2016.

[29]   Y. Yeo and K. Park, "Control of encapsulation efficiency and initial burst in polymeric microparticle systems," Arch. Pharm. Res., vol. 27, no. 1, p. 1, 2004.

[30]   R. C. Mehta, B. C. Thanoo, and P. P. Deluca, "Peptide containing microspheres from low molecular weight and hydrophilic poly(d,l-lactide-co-glycolide)," J. Control. Release, vol. 41, no. 3, pp. 249–257, 1996.

5

Chapter 6

A single injection with sustained-release microspheres and a prime-boost injection of bovine serum albumin elicit the same IgG antibody response in mice

Renée S. van der Kooij [1], Martin Beukema [2], Anke L. W. Huckriede [2], Johan Zuidema [3], Rob Steendam [3], Henderik W. Frijlink [1], and Wouter L. J. Hinrichs [1]

[1] Department of Pharmaceutical Technology and Biopharmacy, University of Groningen, Antonius Deusinglaan 1, 9713 AV Groningen, The Netherlands

[2] Department of Medical Microbiology and Infection Prevention, University Medical Center Groningen, University of Groningen, Antonius Deusinglaan 1, 9713 AV Groningen, The Netherlands

[3] InnoCore Pharmaceuticals, L.J. Zielstraweg 1, 9713 GX Groningen, The Netherlands

Abstract

Although vaccination is still considered to be the cornerstone of public health care, the increase in vaccination coverage has stagnated for many diseases. Most of these vaccines require two or three doses to be administered across several months or years. Single-injection vaccine formulations are an effective method to overcome the logistical barrier to immunization that is posed by these multiple-injection schedules. Here, we developed subcutaneously (s.c.) injectable microspheres with a sustained release of the model antigen bovine serum albumin (BSA). The microspheres were composed of blends of two novel biodegradable multi-block copolymers consisting of amorphous, hydrophilic poly(ε-caprolactone)-poly(ethylene glycol)-poly(ε-caprolactone) (PCL-PEG-PCL) blocks and semi-crystalline poly(dioxanone) (PDO) blocks of different block sizes. *In vitro* studies demonstrated that the release of BSA could be tailored over a period of approximately four to nine weeks by changing the blend ratio of both polymers. Moreover, it was found that BSA remained structurally intact during release. Microspheres exhibiting sustained release of BSA for six weeks were selected for the *in vivo* study in mice. The induced BSA-specific IgG antibody titers increased up to four weeks after administration and were of the same magnitude as found in mice that received a priming and a booster dose of BSA in phosphate-buffered saline (PBS). Determination of the BSA concentration in plasma showed that *in vivo* release probably took place up to at least four weeks, although plasma concentrations peaked already one week after administration. The sustained-release microspheres might be a viable alternative to the conventional prime-boost immunization schedule, but a clinically relevant antigen should be incorporated to assess the full potential of these microspheres in practice.

6.1 Introduction

Although vaccination is one of the most successful medical interventions in history, coverage has not improved over the last decade for several diseases. In 2021, 18.2 million infants worldwide remained unvaccinated with the three-dose diphtheria-tetanus-pertussis (DTP3) vaccine and an additional 6.8 million only received an initial dose. This highlights a lack of access to immunization services, which is especially a problem in low- and middle-income countries [1,2]. To improve global vaccination coverage, the World Health Organization set up the Immunization Agenda 2030, with one of the objectives being the development of new vaccines, technologies, and improved products [3]. An example of an improved vaccine product is a single-injection vaccine formulation, such as a microsphere-based formulation, for vaccines that normally require multiple doses [4,5]. With this technology, the problem of the 6.8 million infants that were only partially vaccinated with the DTP3 vaccine could, for instance, be solved.

In a previous study, we developed polymeric core-shell microspheres that released the model antigen bovine serum albumin (BSA) after a lag time of three to seven weeks [6]. By co-injecting these microspheres together with a solution of BSA, a pulsatile release profile could potentially be obtained that mimics the current prime-boost immunization schedule with multiple doses at specific time intervals. Incorporation of a clinically used antigen into such a pulsatile-release formulation might result in a prolonged immunological response after only a single administration, thereby eliminating the need for booster injections. Although such pulsatile-release formulations that mimic the prime-boost immunization schedule are known to be safe and effective [4,7,8], alternative antigen release kinetics, such as sustained release, have proven to induce strong immune responses as well [9–11]. Moreover, sustained-release formulations are often easier to develop and manufacture and cause fewer side effects than pulsatile-release formulations [12]. As only low levels of antigen are generated upon release from the formulation, there is a limited amount of antigen systemically available during the entire period of release. It is, therefore, worthwhile to investigate the immunological response to such a formulation. In addition, sustained release more closely resembles a natural infection, because the immune system is continuously exposed to an increasing level of antigens during the course of the infection, which is usually several days or weeks [13]. The majority of the single-injection vaccine formulations described in the literature are based on the biocompatible and biodegradable polymer poly(DL-lactide-*co*-glycolide) (PLGA) [4,9]. This polymer has the advantage of being the most extensively investigated polymer in the field of controlled release and has tunable release kinetics [14]. Hydrolytic degradation of PLGA, however, might lead to accumulation of the acidic degradation products lactic acid and glycolic acid, resulting in a pH drop within the microspheres. This might affect the structural integrity and lead to the incomplete release of the incorporated (proteinaceous) antigen [15–17]. Hence, alternative polymers enabling release that is mainly diffusion-controlled are highly desired, as the development of an acidic microclimate is prevented.

In this study, injectable sustained-release microspheres were developed that could serve as a single-injection vaccine formulation. These monolithic microspheres consisted of biodegradable multi-block copolymers in which BSA was incorporated. These

phase-separated multi-block copolymers were composed of amorphous, hydrophilic poly(ε-caprolactone)-poly(ethylene glycol)-poly(ε-caprolactone) (PCL-PEG-PCL) blocks and semi-crystalline poly(dioxanone) (PDO) blocks. Such PEG-based polymers swell when brought into an aqueous environment, thereby allowing the gradual release of the model antigen by diffusion and avoiding the accumulation of acidic degradation products [18–20]. An acidic microclimate is, therefore, not formed, in contrast to PLGA-based systems. This, altogether, could allow for sustained release of structurally intact BSA over several weeks. The two multi-block copolymers used in this study differed in the weight ratio of the amorphous and semi-crystalline block, the PEG molecular weight, and the total weight fraction of PEG. We hypothesized that the release duration could be tailored by varying the blend ratio of the polymers. The BSA-loaded microspheres that most closely resembled the target *in vitro* release profile, that is, a linear or near-linear release over four to six weeks, were subcutaneously (s.c.) administered in mice as an *in vivo* proof-of-concept study. The induced BSA-specific IgG antibody responses for up to eight weeks and the BSA plasma concentration for up to four weeks were measured to determine whether the microspheres could serve as an alternative to the conventional prime-boost immunization schedule.

6.2 Materials and methods

6.2.1 Materials

p-Dioxanone was obtained from HBCChem, Inc. (San Carlos, CA, USA). Anhydrous 1,4-butanediol (BDO), ε-caprolactone, and PEG with a molecular weight of 1000 g/mol (PEG_{1000}) and 3000 g/mol (PEG_{3000}) were purchased from Thermo Fisher Scientific (Waltham, MA, USA). Stannous octoate was purchased from Sigma-Aldrich (Zwijndrecht, The Netherlands). 1,4-Butanediisocyanate (BDI) and acetonitrile were obtained from Actu-All Chemicals B.V. (Oss, The Netherlands). Polyvinyl alcohol (PVA; 5-88 EMPROVE®, 85–89% hydrolyzed), hydrogen peroxide, and sulfuric acid were purchased from Merck (Darmstadt, Germany). Sodium azide, Tween 20, dichloromethane (DCM), dimethyl sulfoxide (DMSO), and octane were purchased from Thermo Fisher Scientific (Waltham, MA, USA). BSA, sodium chloride (NaCl), sodium dodecyl sulfate (SDS), and *o*-phenylenediamine dihydrochloride (OPD) tablets were obtained from Sigma-Aldrich (St. Louis, MO, USA). Sodium hydroxide was obtained from VWR International Ltd. (Leicestershire, UK). Sodium carboxymethyl cellulose (CMC; Blanose™ 7HF PH) was purchased from Ashland (Covington, KY, USA). BSA sample diluent was from Cygnus Technologies (Southport, NC, USA), and horseradish peroxidase (HRP)-linked goat anti-mouse IgG antibody (1 mg/mL) was from Southern Biotech (Birmingham, AL, USA). For the phosphate-perchlorate buffer and the *in vitro* release medium, sodium dihydrogen phosphate dihydrate ($NaH_2PO_4 \cdot 2H_2O$) and disodium hydrogen phosphate (Na_2HPO_4) were purchased from Thermo Fisher Scientific (Waltham, MA, USA) and sodium perchlorate monohydrate ($NaClO_4 \cdot H_2O$) from VWR International Ltd. (EMSURE®, Leicestershire, UK). For the carbonate-bicarbonate buffer, sodium carbonate (Na_2CO_3) and sodium bicarbonate ($NaHCO_3$) were obtained from Merck (Darmstadt, Germany). For the BSA-specific IgG antibody ELISA, NaCl, potassium dihydrogen phosphate (KH_2PO_4), and Na_2HPO_4 were purchased from Merck (Darmstadt, Germany), sodium dihy-

drogen phosphate (NaH_2PO_4) from VWR International Ltd. (EMSURE®, Leicestershire, UK), and Tween 20 from Sigma-Aldrich (St. Louis, MO, USA). Gibco™ sterile-filtered 1X phosphate-buffered saline (PBS; 155 mM NaCl, 1.06 mM KH_2PO_4, 2.97 mM Na_2H-PO_4·$7H_2O$, pH 7.4) was purchased from Thermo Fisher Scientific (Waltham, MA, USA). This PBS was used for all experiments, unless otherwise stated. Sterile 10X PBS (1.5 M NaCl, 20 mM KH_2PO_4, 80 mM NaH_2PO_4, 30 mM KCl, pH 7.4) was obtained from VWR International Ltd. (Leicestershire, UK). Ultrapure water with a resistivity of 18.2 MΩ was obtained from a Millipore Milli-Q Integral 3 (A10) purification system and used for all experiments.

6.2.2. Polymer synthesis and characterization

Poly(ether ester urethane) multi-block copolymers composed of hydrophilic PCL-PEG-PCL and semi-crystalline PDO prepolymer blocks were synthesized and characterized using similar procedures as previously described [18,20].

PDO prepolymer with a target molecular weight of approximately 2800 g/mol was prepared of 356.5 or 228.3 g *p*-dioxanone in the bulk at 80 °C using 11.5 or 6.7 g anhydrous BDO to initiate the ring-opening polymerization for polymer A and B, respectively. Stannous octoate was used as a catalyst at a monomer/catalyst molar ratio of approximately 25.

[PCL-PEG$_{3000}$-PCL] prepolymer with a target molecular weight of 4000 g/mol and [PCL-PEG$_{1000}$-PCL] prepolymer with a target molecular weight of 2000 g/mol were synthesized similarly using 61.2 g ε-caprolactone, 183.5 g PEG$_{3000}$, and 31.3 mg stannous octoate for [PCL-PEG$_{3000}$-PCL], and 495.9 g ε-caprolactone, 500.9 g PEG$_{1000}$, and 140.1 mg stannous octoate for [PCL-PEG$_{1000}$-PCL]. The mixture was magnetically stirred at 160 °C for 69 h ([PCL-PEG$_{3000}$-PCL]) or 73 h ([PCL-PEG$_{1000}$-PCL]) and then cooled to room temperature.

Thereafter, PDO prepolymer was chain-extended with [PCL-PEG$_{3000}$-PCL] or [PCL-PEG$_{1000}$-PCL] prepolymer using BDI to obtain 20[PCL-PEG$_{3000}$-PCL]-b-80[PDO] or 50[PCL-PEG$_{1000}$-PCL]-b-50[PDO] multi-block copolymer. To this end, approximately 300 g of [PDO] and 75 g of [PCL-PEG$_{3000}$-PCL] were dissolved in dry 1,4-dioxane (80 °C, 30 wt-% solution), after which 20 g of BDI was added to the solution. For 50[PCL-PEG$_{1000}$-PCL]-b-50[PDO], 189.3 g of [PDO] and 189.2 g of [PCL-PEG$_{1000}$-PCL] were dissolved in dry 1,4-dioxane (80 °C, 30 wt-% solution), after which 21.10 g of BDI was added to the solution. Then, the reaction mixture was mechanically stirred for 20 h. Finally, 1,4-dioxane was removed from the reaction mixture by precipitation and vacuum drying. A schematic representation of the composition of the multi-block copolymers is displayed in Figure 1.

The synthesized multi-block copolymers 20[PCL-PEG$_{3000}$-PCL]-80[PDO] (polymer A) and 50[PCL-PEG$_{1000}$-PCL]-50[PDO] (polymer B) were analyzed for chemical composition, molecular weight, intrinsic viscosity, residual 1,4-dioxane content, and thermal properties (Table 1). Of polymer A, two different batches were prepared (hereafter referred to as polymer A_1 and A_2) that differed slightly in their physicochemical characteristics. The caprolactate/PEG and dioxanonate/PEG molar ratios and the weight ratio of the PCL-PEG-PCL/PDO block were determined using ^{1}H NMR analysis. This demonstrated that the actual composition of the multi-block copolymers was in agreement with
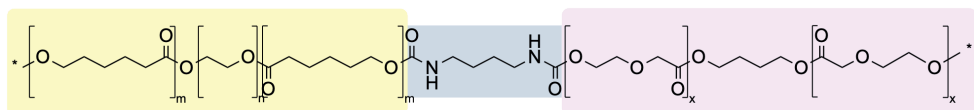
Figure 1. Schematic representation of the general chemical composition of the multi-block copolymers used in this study. In yellow shading: hydrophilic poly(ε-caprolactone)-poly(ethylene glycol)-poly(ε-caprolactone) (PCL-PEG-PCL) block (m: PCL, n: PEG). In blue shading: 1,4-butanediisocyanate (BDI)-based urethane linker. In purple shading: semi-crystalline 1,4-butanediol (BDO)-initiated poly(dioxanone) (PDO) block (x: PDO). The amorphous and semi-crystalline blocks are randomly distributed. The asterisks (*) indicate the possibility of having repeating subunits within the chemical structure. Polymer A and B differ in the weight ratio of the blocks within the copolymer (PCL-PEG-PCL block vs. PDO block), the molecular weight of PEG, and the total PEG weight fraction.

Table 1. Characterization of the multi-block copolymers used in this study.

	Polymer A$_1$	Polymer A$_2$	Polymer B
	20[PCL-PEG$_{3000}$-PCL]-80[PDO]		**50[PCL-PEG$_{1000}$-PCL]-20[PDO]**
Molar caprolactate/PEG ratio (1H NMR)	6.8 (6.4 in-weight)	6.4 (6.4 in-weight)	8.3 (8.6 in-weight)
Molar dioxanonate/PEG ratio (1H NMR)	141.6 (147.6 in-weight)	155.2 (147.5 in-weight)	18.5 (18.9 in-weight)
Weight ratio PCL-PEG-PCL/PDO block (1H NMR)	21.2/78.8	19.6/80.4	49.9/50.1
M_n (×10^4 g/mol)	2.8	1.5	3.6
M_w (×10^4 g/mol)	4.3	4.5	6.7
Intrinsic viscosity (dL/g)	0.70	0.69	0.73
1,4-dioxane content (ppm)	<18	<18	<18
T_g (°C)	−15	−14	−57 and −23
T_m (°C)	34 and 88	34 and 89	88

the targeted composition. The number average molecular weight (M_n) and the weight average molecular weight (M_w) were determined using gel permeation chromatography, which yielded an M_n of 2.8 × 10^4 g/mol and M_w of 4.3 × 10^4 g/mol for polymer A$_1$ and an M_n of 1.5 × 10^4 g/mol and M_w of 4.5 × 10^4 g/mol for polymer A$_2$. The M_n and M_w of polymer B were 3.6 × 10^4 g/mol and 6.7 × 10^4 g/mol, respectively. The intrinsic viscosity was approximately 0.7 dL/g for polymer A and 0.73 dL/g for polymer B, as determined with an Ubbelohde viscometer. The residual 1,4-dioxane contents as determined by gas chromatography were <18 ppm, indicating successful removal of the solvent. Modulated differential scanning calorimetry (MDSC) was used to determine the thermal behavior of the multi-block copolymers. In brief, 4–8 mg of sample was heated from −85 to 120 °C at a rate of 2 °C/min and a modulation amplitude of 0.42 °C/80 s. The glass transition temperature (T_g, midpoint) and melting temperature (T_m, maximum of endothermic peak) were determined using the reversed heat flow curve. Polymer A exhibited a T_g at approximately −15 °C, which is attributed to the amorphous PCL-PEG-PCL segments. Polymer B exhibited two T_g values at −57 and −23 °C, which can be ascribed to the amorphous PCL-PEG-PCL segments and the amorphous domains of the PDO block, respectively. Both multi-block copolymers exhibited a T_m at approximately 88 °C due to melting of the crystalline PDO segments. Polymer A exhibited another T_m at 34 °C, which is attributed to melting of PEG crystals.

6.2.3 Microsphere production

BSA-loaded and placebo microspheres with a target diameter of 40 μm were produced by a membrane-assisted water-in-oil-in-water emulsion solvent extraction/evaporation method, similar to a previously described method [21]. In brief, the polymer solution was prepared by dissolving polymer A and B in the desired weight ratio in DCM to obtain a 15 wt-% solution, and filtering the solution over a 0.2 μm polytetrafluoroethylene filter. The BSA solution was prepared by dissolving BSA in PBS at a concentration of 200 mg/mL and filtering the solution over a 0.22 μm polyethersulfone filter. Subsequently, the polymer solution was homogenized with the 200 mg/mL solution of BSA in PBS (for BSA-loaded microspheres) or PBS only (for placebo microspheres) using an Ultra-Turrax®. The volume of BSA solution to be added was calculated to obtain a 5 wt-% target BSA loading, which resulted in a polymer solution to BSA solution ratio of 21 *v/v*. For the placebo microspheres, the volume of PBS to be added was calculated based on this volume ratio. The resulting primary emulsion, i.e., the dispersed phase, was injected into a continuous phase consisting of 0.4 wt-% PVA and 5 wt-% NaCl in water, by pumping the emulsion through a stainless steel membrane with 20 μm pores (20 μm × 200 μm, hydrophilic ringed stainless steel membrane; Micropore Technologies, Redcar, UK). The primary emulsion was injected at a speed of 1.3 mL/min using a Nexus 3000 syringe pump (Chemyx Inc., Stafford, TX, USA). For all formulations, a dispersed phase to continuous phase ratio of 150 *v/v* was used. The secondary emulsion was stirred at room temperature with a magnetic stirrer to extract and evaporate DCM. Next, the solidified microspheres were washed five times with 250 mL water and collected on a 5 μm hydrophilic polyvinylidene fluoride filter. Microspheres were freeze-dried using a Christ Alpha 2–4 LSC plus freeze-dryer (Martin Christ Gefriertrocknungsanlagen GmbH, Osterode am Harz, Germany) according to a program previously described and then stored at −20 °C [6]. The formulation and process parameters that were not mentioned above can be found in Table 2.

Table 2. Experimental parameters and settings of different bovine serum albumin (BSA)-loaded and placebo microsphere formulations.

Formulation Parameters		Formulation					
		A	**B**	**C**	**D**	**E**	**F**
Weight ratio polymer A:polymer B [1]		100:0	92.5:7.5	85:15	75:25	50:50	92.5:7.5
Target BSA loading (wt-%)		5	5	5	5	5	n.a. [2]
Batch size (g)		1.5	3.5	3.5	3.5	1.5	3.5
Ultra-Turrax®	Speed (rpm)	21,000	25,000	25,000	25,000	21,000	25,000
	Time (s)	40	60	60	60	40	60
Extraction	Vessel size (L)	2	5	5	5	2	5
	Stirrer type	Anchor-type stirring shaft	Stirring bar (10.8 × 2.6 cm)	Stirring bar (10.8 × 2.6 cm)	Stirring bar (10.8 × 2.6 cm)	Anchor-type stirring shaft	Stirring bar (10.8 × 2.6 cm)
	Stirrer speed (rpm)	200	75	75	75	200	75
	Airflow (L/min)	5	10	10	10	5	10
	Time (h)	3	4	4	4	3	4

[1] Polymer A_1 was used for the preparation of formulation A and E; polymer A_2 was used for formulation B, C, D, and F. [2] Formulation F consisted of placebo microspheres that did not contain any BSA.

The theoretical PEG, PCL, PDO, BDO, and BDI content of the microspheres prepared from different blend ratios of polymer A and B as determined from the in-weights is shown in Table 3.

Table 3. Theoretical PEG, PCL, PDO, BDO, and BDI content of microspheres prepared from different weight ratios of polymer A and B.

Ratio Polymer A: Polymer B	Total PEG (wt-%)	PEG_{3000} (wt-%)	PEG_{1000} (wt-%)	PCL (wt-%)	PDO (wt-%)	BDO (wt-%)	BDI (wt-%)
100:0	15	15	0	4	73	3	5
92.5:7.5	15.675	13.875	1.8	5.425	70.975	2.925	5
85:15	16.35	12.75	3.6	6.85	68.95	2.85	5
75:25	17.25	11.25	6	8.75	66.25	2.75	5
50:50	19.5	7.5	12	13.5	59.5	2.5	5

6.2.4 Microsphere size analysis

For all microsphere formulations, the particle size expressed as the volume median diameter (d50) and the particle size distribution expressed as the coefficient of variation (CV) were determined with a laser diffraction particle size analyzer (Horiba LA-960, HORIBA Ltd., Kyoto, Japan). Before measurement, microspheres were dispersed in demineralized water and the obtained suspension was added to a fraction cell equipped with a magnetic stirrer to prevent sedimentation of the particles. All samples were measured immediately after addition to the cell, after which a volume-weighted size distribution plot was established according to the Fraunhofer diffraction theory. The d10 and d90 of the particle size distribution were reported as well, indicating the particle diameter at which 10% and 90% of the distribution, respectively, falls below. The CV was calculated from the d50 and the standard deviation (SD) of the distribution according to Equation (1).

$$CV = \frac{SD}{d50} \times 100\% \qquad (1)$$

6.2.5 Morphology of microspheres

The surface morphology of the dried microspheres was examined using a NeoScope JCM-5000 scanning electron microscope (SEM; JEOL Ltd., Tokyo, Japan) under high vacuum and a secondary electron detector. SEM images were taken at different magnifications ranging from 50× to 1500×. The acceleration voltage was set at 10 kV, the probe current to standard, and the filament setting to long life. Prior to imaging, the microspheres were fixed onto metal sample stubs using double-sided adhesive carbon tape and sputter-coated with gold. The internal morphology was examined by mixing the microspheres with an organic solvent-free adhesive (UHU® Twist & Glue Renature, Bühl, Germany). After air-drying for 2 days and cooling for 30 min at −70 °C, the samples were cut with a razor blade into five equal pieces. The obtained cross sections were imaged with SEM as described above.

6.2.6 Protein content of microspheres

The actual BSA loading of the microspheres was determined with the bicinchoninic acid

(BCA) assay. To this end, 10 mg of microspheres was accurately weighed in triplicate in a glass tube with screw cap. Next, 1 mL of DMSO was added, and the tubes were placed in a heating block at 80 °C and vortexed to completely dissolve the polymer. After dissolution, 5 mL of 0.5 wt-% SDS in 0.05 M sodium hydroxide was added, and the tubes were placed on a roller mixer (60 rpm) overnight at room temperature to solubilize and degrade the protein. Subsequently, 100 μL of the resulting solution was pipetted into another glass tube for further analysis. BCA working reagent was prepared by mixing an alkaline BCA solution with a 4 wt-% aqueous copper(II) sulfate solution (Pierce™ BCA assay kit, Thermo Scientific, Rockford, IL, USA) in a ratio of 50 *v/v*, and 2 mL of the obtained working reagent was added to the tubes containing the supernatant. The tubes were vortexed and placed in a heating block at 60 °C for 30 min, after which they were cooled to room temperature and again vortexed. Samples were transferred to a plastic cuvette, and the absorbance was immediately measured at 562 nm. An eight-point calibration curve was constructed by spiking known amounts of BSA to a glass tube, and thereafter following the same procedure as described above. The calibration curve was plotted using a quadratic fit and a 1/X weighting factor to determine the actual BSA loading. The actual BSA loading was used to calculate the encapsulation efficiency (EE) according to Equation (2).

$$EE = \frac{\text{Actual loading}}{\text{Target loading}} \times 100\% \tag{2}$$

6.2.7 In vitro *release of microspheres*

The *in vitro* release of BSA from the microsphere formulations was measured by accurately weighing 20 mg of microspheres in a 2 mL vial and suspending them in 1.8 mL of release medium (100 mM $NaH_2PO_4.2H_2O$, 0.2 wt-% NaCl, 0.025 *v/v*% Tween 20, 0.02 wt-% sodium azide, pH 7.4, 290 mOsm/kg). In order to maintain the release medium at 37 °C, the vials were placed on a roller mixer (40 rpm) in an oven. At predetermined time intervals, the vials were placed in a centrifuge for 5 min at 4000× *g*. Next, 1.6 mL of the supernatant was collected and replaced by fresh release medium. BSA concentration in the collected release medium was determined by size-exclusion ultra-performance liquid chromatography (SE-UPLC) with fluorescence detection (λ_{ex} = 230 nm and λ_{em} = 330 nm). In brief, an ACQUITY UPLC Protein BEH SEC column (200 Å, 1.7 μm particle size, 4.6 × 150 mm, Waters, Milford, MA, USA) and a mixture of 50 mM phosphate, 0.4 M perchlorate buffer (pH 6.3) and acetonitrile (90:10, *v/v*) as mobile phase were used for the quantification of BSA. The liquid flow rate of this mobile phase was 0.3 mL/min. The injection volume was 5 μL and the total run time was 8.5 min. The peak areas of the main BSA peak, fragments of BSA, and aggregates of BSA were integrated at a retention time of 4.40 min, 4.67 min, and 2.00 min, respectively. An eight-point calibration curve was plotted using a quadratic fit and a 1/(X × X) weighting factor to determine the BSA concentration in the samples. For quantification of the total BSA concentration, that is, the concentration of all BSA-related compounds together, the areas of all peaks at a retention time of 2.00 to 6.00 min were integrated. As a semi-quantitative measure for the integrity of the released BSA, the BSA concentration calculated from the main BSA peak was di-

vided by the total BSA concentration. All *in vitro* release curves represent the release of all BSA-related compounds together, unless otherwise stated.

6.2.8 Residual DCM content of microspheres

The residual DCM content in the microspheres was determined with an Agilent 6850 gas chromatograph (GC; Agilent Technologies, Santa Clara, CA, USA) equipped with a flame ionization detector, a CombiPal CTC headspace sampler, and a DB-624 column (30 m × 0.53 mm, 3 μm). As carrier gas, helium with a flow of 7 mL/min was used. The split injection mode was used with a split ratio of 1:15. The initial column temperature was 40 °C maintained for 5 min and then raised (10 °C/min) to 100 °C with a hold time of 1 min. Finally, the temperature was raised to 250 °C with 50 °C/min for 4 min. The syringe and incubation temperatures were 140 °C and 120 °C, respectively. For each formulation, 100 mg of microspheres was accurately weighed in duplicate and dissolved in 5 mL DMSO with 9.4 μg/mL octane as internal standard. Then, 2 mL of the headspace layer was injected into the GC for analysis. An eight-point calibration curve was plotted using a linear fit and a 1/X weighting factor to determine the DCM concentration from the peak area.

6.2.9 Endotoxin level in microspheres

The endotoxin levels in the microsphere formulations that were intended for the *in vivo* proof-of-concept study were determined with the Limulus amoebocyte lysate (LAL) test using a chromogenic kinetic method at a sensitivity of 0.005 EU/mL. To this end, 1 mL of DMSO was added to 50 mg of accurately weighed microspheres in duplicate, heated to 70 °C in a water bath for 1 min, and vortexed for 20 s to completely dissolve the sample. After dissolution, LAL reagent water was added to the sample (1:50 dilution), and the diluted sample and LAL/substrate reagent were added to each well of a microtiter plate. Then, the absorbance of each well was read at 405 nm and 37 °C, and this initial reading was used as the blank for the corresponding well. Subsequently, the absorbance of each well was read continuously throughout the assay. The time elapsed until the appearance of a yellow color, i.e., an increase of 0.2 absorbance units from the initial reading, was determined for each well, and this reaction time was inversely proportional to the endotoxin level in the sample. A standard curve of reaction time vs. endotoxin concentration was used to calculate the endotoxin concentration in the unknown samples. LAL reagent water was included as a negative control, and a positive product control (PPC) was prepared at a final concentration of 0.5 EU/mL. All standards and controls were assayed in duplicate as well.

6.2.10 Animal experiments

Female CB6F1 (C57Bl/6 x BALB/c F1) mice were obtained from Charles River Laboratories (Sulzfeld, Germany). At the start of the study, the mice were eight to nine weeks old and weighed approximately 20 g. The animals were co-housed with a total number of three to six mice in individually ventilated cages and received a 12 h light/dark cycle. All animals received the rodent diet SAFE® A40 (SAFE Diets, Augy, France) and tap water *ad libitum*. At least five days before the start of the experiment, the mice were imported to the laboratory to assure proper acclimatization. All *in vivo* experiments were conducted in accordance with Timeline Bioresearch AB ethical permit number 5.8.18-20232/2020.

For the *in vivo* proof-of-concept study, 48 mice were divided into nine groups. The treatment groups (groups A, B, and C) and positive control (plus treatment or placebo) groups (groups D to G) all contained 6 mice. The negative control groups (groups H and I) contained 3 mice. An overview of the experimental groups and the corresponding formulations used for the immunization study is given in Table 4.

Table 4. Overview of the groups and the corresponding formulations used for the *in vivo* immunization study in mice.

Group	Type of Group	Formulation Composition	Administration	Total Dose	Average Daily Dose	Week of Administration	Number of Animals
A	Treatment	BSA-MSP in CMC solution [1]	7.28 mg MSP-F in 193 µL CMC solution [1]	250 µg	7.1 µg [2]	0	6
B	Treatment	BSA-MSP in CMC solution	14.6 mg MSP-F in 187 µL CMC solution	500 µg	14.3 µg [2]	0	6
C	Treatment	BSA-MSP in CMC solution	29.2 mg MSP-F in 174 µL CMC solution	1000 µg	28.6 µg [2]	0	6
D	Positive control/ treatment	BSA in PBS + BSA-MSP in CMC solution	500 µg BSA in 100 µL PBS + 14.6 mg MSP-B in 87 µL CMC solution [1]	1000 µg (500 µg + 500 µg)	514.3 µg on day 1, 14.3 µg for remaining days [2]	0	6
E	Positive control/ placebo	BSA in PBS + placebo MSP in CMC solution	500 µg BSA in 100 µL PBS + 14.6 mg MSP-F in 87 µL CMC solution	500 µg	500 µg on day 1	0	6
F	Positive control	BSA in PBS (prime-boost)	500 µg BSA in 200 µL PBS (at 0 and 3 weeks)	1000 µg (500 µg + 500 µg)	500 µg on day 1, 500 µg on day 22	0 and 3	6
G	Positive control	BSA in PBS (prime-boost)	28.6 µg BSA in 200 µL PBS (at 0 and 3 weeks)	57.1 µg (28.6 µg + 28.6 µg)	28.6 µg on day 1, 28.6 µg on day 22	0 and 3	6
H	Negative control	PBS	200 µL PBS (at 0 and 3 weeks)	-	-	0 and 3	3
I	Negative control	CMC solution	200 µL CMC solution	-	-	0	3

[1] MSP = microspheres, MSP-B = microspheres of formulation B, MSP-F = microspheres of formulation F. [2] Assuming an *in vivo* release duration of five weeks.

All formulations were administered as a 100 or 200 µL s.c. injection in the scruff of the neck under isoflurane anesthesia, and were given at day 0, unless otherwise stated. For the microspheres, 0.6 wt-% CMC solution in 10X PBS was used as the injection vehicle, whereas PBS was used for the administration of BSA solution. All treatment groups (groups A to D) were immunized with microspheres of formulation B, and the placebo group (group E) received an injection of microspheres of formulation F. The amount of microspheres to be administered was calculated from the desired dose of BSA (250, 500, or 1000 µg BSA) and the actual BSA loading of the microspheres, corrected for the percentage released *in vitro* after five weeks of incubation. The microspheres of groups A, B and D, and C are hereafter referred to as 250, 500, and 1000 µg BSA-microspheres, respectively. Mice of groups F and G received an injection of BSA in PBS at weeks 0 and 3, where the timing of the booster immunization was based on the experimental setup of previous immunization studies [7,22,23].

Blood samples were taken prior to administration and 1, 2, 3, 4, 6, and 8 weeks

after the first administration. In total, seven blood samples were obtained from each mouse. At all time points up to six weeks, 100 μL of blood was collected in K3-EDTA tubes by sublingual bleeding and immediately placed on melting ice. During blood sampling, mice were fully conscious as no anesthesia was used, so they were gently restrained by the scruff of the neck. For the last sampling point, mice were euthanized by cervical dislocation, and all blood was collected and processed for further analysis. Then, 40 μL of plasma was prepared by centrifuging the blood samples at 1800× g and 4 °C for 10 min and collecting the supernatant. The obtained aliquots were placed on dry ice and eventually stored at −80 °C prior to analysis. All plasma samples were analyzed by ELISA to investigate the BSA-specific IgG antibody response of the mice. Plasma samples from weeks 1 to 4 were also tested by ELISA to determine the BSA levels.

6.2.11 ELISA for BSA-specific IgG antibody titers
BSA-specific IgG antibody titers in plasma were determined by indirect ELISA. Flat-bottom high binding 96-well microplates (Greiner Bio-One, Kremsmünster, Austria) were coated overnight at 37 °C with 0.3 μg BSA (100 μL 3 μg/mL BSA solution in 0.05 M carbonate-bicarbonate buffer, pH 9.6–9.8) per well. PBS composed of 154 mM NaCl, 0.882 mM KH_2PO_4, and 11.4 mM Na_2HPO_4 and the same PBS supplemented with 0.05 v/v% Tween 20 (PBS-T) were prepared as wash solution. PBS-T was also used to remove detection antibodies. The plates were washed once with the 0.05 M carbonate–bicarbonate buffer and twice with PBS-T. Then, 1:100 dilutions of plasma samples in PBS-T were prepared and added in twofold serial dilutions to the plates, with each well containing 100 μL of a dilution. Untreated wells, i.e., wells that did not contain any plasma sample, were used to determine the plate background. After incubating the plates for 1.5 h at 37 °C, the plates were washed three times with PBS-T. Next, the plates were incubated for 1 h at 37 °C with 100 μL of a 1:5000 v/v dilution of HRP-linked goat anti-mouse IgG antibody in PBS-T to detect bound IgG antibodies. Plates were again washed three times with PBS-T and once with PBS. Then, 100 μL staining solution (20 mg OPD, 20 μL hydrogen peroxide in 100 mL 0.1 M phosphate buffer, pH 5.6) was added to each well and incubated for 30 min at room temperature shielded from light. The colorimetric reaction was stopped by adding 50 μL 2 M sulfuric acid to the wells. Absorbance was measured at 492 nm and OD values were corrected for the mean plate background. IgG antibody titers were expressed as $\log_2$ values of the reciprocal of the plasma sample dilution that corresponded to a corrected OD value of 0.2 at a wavelength of 492 nm, which was determined as the cut-off value. Samples with readings for the least diluted plasma lower than the cut-off value were assigned an IgG antibody titer of 5.64 $\log_2$, corresponding to a dilution of 1:50, which would be one dilution below the starting dilution of 1:100.

6.2.12 ELISA for BSA quantification
Plasma BSA levels were determined with a commercial BSA ELISA kit (F030; Cygnus Technologies, Southport, NC, USA) according to the manufacturer's instructions. Due to limited sample volume, plasma samples were diluted at least 1:2 with BSA sample diluent and analyzed only once (n = 1). Absorbance was measured at 450 nm using a microplate reader, and BSA concentrations were determined from a five-point calibration curve (calibration range 0.5–32 ng/mL). Some plasma samples were applied in higher

dilutions of up to 1:50 to fall within the working range of the assay.

6.2.13 Statistical analysis
All microsphere formulations (A to F, Table 2) were produced once (*n* = 1). All measurements were performed in triplicate (*n* = 3), and data were presented as mean ± SD, unless otherwise stated. The IgG titer-time data were analyzed using GraphPad Prism version 9.1.2 (La Jolla, CA, USA). The area under the IgG titer–time curve (AUC) values were obtained, and data were checked for normality using the Shapiro–Wilk test. Differences between all groups were assessed using the ordinary one-way analysis of variance (ANOVA), followed by Tukey's multiple comparisons test for both AUC values and week 8 IgG titers. Differences between the analyzed groups were considered significant if $p < 0.05$ (* $p < 0.05$, ** $p < 0.01$).

6.3 Results and discussion

6.3.1 Properties of microspheres of different polymer blend ratios
Blends of polymer A and B with different weight ratios were used to prepare BSA-loaded microspheres with a 5 wt-% target loading and placebo microspheres. The polymer blend ratio and the incorporation of BSA did not seem to affect the microsphere size and size distribution, as can be seen in Table 5.

Table 5. Characteristics of BSA-loaded and placebo microsphere formulations prepared with different polymer blend ratios [1].

Formulation	Ratio Polymer A: Polymer B	d10 (µm)	d50 (µm)	d90 (µm)	CV (%)	Actual Loading (wt-%)	EE (%)
A	100:0	30.4	38.7	50.5	21.0	4.4 ± 0.1	87.4 ± 1.0
B	92.5:7.5	30.8	39.9	52.4	21.8	4.5 ± 0.5	89.9 ± 10.0
C	85:15	30.6	39.5	51.5	21.7	4.9 ± 0.3	97.3 ± 5.5
D	75:25	30.5	39.2	51.4	21.9	4.9 ± 0.2	96.9 ± 4.5
E	50:50	29.9	39.0	51.6	24.5	5.1 ± 1.3	101.7 ± 26.4
F	92.5:7.5	31.2	42.7	58.2	27.4	n.a. [2]	n.a. [2]

[1] Blend ratio 92.5:7.5 (in grey) was selected for the *in vivo* proof-of-concept study in mice. [2] Formulation F consisted of placebo microspheres that did not contain any BSA.

All formulations had an average particle size of approximately 40 µm. This size enables parenteral administration of the microspheres through a small-gauge hypodermic needle while preventing premature uptake by cells engaging in phagocytosis [24,25]. Moreover, all microsphere formulations had a narrow particle size distribution as reflected by the relatively low CV values. This was the result of a well-defined localized shear and geometry-controlled generation of droplets in the membrane-assisted emulsification process [26]. The morphology of the microspheres was examined using SEM. Representative images of BSA-loaded microspheres composed of a 92.5:7.5 polymer blend (formulation B) are depicted in Figure 2, with Figure 2a,b revealing the surface morphology and Figure 2c,d the internal morphology. Figure 2a,b show that the microspheres had a spherical shape and a smooth and non-porous surface. As expected, images of the internal morphology (Figure 2c,d) display a monolithic matrix with numerous small pores,
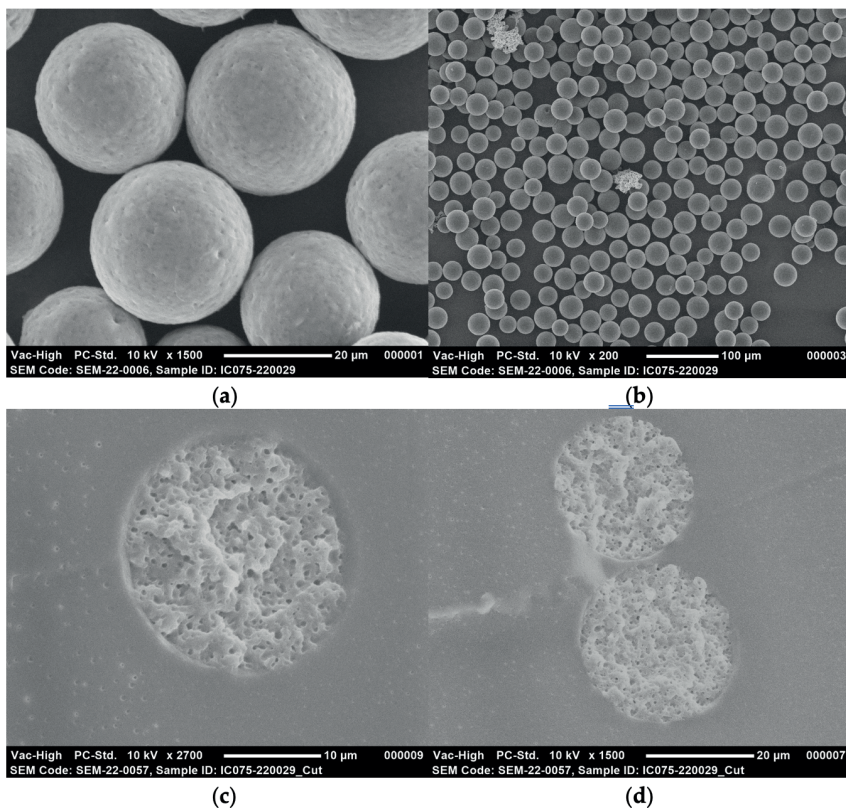
6

Figure 2. Representative scanning electron microscopy (SEM) images of microspheres loaded with 4.5 wt-% BSA (formulation B): (**a**) 1500× magnification; (**b**) 200× magnification; (**c**) Cross-sectioned microsphere at 2700× magnification; (**d**) Cross-sectioned microspheres at 1500× magnification.

resulting from the fine primary emulsion used in the preparation of the microspheres. The porosity was homogeneous throughout the cross section of the particles, which implies that BSA was homogeneously distributed throughout the microspheres. A non-porous surface, small internal pores, and a homogeneous drug distribution are critical to obtaining a high EE and low initial burst release [27]. Indeed, the EE of BSA was high for all formulations (>85%, Table 5). The high EE can be attributed to the relatively high molecular weight of the polymers (M_w 4.3–6.7 × 10^4 g/mol) and concentration of the polymer solution (15 wt-%), resulting in a relatively high viscosity of the polymer solution [28,29]. The high polymer solution to BSA solution ratio (21 *v/v*) [30] and the addition of NaCl to the continuous phase probably contributed to these high EE values as well [31].

6.3.2 In vitro release of BSA from microspheres of different polymer blend ratios
We investigated the suitability of a blend of multi-block copolymers A and B in obtaining microspheres with a low initial burst and linear or near-linear *in vitro* release of the complete BSA payload within four to six weeks. The effect of the polymer blend ratio on the *in vitro* release of BSA from the microspheres is presented in Figure 3.
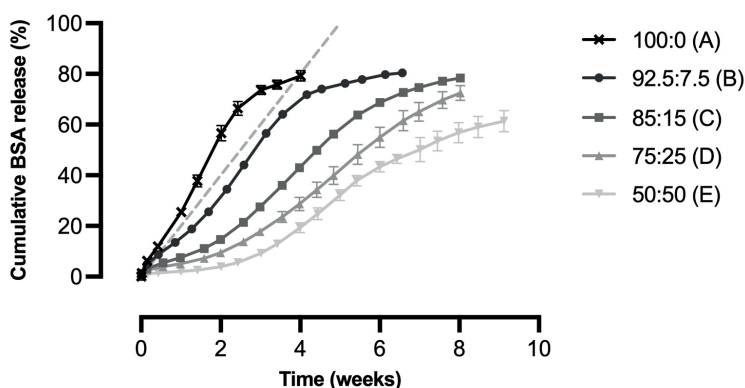
Figure 3. Cumulative *in vitro* release of BSA from microspheres composed of polymer A and polymer B in different blend ratios (*n* = 3). The cumulative release is expressed as the percentage of the total amount of BSA incorporated into the microspheres. The dashed line represents the target release profile of the microspheres with a linear release of BSA over a period of five weeks.

For all formulations, the initial burst release, defined as the percentage of BSA released after one day, was minimal (1 to 6%). Moreover, all release profiles showed a similar trend with an initial slow release followed by a faster release after which the release again slowed down. In particular, the microspheres composed of a relatively high percentage of polymer B exhibited such a sigmoidal release profile. The *in vitro* release rate was clearly influenced by the polymer blend ratio, as the release rate decreased with an increasing weight fraction of polymer B. Formulation A, which was composed of 100% of polymer A, demonstrated the highest release rate, with a cumulative release of approximately 80% after four weeks. The lowest release rate was obtained with formulation E, composed of a 50:50 polymer blend that exhibited a cumulative BSA release of only 20% after four weeks.

For bulk degrading polymers such as the polymers used in this study, drug release from the polymeric matrix is determined by the drug solubility, drug diffusion, drug load, polymer swelling, polymer degradation, or a combination of these factors [19,32]. For a hydrophilic protein with a high molecular weight, such as BSA (6.6×10^4 g/mol), diffusion through the hydrated polymer matrix is dependent on the degree of swelling and degradation of the polymer matrix, as these determine the mesh size of the matrix [19]. If a mesh size larger than the protein size is reached through swelling and/or degradation, the protein will be released from the polymer matrix [19,33]. To obtain a better understanding of the *in vitro* release profile, it is important to determine whether the prepared microspheres exhibit diffusion- or degradation-controlled release.

In previous studies, controlled-release microspheres [20,21,34] and implants [19] were prepared from semi-crystalline, phase-separated multi-block copolymers similar to the polymers used in this study. These polymers also consisted of amorphous PCL-PEG-PCL blocks, but the semi-crystalline blocks were composed of poly(L-lactide) (PLLA) [20,21,34] or PCL [19] instead of PDO. In two of these studies, *in vitro* release and polymer degradation were assessed to gain insight into the release mechanisms in play. Results suggested that *in vitro* release was primarily driven by diffusion [19,21]. *In*

vitro release data of several proteins were fitted into different kinetic models and in most cases, diffusion-controlled release was indicated. For the *in vitro* degradation studies, polymer-only microspheres [21] and implants [19] were incubated in a release medium at 37 °C, and the mass loss was determined over time. Although mass loss only gives an indication of the formation of water-soluble degradation products and degradation products that are not (yet) soluble in water will have formed as well, it does give information on the contribution of polymer degradation to the release kinetics. Only a slight mass loss was observed during the first week after incubation, which was ascribed to the preferential hydrolysis of the PEG-PCL bonds, and the subsequent dissolution and diffusion of PEG. During the remainder of the study (i.e., three [21] and nineteen [19] weeks), the sample mass hardly changed, and the molecular weight of the polymers decreased only slowly. This indicated that hydrolysis of ester bonds in the PLLA and PCL blocks was limited and that no substantial degradation had occurred within the timeframe of the degradation studies, due to slow *in vitro* degradation of PLLA and PCL and its copolymers. Based on the extrapolation of previously obtained data, the anticipated *in vitro* degradation time of PLLA-based multi-block copolymers is three to four years [35]. For the PCL-based multi-block copolymers, this is expected to be the same [36]. Therefore, the release from such multi-block copolymers was assumed to be mainly driven by other mechanisms than degradation.

In order to obtain faster degrading microspheres with a more acceptable balance between BSA release and polymer erosion, the faster degrading polymer PDO was used as the semi-crystalline block. The homopolymer has a degradation time of six months [36–38], and *in vitro* degradation of PDO-based multi-block copolymers is anticipated to be 9 to 24 months [35]. Although PDO-based multi-block copolymers degrade significantly faster than PLLA- and PCL-based multi-block copolymers, it is not expected that degradation of the semi-crystalline PDO block played a significant role in the *in vitro* release of BSA, as substantial degradation is unlikely to have occurred within the timeframe of the *in vitro* release studies (i.e., four to nine weeks) [36–38]. Therefore, as in previous studies, the release of BSA from the microspheres was mainly controlled by the amorphous PCL-PEG-PCL block. It is assumed that the release was partially driven by diffusion, as the high swelling degree and water solubility of the PEG blocks within the multi-block copolymer allowed the initial, diffusion-controlled release of BSA [18]. This occurred via dissolution and subsequent diffusion of the antigen through the swollen polymer matrix [19,21]. Release, however, was probably not solely diffusion-controlled but involved some degradation of the PCL-PEG-PCL block as well, which is also reflected in the sigmoidal release profile that was observed for the different microsphere formulations (Figure 3). It is assumed that ongoing degradation of the PCL-PEG-PCL blocks further increased the mesh size of the polymer matrix, which eventually accelerated the release. Especially for the formulations composed of a relatively high amount of polymer B, swelling of the polymer matrix was insufficient to cause an initial fast release of the high molecular weight BSA due to the presence of small-sized PEG blocks (Table 3). This resulted in a sort of lag phase directly after the start of the *in vitro* release study, after which the release rate increased. Apparently, some degradation and/or increased swelling of the polymer matrix over time was required for BSA to be released from the microspheres.

As expected, the BSA release rate from microspheres composed of polymer A and B was dependent on the polymer blend ratio, as the release rate decreased with an increasing weight fraction of polymer B (Figure 3). The slower release induced by polymer B can be explained by the fact that this polymer is less swellable and degrades slower than polymer A. As the release of BSA from the microspheres is assumed to be both diffusion- and degradation-controlled, the release rate is determined by an interplay between the PEG molecular weight, the total PEG content, the PCL content, and the PDO content of the polymer blends. The interplay between the PEG molecular weight and the total PEG content was previously described for the PLLA-based multi-block copolymers [20,21]. A comparison of polymer B with polymer A demonstrates a lower PEG molecular weight (1000 vs. 3000 g/mol), which explains the decreased release rate with an increasing weight fraction of polymer B, as PEG blocks swell due to the uptake of water. Due to the lower molecular weight of PEG in the PCL-PEG-PCL blocks, polymer B absorbs less water causing slower hydrolytic cleavage of the polymer backbone and a lower swelling degree. This eventually results in a slower release. The difference between the two polymers was also reflected in the mass loss. After incubation of polymer-only microspheres prepared from polymer A, a minor mass loss of <10% was observed after 30 days and <20% after 50 days [35]. For PDO-based multi-block copolymers comparable to polymer B, this was even less [35]. Polymer B does contain a higher total PEG content (24 vs. 15 wt-%), but this did not compensate for the PEG molecular weight. In this case, a high molecular weight of PEG is apparently more important to create a polymeric network that swells enough to allow the diffusion of the high molecular weight BSA, than a high total PEG content is for the formation of such a hydrated network. Moreover, the PCL content was higher for polymer B than for polymer A (25 vs. 5 wt-%), while the PDO content was lower (50 vs. 80 wt-%), as shown in Table 3. As PCL degrades slower than PDO, polymer B is expected to degrade slower than polymer A, resulting in a lower release rate. A higher PCL content also results in a lower swelling degree due to its hydrophobicity, thereby causing a decreased release rate [39].

We aimed to develop a formulation that exhibited a continuous release of BSA for approximately four to six weeks. Microspheres prepared from a 92.5:7.5 blend of polymer A and B (formulation B) exhibited near-linear release kinetics for up to four weeks, after which the release of BSA continued in a slower fashion for another two weeks. In addition, a high cumulative release of 80% was obtained during the course of the *in vitro* release study. Since these microspheres best met our target *in vitro* release profile, this formulation was selected for the *in vivo* proof-of-concept study. Figure 4a presents the results of the *in vitro* release study with this formulation, showing both the total and the intact BSA release from the microspheres. Protein denaturation and aggregation are common problems for protein-loaded microspheres, as they are subjected to many stress factors upon incubation, such as hydration and elevated temperatures [4,25]. Although the integrity of the released BSA was not tested directly, we did measure the percentage of BSA that was released as fragments or aggregates, which indicated how well the structural integrity was maintained during incubation. During the first four weeks, the integrity of the released BSA was high (>90%, Figure 4b). Only at the end of the *in vitro* release study did the integrity decrease drastically, as the release mainly consisted of aggregates of BSA. These aggregates are larger than BSA itself and are,

Figure 4. *In vitro* release of BSA from microspheres composed of polymer A and polymer B in the blend ratio 92.5:7.5 (formulation B, *n* = 3): (**a**) Cumulative total and intact release vs. time. (**b**) Total and intact BSA concentration and corresponding integrity of samples at each individual time point.

therefore, probably released more slowly. During the major part of the *in vitro* release study, however, aggregates and fragments of BSA were absent and the cumulative intact release was even >70%.

Furthermore, the average daily *in vitro* release fromformulation B for different doses of BSA was plotted in Figure 5.
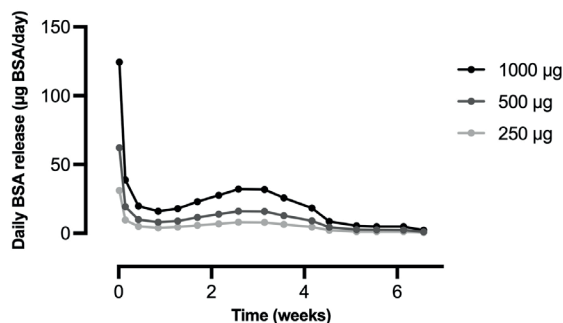
Figure 5. Average daily *in vitro* release of BSA from microspheres composed of polymer A and polymer B in the blend ratio 92.5:7.5 (formulation B, *n* = 3). The average daily *in vitro* release was calculated by dividing the absolute amount of BSA (in µg) that was released between two sampling points by the time between those sampling points. The different curves represent different amounts of microspheres corresponding to a total BSA content of 250, 500, or 1000 µg.

A relatively high daily release is visible during the first day of incubation and especially during the first two hours due to a small initial burst release. Apart from day one, the average daily release was rather constant during the first four weeks of the release study. A slight increase in the daily release was observed up to approximately three weeks, followed by a decrease during the remaining weeks of the release study, which is typical for a sigmoidal release profile.

6.3.3 Residual DCM content and endotoxin analysis of microspheres intended for the in vivo *study*

The residual DCM content in the microspheres of formulation B and the corresponding placebo microspheres (formulation F) was measured to determine whether the removal of the toxic organic solvent was effective. The DCM content of formulation B and F was 295 and 294 ppm, respectively, which is well below the ICH concentration limit of 600 ppm [40]. The permissible daily exposure for humans is 6 mg/day [40]. When this value is corrected for the body weight of a mouse (20 g) and for the factor that accounts for the extrapolation between both species (12), a permissible daily exposure of 28.8 µg/day is found for mice. As the highest amount of microspheres to be administered is 29.2 mg, the maximum DCM exposure will be only 8.6 µg, which is below the permissible daily exposure as well. Although there are only limited data available on DCM toxicity after parenteral administration, no increased risk of tumor development was observed in mice after oral administration of DCM doses up to 5 mg/day [41]. Therefore, no carcinogenic effects are expected from the prepared microspheres. In addition, the endotoxin level in both formulations was quantified as it is an important factor for microspheres intended for immunological studies. The LAL test confirmed that both formulations did not contain detectable levels of endotoxin (<5 EU/g microspheres). Therefore, it is not expected that any undefined immune responses will be induced by endotoxins from the microspheres. Overall, both formulations complied with all requirements for use in the *in vivo* proof-of-concept study.

6.3.4 IgG antibody response and kinetics of microspheres in vivo

Based on the *in vitro* release results, the BSA-loaded microspheres prepared from a 92.5:7.5 blend of polymer A and B (formulation B) and the corresponding placebo microspheres (formulation F) were chosen for the *in vivo* proof-of-concept study in mice. The microspheres containing the model antigen BSA were s.c. injected to investigate whether the formulation could elicit a BSA-specific IgG antibody response. Different amounts of the microspheres were injected into the subcutaneous tissue to test the effect of the dose of BSA on the humoral immune response. A positive control/treatment group was included to determine whether priming with BSA in PBS could enhance the antibody response induced by the microspheres. A positive control/placebo group was included to investigate the potential adjuvant effect of the polymers. In addition, two positive controls consisting of a high- and low-dose prime-boost injection of BSA in PBS were included to compare the antibody titers induced by a prime-boost immunization schedule with the titers induced by the microspheres. Two negative controls consisting of PBS and CMC solution were included to confirm that the vehicles did not induce BSA-specific IgG antibodies. For all groups, the BSA-specific IgG antibody titers in the mouse plasma were determined over time, up to eight weeks after administration.

As expected, no IgG antibody response was induced after administration of the injection vehicles to the negative control groups. For the other groups, the systemic BSA-specific IgG antibody titers over time after administration of different BSA and placebo formulations are shown in Figure 6 (see Figure S1 in the Supplementary Materials for the IgG antibody titers of the individual mice). In addition, the final IgG antibody titers as measured at week 8 are shown in Figure 7.
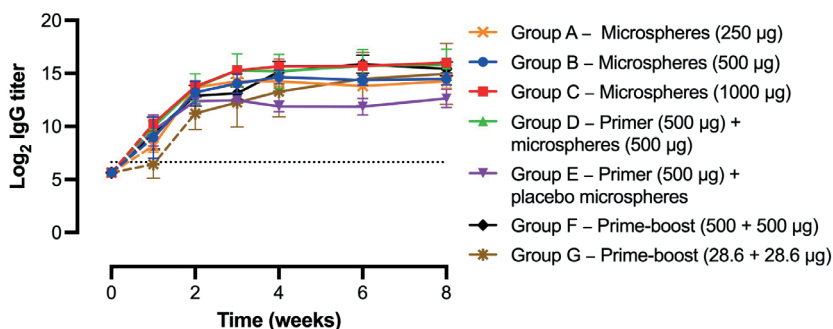
6

Figure 6. BSA-specific IgG antibody titers in mouse plasma over time after immunization with different BSA formulations (group A to G). The averages of the antibody levels measured in all mice were calculated for each group ($n = 6$ per group) and presented for all groups together. The dotted line represents the cut-off value for the IgG antibody titer, i.e., a titer of 6.64 $\log_2$, corresponding to the starting dilution of the plasma samples of 1:100. Values below this titer could not be measured. Samples with a reading for the least diluted plasma (i.e., 100× diluted) lower than the cut-off value were assigned an IgG antibody titer of 5.64 $\log_2$, corresponding to a dilution of 1:50, which would be one dilution below the starting dilution. Dashed lines were used to connect the data points with a titer of 5.64 $\log_2$ to the next data point. The negative control groups receiving PBS (group H) and CMC solution (group I) are not presented in this figure.

Figure 7. Week 8 IgG titer for each individual mouse of group A to G. Statistical comparisons between the mice of the different groups were performed using the ordinary ANOVA, followed by Tukey's multiple comparisons test (* p < 0.05, ** p < 0.01). For clarity reasons, statistical comparison is only indicated where p < 0.05 (*) or p < 0.01 (**), and differences for all other comparisons were non-significant. The negative control groups receiving PBS (group H) and CMC solution (group I) are not presented in this figure. MSP = microspheres.

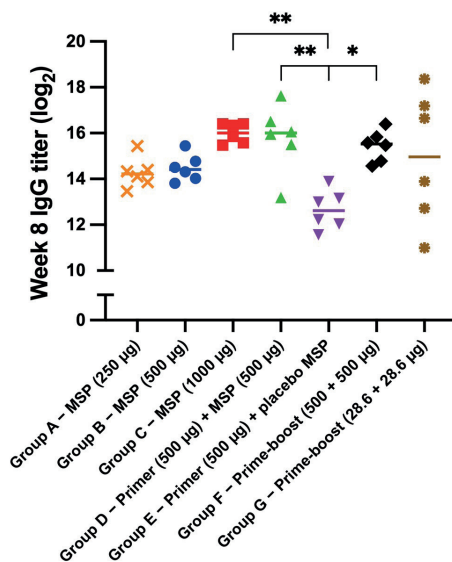The AUC values of the antibody titer vs. time graphs from Figure S1 were calculated for each individual mouse of groups A to G as shown in Figure S2. All mice that received BSA-loaded microspheres had elevated antibody titers from week 1 onwards, which in-

dicates that the microspheres were effective in inducing an immune response. To assess the performance of the sustained-release microspheres in relation to the conventional prime-boost immunization schedule, a high-dose prime and booster injection of BSA in PBS (500 + 500 μg BSA) were administered to mice in group F at weeks 0 and 3, respectively. As expected, antibody titers increased up to week 2, remained steady up to week 3, and again increased and stabilized at week 4 (Figure 6). In other words, the antibody titers spiked following the prime and the booster injection, which demonstrates that the conventional prime-boost immunization schedule was effective as well. Comparison of group C (1000 μg BSA-microspheres) and F (prime-boost 500 + 500 μg BSA) demonstrates that the (week 8) antibody titers as well as the AUC values of both groups were not significantly different. This shows that sustained release of BSA from the microspheres did not result in immunological tolerance toward the model antigen within the tested time frame. The induction of tolerance toward the antigen, causing the vaccine to be ineffective, has previously been related to the sustained release of the antigen from the formulation [42–44]. Clear evidence is, however, lacking [45], and apparently was not found in our study either. When the same total dose of BSA was given, microspheres and a prime-boost injection of BSA in PBS induced a similar IgG antibody response, so the sustained-release microspheres could be a viable alternative to the conventional prime-boost immunization schedule.

Interestingly, mice of group E that received a prime injection of 500 μg BSA in PBS and a mock immunization of placebo microspheres demonstrated a rather different immune response. Here, the antibody titers peaked already after two weeks, after which no further increase in titer was observed (Figure 6). For this group, the final IgG antibody titer at week 8 was significantly lower than that of groups C and F ($p < 0.01$ for 1000 μg BSA-microspheres and $p < 0.05$ for prime-boost 500 + 500 μg BSA). The AUC value was also significantly lower than that of group C. Even though the total administered dose of BSA was lower than for groups C and F, these results suggest that a priming dose alone is not sufficient to elicit a strong immune response over time, and that a booster injection or a continuous release of antigen is required. Although the difference was not statistically significant, the fact that the AUC value and week 8 antibody titer of group E were also lower than those of group B (500 μg BSA-microspheres), which did receive the same total dose of BSA, supports this conclusion. A single-injection vaccine formulation such as the microspheres would then have the preference over the conventional prime-boost vaccine. Apart from one outlier, mice that received both a prime injection of 500 μg BSA in PBS and 500 μg BSA-microspheres (group D, Figure 6) showed an antibody response that strongly resembled the response in group C (1000 μg BSA-microspheres), as the total administered dose of BSA was the same. Apparently, priming with BSA in PBS in addition to the sustained-release microspheres does not enhance the antibody response and, therefore, does not have a preference over the administration of microspheres only.

Furthermore, the fact that (week 8) antibody titers and AUC values were similar for groups C and F suggests that the microspheres did not possess any adjuvant activity for the encapsulated model antigen, as was observed previously for PLGA-based single-administration vaccine formulations [7,46,47]. Comparison of group E (500 μg BSA in PBS + placebo microspheres) and F (prime-boost 500 + 500 μg BSA) confirmed this suspicion, as the IgG antibody titer at week 3 was similar for both groups (12.5 ± 0.1 and

6

13.1 ± 0.6 $\log_2$, respectively).

Mice in the treatment groups (groups A to C) received different amounts of microspheres that were expected to deliver an amount of 250, 500, and 1000 µg BSA, respectively, into the subcutaneous tissue. The antibody responses measured in these groups all followed a similar trend, with an increasing titer up to four weeks, after which it leveled off (Figure 6). A clear difference between the groups is, however, visible at week 1, which demonstrates that the development of high antibody titers takes more time at lower doses. Moreover, the week 8 antibody titer in group C was 3.1- and 2.8-fold higher than in group A and B, respectively (Figure 7), although the differences were not significant ($p > 0.05$). The AUC values raised by immunization with different doses of BSA-loaded microspheres were not significantly different either (Figure S2). Possibly, the difference between the administered doses was not large enough and the doses were all relatively high, which caused only a small difference in immune response. In another study with BSA-loaded microspheres, the influence of the dose on the magnitude of the induced antibody response was more clearly visible [8]. Here, a high dose of BSA (431 µg) elicited 13- and 8-fold higher antibody titers than a low dose of BSA (i.e., 64 µg) at the first and last time point of the *in vivo* study, respectively. It should, however, be noted that the microspheres in this specific study displayed a pulsatile release of BSA instead of sustained release, which impedes direct comparison.

Finally, mice receiving a high- and a low-dose prime-boost injection of BSA in PBS were compared in terms of IgG antibody response. The dose of the high-dose prime-boost injection (500 + 500 µg BSA, group F) was based on the total dose of the sustained-release microspheres from group C, and the dose of the low-dose prime-boost injection (28.6 + 28.6 µg BSA, group G) was based on the average daily dose of the microspheres. All mice in the high-dose prime-boost group developed high titers of BSA-specific IgG antibodies. However, high variability in antibody titers was observed in the low-dose prime-boost group. These results are in line with a study by Guarecuco et al., where a greater variability in antibody response was observed for a low-dose than for a high-dose BSA formulation [8]. This probably indicates that in some mice of group G, the amount of antigen reaching the draining lymph nodes was sufficient for B cell activation, while in other mice this was not the case [48].

For most of the mice from the treatment groups (groups A to C), IgG antibody titers continued to increase up to four weeks after administration of the formulations, which can be considered an indirect indication of sustained release of BSA from the microspheres. After these four weeks, antibody titers hardly increased, which suggests that the release of BSA from the microspheres had ceased. These results are in line with the *in vitro* release data (Figure 4a), where the vast majority of the encapsulated BSA was released in a near-linear fashion over a period of four weeks. The development of antigen-specific antibodies, however, takes approximately one week [7,49]. An increase in IgG antibody titers up to four weeks, therefore, suggests an *in vivo* release duration of only three weeks. This indicates that the release of BSA was faster *in vivo* than *in vitro*, probably due to accelerated microsphere degradation *in vivo*, for instance, caused by increased liquid uptake into the polymer and foreign body responses [8,50,51]. Lipids and other biological molecules can act as plasticizers or affect the surface tension, which enhances water uptake. Moreover, free radicals, acidic products, or enzymes produced

by macrophages that form around the microspheres can accelerate polymer degradation. To gain more insight into the *in vivo* pharmacokinetics of BSA, plasma samples from weeks 1 to 4 of groups A to G were analyzed for BSA levels as well (Figure 8).
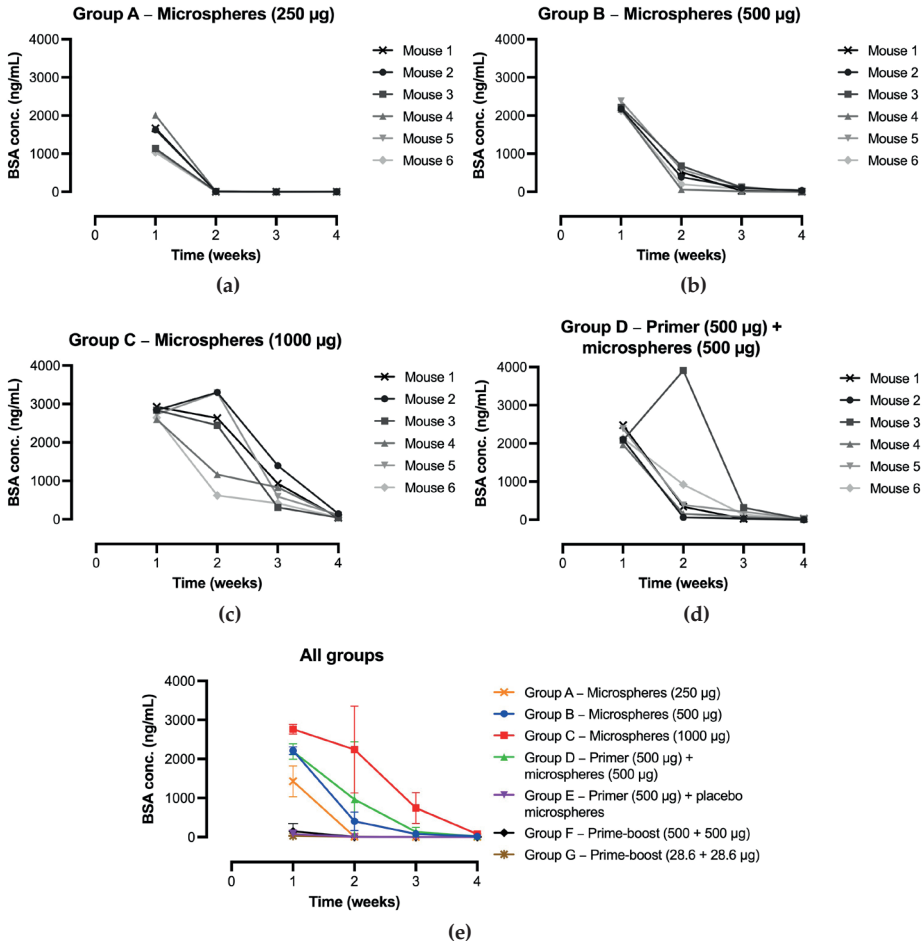
Figure 8. BSA levels in mouse plasma over time after immunization with different BSA formulations (group A to D). Mice (*n* = 6 per group) were immunized with: (**a**) 250 µg BSA-microspheres in CMC solution; (**b**) 500 µg BSA-microspheres in CMC solution; (**c**) 1000 µg BSA-microspheres in CMC solution; and (**d**) 500 µg BSA in PBS together with 500 µg BSA-microspheres in CMC solution. (**e**) The averages of the BSA levels measured in all mice were calculated for each group (group A to G) and presented for all groups together.

Sustained release of BSA from the microspheres into the systemic circulation was demonstrated, with plasma BSA concentrations being dependent on the administered dose, as expected. Peak plasma concentrations were 1429 ± 397, 2214 ± 99, and 2762 ± 127 ng BSA/mL for 250, 500, and 1000 µg BSA, respectively. For most of the mice receiving BSA-loaded microspheres, the highest plasma BSA concentration was measured one week after administration, followed by a strong decline in the concentration (Figure 8a–d). After

four weeks, only low levels of BSA were still measured. In contrast, the highest release rate *in vitro* was reached after three weeks of incubation (Figure 5), which indicates that the release of BSA from the microspheres was indeed faster *in vivo* than *in vitro*. It is, however, also possible that the decline in BSA plasma concentration after one week was due to antibody formation, as was previously observed by van Dijk et al. after injection of sustained-release microspheres containing a human serum albumin construct [34]. Likewise, in our study, the induced antibodies might have formed a complex with BSA, which prevented the model antigen from binding to the capture antibodies of the ELISA and, thus, from being detected with the assay. Furthermore, the theoretical plasma BSA concentrations of weeks 2 to 4 can be calculated based on the actual plasma BSA concentrations of the previous week, assuming a BSA half-life of 1 day [52,53]. For almost all mice of groups B to D, the actual plasma BSA concentrations of weeks 2 to 4 were higher than the theoretical concentrations. This suggests that at least some release of BSA from the microspheres was still ongoing during these weeks.

Altogether, these findings demonstrate that single-injection microspheres providing a sustained release of BSA can induce strong humoral immune responses in mice, with antibody titers similar to the immune response induced by a prime-boost injection of BSA in PBS. Sustained-release microspheres, therefore, might be a viable alternative to the conventional prime-boost immunization schedule. Further research is, however, needed to determine whether the developed microspheres are also suitable for the delivery of a clinically relevant vaccine and which dose of antigen is optimal for strong antibody induction. In this study, relatively high doses of BSA were administered, while lower doses might have been sufficient as well. Once a clinically relevant antigen has been incorporated, IgG subclasses (e.g., IgG1 and IgG2a) and cellular immune responses could be determined in addition to total IgG. This will provide insight into qualitative aspects of the immune response induced by sustained-release microspheres. Moreover, tailoring the release duration to the specific needs of a vaccine is essential for the use of the sustained-release microspheres for a broad variety of vaccines. According to the *in vitro* release results, the release duration could be varied by varying the blend ratio of the polymers used but changing the composition of the polymers is an option as well. However, establishing an *in vitro-in vivo* correlation remains difficult, as there are many factors in play that affect the pharmacokinetics of an antigen. Examples are plasma clearance and antibody formation, but also lymphatic uptake and metabolism, interference of components of the s.c. extracellular matrix, and protein degradation at the injection site [34]. Determining the *in vivo* release or the plasma concentration as a surrogate indicator of release is, therefore, recommended.

6.4 Conclusion

Novel multi-block copolymers composed of amorphous, hydrophilic PCL-PEG-PCL blocks and semi-crystalline PDO blocks were used to produce sustained-release microspheres containing the model antigen BSA. The membrane emulsification method enabled the production of uniformly sized particles with the desired size and morphology and high EE. *In vitro* release studies showed that the release rate could be modulated by adjusting the blend ratio of the two multi-block copolymers. All formulations exhibited

sustained release of BSA with low initial burst. Microspheres consisting of a 92.5:7.5 polymer blend released BSA *in vitro* in a near-linear fashion over a period of approximately four weeks, after which BSA continued to slowly diffuse out for another two weeks. We demonstrated that these microspheres were able to induce a strong BSA-specific IgG antibody response *in vivo* after s.c. administration in mice. The immune response was equal to that elicited by a prime-boost injection of BSA in PBS administered at 0 and 3 weeks, and the IgG titers followed the same pattern as the *in vitro* BSA release. Pharmacokinetic analysis of the microspheres demonstrated that *in vivo* release of BSA was probably ongoing up to at least four weeks as well, although peak plasma concentrations were already reached one week after administration and after four weeks only low levels of BSA were still detected. This suggests that the release of BSA was faster *in vivo* than *in vitro*, although the early decline in plasma BSA concentration might also have been caused by the formation and subsequent elimination of antigen–antibody complexes. Converting *in vitro* release and plasma concentration profiles into *in vivo* release profiles, thus, remains a challenge. This research shows the potential of sustained-release microspheres as an alternative to the conventional prime-boost immunization schedule. Ultimately, this technology could contribute to the development of single-injection vaccines and improvements in global vaccination coverage. Further studies with a clinically relevant antigen are, however, necessary to evaluate the clinical potential of the microspheres.

Funding

Acknowledgments

References

[1]   WHO, "Immunization Coverage," 2022. [Online]. Available: https://www.who.int/news-room/fact-sheets/detail/immunization-coverage. [Accessed: 14-Dec-2022].

[2]   H.A. Ali, A.M. Hartner, S. Echeverria-Londono, J. Roth, X. Li, K. Abbas, A. Portnoy, E. Vynnycky, K. Woodruff, N.M. Ferguson, and others, "Vaccine equity in low and middle income countries: a systematic review and meta-analysis," Int. J. Equity Health, vol. 21, no. 1, p. 82, 2022.

[3]   WHO, "Immunization Agenda 2030," 2021. [Online]. Available: https://www.who.int/docs/default-source/immunization/strategy/ia2030/ia2030-document-en.pdf. [Accessed: 25-Oct-2022].

[4]   K.J. McHugh, R. Guarecuco, R. Langer, and A. Jaklenec, "Single-injection vaccines: Progress, challenges, and opportunities," J. Control. Release, vol. 219, pp. 596–609, 2015.

[5]   J.L. Cleland, A. Lim, L. Barrón, E.T. Duenas, and M.F. Powell, "Development of a single-shot subunit vaccine for HIV-I: Part 4. Optimizing microencapsulation and pulsatile release of MN rgp120 from biodegradable microspheres," J. Control. Release, vol. 47, no. 2, pp. 135–150, 1997.

[6]   R.S. van der Kooij, R. Steendam, J. Zuidema, H. Frijlink, and W.L.J. Hinrichs, "Microfluidic production of polymeric core-shell microspheres for the delayed pulsatile release of bovine serum albumin as a model antigen," Pharmaceutics, vol. 13, no. 11, p. 1854, 2021.

[7]   K. Amssoms, P.A. Born, M. Beugeling, B. De Clerck, E. Van Gulck, W.L.J. Hinrichs, H.W. Frijlink, N. Grasmeijer, G. Kraus, R. Sutmuller, and others, "Ovalbumin-containing core-shell implants suitable to obtain a delayed IgG1 antibody response in support of a biphasic pulsatile release profile in mice," PLoS One, vol. 13, no. 8, p. e0202961, 2018.

[8]   R. Guarecuco, J. Lu, K.J. McHugh, J.J. Norman, L.S. Thapa, E. Lydon, R. Langer, and A. Jaklenec, "Immunogenicity of pulsatile-release PLGA microspheres for single-injection vaccination," Vaccine, vol. 36, no. 23, pp. 3161–3168, 2018.

[9]   J.L. Cleland, "Single-administration vaccines: controlled-release technology to mimic repeated immunizations," Trends Biotechnol., vol. 17, no. 1, pp. 25–29, 1999.

[10]   L. Feng, X. Qi, X. J. Zhou, Y. Maitani, S. C. Wang, Y. Jiang, and T. Nagai, "Pharmaceutical and immunological evaluation of a single-dose hepatitis B vaccine using PLGA microspheres," J. Control. Release, vol. 112, pp. 35–42, 2006.

[11]   M. Singh, A. Singh, and G. P. Talwar, "Controlled delivery of diphtheria toxoid using biodegradable poly(d,l-lactide) microcapsules," Pharm. Res., vol. 8, pp. 958–961, 1991.

[12]   G. Du and X. Sun, "Current advances in sustained release microneedles," Pharm. Front., vol. 2, pp. e11–e22, 2020.

[13]   W. Li, J. Meng, X. Ma, J. Lin, and X. Lu, "Advanced materials for the delivery of vaccines for infectious diseases," Biosaf. Health, vol. 4, pp. 95–104, 2022.

[14]   H. K. Makadia and S. J. Siegel, "Poly lactic-co-glycolic acid (PLGA) as biodegradable controlled drug delivery carrier," Polymers, vol. 3, pp. 1377–1397, 2011.

[15]   L. Duque, M. Körber, and R. Bodmeier, "Improving release completeness from PLGA-based implants for the acid-labile model protein ovalbumin," Int. J. Pharm., vol. 538, pp. 139–146, 2018.

[16]   A. Giteau, M. C. Venier-Julienne, A. Aubert-Pouëssel, and J. P. Benoit, "How to achieve sustained and complete protein release from PLGA-based microparticles?," Int. J. Pharm., vol. 350, pp. 14–26, 2008.

[17]   M. L. Houchin and E. M. Topp, "Chemical degradation of peptides and proteins in PLGA: A review of reactions and mechanisms," J. Pharm. Sci., vol. 97, pp. 2395–2404, 2008.

[18]   M. Stanković, H. de Waard, R. Steendam, C. Hiemstra, J. Zuidema, H. W. Fri-

jlink, and W. L. J. Hinrichs, "Low temperature extruded implants based on novel hydrophilic multiblock copolymer for long-term protein delivery," Eur. J. Pharm. Sci., vol. 49, pp. 578–587, 2013.

[19]   M. Stanković, J. Tomar, C. Hiemstra, R. Steendam, H. W. Frijlink, and W. L. J. Hinrichs, "Tailored protein release from biodegradable poly(ε-caprolactone-PEG)-b-poly(ε-caprolactone) multiblock-copolymer implants," Eur. J. Pharm. Biopharm., vol. 87, pp. 329–337, 2014.

[20]   N. Teekamp, F. Van Dijk, A. Broesder, M. Evers, J. Zuidema, R. Steendam, E. Post, J. L. Hillebrands, H. W. Frijlink, K. Poelstra, et al., "Polymeric microspheres for the sustained release of a protein-based drug carrier targeting the PDGFβ-receptor in the fibrotic kidney," Int. J. Pharm., vol. 534, pp. 229–236, 2017.

[21]   K. C. Scheiner, R. F. Maas-Bakker, T. T. Nguyen, A. M. Duarte, G. Hendriks, L. Sequeira, G. P. Duffy, R. Steendam, W. E. Hennink, and R. J. Kok, "Sustained release of vascular endothelial growth factor from poly(ε-caprolactone-PEG-ε-caprolactone)-b-poly(l-lactide) multiblock copolymer microspheres," ACS Omega, vol. 4, pp. 11481–11492, 2019.

[22]   M. Igartua, R. M. Hernández, A. Esquisabel, A. R. Gascón, M. B. Calvo, and J. L. Pedraz, "Enhanced immune response after subcutaneous and oral immunization with biodegradable PLGA microspheres," J. Control. Release, vol. 56, pp. 63–73, 1998.

[23]   B. R. Conway, J. Eyles, and H. O. Alpar, "A comparative study on the immune responses to antigens in PLA and PHB microspheres," J. Control. Release, vol. 49, pp. 1–9, 1997.

[24]   G. Lemperle, "Biocompatibility of injectable microspheres," Biomed. J. Sci. Tech. Res., vol. 2, pp. 2296–2306, 2018.

[25]   M. Ye, S. Kim, and K. Park, "Issues in long-term protein delivery using biodegradable microparticles," J. Control. Release, vol. 146, pp. 241–260, 2010.

[26]   G. T. Vladisavljević, "Structured microparticles with tailored properties produced by membrane emulsification," Adv. Colloid Interface Sci., vol. 225, pp. 53–87, 2015.

[27]   F. Qi, J. Wu, Q. Fan, F. He, G. Tian, T. Yang, G. Ma, and Z. Su, "Preparation of uniform-sized exenatide-loaded PLGA microspheres as long-effective release system with high encapsulation efficiency and bio-stability," Colloids Surfaces B Biointerfaces, vol. 112, pp. 492–498, 2013.

[28]   R. Bodmeier and J. W. McGinity, "Solvent selection in the preparation of poly(dl-lactide) microspheres prepared by the solvent evaporation method," Int. J. Pharm., vol. 43, pp. 179–186, 1988.

[29]   H. Rafati, A.G.A. Coombes, J. Adler, J. Holland, and S.S. Davis, "Protein-loaded poly(dl-lactide-co-glycolide) microparticles for oral administration: formulation, structural and release characteristics," J. Control. Release, vol. 43, pp. 89-102, 1997.

[30]   S. Mao, J. Xu, C. Cai, O. Germershaus, A. Schaper, and T. Kissel, "Effect of WOW process parameters on morphology and burst release of FITC-dextran loaded PLGA microspheres," Int. J. Pharm., vol. 334, pp. 137-148, 2007.

6

[31]   T. Arakawa and S.N. Timasheff, "Preferential interactions of proteins with salts in concentrated solutions," Biochemistry, vol. 21, pp. 6545-6552, 1982.

[32]   Y. Fu and W.J. Kao, "Drug release kinetics and transport mechanisms of non-degradable and degradable polymeric delivery systems," Expert Opin. Drug Deliv., vol. 7, pp. 429-444, 2010.

[33]   R. van Dijkhuizen-Radersma, S. Métairie, J.R. Roosma, K. de Groot, and J.M. Bezemer, "Controlled release of proteins from degradable poly(ether-ester) multiblock copolymers," J. Control. Release, vol. 101, pp. 175-186, 2005.

[34]   F. Van Dijk, N. Teekamp, L. Beljaars, E. Post, J. Zuidema, R. Steendam, Y.O. Kim, H.W. Frijlink, D. Schuppan, K. Poelstra, et al., "Pharmacokinetics of a sustained release formulation of PDGFβ-receptor directed carrier proteins to target the fibrotic liver," J. Control. Release, vol. 269, pp. 258-265, 2018.

[35]   H. Haitjema, R. Steendam, C. Hiemstra, J. Zuidema, A. Doornbos, and T. Nguyen, "Biodegradable, phase separated, thermoplastic multi-block copolymer," PCT Patent No. WO 2021/066650 A1, Apr. 8, 2021.

[36]   J.C. Middleton and A.J. Tipton, "Synthetic biodegradable polymers as orthopedic devices," Biomaterials, vol. 21, pp. 2335-2346, 2000.

[37]   S. Heene, S. Thoms, S. Kalies, N. Wegner, P. Peppermüller, N. Born, F. Walther, T. Scheper, and C.A. Blume, "Vascular network formation on macroporous polydioxanone scaffolds," Tissue Eng. Part A, vol. 27, pp. 1239-1249, 2021.

[38]   M. Zilberman, K.D. Nelson, and R.C. Eberhart, "Mechanical properties and in vitro degradation of bioresorbable fibers and expandable fiber-based stents," J. Biomed. Mater. Res. Part B Appl. Biomater., vol. 74B, pp. 792-799, 2005.

[39]   P. Kotcharat, P. Chuysinuan, T. Thanyacharoen, S. Techasakul, and S. Ummartyotin, "Development of bacterial cellulose and polycaprolactone (PCL) based composite for medical material," Sustain. Chem. Pharm., vol. 20, p. 100404, 2021.

[40]   European Medicines Agency, "ICH Guideline Q3C (R8) on Impurities: Guideline for Residual Solvents," 2021. [Online]. Available: https://www.ema.europa.eu/en/documents/regulatory-procedural-guideline/ich-guideline-q3c-r8-impurities-guideline-residual-solvents-step-5_en.pdf. [Accessed: Oct. 25, 2022].

[41]   D. G. Serota, A. Thakur, B. Ulland, J. Kirschman, N. Brown, and R. H. Coots, "A two-year drinking-water study of dichloromethane in rodents. II. Mice," Food Chem. Toxicol., vol. 24, pp. 959–963, 1986.

[42]   D. W. Dresser and G. Gowland, "Immunological paralysis induced in adult rabbits by small amounts of a protein antigen," Nature, vol. 203, pp. 733–736, 1964.

[43]   F. J. Dixon and P. H. Maurer, "Immunologic unresponsiveness induced by protein antigens," J. Exp. Med., vol. 101, pp. 245–257, 1955.

[44]   N. A. Mitchison, "Induction of immunological paralysis in two zones of dosage," Proc. R. Soc. Lond. B, vol. 161, pp. 275–292, 1964.

[45]   S. Lofthouse, "Immunological aspects of controlled antigen delivery," Adv. Drug Deliv. Rev., vol. 54, pp. 863–870, 2002.

[46]   E. C. Lavelle, M. K. Yeh, A. G. A. Coombes, S. S. Davis, "The stability and immunogenicity of a protein antigen encapsulated in biodegradable microparticles based on blends of lactide polymers and polyethylene glycol," Vaccine, vol. 17,

pp. 512–529, 1999.

[47]   D. T. O'Hagan, D. Rahman, J. P. McGee, H. Jeffery, M. C. Davies, P. Williams, S. S. Davis, and S. J. Challacombe, "Biodegradable microparticles as controlled release antigen delivery systems," Immunology, vol. 73, pp. 239–242, 1991.

[48]   B. A. Heesters, C. E. van der Poel, A. Das, and M. C. Carroll, "Antigen presentation to B cells," Trends Immunol., vol. 37, pp. 844–854, 2016.

[49]   O. Leo, A. Cunningham, and P.L. Stern, "Vaccine immunology," Perspect. Vaccinol., vol. 1, pp. 25–59, 2011.

[50]   M. Sandor, J. Harris, and E. Mathiowitz, "A novel polyethylene depot device for the study of PLGA and P(FASA) microspheres in vitro and in vivo," Biomaterials, vol. 23, pp. 4413–4423, 2002.

[51]   M.A. Tracy et al., "Factors affecting the degradation rate of poly(lactide-co-glycolide) microspheres in vivo and in vitro," Biomaterials, vol. 20, pp. 1057–1062, 1999.

[52]   A. Nguyen et al., "The pharmacokinetics of an albumin-binding Fab (AB.Fab) can be modulated as a function of affinity for albumin," Protein Eng. Des. Sel., vol. 19, pp. 291–297, 2006.

[53]   D. Stevens, R. Eyre, and R. Bull, "Adduction of hemoglobin and albumin in vivo by metabolites of trichloroethylene, trichloroacetate, and dichloroacetate in rats and mice," Fundam. Appl. Toxicol., vol. 19, pp. 336–342, 1992.

6
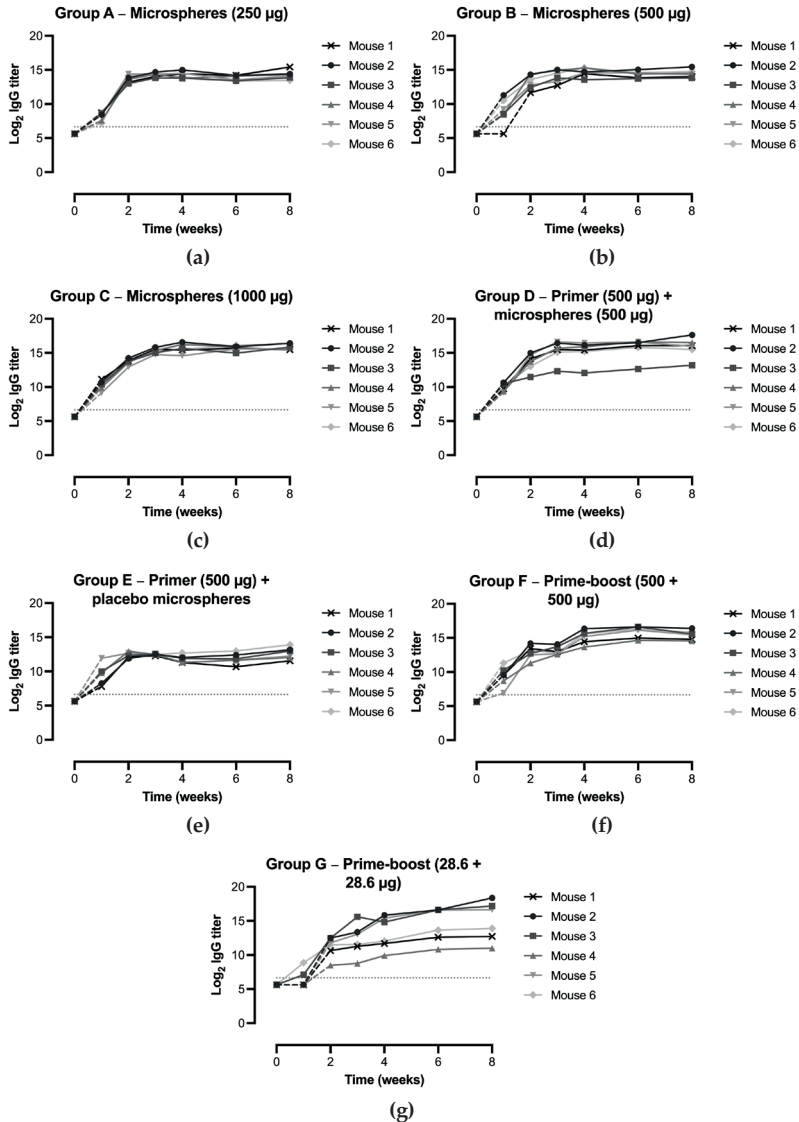
Figure S1. BSA-specific IgG antibody titers in mouse plasma over time after immunization with different BSA formulations (group A to G). Mice (n = 6 per group) were immunized with: (a) 250 μg BSA-microspheres in carboxymethyl cellulose (CMC) solution; (b) 500 μg BSA-microspheres in CMC solution; (c) 1000 μg BSA- microspheres in CMC solution; (d) 500 μg BSA in phosphate-buffered saline (PBS) together with 500 μg BSA- microspheres in CMC solution; (e) 500 μg BSA in PBS together with placebo microspheres in CMC solution; (f) 500 + 500 μg BSA in PBS, prime injection (week 0) and booster injection (week 3); and (g) 28.6 + 28.6 μg BSA in PBS, prime injection (week 0) and booster injection (week 3). The dotted lines represent the cut-off value for the IgG antibody titer, i.e. a titer of 6.64 $\log_2$, corresponding to the starting dilution of the plasma samples of 1:100. Values below this titer could not be measured. Samples with a reading for the least diluted plasma (i.e. 100x diluted) lower than the cut-off value were assigned an IgG antibody titer of 5.64 $\log_2$, corresponding to a dilution of 1:50, which would be

one dilution below the starting dilution. For these samples, dashed lines were used to connect the data point below the cut-off value with the next time point. The negative control groups receiving PBS (group H) and CMC solution (group I) are not presented in this figure.
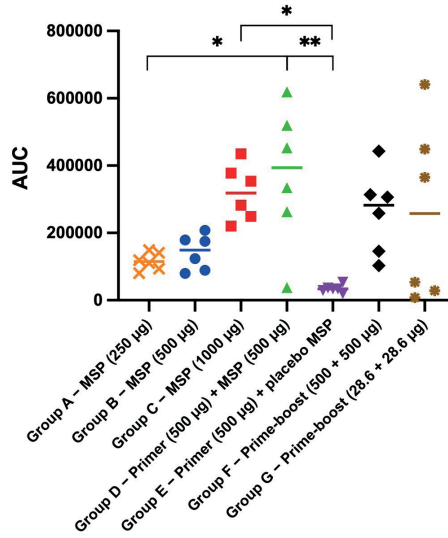
Figure S2. Area under the IgG titer–time curve (AUC) values of the BSA-specific IgG antibody titer vs. time graph (Figure S1). Statistical comparisons between the mice of the different groups were performed using the ordinary ANOVA, followed by Tukey's multiple comparisons test (* $p < 0.05$, ** $p < 0.01$). For clarity reasons, statistical comparison is only indicated where $p < 0.05$ (*) or $p < 0.01$ (**), and differences for all other comparisons were non-significant. The negative control groups receiving PBS (group H) and CMC solution (group I) are not presented in this figure. MSP = microspheres.

# Chapter 7

General discussion

In the previous chapters, several potential single-administration vaccine formulations based on different concepts were presented and discussed. Both *in vitro* and *in vivo* experiments have given insight into the opportunities and challenges associated with the developed formulations and single-administration vaccines in general. Here, a general discussion of the previous chapters will be provided in which the results of the different formulations will be united. In addition, some perspectives on further research to progress toward clinical application will be presented.

7.1 General discussion

7.1.1 Choice of (model) antigen

In this thesis, several model antigens and compounds have been used in the development of a single-administration vaccine formulation. The choice for a model antigen or compound instead of a clinically relevant antigen had three reasons. First of all, the aim of this research was the development of a single-administration vaccine formulation that could be used for multiple (types of) vaccines instead of one particular vaccine. By obtaining a mechanistic understanding of the different formulations, the most optimal concept can be selected and, subsequently, tailored to the needs of a specific clinically relevant vaccine. Second, most vaccines, whether they are live attenuated or inactivated pathogens, protein-, mRNA-, or polysaccharide-based, are physically and chemically unstable [1]. For example, many vaccines are very sensitive to heat and sometimes cold, causing a decline in potency when exposed to elevated or freezing temperatures during production, storage, and/or release [2-4]. However, other factors can compromise the vaccine's integrity as well, such as interfacial, shear, and drying stresses during formulation and hydration during (*in vitro*) release. Moreover, protein-based based vaccines tend to denature, aggregate, or undergo chemical degradation, even under mild conditions, which ultimately affects their therapeutic activity [5]. These stability issues might greatly impair the formulation research, which could be circumvented by using (stable) model antigens or compounds. Last, most clinically relevant antigens are rather expensive as their complex structure requires complex production methods. Especially in the preformulation stage of the development, relatively large amounts of antigen are needed, resulting in high costs. Cheaper model antigens or compounds are therefore a good alternative.

Examples of frequently used (proteinaceous) model antigens are serum albumin [6-8] and ovalbumin (OVA) [9-11], as they are affordable, well characterized, easy to analyze, and rather stable compared to many clinically used vaccines. Moreover, previous studies have shown that these model antigens are capable of inducing strong immune responses in mice upon parenteral administration [6,7,9,12], allowing for *in vivo* evaluation of the release kinetics resulting in an immune response. The model antigen used in this thesis (chapters 4 to 6) was bovine serum albumin (BSA), a fairly stable and highly water-soluble serum albumin protein derived from cows. Therefore, it can induce BSA-specific immune responses in commonly used animal models, such as mice and rats, as it is a foreign protein to these species. BSA has a molecular weight of 66 kDa and is, thus, a medium-sized protein. The dimensions of clinically relevant antigens, however, vary greatly. For example, tetanus toxoid is larger (150 kDa [1])

than BSA, while the hepatitis B surface antigen (HBsAg) is smaller (24 kDa [13]). Live attenuated and inactivated pathogens, on the other hand, are obviously much larger, as they are whole organisms or cells that have been modified or inactivated, respectively. This demonstrates that a model antigen, as the name already implies, only serves as a model, and that extensive testing with the clinically relevant antigen in question is still necessary. Moreover, it is not possible to have all physicochemical properties (e.g. size, isoelectric point and charge, hydrophilicity and water solubility) of the model antigen equal to those of the clinically relevant antigen. Especially for model antigens such as BSA, their high (conformational and thermal) stability is often not a good representation of clinically relevant antigens as these are they are generally more vulnerable to denaturation, aggregation, and degradation processes as described above. The transition to a clinically relevant antigen can, therefore, be challenging.

For the prototype based on a physical mixture of poly(lactic-*co*-glycolic acid) (PLGA) (chapter 3), blue dextran (BD) was used as a model antigen for bacterial polysaccharide-based vaccines [14]. Blue dextran is a polysaccharide (dextran) labeled with a blue dye (Cibacron blue F3GA) and is available in a wide range of molecular weights, offering the potential to be used as a model for a wide variety of (polysaccharide-based) vaccines. In this thesis, large (2000 kDa) and moderately sized (70 kDa) BD were used. The physical mixture concept could only be applied to polysaccharide-based antigens, as it was unsuitable for the pulsatile delivery of protein-based (model) antigens, such as OVA and BSA. *In vitro* release studies (data not shown in this thesis) demonstrated that physically mixed PLGA compacts encapsulating OVA released approximately 60% of the totally incorporated OVA within the first day, which could serve as the prime dose. However, no delayed pulsatile release of OVA was observed after the release of this prime dose. The absence of a delayed pulsatile release might be due to the close contact of the protein with the polymer, and due to the porous structure combined with the release mechanism of the compact. Upon incubation, water immediately penetrated through the pores into the compact. After a certain period, these pores closed causing water to be entrapped within the compact. This initiated the hydrolysis of PLGA, which caused acidic degradation products of PLGA (lactic and glycolic acid) to accumulate within the polymer matrix [15,16]. This acidic microclimate probably resulted in degradation of the remaining OVA, and thereby, the absence of a delayed pulsatile release [17]. As expected, physically mixed PLGA compacts containing BD did exhibit the desired biphasic pulsatile release profile. This indicates that the concept might be suitable for the pulsatile delivery of bacterial polysaccharide-based vaccines, though incorporation of a clinically relevant antigen and assessment of the structural integrity of the released antigen is still required. Next to BD, the small molecule theophylline (180 Da) was incorporated as a model drug into the physically mixed PLGA compacts. Though theophylline is not representative of antigens, the drug was released from the compacts in a pulsatile manner, similar to the release profile of BD. As the main aim of this chapter was to investigate the mechanism behind this biphasic pulsatile release profile and as it was found that the release profile was not influenced by the molecular weight of the model compound, theophylline was considered to be a suitable model drug. Moreover, the physical mixture prototype was based on a previous study by Murakami et al. in which a PLGA-based device was developed that displayed a biphasic pulsatile release profile [18]. This device also

7

contained theophylline as a model drug, which allowed comparison between both studies. For the core-shell prototype, theophylline was also used as a model drug. BD was not incorporated into the core-shell compacts, because for these compacts, the focus was on protein-based vaccines. With a core-shell structure, the antigen is physically separated from the polymer phase, which might reduce the stresses caused by polymer-protein interactions. It was therefore assumed that obtaining a delayed pulsatile release profile is possible for these compacts in contrast to the physically mixed compacts. Such core-shell compacts containing the model antigen OVA and the clinically relevant antigen respiratory syncytial virus pre-fusion protein were developed by Amssoms et al. [9] and Beugeling et al. [19], respectively. In both studies, a delayed pulsatile release profile could indeed be obtained, though the release was incomplete. By applying a fast-dissolving coating containing the antigen onto the compacts, a biphasic pulsatile release of a protein-based antigen could possibly be obtained.

Taken together, it can be concluded that various model antigens and compounds can be used as an alternative to the clinically relevant antigen. BSA showed good results as a model antigen for protein-based antigens, as it was highly stable, easy to measure, and able to induce a BSA-specific immune response in mice. For polysaccharide-based vaccines, BD is very suitable as it functions well as a release marker due to its blue color and is available in a wide range of molecular weights. However, as already mentioned above, a model antigen only serves as a model and the ideal model antigen is, in fact, only the clinically relevant antigen itself. Especially for complex and novel types of vaccines, such as the COVID-19 mRNA vaccines, a model compound can never fully replace the vaccine of interest, so follow-up experiments with the clinically used vaccine are essential. Also, mRNA vaccines do not contain the antigen itself, but introduce a piece of mRNA into the vaccinee's body that encodes the antigen of interest. A different type of model compound is therefore required in the development of a single-administration vaccine formulation than for the antigen-based vaccines.

7.1.2 Choice of polymer

In chapters 3 to 5 of this thesis, the focus was on the biocompatible and biodegradable polymer PLGA, as it is the most widely investigated polymer and can be prepared at different lactide:glycolide molar ratios and molecular weights [15]. These variations allow for a relatively simple tuning of the physicochemical properties, such as degradation rate and glass transition temperature (T_g). For already many years, PLGA has been used in commercial pharmaceutical products for the delivery of small molecule drugs and (small) peptides [20]. Examples are the long-acting injectable microsphere formulations Risperdal Consta and Sandostatin LAR for the delivery of the small molecule drug risperidone (410 Da) and the small peptide octreotide (1.02 kDa), respectively. The compatibility of PLGA with proteins is, however, poor, which often results in instability and consequently incomplete release of the intact protein [17]. This issue has been extensively described in the literature and has been attributed to different factors [21-24]. These stress factors can compromise the structural integrity of the protein during production, storage, and release. Especially during release, many processes might occur that lead to an incomplete release of the protein, such as protein aggregation, hydrolysis, and adsorption to and/or interactions with the polymer matrix [17,23]. These processes

might render the (proteinaceous) antigen inactive and sometimes even cause unforeseen side effects or toxicity [25]. One of the main causes for physical or chemical instability is the formation of an acidic microenvironment within the formulation, which is created by the degradation products of PLGA, i.e. lactic and glycolic acid [16,26]. Examples of acid-catalyzed protein degradation reactions described in the literature are (amide bond) hydrolysis, deamidation, dimerization, and conformational changes [27]. Interactions between PLGA and the encapsulated protein are, for instance, caused by electrostatic interactions and hydrophobic polymer surfaces resulting in protein adsorption to the polymer [28]. Also, reactive ester bonds in PLGA can lead to acylation of the protein [27]. For peptides, the same stability issues may occur, although PLGA is better compatible with small hydrophilic peptides, such as octreotide and leuprolide (1.21 kDa, Lupron Depot), than with proteins [29,30]. This might be due to their relatively small size, which causes them to be less prone to chemical degradation and denaturation, as they have a simpler three-dimensional structure [31]. Also, their hydrophilic nature reduces the risk of aggregation and precipitation, and the fact that these small peptides are relatively stable in acidic environments explains why the development of an acidic microclimate is less of a problem [31,32]. These peptides can, however, be susceptible to acylation upon interaction with PLGA [33,34].

In chapter 4, an incomplete release of BSA from PLGA microspheres was observed as expected. The total release percentage varied from approximately 30 to 60% of the incorporated amount of BSA, though for some formulations, the release still seemed to be ongoing. Apparently, even for a stable protein such as BSA, complete release from a PLGA-based formulation is difficult to achieve. Also, physically separating the model antigen from the polymer phase did not (completely) prevent issues related to the incompatibility between BSA and PLGA. In chapter 5, incorporation of BSA unfortunately failed and the completeness of release could therefore not be determined. As already mentioned above, physically mixed PLGA compacts (chapter 3) containing OVA did not release any model antigen at all after the lag phase. Here, only an initial release of OVA serving as the prime dose was observed. One strategy to improve the stability of a protein within a PLGA-based formulation is the incorporation of stabilizing excipients that protect the protein from several stress factors that can cause such protein instability [1,35]. Examples are (divalent cation) salts or inorganic bases, such as $MgOH_2$, which acts as an acid neutralizer and can, thus, prevent a pH drop within the formulation upon degradation of the polymer [36,37]. Other options are the incorporation of sugars, surfactants, and buffers, though these have been employed with varying degrees of success [35,38]. Some of these methods resulted in an increased release percentage, but none of them in a complete release. Also, the effectivity is partially dependent on the antigen that is used [35], and the incorporation of these excipients might affect the release rate. It can thus be concluded that alternative polymers with improved protein compatibility are highly desired.

An example of biodegradable polymers with improved protein compatibility are the novel poly(ether ester urethane) multi-block copolymers used in chapter 6 [39]. These phase-separated multi-block copolymers can consist of both amorphous and semi-crystalline blocks, and the amorphous block usually contains the hydrophilic polymer poly(ethylene glycol) (PEG) [40-42]. Upon contact with water, these PEG blocks will

7

swell, causing the incorporated (model) antigen to diffuse out. On the other hand, the semi-crystalline block provides mechanical strength and enables prolonged release of the incorporated (model) antigen [39]. Besides PEG, the multi-block copolymers can be composed of several different polymers, such as poly(DL-lactide) (PDLLA), poly(L-lactide), polyglycolide, poly(ε-caprolactone) (PCL), and poly(dioxanone) (PDO). Due to the swelling of the PEG blocks, the release mechanism from the multi-block copolymers contrasts with the release mechanism from a PLGA-based matrix [43]. Release from a PLGA-based matrix is usually degradation-controlled, while release from the multi-block copolymers takes place by diffusion before substantial degradation of the polymer has occurred. The formation of acidic degradation products during release causing pH-induced degradation of the incorporated compounds is thereby prevented. Moreover, the multi-block copolymers are known to generate fewer degradation products than PL(G)A, and the acidic degradation products that are generated during release can diffuse out through the swollen polymer matrix and, therefore, do not accumulate within the formulation. In chapter 6, monolithic microspheres were prepared from blends of two multi-block copolymers composed of amorphous, hydrophilic PCL-PEG-PCL blocks and semi-crystalline PDO blocks. Swelling of the PEG blocks upon incubation of the microspheres in *in vitro* release medium caused the model antigen BSA to be gradually released by diffusion over several weeks. Because the homopolymer PDO has a degradation time of approximately six months [44,45] and *in vitro* degradation of PDO-based multi-block copolymers is anticipated to be 9 to 24 months [39], it was not expected that extensive degradation of the semi-crystalline PDO block had occurred during the course of the *in vitro* release studies (i.e. four to nine weeks). Hence, the PDO block probably did not play a significant role in the release of BSA. We hypothesize that (initial) BSA release was caused by diffusion of the model antigen through the swollen polymer matrix, while some degradation of the PCL-PEG-PCL blocks further increased the mesh size of the matrix, thereby accelerating release. This release mechanism resulted in a reasonably high release completeness of up to 80% for all formulations, of which most of the BSA (> 70%) was released in its intact form. Furthermore, it was demonstrated that the release rate of BSA from the microspheres could be tuned by varying the blend ratio of the polymers used. These polymers differed in the ratio of the amorphous and semi-crystalline block, the molecular weight of the amorphous block, and the molecular weight of PEG in the amorphous block. These parameters together determined the total PEG content in the multi-block copolymer, which was also different for both polymers. This shows that the multi-block copolymers offer endless possibilities in varying their composition, which enables tailoring of the degradation rate and release of the (model) antigen from the formulation.

7.1.3 Choice of formulation type and production method

Besides different model antigens and polymers, multiple formulation types and production methods have been explored in this thesis in the search of an ideal single-administration vaccine formulation. In chapter 3, PLGA- and PDLLA-based polymer compacts were developed that exhibited a (biphasic or delayed) pulsatile release profile of the model compounds theophylline and BD. These compacts were based on a study by Murakami et al., in which PLGA-based mini-depot compacts (1.3, 3, and 5 mm diameter)

were prepared by compression of PLGA nanoparticles and theophylline [18]. The mini-depot compacts were intended to be used as an implantable depot and exhibited a biphasic pulsatile release profile. As the mechanism behind the biphasic pulsatile release from these compacts was not fully clear and the preparation of nanoparticles used for the compaction process was rather complex, we prepared similar compacts by direct compaction of a physical mixture of the freeze-dried model compound (theophylline or BD) and the ground polymer (PLGA or PDLLA). In addition, core-shell compacts were prepared that consisted of a core containing theophylline and a PDLLA shell. The physically mixed compacts exhibited the desired biphasic pulsatile release profile, and the core-shell compacts exhibited a delayed pulsatile release profile. Direct compaction offers several advantages over other production methods, for example the fact that it is a relatively simple, one- or two-step step method and that no organic solvent is used [17]. For most compacts, no heating was used either, though an additional heating step after the compaction procedure was required for the core-shell compacts composed of PDLLA (0.5 dL/g) to obtain a delayed pulsatile release. In this study, however, rather large compacts were obtained (physically mixed compacts: 6 x 2 x 2 mm, core-shell compacts: 9 x 5 x 5 mm). Due to this larger size, the compacts were not injectable but required surgical insertion. The formulations were therefore not suitable for clinical application and only served as a prototype.

Miniaturization of the core-shell polymer compacts might be possible using hot melt extrusion (HME) [46], which is a common technique for the production of injectable implants. Such implants are usually prepared in the form of small rods with an outer diameter small enough to be injected with a thin, high-gauge hypodermic needle. Most vaccines are administered with a 22 to 25G needle (outer diameter of 711 to 508 μm) [47], and although examples exist of drug formulations that are administered with a needle as large as 14G (outer diameter of 2.108 mm) [48], this is probably too painful for the vaccinee to be used in clinical practice [49,50]. We consider an 18G hypodermic needle (inner diameter of 838 μm) to be the maximum size for clinical application, which means that the implants should have a maximum outer diameter of approximately 700 μm. HME has shown to be capable of producing monolithic implants with an outer diameter of 700 μm or less, for instance the currently marketed PLGA-based Ozurdex implant for intravitreal application, which has an outer diameter of 460 mm [51]. Yet, it is unknown if this is also possible for core-shell implants, as a more complex extrusion setup is required to obtain a core-shell structure. For example, a co-extrusion die can be used to produce implants that consist of a polymeric core containing the (model) antigen surrounded by a polymeric shell [52,53]. It is, however, also possible to use commercially available tubular extrusions that are composed of a biocompatible and biodegradable polymer, for instance those manufactured by Zeus Industrial Products, Inc. [54]. In a study by Beugeling et al., such commercially available microtubes composed of PLGA were used in the development of a single-injection vaccine formulation [19]. These microtubes were non-porous and had an outer diameter of approximately 700 μm. As expected, the microtubes filled with the model drug aminophylline exhibited a delayed pulsatile release profile with a lag time of 3.5 weeks. In the preformulation and early formulation stage of the development, such microtubes can also be prepared manually. For example, immersing a needle into a polymer solution and withdrawing

7

it at a controlled rate might result in a thin, uniform coating around the needle. This process, often referred to as dip coating, can be repeated multiple times to obtain the desired coating thickness [55]. After immersion, the organic solvent is extracted and the microtubes are dried to solidify the polymer. This also gives more freedom in the choice of polymer the microtube is composed of. The disadvantage of both microtubes and co-extruded implants is, however, the fact that an extra closing step is required to prevent immediate release of the incorporated (model) antigen from the ends of the implants. In the study with the PLGA microtubes, the ends were closed with a viscous mixture of PLGA and acetone, which was manually formed as a bulb-shaped plug around the microtube (data not shown). This increased the outer diameter of the microtubes, which disabled injection with an 18G needle. An alternative method for closing the microtubes is therefore necessary, for instance the use of micro-molding to prepare a polymeric plug that fits into the microtubes. Miniaturization of the polymer compacts, however, was not attempted in this thesis, as the development of injectable microspheres seemed to be more promising than miniaturization of the compacts, and therefore gained the full attention in the remainder of the thesis.

In chapters 4 to 6, microspheres were developed as a potential single-administration vaccine formulation. For microspheres intended as a controlled-release vaccine formulation, the size is of great importance as well. First of all, the microspheres have to be administered with a subcutaneous or intramuscular injection, which means that the particles should be small enough to go through a thin hypodermic needle [56]. To minimize the risk of needle blockages, the size of the microspheres should be well below the inner diameter of the needle. For spherical particles in dry granular flow tests, the orifice-to-particle size ratio should be at least 6 to reduce the clogging probability to zero [57], though this ratio can probably be lower when the microspheres are administered in a carboxymethyl cellulose (CMC) solution. Also, the clogging probability depends to a great extent on the concentration of the microspheres in the CMC solution [58]. Nevertheless, we aimed at a particle size of < 50 μm to ensure that the microspheres could be administered with a 22 to 25G needle (inner diameter of 394 to 241 μm). In addition, particles < 20 μm will be phagocytosed prematurely by immune cells or other cells, which is undesired [59]. All microsphere formulations prepared in this thesis had a median particle diameter of 30 to 50 μm and thus fulfilled the requirements. Not only the particle size but also the particle size distribution greatly influences the injectability of the microspheres. A broad particle size distribution can impair the injection, even if the median diameter of the microspheres is small. The particle size distribution, which is expressed as the coefficient of variation (CV), depends on the applied production method. The maximum acceptable CV value is often chosen arbitrarily, as it is determined by several factors, such as the intended application and needle size. For the core-shell microspheres in chapter 4, we aimed at CV values of < 10%, as one of the objectives was to investigate the influence of the shell thickness of the microspheres on the *in vitro* release profile. Monodisperse microspheres with shells of uniform thickness were therefore desired. Highly monodisperse particles with CV values of < 10% could indeed be generated using droplet microfluidics, as the emulsion that ultimately formed the microspheres was produced drop by drop instead of in bulk. In chapters 5 and 6, we aimed at CV values of < 30%, as the particle size distribution

was less important in these studies. Replacement of the first microfluidic chip with the flow-through ultrasonic cell somewhat affected the particle size distribution, as for some formulations, CV values increased from < 10% to up to 20% (chapter 5). The CV values were, however, the highest (20 to 30%) with the membrane emulsification method (chapter 6), as the double emulsion was no longer produced drop by drop. It should be noted that in this thesis, two different methods were used for the determination of the particle size. In chapters 4 and 5, light microscopy combined with ImageJ software was used to measure each particle individually due to limited amount of sample, while the size of the microspheres in chapter 6 was measured with laser diffraction analysis. Laser diffraction analysis is in general a more reliable method than manual measurement as a significantly larger number of particles are analyzed (20000 vs. 20 or 50). Nevertheless, in all chapters, scanning electron microscopy (SEM) images demonstrate (rather) uniformly sized particles, and all measured d90 values were well below the maximum particle size of 100 µm. Also, the monolithic microspheres with CV values of 20 to 30% could easily be administered to mice using a 23G needle. It is therefore expected that all developed formulations were suitable for injection with a thin, high-gauge needle.

In order to obtain a delayed pulsatile or a sustained release profile, core-shell and monolithic microspheres were prepared, respectively. For the compacts, the core-shell concept was also applied to obtain a delayed pulsatile release profile. In addition, the physical mixture concept was applied to the compacts. Though these compacts can be regarded as a monolithic formulation as well, a biphasic pulsatile release profile instead of a sustained release profile was obtained as a porous compact was prepared from a polymer with a T_g when moisturized below body temperature. Upon incubation in release medium at 37 °C, one part of the incorporated model compound was immediately released by diffusion through the pores of the compact, but further release was inhibited as the pores closed due to viscous flow of the polymer, because it transitioned to the rubbery state. This resulted in a lag phase, after which the remaining model compound was released as a pulse due to rupture of the compact resulting from degradation of the polymer [60].

Both internal structures (core-shell and monolithic) have their advantages and disadvantages. First of all, core-shell microspheres are known to offer some advantages over monolithic microspheres in terms of particle characteristics. Multiple studies have shown that higher EE values could be obtained with core-shell microspheres than with monolithic microspheres as described in chapter 2 [61-65]. In this thesis, high EE values of up to 99% could indeed obtained for the core-shell microspheres prepared in chapter 4, though the formulation with the highest shell thickness (7.4 µm) had an EE of only 23%. This could probably be ascribed to the relatively thick shell of these microspheres, which caused slow solidification of the polymeric shells and thus facilitated the diffusion of BSA out of the cores during production. The same phenomenon was observed for the core-shell microspheres prepared in chapter 5, which all had a negligible EE, as the production settings applied in this chapter only yielded microspheres with a shell thickness > 7.4 µm. Apparently, core-shell microspheres do not always exhibit high EE values, but optimization of the production settings might lead to EE values of > 80%. Moreover, the monolithic microspheres prepared in chapter 6 had a high EE (> 85%) as well. This could be attributed to the appropriate settings for several formulation and

production parameters and to the choice of polymer. Regarding the formulation and production parameters, a sufficiently high molecular weight of the polymers, polymer concentration, and polymer solution to BSA solution ratio [66-68], and the addition of NaCl to the continuous phase [69] probably contributed to these high EE values. Regarding the choice of polymer, we selected a polymer blend that is swellable enough to allow diffusion of BSA out of the microspheres within approximately six weeks of *in vitro* release, but not too swellable to cause BSA to immediately diffuse out during microsphere production. Besides EE, a core-shell structure might offer improved control over the release kinetics of the encapsulated (model) antigen, as it is possible to independently tune the composition and dimensions of the core and shell phase. For instance, if a surface-eroding polymer is used for the shell phase, it might be possible to tune the lag time by simply varying the shell thickness [70,71]. The initial burst release, defined as the percentage of antigen released after one day, is often also lower for core-shell microspheres than for monolithic microspheres, as the shell layer presents a diffusion barrier to the antigen in the core (chapter 2) [61,72,73]. For the BSA-loaded core-shell microspheres prepared in chapter 4, the initial burst release was indeed low (0 to 3%), though one formulation showed a burst release of 14%. This could probably be attributed to the thin shells of these particles, as some fractured particles were visible on SEM images, causing premature release of BSA. Nonetheless, the initial burst release was also low for the monolithic microspheres prepared in chapter 6 (1 to 6%). A non-porous surface, small internal pores, and a homogeneous drug distribution as observed on SEM images probably contributed to this low initial burst release [74].

A great disadvantage of a core-shell formulation in general is the fact that it exhibits a delayed pulsatile release profile, and thus, only serves as the booster dose. Therefore, the addition of the prime dose is always required to obtain a biphasic pulsatile release profile. For compacts or implants, a thin rapidly dissolving coating containing the (model) antigen could be applied onto the outer surface of the formulation to obtain an immediate release of the prime dose. As an alternative, a rapidly dissolving implant containing the (model) antigen could be injected together with the controlled-release implant by placing it in the same needle. For microspheres, a separate immediate-release formulation of the (model) antigen could be injected together with the microspheres. This is preferably a formulation of the antigen in the dry state that is stable at ambient conditions, for instance the antigen dried with a stabilizing sugar [75-77]. The microspheres can be mixed with the dried antigen powder, which can be suspended in a CMC solution just before injection. In these ways, for both implants and microspheres, the prime and booster dose can be administered together in one injection and cold chain storage and transportation is not needed as the primer is in the dry state as well. Furthermore, core-shell formulations usually require more complex production methods. For the core-shell compacts, a two-step compaction procedure was required instead of a one-step procedure for the physically mixed compacts. The same counts for the injectable implants described above. HME has proven its capability of producing monolithic implants, which only requires the preparation and subsequent extrusion of a mixture of the (model) antigen and the polymer [46]. For the core-shell implants, on the other hand, a more complex co-extrusion method is required to obtain a shell layer around the core phase [52,53,78]. It is also possible to purchase or produce microtubes and fill these with the (model) antigen,

though this may be too laborious for large-scale production. Nonetheless, in both cases, an additional step to close the ends of the implants is needed to obtain a delayed pulsatile release profile. Monolithic microspheres are generally also easier to produce than core-shell microspheres. For a water-soluble (model) antigen such as BSA, an aqueous solution of the (model) antigen can be emulsified with a solution of the polymer in an organic solvent using, for instance, high-speed or ultrasonic homogenization [79]. Subsequently, the prepared emulsion should be formed into microspheres, for instance using a single microfluidic chip or using the membrane-assisted emulsification method as explained in chapter 6. These are rather straightforward and robust methods that do not require a lot of fine-tuning. For the production of the core-shell microspheres, the same methods could be applied, but the formation of a core-shell structure would then rely on coalescence of the inner water droplets. In this thesis, for instance, a primary water-in-oil emulsion of BSA solution in PLGA solution was prepared inline (using a microfluidic chip with a hydrophobic surface as in chapter 4 or a flow-through ultrasonic cell as in chapter 5). The obtained primary emulsion was pumped into a microfluidic chip with a hydrophilic surface to generate a water-in-oil-in-water double emulsion that formed the basis for the desired core-shell structure. The inner water droplets became close-packed upon collection of the microspheres and coalesced during freeze-drying, thereby forming a single core. It is, however, unknown whether coalescence will also take place when other polymers than low molecular weight PL(G)A are used. If this is not the case, the setup from chapter 4 with two microfluidic chips placed in series could be used to produce microspheres that contain exactly one (large) inner water droplet instead of multiple small inner water droplets. However, this is very difficult to achieve as small fluctuations in flow cannot completely be avoided (chapter 2). In addition, droplet microfluidics has the disadvantage of a low production speed, with microspheres being produced at a throughput of approximately 50-300 mg/h with a single microfluidic junction [80]. The production can be scaled up by placing multiple microfluidic chips in parallel that operate with a minimum number of pumps [80,81]. Large-scale production of solid lipid nanoparticles using microfluidics has, for instance, proven to be possible for the mRNA-based COVID-19 vaccines [82,83], but these particles did not possess a core-shell structure. It might therefore be necessary to explore other production techniques for core-shell microspheres as well. As described in chapter 3, coaxial electrospraying and precision particle fabrication seem to be promising methods as both are continuous processes that generate particles with a narrow particle size distribution and, generally, a high EE. Moreover, the production speed of both methods is much higher than with a single microfluidic chip and a wide variety of materials can be used.

Altogether, it can be concluded that both implants and microspheres can be used as a single-administration vaccine formulation. Microspheres have the advantage that they can usually be administered with a thinner needle than implants, and that monolithic microspheres can be produced with several commonly used and/or robust methods, such as the method described in chapter 6. Moreover, the monolithic microspheres prepared in chapter 6 already show a great potential as a single-administration vaccine, as high BSA-specific IgG antibody titers were induced in mice that received a subcutaneous injection of the six-weeks sustained-release formulation. The induced antibody titers were even similar to those measured in mice that received a prime-boost injection of BSA

7

in PBS administered at 0 and 3 weeks. This suggests that monolithic microspheres might be a good alternative to the current multiple-injection vaccination schedule. Production of core-shell microspheres is more difficult, but several options exist that are worth exploring.

7.2 Directions for further research

In this thesis, several promising formulations have been developed that could contribute to the development of a single-administration vaccine. A (biphasic or delayed) pulsatile release of a polysaccharide-based model antigen (BD) and a protein-based model antigen (BSA) could successfully be obtained with the physically mixed polymer compacts and the core-shell microspheres, respectively. A sustained release of a protein-based model antigen (BSA) could be obtained with the monolithic microspheres. However, the physically mixed polymer compacts were not suitable for protein-based antigens and were not injectable. With the core-shell microspheres, a complete release of a protein-based model antigen could not be achieved as well, and these microspheres were only able to administer the booster dose. The full development of an injectable formulation that exhibits a complete, biphasic pulsatile release of a protein-based, clinically relevant antigen is therefore still required. Ultimately, the performance of the developed formulation should be evaluated *in vivo* in a relevant animal model and compared with a sustained-release single-administration vaccine formulation in terms of immune responses. In such a study, both formulations should be compared with the currently applied multiple-injection regimen as well.

7.2.1 Production of core-shell microspheres or implants exhibiting a complete pulsatile release of a protein-based (model) antigen

For the core-shell microspheres, PLGA should be replaced by other polymers, e.g. the phase-separated multi-block copolymers used in chapter 6, to obtain a complete pulsatile release of a protein-based (model) antigen. Due to PLGA-related stability issues, only 30 to 60% of BSA was released from the core-shell microspheres prepared in chapter 4. It is expected that the release completeness can be improved if a polymer is used that is better compatible with proteins than PLGA. It is, however, unknown whether microspheres with a core-shell structure can be obtained with the same production method as used in chapter 4, as the formation of a core-shell structure relied on the coalescence of the inner water droplets. Coalescence might not take place when PLGA is replaced by another polymer, as this might increase the viscosity of the polymer phase and reduce the interfacial tension between the polymer and water phase, thereby stabilizing the inner water droplets [84]. The viscosity could probably be tuned by lowering the polymer concentration, but it is unknown to which extent this will aid in the coalescence of the inner water droplets. The same applies to the production method applied in chapter 5, though in this study, a flow-through ultrasonic cell was used for the emulsification of the inner water phase containing the model antigen and the oil phase containing the polymer. With this adjustment, channel blockages were prevented, and higher production rates could be obtained. Incorporation of a model antigen, however, did not succeed due to increased shell thickness, which caused BSA to diffuse out of

the microspheres. Nonetheless, this production method is worth further investigating for the preparation of core-shell microspheres. A combination of a sufficiently low polymer concentration and a sufficiently low flow rate ratio of the shell and core phase might reduce the shell thickness and, thereby, improve the EE. The last option is using a completely different production method. Examples are coaxial electrospraying or precision particle fabrication as previously described, but fluidized bed coating is an option as well. With fluidized bed coating, a thin polymeric coating can be applied onto solid (polymeric) cores containing the (model) antigen, though this technique is usually only suitable for cores larger than 100 µm [85,86]. In this case, the cores should be highly water-soluble and/or porous to obtain a pulsatile release instead of a sustained release after the lag phase.

As an alternative to the core-shell microspheres, core-shell implants could be prepared using co-extrusion. A co-extrusion die allows the simultaneous processing of two different polymers through separate coaxial channels [52,53,78]. In contrast to compaction, the core phase must consist of a polymer containing the (model) antigen as the (model) antigen itself cannot be extruded. Yet, even the most thermostable vaccines, such as tetanus and diphtheria toxoid, lose potency after only a few hours when subjected to temperatures > 60 °C [3], though it is unknown whether they do remain intact when the exposure is only short (i.e. during extrusion). Repka et al. showed that the thermally unstable drug hydrocortisone remained intact upon incorporation into hydroxypropylcellulose films using hot-melt extrusion at 170 °C when the residence time of the material in the extruder was less than 2 minutes [87]. Nevertheless, the (model) antigen should preferably be extruded at relatively low temperatures, which means that a polymer with a relatively low melting temperature (T_m) (or T_g in case of a fully amorphous polymer) should be used for the core phase. In addition, the polymer should be highly swellable and fast releasing to obtain a pulsatile release. Examples of such polymers are PEG, polyethylene oxide (PEO) [88], and multi-block copolymers with a high PEG content, though the temperature required for extrusion of PEG and PEO depends on their molecular weight [89]. The (model) antigen of interest can be spray-dried with a stabilizing excipient and mixed with the polymer before extrusion. For the shell layer, the T_m or T_g of the polymer is less important as the shell layer is physically separated from the core layer containing the (model) antigen. Also, the barrel temperatures of the core and the shell phase can be regulated independently [78], which means that a higher extrusion temperature can be used for the shell phase than for the core phase, thereby preventing that the structural integrity of the incorporated (model) antigen is compromised. Both the core and shell phase do, however, need to flow through the die under the same temperature conditions [52,88]. Altogether, PLGA as shell material might still be an option, even though it requires a high extrusion temperature (> 90 °C) [90]. The lactide:glycolide molar ratio, molecular weight, and end-capping of PLGA can be selected based on the desired degradation rate and, thereby, lag time. It is, however, also possible to use different types of polymers, such as the phase-separated multi-block copolymers, preferably those that require relatively low extrusion temperatures. Another upcoming method for the production of polymeric implants is 3D-printing. This technique allows for the production of controlled-release implants in various shapes and sizes using a wide variety of polymers [91]. Injectable rods with a

7

core-shell structure have also been prepared with the method [92], but it is unknown whether this method can be applied to different polymers such as the PEG-based multi-block copolymers as well.

7.2.2 Incorporation of clinically relevant antigens

Obviously, the developed formulations that showed the most promising results as a single-administration vaccine should be tested with clinically relevant antigens instead of model antigens. Several different types of vaccines exist, which can roughly be divided into live attenuated pathogens, inactivated pathogens, subunits, polysaccharides and polysaccharide protein conjugates, toxoids, mRNA, and viral vectors [93,94]. Starting with a subunit or toxoid antigen would be preferred, as these are the most investigated antigens for single-administration vaccine formulations [1]. For example, the hepatitis B surface antigen (24 kDa) could be incorporated, as this antigen has previously been used in numerous studies on single-administration vaccines [95,96] and has shown to be rather stable, even at slightly acidic pH (5-6) and elevated temperatures (37 °C) [3,13]. In addition, this vaccine is currently administered as a three-dose series, with the second and third dose administered at one and six months after the first dose, respectively [95]. This means that pulsatile-release formulations are envisaged with a pulse after a lag time of one month and six months, which should be possible with, for example, the PDO-based multi-block copolymers. For the sustained-release formulations, the target release duration is six months as well, though it should be examined if this is indeed the ideal release duration. Tetanus and diphtheria toxoid (150 and 62 kDa [97], respectively) have been extensively studied as well, as toxoids are among the most thermostable antigens used in vaccines [1], with no significant loss of potency after exposure to 37 °C for several weeks [3]. Both toxoids are usually injected as part of a five-dose multivalent DTaP vaccine being administered at the ages of 2, 4, 6, 15-18 months, and 4-6 years [98]. It might be possible to combine at least the first three doses into a single-injection vaccine formulation, which means that the formulation should exhibit a pulsatile release profile with a pulse after two and four months or a sustained release profile with a release duration of approximately four months. With the PDO-based multi-block copolymers used in this thesis, 20[PCL-PEG$_{3000}$-PCL]-80[PDO] and 50[PCL-PEG$_{1000}$-PCL]-50[PDO], a total release duration of approximately four to nine weeks could be obtained for BSA. The release rate decreased with an increasing weight fraction of 50[PCL-PEG$_{1000}$-PCL]-50[PDO] in the polymer blend, as this polymer consisted of PEG blocks with a lower molecular weight. Hence, this polymer absorbed less water, resulting in a lower swelling degree and a slower release. Therefore, the release could probably be prolonged by using only this polymer (i.e. not blended with 20[PCL-PEG$_{3000}$-PCL]-80[PDO]). A further prolongation of the release might be achieved by making small adjustments to the multi-block copolymer 50[PCL-PEG$_{1000}$-PCL]-50[PDO], such as reducing the weight percentage of the amorphous PCL-PEG-PCL block or the PEG molecular weight, or a combination of both. For the core-shell microspheres, using a surface-eroding polymer such as a poly(ortho ester) might be a good strategy [70,71]. These polymers degrade from the surface in contrast to bulk-degrading polymers that degrade throughout the whole microsphere. Degradation products, therefore, do not accumulate within the microspheres and it might be possible to tune the lag time by varying the shell thickness.

7.2.3 In vivo *immune response study to compare pulsatile- and sustained-release formulations*
In vivo immune response studies should be performed with the developed formulations to directly compare the pulsatile-release and sustained-release formulations in appropriate animal models. In addition, the formulations must be compared with the currently applied multiple-injection regimen to determine whether they can actually be a viable alternative for vaccines requiring multiple doses. To mimic the prime-boost regimen, the core-shell microspheres exhibiting a delayed pulsatile release should be injected together with a separate immediate-release formulation of the antigen that serves as the prime dose. This immediate-release formulation of the antigen should ideally be in the dry state. To gain more insight into the induced immune responses, determination of IgG subclasses and cellular immune responses is recommended in addition to total IgG. The protective efficacy of immunization with the single-administration vaccine formulations could be assessed by challenging the animals with a lethal dose of the pathogen in question and monitoring the animals for disease severity and/or survival rate.

References

[1]   K. J. McHugh, R. Guarecuco, R. Langer, and A. Jaklenec, "Single-injection vaccines: Progress, challenges, and opportunities," J. Control. Release, vol. 219, pp. 596–609, 2015.

[2]   D. T. Brandau, L. S. Jones, C. M. Wiethoff, J. Rexroad, and C. R. Middaugh, "Thermal Stability of Vaccines," J. Pharm. Sci., vol. 92, no. 2, pp. 218–231, 2003.

[3]   A. Galazka, J. Milstien, and M. Zaffran, "Thermostability of vaccines: global programme for vaccines and immunization," World Heal. Organ. Geneva, vol. 64, 1998.

[4]   M. N. Uddin and M. A. Roni, "Challenges of Storage and Stability of mRNA-Based COVID-19 Vaccines," Vaccines, vol. 9, no. 9. 2021.

[5]   M. Akbarian and S.-H. Chen, "Instability Challenges and Stabilization Strategies of Pharmaceutical Proteins," Pharmaceutics, vol. 14, no. 11. 2022.

[6]   R. Guarecuco et al., "Immunogenicity of pulsatile-release PLGA microspheres for single-injection vaccination," Vaccine, 2017.

[7]   M. Igartua, R. M. Hernández, A. Esquisabel, A. R. Gascón, M. B. Calvo, and J. L. Pedraz, "Enhanced immune response after subcutaneous and oral immunization with biodegradable PLGA microspheres," J. Control. Release, vol. 56, no. 1, pp. 63–73, 1998.

[8]   B. R. Conway, J. E. Eyles, and H. O. Alpar, "A comparative study on the immune responses to antigens in PLA and PHB microspheres," J. Control. Release, vol. 49, no. 1, pp. 1–9, 1997.

[9]   K. Amssoms et al., "Ovalbumin-containing core-shell implants suitable to obtain a delayed IgG1 antibody response in support of a biphasic pulsatile release profile in mice," PLoS One, vol. 13, no. 8, p. e0202961, Aug. 2018.

[10]   B. A. Bailey, K.-G. H. Desai, L. J. Ochyl, S. M. Ciotti, J. J. Moon, and S. P. Schwendeman, "Self-encapsulating Poly(lactic-co-glycolic acid) (PLGA) Microspheres for Intranasal Vaccine Delivery," Mol. Pharm., vol. 14, no. 9, pp. 3228–3237, Sep. 2017.

7

[11]   G. Du et al., "Intradermal vaccination with hollow microneedles: A comparative study of various protein antigen and adjuvant encapsulated nanoparticles," J. Control. Release, vol. 266, pp. 109–118, 2017.

[12]   B. A. Bailey, L. J. Ochyl, S. P. Schwendeman, and J. J. Moon, "Toward a Single-Dose Vaccination Strategy with Self-Encapsulating PLGA Microspheres," Adv. Healthc. Mater., vol. 6, no. 12, p. 1601418, Jun. 2017.

[13]   L. Shi, M. J. Caulfield, R. T. Chern, R. A. Wilson, G. Sanyal, and D. B. Volkin, "Pharmaceutical and immunological evaluation of a single-shot hepatitis B vaccine formulated with PLGA microspheres," J. Pharm. Sci., vol. 91, no. 4, pp. 1019–1035, Apr. 2002.

[14]   A. Weintraub, "Immunology of bacterial polysaccharide antigens," Carbohydr. Res., vol. 338, no. 23, pp. 2539–2547, 2003.

[15]   H. K. Makadia and S. J. Siegel, "Poly Lactic-co-Glycolic Acid (PLGA) as Biodegradable Controlled Drug Delivery Carrier," Polymers (Basel)., vol. 3, no. 3, pp. 1377–1397, Sep. 2011.

[16]   K. Fu, D. W. Pack, A. M. Klibanov, and R. Langer, "Visual Evidence of Acidic Environment Within Degrading Poly(lactic-co-glycolic acid) (PLGA) Microspheres," Pharm. Res., vol. 17, no. 1, pp. 100–106, 2000.

[17]   M. van de Weert, W. E. Hennink, and W. Jiskoot, "Protein Instability in Poly(Lactic-co-Glycolic Acid) Microparticles," Pharm. Res., vol. 17, no. 10, pp. 1159–1167, 2000.

[18]   H. Murakami, M. Kobayashi, H. Takeuchi, and Y. Kawashima, "Utilization of poly(dl-lactide-co-glycolide) nanoparticles for preparation of mini-depot tablets by direct compression," J. Control. Release, vol. 67, no. 1, pp. 29–36, 2000.

[19]   M. Beugeling et al., "Development of a Stable Respiratory Syncytial Virus Pre-Fusion Protein Powder Suitable for a Core-Shell Implant with a Delayed Release in Mice: A Proof of Concept Study," Pharmaceutics, vol. 11, no. 10. Department of Pharmaceutical Technology and Biopharmacy, University of Groningen, Antonius Deusinglaan 1, 9713 AV Groningen, The Netherlands. m.beugeling@rug.nl., 2019.

[20]   K. Park et al., "Injectable, long-acting PLGA formulations: Analyzing PLGA and understanding microparticle formation," J. Control. Release, vol. 304, pp. 125–134, 2019.

[21]   L. Duque, M. Körber, and R. Bodmeier, "Improving release completeness from PLGA-based implants for the acid-labile model protein ovalbumin," Int. J. Pharm., vol. 538, no. 1, pp. 139–146, 2018.

[22]   Z. Ghalanbor, M. Körber, and R. Bodmeier, "Interdependency of protein-release completeness and polymer degradation in PLGA-based implants," Eur. J. Pharm. Biopharm., vol. 85, no. 3, Part A, pp. 624–630, 2013.

[23]   A. Giteau, M. C. Venier-Julienne, A. Aubert-Pouëssel, and J. P. Benoit, "How to achieve sustained and complete protein release from PLGA-based microparticles?," Int. J. Pharm., vol. 350, no. 1, pp. 14–26, 2008.

[24]   K. Fu, A. M. Klibanov, and R. Langer, "Protein stability in controlled-release systems," Nat. Biotechnol., vol. 18, no. 1, pp. 24–25, 2000.

[25]   J. L. Cleland, M. F. Powell, and S. J. Shire, "The development of stable protein

formulations: a close look at protein aggregation, deamidation, and oxidation," Crit. Rev. Ther. Drug Carrier Syst., vol. 10, no. 4, pp. 307–377, 1993.

[26]   Y. Liu and S. P. Schwendeman, "Mapping Microclimate pH Distribution inside Protein-Encapsulated PLGA Microspheres Using Confocal Laser Scanning Microscopy," Mol. Pharm., vol. 9, no. 5, pp. 1342–1350, May 2012.

[27]   M. L. Houchin and E. M. Topp, "Chemical Degradation of Peptides and Proteins in PLGA: A Review of Reactions and Mechanisms," J. Pharm. Sci., vol. 97, no. 7, pp. 2395–2404, 2008.

[28]   S. Mohammadi-Samani and B. Taghipour, "PLGA micro and nanoparticles in delivery of peptides and proteins; problems and approaches," Pharm. Dev. Technol., vol. 20, no. 4, pp. 385–393, May 2015.

[29]   X. Li, Z. Zhang, A. Harris, and L. Yang, "Bridging the gap between fundamental research and product development of long acting injectable PLGA microspheres," Expert Opin. Drug Deliv., vol. 19, no. 10, pp. 1247–1264, Oct. 2022.

[30]   T. Estey, J. Kang, S. P. Schwendeman, and J. F. Carpenter, "BSA Degradation Under Acidic Conditions: A Model For Protein Instability During Release From PLGA Delivery Systems," J. Pharm. Sci., vol. 95, no. 7, pp. 1626–1639, 2006.

[31]   L. R. Brown, "Commercial challenges of protein drug delivery," Expert Opin. Drug Deliv., vol. 2, no. 1, pp. 29–42, Jan. 2005.

[32]   W. Jiang, R. K. Gupta, M. C. Deshpande, and S. P. Schwendeman, "Biodegradable poly(lactic-co-glycolic acid) microparticles for injectable delivery of vaccine antigens," Adv. Drug Deliv. Rev., vol. 57, no. 3, pp. 391–410, 2005.

[33]   S. P. Schwendeman, R. B. Shah, B. A. Bailey, and A. S. Schwendeman, "Injectable controlled release depots for large molecules," J. Control. Release, vol. 190, pp. 240–253, 2014.

[34]   T. Li et al., "Characterization of attributes and in vitro performance of exenatide-loaded PLGA long-acting release microspheres," Eur. J. Pharm. Biopharm., vol. 158, pp. 401–409, 2021.

[35]   L. (Lucy) Chang and M. J. Pikal, "Mechanisms of protein stabilization in the solid state," J. Pharm. Sci., vol. 98, no. 9, pp. 2886–2908, Sep. 2009.

[36]   G. Zhu, S. R. Mallery, and S. P. Schwendeman, "Stabilization of proteins encapsulated in injectable poly (lactide- co-glycolide)," Nat. Biotechnol., vol. 18, no. 1, pp. 52–57, 2000.

[37]   J. Kang and S. P. Schwendeman, "Comparison of the effects of Mg(OH)2 and sucrose on the stability of bovine serum albumin encapsulated in injectable poly(d,l-lactide-co-glycolide) implants," Biomaterials, vol. 23, no. 1, pp. 239–245, 2002.

[38]   W. Wang, "Lyophilization and development of solid protein pharmaceuticals," Int. J. Pharm., vol. 203, no. 1, pp. 1–60, 2000.

[39]   H. Haitjema, R. Steendam, C. Hiemstra, J. Zuidema, A. Doornbos, and T. Nguyen, "Biodegradable, phase separated, thermoplastic multi-block copolymer," PCT Patent No. WO 2021/066650 A1, 2021.

[40]   M. Stanković et al., "Low temperature extruded implants based on novel

7

hydrophilic multiblock copolymer for long-term protein delivery," Eur. J. Pharm. Sci., vol. 49, no. 4, pp. 578–587, 2013.

[41]   N. Teekamp et al., "Polymeric microspheres for the sustained release of a protein-based drug carrier targeting the PDGFβ-receptor in the fibrotic kidney," Int. J. Pharm., vol. 534, no. 1, pp. 229–236, 2017.

[42]   K. C. Scheiner et al., "Sustained Release of Vascular Endothelial Growth Factor from Poly(ε-caprolactone-PEG-ε-caprolactone)-b-Poly(l-lactide) Multiblock Copolymer Microspheres," ACS Omega, vol. 4, no. 7, pp. 11481–11492, Jul. 2019.

[43]   S. Fredenberg, M. Wahlgren, M. Reslow, and A. Axelsson, "The mechanisms of drug release in poly(lactic-co-glycolic acid)-based drug delivery systems--a review.," Int. J. Pharm., vol. 415, no. 1–2, pp. 34–52, 2011.

[44]   J. C. Middleton and A. J. Tipton, "Synthetic biodegradable polymers as orthopedic devices," Biomaterials, vol. 21, no. 23, pp. 2335–2346, 2000.

[45]   S. Heene et al., "Vascular Network Formation on Macroporous Polydioxanone Scaffolds," Tissue Eng. Part A, vol. 27, no. 19–20, pp. 1239–1249, Jan. 2021.

[46]   M. Stanković, H. W. Frijlink, and W. L. J. Hinrichs, "Polymeric formulations for drug release prepared by hot melt extrusion: application and characterization," Drug Discov. Today, vol. 20, no. 7, pp. 812–823, 2015.

[47]   Centers for Disease Control and Prevention (CDC), "Vaccine Administration - General Best Practice Guidelines for Immunization: Best Practices Guidance of the Advisory Committee on Immunization Practices (ACIP)," 2023. [Online]. Available: https://www.cdc.gov/vaccines/hcp/acip-recs/general-recs/administration.html. [Accessed: 09-Feb-2023].

[48]   Tersera Therapeutics, "ZOLADEX® (goserelin implant) 10.8 mg - Highlights of prescribing information," 2020. [Online]. Available: https://documents.tersera.com/zoladex-us/10.8mg_MagnumPI.pdf. [Accessed: 09-Feb-2023].

[49]   P. V Beirne, S. Hennessy, S. L. Cadogan, F. Shiely, T. Fitzgerald, and F. MacLeod, "Needle size for vaccination procedures in children and adolescents," Cochrane Database Syst. Rev., no. 6, 2015.

[50]   L. Arendt-Nielsen, H. Egekvist, and P. Bjerring, "Pain following controlled cutaneous insertion of needles with different diameters," Somatosens. Mot. Res., vol. 23, no. 1–2, pp. 37–43, Jan. 2006.

[51]   E. Lehner, D. Gündel, A. Liebau, S. Plontke, and K. Mäder, "Intracochlear PLGA based implants for dexamethasone release: Challenges and solutions," Int. J. Pharm. X, vol. 1, p. 100015, 2019.

[52]   A.-K. Vynckier, L. Dierickx, J. Voorspoels, Y. Gonnissen, J. P. Remon, and C. Vervaet, "Hot-melt co-extrusion: requirements, challenges and opportunities for pharmaceutical applications," J. Pharm. Pharmacol., vol. 66, no. 2, pp. 167–179, Feb. 2014.

[53]   S. Tambe, D. Jain, Y. Agarwal, and P. Amin, "Hot-melt extrusion: Highlighting recent advances in pharmaceutical applications," J. Drug Deliv. Sci. Technol., vol. 63, p. 102452, 2021.

[54]   Zeus Industrial Products Inc., "Tech Sheet - AbsorvTM Products," 2021. [Online]. Available: https://www.zeusinc.com/wp-content/uploads/2021/01/Absorv-Biomaterial-V2R2.pdf. [Accessed: 14-Feb-2023].

[55] N. Argarate et al., "Biodegradable Bi-layered coating on polymeric orthopaedic implants for controlled release of drugs," Mater. Lett., vol. 132, pp. 193–195, 2014.

[56] M. Ye, S. Kim, and K. Park, "Issues in long-term protein delivery using biodegradable microparticles," J. Control. Release, vol. 146, no. 2, pp. 241–260, 2010.

[57] A. Hafez, Q. Liu, T. Finkbeiner, R. A. Alouhali, T. E. Moellendick, and J. C. Santamarina, "The effect of particle shape on discharge and clogging," Sci. Rep., vol. 11, no. 1, p. 3309, 2021.

[58] M. Sarmadi et al., "Modeling, design, and machine learning-based framework for optimal injectability of microparticle-based drug formulations," Sci. Adv., vol. 6, no. 28, p. eabb6594, Feb. 2023.

[59] G. Lemperle, "Biocompatibility of Injectable Microspheres," Biomed. J. Sci. & Tech. Res., vol. 2, no. 1, pp. 2296–2306, 2018.

[60] I. Mylonaki, E. Allémann, F. Delie, and O. Jordan, "Imaging the porous structure in the core of degrading PLGA microparticles: The effect of molecular weight," J. Control. Release, vol. 286, pp. 231–239, 2018.

[61] A. Navaei, M. Rasoolian, A. Momeni, S. Emami, and M. Rafienia, "Double-walled microspheres loaded with meglumine antimoniate: preparation, characterization and in vitro release study.," Drug Dev. Ind. Pharm., vol. 40, no. 6, pp. 701–710, Jun. 2014.

[62] M. Zamani, M. P. Prabhakaran, E. S. Thian, and S. Ramakrishna, "Protein encapsulated core–shell structured particles prepared by coaxial electrospraying: Investigation on material and processing variables," Int. J. Pharm., vol. 473, no. 1–2, pp. 134–143, Oct. 2014.

[63] Y. Xia, Q. Xu, C. Wang, and D. W. Pack, "Protein Encapsulation in and Release from Monodisperse Double-Wall Polymer Microspheres," J. Pharm. Sci., vol. 102, no. 5, pp. 1601–1609, May 2013.

[64] S. Hiraoka, S. Uchida, and N. Namiki, "Preparation and Characterization of High-Content Aripiprazole-Loaded Core–Shell Structure Microsphere for Long-Release Injectable Formulation," Chem. Pharm. Bull., vol. 62, no. 7, pp. 654–660, 2014.

[65] J. Wu et al., "Fabrication and characterization of monodisperse PLGA–alginate core–shell microspheres with monodisperse size and homogeneous shells for controlled drug release," Acta Biomater., vol. 9, no. 7, pp. 7410–7419, Jul. 2013.

[66] R. Bodmeier and J. W. McGinity, "Solvent selection in the preparation of poly(dl-lactide) microspheres prepared by the solvent evaporation method," Int. J. Pharm., vol. 43, no. 1, pp. 179–186, 1988.

[67] H. Rafati, A. G. A. Coombes, J. Adler, J. Holland, and S. S. Davis, "Protein-loaded poly(dl-lactide-co-glycolide) microparticles for oral administration: formulation, structural and release characteristics," J. Control. Release, vol. 43, no. 1, pp. 89–102, 1997.

[68] S. Mao, J. Xu, C. Cai, O. Germershaus, A. Schaper, and T. Kissel, "Effect of WOW process parameters on morphology and burst release of FITC-dextran loaded PLGA microspheres," Int. J. Pharm., vol. 334, no. 1, pp. 137–148, 2007.

7

[69]   T. Arakawa and S. N. Timasheff, "Preferential interactions of proteins with salts in concentrated solutions," Biochemistry, vol. 21, no. 25, pp. 6545–6552, Dec. 1982.

[70]   P. Wuthrich, S. Y. Ng, B. K. Fritzinger, K. V Roskos, and J. Heller, "Pulsatile and delayed release of lysozyme from ointment-like poly(ortho esters)," J. Control. Release, vol. 21, no. 1, pp. 191–200, 1992.

[71]   S. Lyu and D. Untereker, "Degradability of Polymers for Implantable Biomedical Devices," International Journal of Molecular Sciences, vol. 10, no. 9. pp. 4033–4065, 2009.

[72]   W. Zheng, "A water-in-oil-in-oil-in-water (W/O/O/W) method for producing drug-releasing, double-walled microspheres," Int. J. Pharm., vol. 374, no. 1, pp. 90–95, 2009.

[73]   C.-D. Xiao, X.-C. Shen, and L. Tao, "Modified emulsion solvent evaporation method for fabricating core–shell microspheres," Int. J. Pharm., vol. 452, no. 1–2, pp. 227–232, Aug. 2013.

[74]   F. Qi et al., "Preparation of uniform-sized exenatide-loaded PLGA microspheres as long-effective release system with high encapsulation efficiency and bio-stability," Colloids Surfaces B Biointerfaces, vol. 112, pp. 492–498, 2013.

[75]   M. A. Mensink, H. W. Frijlink, K. van der Voort Maarschalk, and W. L. J. Hinrichs, "How sugars protect proteins in the solid state and during drying (review): Mechanisms of stabilization in relation to stress conditions," Eur. J. Pharm. Biopharm., vol. 114, pp. 288–295, 2017.

[76]   J.-P. Amorij, A. Huckriede, J. Wilschut, H. W. Frijlink, and W. L. J. Hinrichs, "Development of Stable Influenza Vaccine Powder Formulations: Challenges and Possibilities," Pharm. Res., vol. 25, no. 6, pp. 1256–1273, 2008.

[77]   W. F. Tonnis, J.-P. Amorij, M. A. Vreeman, H. W. Frijlink, G. F. Kersten, and W. L. J. Hinrichs, "Improved storage stability and immunogenicity of hepatitis B vaccine after spray-freeze drying in presence of sugars," Eur. J. Pharm. Sci., vol. 55, pp. 36–45, 2014.

[78]   D. Leister, K. Paulsen, I. Ruff, K. C. Schwan, S. Nunn, and M. Long, "Thermo Scientific Poster Note - Product Quality Control of a HME Co-Extrudate Using a Raman Imaging Microscope," 2015. [Online]. Available: https://tools. thermofisher.com/content/sfs/brochures/PN52687-EN-PITTCON2015-QC-of-HME-with-Extruders-and-Raman-imaging.pdf. [Accessed: 09-Feb-2023].

[79]   N. Teekamp, L. F. Duque, H. W. Frijlink, W. L. Hinrichs, and P. Olinga, "Production methods and stabilization strategies for polymer-based nanoparticles and microparticles for parenteral delivery of peptides and proteins," Expert Opin. Drug Deliv., vol. 12, no. April 2017, pp. 1–21, 2015.

[80]   F. Ramazani et al., "Strategies for encapsulation of small hydrophilic and amphiphilic drugs in PLGA microspheres: State-of-the-art and challenges," Int. J. Pharm., vol. 499, no. 1–2, pp. 358–367, 2016.

[81]   W. J. Duncanson, T. Lin, A. R. Abate, S. Seiffert, R. K. Shah, and D. A. Weitz, "Microfluidic synthesis of advanced microparticles for encapsulation and controlled release," Lab Chip, vol. 12, no. 12, pp. 2135–2145, 2012.

[82]   C. B. Roces et al., "Manufacturing Considerations for the Development of Lipid

Nanoparticles Using Microfluidics," Pharmaceutics, vol. 12, no. 11. 2020.

[83]   Y.-S. Lin, C.-M. Cheng, and C.-F. Chien, "How Smart Manufacturing Can Help Combat the COVID-19 Pandemic," Diagnostics, vol. 11, no. 5. 2021.

[84]   F. Y. Ushikubo and R. L. Cunha, "Stability mechanisms of liquid water-in-oil emulsions," Food Hydrocoll., vol. 34, pp. 145–153, 2014.

[85]   E. S. Nuwayser and W. A. Nucefora, "Composite core coated microparticles and process of preparing same," US Patent 4568559, 1984.

[86]   E. S. Nuwayser and W. A. Nucefora, "Controlled release composite core coated microparticles," US Patent 4623588, 1985.

[87]   M. A. Repka, T. G. Gerding, S. L. Repka, and J. W. McGinity, "Influence of Plasticizers and Drugs on the Physical-Mechanical Properties of Hydroxypropylcellulose Films Prepared by Hot Melt Extrusion," Drug Dev. Ind. Pharm., vol. 25, no. 5, pp. 625–633, Jan. 1999.

[88]   L. Dierickx, J. P. Remon, and C. Vervaet, "Co-extrusion as manufacturing technique for multilayer mini-matrices with dual drug release," Eur. J. Pharm. Biopharm., vol. 85, no. 3, Part B, pp. 1157–1163, 2013.

[89]   R. Paberit et al., "Cycling Stability of Poly(ethylene glycol) of Six Molecular Weights: Influence of Thermal Conditions for Energy Applications," ACS Appl. Energy Mater., vol. 3, no. 11, pp. 10578–10589, Nov. 2020.

[90]   Z. Ghalanbor, M. Körber, and R. Bodmeier, "Improved Lysozyme Stability and Release Properties of Poly(lactide-co-glycolide) Implants Prepared by Hot-Melt Extrusion," Pharm. Res., vol. 27, no. 2, pp. 371–379, 2010.

[91]   V. Domsta and A. Seidlitz, "3D-Printing of Drug-Eluting Implants: An Overview of the Current Developments Described in the Literature," Molecules, vol. 26, no. 13. 2021.

[92]   J. Y. Won et al., "3D printing of drug-loaded multi-shell rods for local delivery of bevacizumab and dexamethasone: A synergetic therapy for retinal vascular diseases," Acta Biomater., vol. 116, pp. 174–185, 2020.

[93]   D. Baxter, "Active and passive immunity, vaccine types, excipients and licensing," Occup. Med. (Chic. Ill)., vol. 57, no. 8, pp. 552–556, Dec. 2007.

[94]   X. Han, P. Xu, and Q. Ye, "Analysis of COVID-19 vaccines: Types, thoughts, and application," J. Clin. Lab. Anal., vol. 35, no. 9, p. e23937, Sep. 2021.

[95]   L. Feng et al., "Pharmaceutical and immunological evaluation of a single-dose hepatitis B vaccine using PLGA microspheres," J. Control. Release, vol. 112, no. 1, pp. 35–42, 2006.

[96]   M. Singh et al., "Controlled release microparticles as a single dose hepatitis B vaccine: evaluation of immunogenicity in mice," Vaccine, vol. 15, no. 5, pp. 475–481, 1997.

[97]   M. Singh, A. Singh, and G. P. Talwar, "Controlled Delivery of Diphtheria Toxoid Using Biodegradable Poly(D,L-Lactide) Microcapsules," Pharm. Res., vol. 8, no. 7, pp. 958–961, 1991.

[98]   Centers for Disease Control and Prevention (CDC), "Vaccine Information Statement - DTaP (Diphtheria, Tetanus, Pertussis) VIS," 2021. [Online]. Available: https://www.cdc.gov/vaccines/hcp/vis/vis-statements/dtap.html. [Accessed: 09-Feb-2023].

7

Appendices

Summary
Samenvatting
Biography and list of publications
Dankwoord

Summary

Although vaccination is considered one of the most important medical advances of the past centuries, the vaccination coverage for many vaccines has not increased in the past decade. One of the main reasons for a low vaccination coverage is limited access to vaccination services, especially in second- and third-world countries. For vaccines that require multiple doses for optimal protection against the pathogen in particular, vaccination coverage is often lower than for vaccines that require only one dose. The reason for this lower vaccination coverage is that, in the current vaccination schedule, multiple doses are administered through multiple injections. Such a vaccination schedule consists of the administration of a first dose (primer), followed by the administration of a second and sometimes even a third or fourth dose (booster) several weeks, months, or years later, and is therefore also called a prime-boost schedule. The vaccination coverage could possibly be improved by developing an alternative vaccine formulation where a single injection is sufficient for vaccines that require multiple doses. Such an injectable formulation should include both the primer and booster dose(s), thereby eliminating the need for multiple injections. An example is the incorporation of the antigen into a matrix consisting of a biocompatible and biodegradable polymer, which causes the antigen to be released from the formulation in a controlled manner. For this purpose, the formulation can exhibit a pulsatile or sustained release profile of the antigen. In a pulsatile release profile, a part of the antigen is released immediately after administration, while the remaining antigen is released in a pulse after a certain, preferably adjustable, time period. In a sustained release profile, the antigen is slowly released over a certain period of time. Moreover, various formulation types, such as microspheres or implants, and various polymers can be used. In this thesis, different types of formulations with both a pulsatile and sustained release profile have been developed and evaluated, which could provide an alternative to vaccines that require multiple injections. One of these formulations was based on microspheres with a so-called core-shell structure. Many different methods are possible for producing core-shell microspheres, each with its own advantages and disadvantages (**chapter 2**). However, it is also possible to develop implants with a core-shell structure. This concept was investigated in **chapter 3**, where a prototype of a core-shell implant was developed using direct compaction. This prototype consisted of a core in which the antigen was incorporated, surrounded by a polymeric shell. Additionally, a prototype of an implant was developed by means of direct compaction of a physical mixture of the antigen and the polymer. Poly(DL-lactide-*co*-glycolide) (PLGA) with a molar DL-lactide:glycolide ratio of 50:50 and poly(DL-lactide) (PDLLA) with two different molecular weights were used for the compacts. *In vitro* release studies were performed with theophylline as a model drug for the compacts of a physical mixture, which demonstrated that approximately half of the incorporated theophylline was released immediately, while the remaining part was released in a pulse after a lag time of several weeks. However, such a biphasic release profile was only obtained when the glass transition temperature of the moisturized polymer was above the compaction temperature, but below the temperature of the release medium. It was also shown that the lag time could be extended by increasing the lactide content of the polymer (PDLLA

instead of PLGA), and that the molecular weight of the incorporated release marker had no effect on the release profile. For the latter, labeled dextran (70 and 2000 kDa) was used as a model polysaccharide to investigate whether the developed compacts were suitable for polysaccharide-based antigens, such as some bacterial vaccines. The compacts were indeed suitable for the delivery of polysaccharide-based antigens, but not for the delivery of protein-based antigens. For the core-shell compacts, theophylline was again used as a model drug and PDLLA as polymer. When the glass transition temperature of PDLLA was below the compaction temperature or the temperature of the release medium, a delayed pulsatile release could be obtained. The developed compacts were, however, too large for clinical application. In the subsequent research, the focus was therefore on microspheres, including microspheres with a core-shell structure (**chapter 4**). These core-shell microspheres were produced using a method based on microfluidics, in which bovine serum albumin (BSA) was used a model antigen and PLGA with a molar DL-lactide:glycolide ratio of 50:50 and 75:25 as polymer. By placing two microfluidic chips in series, a double emulsion could be formed, which ultimately resulted in the formation of highly monodisperse particles with an average particle size of 35 to 50 μm. *In vitro* release studies showed that BSA was released after a lag time of several weeks and that this lag time could be varied from three to seven weeks by adjusting the molar DL-lactide-glycolide ratio of PLGA. An increase in the lactide content of the polymer resulted in a longer lag time. The BSA loading and shell thickness of the microspheres had no effect on the lag time. The release of BSA from the microspheres was, however, incomplete (30 to 50%). Furthermore, the used production method did have some disadvantages, especially the occurrence of channel blockages in the microfluidic chips. The chip in which the primary emulsion was formed was particularly sensitive to clogging, as this chip had the narrowest channels (14 μm). Therefore, this chip was replaced with a flow-through ultrasonic cell, which also enabled the production of microspheres with a core-shell structure, the desired size (30 to 50 μm), and a narrow particle size distribution (**chapter 5**). PLGA with a molar DL-lactide:glycolide ratio of 50:50 was used as the shell polymer, and BSA was again used as a model antigen. However, the incorporation of BSA did not succeed with the applied production settings, as the maximum encapsulation efficiency (EE) that was obtained was only 4%. These low EE values could probably be attributed to the relatively thick shells of the produced microspheres. Attempts to reduce the shell thickness were, however, not successful, but a combination of a relatively low polymer concentration and a lower flow rate ratio shell/core phase might provide a solution to this problem. Since there are numerous examples in the literature where a sustained release profile induced a strong immune response, attention was shifted to the development of monolithic microspheres for the sustained release of an (model) antigen. These microspheres were produced using membrane emulsification, in which a double emulsion was generated that formed the basis for the microspheres (**chapter 6**). The polymer matrix consisted of two novel multiblock copolymers composed of amorphous, hydrophilic poly(ε-caprolactone)-polyethylene glycol-poly(ε-caprolactone) (PCL-PEG-PCL) blocks and semi-crystalline poly(dioxanone) (PDO) blocks. The used production method and polymers enabled the production of uniform particles with the desired size (40 μm) and high EE. *In vitro*, (blends of) the polymers allowed for the sustained release of BSA from the microspheres over a period of four to nine weeks, depending on the

A

polymer blend ratio. Microspheres consisting of a 92.5:7.5 polymer blend exhibited the most optimal release profile and were therefore selected for the *in vivo* proof-of-concept study. After subcutaneous administration in mice, the microspheres induced a strong BSA-specific IgG antibody response that was equivalent to the immune response induced by a primer (t = 0 weeks) and a booster (t = 3 weeks) injection of BSA. Furthermore, pharmacokinetic analysis indicated that BSA was probably released *in vivo* over a period of four weeks, although peak plasma concentrations were reached already one week after administration, and only low levels of BSA could still be detected after four weeks. The work described in this thesis demonstrated the potential of implants and microspheres with pulsatile or continuous antigen release as an alternative to vaccines that require multiple doses and therefore injections according to the conventional prime-boost vaccination schedule. Hence, the developed formulations could contribute to improving the global vaccination coverage for various vaccines. Nevertheless, this research raised new questions but also offered perspectives for further research, as described in **chapter 7**. This follow-up research may lead to the development of an injectable single-administration vaccine formulation that allows for a complete pulsatile or sustained release of a clinically relevant antigen.

A

Samenvatting

Hoewel vaccinatie beschouwd wordt als één van de belangrijkste medische ontwikkelingen van de afgelopen eeuwen, is de vaccinatiegraad voor veel vaccins in het afgelopen decennium niet toegenomen. Eén van de voornaamste oorzaken van een lage vaccinatiegraad is de beperkte toegang tot vaccinatiediensten, vooral in tweede- en derdewereldlanden. Met name voor vaccins waarbij meerdere doseringen vereist zijn voor een optimale bescherming tegen de ziekteverwekker, is de vaccinatiegraad vaak lager dan voor vaccins waarbij één dosering volstaat. De reden hiervoor is dat meerdere doseringen door middel van meerdere injecties worden toegediend bij het huidige vaccinatieschema. Een dergelijk vaccinatieschema bestaat uit de toediening van een eerste dosis (primer), gevolgd door de toediening van een tweede en soms zelfs derde of vierde dosis (booster) enkele weken, maanden of jaren later en wordt daarom ook wel een prime-boost schema genoemd. De vaccinatiegraad kan mogelijk verbeterd worden door een alternatieve vaccinformulering te ontwikkelen waarbij een enkele injectie volstaat voor vaccins die meerdere doseringen vereisen. Een dergelijke injecteerbare formulering moet zowel de primer als de booster dosis omvatten, om daarmee de noodzaak voor meerdere injecties te elimineren. Een voorbeeld hiervan is het verwerken van het antigeen in een matrix die bestaat uit een biocompatibel en biologisch afbreekbaar polymeer, waardoor het antigeen gecontroleerd wordt afgegeven uit de formulering. Hierbij kan gebruik worden gemaakt van een pulserend of een continu afgifteprofiel van het antigeen uit de formulering. Bij een pulserend afgifteprofiel wordt een deel van het antigeen onmiddellijk na toediening afgegeven, terwijl het resterende antigeen pas na een bepaalde, bij voorkeur instelbare, periode gepulseerd wordt afgegeven. Bij een continu afgifteprofiel wordt het antigeen langzaam afgegeven over een bepaalde periode. Bovendien kan gebruik gemaakt worden van verschillende toedieningsvormen, bijvoorbeeld microsferen of implantaten, en verschillende polymeren. In dit proefschrift zijn verschillende typen formuleringen met zowel een gepulseerd als een continu afgifteprofiel ontwikkeld en geëvalueerd, die daarmee een alternatief zouden kunnen vormen voor vaccins die meerdere injecties vereisen. Eén van deze formuleringen bestaat uit microsferen met een zogeheten kern-schil structuur. Er zijn veel verschillende methodes mogelijk voor het produceren van microsferen met een kern-schil structuur die allen hun eigen voor- en nadelen hebben (**hoofdstuk 2**). Het is echter ook mogelijk om implantaten met een kern-schil structuur te ontwikkelen. Dit concept werd onderzocht in **hoofdstuk 3**, waarbij een prototype van een implantaat met een kern-schil structuur werd ontwikkeld door middel van directe compactie. Dit prototype bestond uit een kern waarin het antigeen zich bevond met daaromheen een schil van een polymeer. Bovendien werd een prototype van een implantaat ontwikkeld dat gebaseerd was op de directe compactie van een fysisch mengsel van het antigeen en het polymeer. Voor de compacten werd gebruik gemaakt van poly(DL-lactide-*co*-glycolide) (PLGA) met een molaire DL-lactide:glycolide ratio van 50:50 en poly(DL-lactide) (PDLLA) met twee verschillende molecuulgewichten. Voor de compacten van een fysisch mengsel werden *in vitro* afgifte studies uitgevoerd met theofylline als modelgeneesmiddel, waarin werd aangetoond dat ongeveer de helft van de geïncorporeerde theofylline direct werd afgegeven, terwijl het

resterende deel pas na enkele weken gepulseerd werd afgegeven. Een dergelijk bifasisch afgifteprofiel werd echter alleen verkregen wanneer de glasovergangstemperatuur van het bevochtigde polymeer boven de compactietemperatuur, maar onder de temperatuur van het afgiftemedium lag. Ook werd aangetoond dat de tijd tot de tweede gepulseerde afgifte verlengd kon worden door het lactidegehalte van het polymeer te verhogen (PDLLA in plaats van PLGA) en dat het molecuulgewicht van de geïncorporeerde afgiftemarker geen effect had op het afgifteprofiel. Voor het laatste werd onder andere gebruik gemaakt van gelabeld dextraan (70 en 2000 kDa) als modelpolysacharide om te onderzoeken of de ontwikkelde compacten geschikt zijn voor op polysacharide gebaseerde antigenen, zoals sommige bacteriële vaccins. Hoewel dit inderdaad het geval was, bleken de compacten niet geschikt te zijn voor de afgifte van op eiwit gebaseerde antigenen. Voor de compacten met een kern-schil structuur werd wederom gebruik gemaakt van theofylline als modelgeneesmiddel en PDLLA als polymeer. Wanneer de glasovergangstemperatuur van PDLLA onder de compactietemperatuur of onder de temperatuur van het afgiftemedium lag, kon een uitgestelde, gepulseerde afgifte worden verkregen. De ontwikkelde compacten waren echter te groot voor klinische toepassing en daarom werd in het vervolgonderzoek de focus gelegd op microsferen, waaronder microsferen met een kern-schil structuur (**hoofdstuk 4**). Deze microsferen werden geproduceerd met een methode gebaseerd op microfluïdica, waarbij bovine serum albumine (BSA) als modelantigeen en PLGA met een molaire DL-lactide:glycolide ratio van 50:50 en 75:25 werden gebruikt. Door twee microfluïdische chips in serie te plaatsen kon een dubbele emulsie worden gevormd, wat uiteindelijke resulteerde in de vorming van zeer monodisperse deeltjes met een gemiddelde deeltjesgrootte van 35 tot 50 µm. *In vitro* afgiftestudies toonden aan dat BSA na enkele weken werd afgegeven, waarbij de tijd tot de uitgestelde afgifte kon worden gevarieerd van drie tot zeven weken door de molaire DL-lactide-glycolide ratio van PLGA aan te passen. Hierbij leidde een hoger lactidegehalte van het polymeer tot een langere vertragingstijd. De schildikte en BSA-belading van de microsferen bleken geen effect te hebben op deze vertragingstijd. De afgifte van BSA uit de microsferen was echter wel incompleet (30 tot 50%). Bovendien had de gebruikte productiemethode wel enkele nadelen, voornamelijk het regelmatig optreden van verstoppingen in de kanalen van de microfluïdische chips. Met name de chip waarin de primaire emulsie gevormd werd, was erg gevoelig voor verstoppingen, aangezien deze chip de smalste kanalen (14 µm) had. Daarom werd deze chip vervangen door een in-line ultrasone cel, waarmee wederom microsferen met een kern-schil structuur, de gewenste grootte (30 tot 50 µm) en een smalle deeltjesgrootteverdeling konden worden verkregen (**hoofdstuk 5**). PLGA met een molaire DL-lactide:glycolide ratio van 50:50 werd gebruikt als polymeer voor de schil en BSA werd nogmaals gebruikt als modelantigeen. Het incorporeren van BSA bleek echter niet mogelijk te zijn met de toegepaste instellingen, aangezien de maximaal behaalde inkapselingsefficiëntie slechts 4% was. Deze lage waarde voor de inkapselingsefficiëntie kon waarschijnlijk worden toegeschreven aan de relatief dikke schillen van de geproduceerde microsferen. Pogingen om de schildikte te verlagen waren niet succesvol, maar een combinatie van een relatief lage polymeerconcentratie en een lagere schil vs. kern volumeverhouding zou wellicht een oplossing kunnen vormen voor dit probleem. Aangezien in de literatuur is aangetoond dat continue afgifte ook tot een efficiënte immuunrespons kan leiden, werd

A

de aandacht verschoven naar de ontwikkeling van monolithische microsferen voor de continue afgifte van een (model)antigeen. Deze microsferen werden geproduceerd met behulp van membraanemulsificatie, waarbij een dubbele emulsie werd gevormd die de basis vormde voor de microsferen (**hoofdstuk 6**). Voor de polymeer matrix werd gebruik gemaakt van twee nieuwe multiblok-copolymeren bestaande uit amorfe, hydrofiele poly(ε-caprolacton)-polyethyleenglycol-poly(ε-caprolacton) (PCL-PEG-PCL)-blokken en semi-kristallijne polydioxanon (PDO)-blokken. De gebruikte productiemethode en polymeren maakten de productie van uniforme deeltjes mogelijk met de gewenste grootte (40 μm) en een hoge inkapselingsefficiëntie. Met (mengsels van) de betreffende polymeren kon *in vitro* een langdurige afgifte van BSA uit de microsferen worden verkregen over een periode van vier tot negen weken, afhankelijk van de mengverhouding van de polymeren. Microsferen bestaande uit een 92,5:7,5 polymeermengsel voldeden het beste aan het beoogde afgifteprofiel en werden daarom geselecteerd voor de *in vivo* proof-of-concept studie. Deze microsferen induceerden na subcutane toediening in muizen een sterke BSA-specifieke IgG-antilichaamrespons, die gelijk was aan de immuunrespons na een primer (t = 0 weken) en een booster (t = 3 weken) injectie van BSA. Bovendien toonde farmacokinetische analyse aan dat BSA *in vivo* waarschijnlijk ook over een periode van vier weken werd afgegeven, hoewel de piekplasmaconcentraties al één week na toediening werden bereikt en vier weken na toediening alleen nog lage niveaus van BSA werden gedetecteerd. Het werk beschreven in dit proefschrift toont het potentieel aan van implantaten en microsferen met gepulseerde of continue afgifte als alternatief voor vaccins die meerdere doseringen en dus injecties vereisen volgens het conventionele prime-boost vaccinatieschema. De ontwikkelde formuleringen zouden daarmee kunnen bijdragen aan de verbetering van de wereldwijde vaccinatiegraad voor verschillende vaccins. Desalniettemin roept het onderzoek nieuwe vragen op, maar biedt het ook perspectieven voor vervolgonderzoek zoals beschreven in **hoofdstuk 7**. Met dit vervolgonderzoek kan mogelijk een injecteerbare formulering worden ontwikkeld die een volledige, gepulseerde of continue afgifte van een klinisch relevant antigeen mogelijk maakt.

A

Author biography

Renée van der Kooij was born on 16 January 1993 in Dronten, The Netherlands. In 2010, she completed her secondary education at Gymnasium Celeanum in Zwolle, The Netherlands. She then started her study Pharmacy at the University of Groningen. During her study, she developed an interest in pharmaceutical technology and controlled drug delivery. She therefore decided to conduct her Bachelor's research project at the pharmaceutical company InnoCore Technologies B.V. (Groningen, The Netherlands) in collaboration with the department of Pharmaceutical Technology and Biopharmacy. This project sparked her enthusiasm and she therefore decided to conduct her Master's research project at the department of Pharmaceutical Technology and Biopharmacy as well, under the supervision of Prof. Dr. H.W. Frijlink and Dr. W.L.J. Hinrichs. In this project, she investigated the suitability of physically mixed poly(DL-lactide-*co*-glycolide)-based compacts as a single-administration vaccine formulation. After obtaining her MSc degree *cum laude*, she started a PhD project at the same department in 2017. This project was again under the supervision of Prof. Dr. H.W. Frijlink and Dr. W.L.J. Hinrichs and in collaboration with InnoCore Technologies B.V. She investigated whether biodegradable polymers could be used for the development of compacts and microspheres as an alternative to the currently applied multiple-injection vaccination schedule, which altogether resulted in this thesis.

List of publications

R.S. van der Kooij, M. Beukema, A.L.W. Huckriede, J. Zuidema, R. Steendam, H.W. Frijlink, W.L.J. Hinrichs, "A single injection with sustained-release microspheres and a prime-boost injection of bovine serum albumin elicit the same IgG antibody response in mice," Pharmaceutics, vol. 15, pp. 676, 2023.

R.S. van der Kooij, R. Steendam, H.W. Frijlink, W.L.J. Hinrichs, "An overview of the production methods for core–shell microspheres for parenteral controlled drug delivery," European Journal of Pharmaceutics and Biopharmaceutics, vol. 170, pp. 24-42, 2022.

R.S. van der Kooij, R. Steendam, J. Zuidema, H.W. Frijlink, W.L.J. Hinrichs, "Microfluidic production of polymeric core-shell microspheres for the delayed pulsatile release of bovine serum albumin as a model antigen," Pharmaceutics, vol. 13, pp. 1854, 2021.

M. Beugeling*, N. Grasmeijer*, P.A. Born, M. van der Meulen, **R.S. van der Kooij**, K. Schwengle, L. Baert, K. Amssoms, H.W. Frijlink, W.L.J. Hinrichs, "The mechanism behind the biphasic pulsatile drug release from physically mixed poly(DL-lactic(-*co*-glycolic) acid)-based compacts," International Joournal of Pharmaceutics, vol. 551, pp. 195-202, 2018.

* Authors contributed equally

A

Dankwoord

In de afgelopen zes jaar zijn er ontzettend veel mensen geweest die direct of indirect een bijdrage hebben geleverd aan de totstandkoming van dit proefschrift. Ik kan met geen woorden beschrijven hoe dankbaar ik ben voor alle begeleiding en steun die ik heb ontvangen van jullie, collega's, vrienden en familie. Het is onmogelijk om iedereen hier persoonlijk te bedanken, maar het feit dat je dit hoofdstuk leest, betekent waarschijnlijk dat ook jij een (belangrijk) onderdeel bent geweest van mijn PhD jaren. Heel erg bedankt voor dat, zonder jullie had ik het niet gekund! Toch wil ik een aantal mensen in het bijzonder bedanken.

Allereerst mijn promotor prof. dr. H.W. Frijlink, **Erik**. Acht jaar geleden begon ik mijn masteronderzoek bij jouw afdeling, waar ik direct kennis maakte met jouw positiviteit, enthousiasme en toewijding. Ik kan me nog goed herinneren dat jij mij zelfs een keer om vijf uur 's middags nog hebt geholpen met het schoonmaken van mijn reageerbuizen. Ik waardeer je behulpzaamheid enorm en ben dan ook erg dankbaar dat ik in 2017 terug mocht komen op de afdeling voor het uitvoeren van mijn PhD project. Ook al heb ik uiteindelijk maar een half jaar bij FTB gewerkt en hebben we weliswaar niet veel direct samengewerkt, er zijn toch veel dingen waar ik je voor wil bedanken. Ondanks je drukke agenda was je altijd bereid om te helpen, al was het maar door het snel reageren op mijn e-mails en het regelen van zaken omtrent mijn promotie. Daarnaast bewonder ik je brede kennis, waardoor je altijd met goede oplossingen en suggesties voor vervolgexperimenten kwam. Tenslotte wil ik je bedanken voor alle vrijheid en mogelijkheden die je mij hebt gegeven tijdens mijn PhD.

Daarna mijn copromotor dr. W.L.J. Hinrichs, **Wouter**. Ik heb enorm veel aan jouw kennis en input gehad! Bedankt voor het steeds maar weer meedenken over verklaringen voor de onverwachtse resultaten en oplossingen voor problemen. Meermaals heb ik je geduld op de proef gesteld door technische problemen (nogmaals sorry daarvoor), maar gelukkig bleef je altijd vriendelijk en behulpzaam. Ik waardeer je humor en je pragmatische instelling en, het is al zo vaak gezegd maar, jouw commentaar op mijn manuscripten hebben ze echt enorm verbeterd. Ik ben ervan overtuigd dat dit proefschrift er zonder jou heel anders uit had gezien. Daarnaast wil ik je bedanken voor je gezelligheid bij de vrijdagmiddagborrels en de etentjes met het Daghapgenootschap. Helaas werd dit door de coronapandemie een stuk minder, maar gelukkig kunnen we op 23 mei nog een laatste keer proosten.

Naast de begeleiding vanuit FTB heb ik ook enorm veel gehad aan de begeleiding vanuit InnoCore. Allereerst **Rob**. Bedankt dat ik 5,5 jaar geleden vanuit FTB naar jullie toe mocht vertrekken. Ik ben heel blij met de kans die ik heb gekregen om een groot deel van mijn PhD project bij InnoCore uit te voeren. Dit is zeker een hele waardevolle toevoeging geweest aan mijn PhD. Daarnaast bewonder ik de enorme kennis die jij hebt, met name over polymeren. Je was vaak erg druk, maar dat belette je niet om tijdens de vrijdagochtendmeetings volop mee te denken over oplossingen en vervolgexperimenten.

Bedankt voor die actieve houding en dat je altijd mijn onderzoek verder wilde helpen. Naast je inhoudelijke input was het ook altijd erg gezellig als je op de vrijdagmiddag nog even aansloot voor een potje tafeltennis met een biertje. Hopelijk kruisen onze wegen elkaar ooit nog eens.

Dan mijn andere begeleider bij InnoCore, **Johan**. Wat ben ik blij dat jij na enige tijd (en heel wat begeleiders verder…) ons projectteam definitief aanvulde! We ontmoetten elkaar al in 2013 toen jij samen met Luisa mijn bacheloronderzoek bij InnoCore begeleidde en het feit dat ik in 2017 weer terug ben gekomen voor mijn PhD project zegt denk ik genoeg. Zonder jouw behulpzaamheid, nuchterheid en praktische instelling was dit proefschrift er zeker niet geweest, maar ook de vele jaren aan kennis die je over microsferen hebt opgedaan was enorm waardevol. Bedankt voor je relativeringsvermogen en gezelligheid. Je was altijd erg goed gezelschap, mede doordat we veel dezelfde hobby's delen (sporten, BBQ'en, borrelen, etc.) hadden we altijd veel leuke gesprekken. Wie weet spreken we elkaar nog eens, maar ik zal je in ieder geval blijven volgen op Strava! ;-)

Wat zou een promotieonderzoek zijn zonder mede-AIO's… **Gerian**, in 2017 kwam ik bij de afdeling FTB en ik had het niet beter kunnen treffen, want ik kwam bij jou op de kamer terecht. Helaas zijn we maar een half jaar kamergenoten geweest, omdat ik naar InnoCore vertrok, maar gelukkig zijn we goede vriendinnen geworden en gebleven. Je bent super gezellig, slim, behulpzaam en af een toe een beetje gek (gelukkig!). We hebben heel veel leuke dingen samen gedaan in de afgelopen jaren en ik ben enorm blij dat ik op 23 mei mag gaan promoveren met jou als paranimf aan mijn zijde. **Annemarie**, ook jij was onmisbaar tijdens mijn PhD de afgelopen jaren! We kenden elkaar al van de studie én ons masteronderzoek, maar op de één of andere manier hadden we toen nog niet door dat we goede vriendinnen zouden kunnen zijn. Ik waardeer je enorme toewijding aan dingen, van werk tot klussen tot onze vriendschap. Bedankt voor je gezelligheid en dat je altijd al mijn vragen wilde beantwoorden. Ik kijk uit naar nog heel veel leuke momenten met z'n drieën!

Mark en **Sebastiaan**, wat zou mijn PhD zonder jullie geweest zijn? Ik kwam bij InnoCore bij jullie op kantoor te zitten en had al snel in de gaten dat mijn jaren heel wat leuker konden worden met jullie als gezelschap. Gelukkig werden we uiteindelijk ook echt vrienden, waar onze whatsappgroep genaamd "Vrienden" het bewijs van is. Bedankt dat ik altijd bij jullie terecht kon met mijn vragen, maar nog veel meer voor alle goede gesprekken, het lachen, maar zelfs ook het huilen. Jullie relativeringsvermogen is voor mij heel belangrijk geweest. We hebben super veel gezellige borrels en kroegavondjes samen gehad en ik had al die momenten met jullie dan ook niet willen missen.

And of course all other (ex-)colleagues at InnoCore, thanks for making me feel welcome right away! Your "gezelligheid" and interest in and suggestions for my research have been an essential part of my PhD project. Especially the Formulation and Process Development department, **Albert**, **Ana**, **Cees**, **Daan**, **Duong**, **Kimberly**, **Maarten**, **Niels**, **Neda**, and all the others that have been part of the department over the last few years, many thanks for everything! I had a great time with all of you and I learned a lot from

A

you. **Inge**, **Ivan**, **Jeroen**, **Kim**, **Lidia**, **Peter**, and many others, thank you for the useful discussions and/or performing analyses for my project.

I would also like to thank all my (ex-)colleagues of the Pharmaceutical Technology and Biopharmacy department. Although I spent only half a year at the PTB department, you were definitely an important part of my PhD years. Thanks for the valuable suggestions for my research, the good atmosphere, and for always welcoming me with opens arms, even when you hadn't seen me in weeks ☺ **Khanh**, thank you for synthesizing the FITC-BSA and for helping me with the CLSM. **Emma**, it was really nice to be your office mate. I enjoyed your company and our good conversations a lot. **Imco**, jij was samen met Gerian en Annemarie onderdeel van onze "fine dining" club. Ik kan me niet herinneren dat we ooit fine zijn gaan dining, maar we hebben met z'n vieren wel erg veel leuke dingen gedaan, waarvan onze reis naar Amerika natuurlijk het hoogtepunt was.

Tijdens mijn PhD project had ik het voorrecht om samen te mogen werken met andere afdelingen van de Rijksuniversiteit Groningen. Allereerst de afdeling Farmaceutische Analyse, **prof. dr. E.M.J. Verpoorte**, bedankt voor de input in het microfluïdica project en voor het doornemen van dit proefschrift als lid van de beoordelingscommissie. Ook veel dank aan **Patty Mulder** en **Jean-Paul Mulder** voor de waardevolle suggesties met betrekking tot de microfluïdische chips. Daarnaast de afdeling Medische Microbiologie en Infectiepreventie, **prof. dr. A.L.W. Huckriede**, bedankt voor het meedenken over de immunologische kant van mijn project, voor het doornemen van de CCD-aanvraag en voor de samenwerking aan hoofdstuk 6 van dit proefschrift. **Martin**, op de valreep mocht ik nog met jou samenwerken, wat uiteindelijk ook heeft geresulteerd in de goedkeuring van onze CCD-aanvraag en in een publicatie. Bedankt voor je onmisbare suggesties en je hulp met de ELISA's, maar natuurlijk ook voor de leuke gesprekken!

Also many thanks to the other two members of the assessment committee, **prof. dr. H. Almeida Santos** and **prof. dr. E. Mastrobattista**, for evaluating this thesis.

Tijdens mijn promotieonderzoek heb ik ook enkele studenten mogen begeleiden. **Mark**, **Stefan**, **Marlyn** en **Tijn**, bedankt voor jullie inzet en waardevolle bijdrage aan dit proefschrift.

Maria Roosen, ik ben erg blij dat ik een afbeelding van uw werk 'Bubbles' als omslag mocht gebruiken voor dit proefschrift, het is precies zo geworden als ik in gedachten had.

Tenslotte alle vrienden en familie die allemaal op hun eigen manier mij hebben gesteund de afgelopen jaren. Allereerst mijn farmacievriendinnen, **Anne**, **Carolien**, **Loïs** en **Marlou**, ik ben zo blij dat wij al meer dan 12 jaar vriendinnen zijn! Bedankt voor jullie interesse en bemoedigingen en ik kijk uit naar de volgende 12 jaar vriendschap. Daarnaast **Aniek**, **Areanne**, **Josine** en **Rosanne**, ook jullie ken ik inmiddels al heel wat jaren. Bedankt voor jullie vriendschap en gezelligheid, die hebben mijn PhD jaren heel wat aangenamer gemaakt! **Henrieke** en **Christina**, ik vind het mega leuk dat ik jullie de

afgelopen jaren weer meer heb gesproken, laten we dat vooral zo houden! Als laatste **Eise**, **Jinke**, **Ellen** en **Pascal**, bedankt voor de gezelligheid en alle keren "even pils", ik ben heel erg blij met jullie als vrienden.

Mijn lieve familie, **Hanna**, **oma**, **Ludo**, **Annelies**, **Hanneke**, **Herman**, **Liza**, **Demi** en **Nouschke**. Bedankt voor jullie gezelschap en interesse. Ik waardeer alle leuke momenten die ik met jullie heb gehad enorm. En natuurlijk mijn lieve schoonfamilie, **Rolf**, **Judith**, **Anita**, **Jaap**, **Martin**, **Mirjam**, **Henk-Jan**, **Melissa**, **Bart** en **Lotte**. Ik ben heel erg blij dat jullie in mijn leven zijn gekomen. Jullie gezelligheid en steun de afgelopen jaren had ik niet willen missen!

Lieve **mam**, wat vind ik het enorm jammer dat jij mijn promotie niet zal kunnen meemaken. Ik houd van je en ik ben dankbaar voor alles wat je voor pap, Hanne en mij hebt betekend.

Lieve **pap**, jouw steun, empathie en relativeringsvermogen zijn onmisbaar voor mij geweest de afgelopen jaren. Bedankt dat je altijd naar me wilt luisteren, zonder twijfel me op allerlei manieren wilt helpen en zoveel van mij houdt. Ik bewonder je enorm als persoon en ben blij dat ik best wel veel op jou lijk.

Lieve **Hanne**, mijn grote zus! Ik ben enorm blij om jou als zus te hebben. Bedankt voor je luisterend oor, je wijsheid en je lieve woorden. Niet alleen ben je super slim, ook bewonder ik je doorzettingsvermogen, je openheid en je interesse. Ik vind het heel bijzonder dat ik 2,5 jaar geleden jouw paranimf mocht zijn en ik kijk er naar uit dat jij op 23 mei de mijne zal zijn!

Lieve **Ralf**, waarbij ik tegen de meeste mensen in dit dankwoord kan zeggen dat dit proefschrift zonder hen er niet was geweest, kan ik bij jou misschien beter zeggen dat dit proefschrift dankzíj jou er bijna niet was geweest ;-) Je hebt wellicht niet altijd achter mijn keuze om mijn promotieonderzoek af te ronden gestaan, maar toch ben je me blijven steunen, ook al was dit niet altijd makkelijk. Ik ben blij dat ik mijn gehele PhD met jou aan mijn zijde heb mogen doorlopen, zonder jou had ik het niet kunnen doen. Bedankt voor je lieve gebaren of soms juist strenge woorden, ik weet dat je altijd het beste met mij voor hebt gehad. Ik ben gek op je en kijk enorm uit naar ons volgende avontuur samen in Peru, we gaan er iets moois van maken.

Renée

A